Application and evaluation of amine based polymers for heavy metals adsorption and recovery from wastewater

Thesis submitted
in partial fulfillment of the requirements for the degree of
Doctor of Philosophy
by

Potsangbam Albino Kumar
Regd. No. 04610409

DEPARTMENT OF CIVIL ENGINEERING
INDIAN INSTITUTE OF TECHNOLOGY GUWAHATI
GUWAHATI-781039, INDIA
July 2009

Dedicated

to

My Loving Parents

Dr. P. BediKumar

&

Prof. (Dr.) Th. Ibetombi Devi

CERTIFICATE

This is to certify that the thesis entitled "Application and evaluation of amine based polymers for heavy metals adsorption and recovery from wastewater" submitted by Potsangbam Albino Kumar (04610409) to the Indian Institute of Technology Guwahati for the degree of Doctor of Philosophy is a record of bonafide research work carried out by him under our supervision and guidance. The thesis work, in our opinion has reached the requisite standard fulfilling the requirement for the degree of Doctor of Philosophy and has not been submitted earlier for award of any degree or diploma to the best of our knowledge and belief.

(Supervior)
Dr. Saswati Chakraborty
Associate Professor
Department of Civil Engineering
Indian Institute of Technology Guwahati

(Co Supervisor)
Dr. Manabendra Ray
Associate Professor
Department of Chemistry
Indian Institute of Technology Guwahati

Guwahati
May, 2010

Acknowledgement

The journey of this research work for the last four and half years has taught me several principles of life. And through this phase, several individuals from different walk of life have come upon to guide, help and support me. It is my privilege to acknowledge those persons who have made the most conspicuous contribution for the completion of my research work and who sought nothing in return from me.

Firstly, I thank my supervisor, Dr. Saswati Chakraborty, for the confidence she placed in me for carrying out the research work. Working under her supervision and being her first PhD student was a huge privilege with her teachings and guidance on ethics of high quality research through her knowledge, understanding, patience, dedications, sacrifice and inspiration. Her constant encouragement throughout the phase of my research work with her complete involvement even during experimental period was truly admiring. The effort she put in my research work was tremendous and complete in all aspects and that taught me the essential qualities of being a dedicated guide.

I would like to gratefully and sincerely thank my co supervisor Dr. Manabendra Ray, for his guidance, understanding, patience, and most importantly, his friendship during the course of the research. His mentorship was paramount in providing a well rounded experience for my long-term career goals. He encouraged me to not only grow as an experimentalist but also as an instructor and an independent thinker.

I would like to express my sincere gratitude to my Doctoral committees, Dr. Baleshwar, Dr. Sharad Ghokhale and Dr. Gopal Das for their constant directions and guidance in moulding my research work. I would like to thank Prof. Talukdar and Prof. Anjan Dutta (former HODs of Civil Engg. Dept) and Prof. S. K. Deb for their help and the facilities provided for completion of the research work. I sincerely would like to thank Dr. M. Jawed for the management skills he taught and trained me for being a future academician, for his valuable advice, inspiration and encouragement.

I appreciate and thanks the help rendered by Jonali Saikia (Scientific Officer) and P. Pathak (Lab attendant) that makes my research experiment complete. I am very much thankful to Jayshree Nath, Deepmoni Deka (Scientific Officer) and Partho (Lab Technician), Center of Environment, IIT Guwahati, for their cooperation and help with equipments and resource during my experimental period in their laboratory. I am very grateful to my friends from Chemistry department, Rik, Ballav, Marjit, and Francis for their valuable help in analysis of reactions and compounds for my research work. I would like to express my gratitude to Mr. Plaubon Basu (Varian, Calcutta) for his help in learning A.A.S. Instrument and also Center for instrument Facility (CIF), IIT Guwahati and CDRI, Lucknow, for allowing analysis of my polymers and samples. The quality level of research work achieved won't be possible without the financial support of Council of Scientific and Industrial Research (CSIR), Govt. of India, through project (No. 22 (0418)/06/EMR-II) and their support is hereby highly acknowledged.

This is a great opportunity to thank my fellow friends with whom I share my pains, sorrows, fun and laughter throughout the whole phase of my research work in IIT Guwahati. It will be impossible to imagine a life in campus without them. The help, support and advice of my seniors and well wisher Dr. Manglem, Tejmani, Dr. Darun, Kabita, Tej Banta, Dr. Girija, Sangeeta, Thoiba, Ashok, Bina are truly invaluable. I am very much obliged to my friend G. Pramod for his tremendous help during my initial phase of this research work. I will be very much indebted if I don't thank my friends from campus, Naim Hossain, Ramu Gantela, Zulker Nain, Biju Prava, Rupak Sarkar, Minaxi Rai, Sachin, Sandip Mondal, Jyoti, Aashish, for their love and affection besides their help, encouragement and support. Dr. Sarbajit, Arun Yendrembam, Genemala Hoabijam and Sonia Nongmaithem, they are the wonderful individuals who keep on pouring unconditional support professionally and personally throughout my stay in campus and close to my heart, and I would like to thank them for their constant support. I specially would like to thank my fellow colleagues Kamal Uddin Ahamad and Lalsangzela Sailo who are more than a friend and brother, for the whole journey they had with me throughout my stay in IIT Guwahati. I would like to highly acknowledge my fellow friends Uttam, Deepak, Santosh, Bihari, Roshan, Joy Shanker, Hemjit, Gautam, Devson,

Ronel and Hudson for their unwavering love, help, support and encouragement during my research.

Most importantly, I would like to thank my loving sisters Dr. Lunalisa and Ruby Miranda, my brother in law Anuj Shanker Saxena and Rahul Dev Sharma for their unwavering love and affection, unending encouragement, support and guidance. I am very much thankful to my wife Mimoda Devi. Her support, encouragement, quiet patience and prayers since the beginning of my research work, were undeniably the bedrock upon which the past four and half years of my life in research have been built. The love and affection of my daughter Ichathoi (Jessica Potsangbam) and her desire to be with me always is the main inspiration in completion of my Thesis. Finally, I thank my parents, for their faith in me and allowing me to be as ambitious as I wanted. It was under their watchful eye that I gained so much drive and an ability to tackle challenges head on.

Potsangbam Albino Kumar

Abstract

The impact of heavy metal pollution on environment due to industrial effluent is a global concern. Adsorption technique is one of the well proven metal removal techniques due to its several advantages over conventional methods like simple and easy operation, low cost, recovery of metal ions etc. Employment of functionalized polymers containing several functional groups such as amines, carboxylate, ether, hydroxyl, sulphate, phenolic, cyanide, chloride, acetate etc., as adsorbent for removal of metal ions has become a recent trend. However many of the reported functionalized polymers have complex synthesis procedure and cost ineffective. Therefore development of low cost functional polymer with easy synthesis procedure, moderate to high metal removal, rapid adsorption kinetics and reusability is necessary.

Amine ($-NH_2$) is known to be one of the most effective metal binding functional group due to presence of lone pair of electron in *sp3* hybridized atom of nitrogen. In the present study, two amine based polymers namely aniline formaldehyde condensate (AFC) and polyaniline (PANI) were synthesized to use as an adsorbent for metal removal from aqueous solution. Aniline was used as the amine source for both the polymers. The obtained polymers however being resinous, solid support were necessary to add in the matrixes of polymers to make granular adsorbent for easy separation of metal-adsorbent after interactions between metal and polymer. For AFC, due to its sticky nature, silica gel was observed as the only suitable support, where as for PANI, jute fibre was selected as the support medium. Synthesis of both the polymers was optimized in terms of metal removal efficiency. During interaction with anionic metal ions hexavalent chromium, maximum removal was achieved by both AFC coated silica gel and PANI-jute at pH 3 due to electrostatic attraction of protonated amines (NH_3^+) of polymer with chromate ion ($HCrO_4^-$). On removal study of cationic metal ions, removal trend of trivalent chromium [Cr(III)] and mercury [Hg(II)] by both the polymers and copper [Cu(II)], cadmium [Cd(II)] and lead [Pb(II)] by PANI-jute trends were observed similar with increase in metal removal with increase in pH. Maximum removals of all cationic metal ions were observed in the pH range of 6-9. The main removal mechanism was due to formation of coordinate bond between deprotonated nitrogen of amine ($-NH_2$) in polymers and cationic metal ions. AFC polymer showed presence of amine group throughout the chain length of the polymer, whereas PANI had amine group only at the terminal end

position. Due to presence of higher amount of amine group, AFC showed more metal uptake (both cationic and anionic metals) than PANI. Desorption studies showed metal recovery of 70-100% by both the polymers for all metals except for Cr(III) due to the high kinetic immobility of it. Since jute is combustible in nature, ignition of Cr(III) contaminated PANI-jute reduced the volume of spent adsorbent by more than 95-99% solving the problem of solid waste disposal as alternative. After desorption both the polymers were reused for several cycles. Through this adsorption-desorption-adsorption process, AFC coated silica gel was regenerated by chloroform extraction process and reused for four cycles with 80% metal removal efficiency whereas PANI-jute could be reused by washing with distilled water for more than six cycles without sacrificing metal removal efficiency. In industrial effluent, metal ions hardly exist as single ions, but as mixture of metals. Therefore adsorption from mixed metal system was studied with both AFC and PANI-jute and observed similar results with adsorption in the order of Cu(II) > Ni(II) > Cr(III) > Hg(II) > Pb(II) > Cd(II). These mixed metals removals followed the preferences dictated by the hard-soft theory of acids and bases and ligand exchange rate of metal ions. Dynamic metal removal studies by column experiments revealed the achievement of removal of highly toxic Hg(II) by AFC coated silica gel and Cr(VI) by PANI-jute with effluent below the permissible limit of 0.05 µg/L for both the metal ions. However, for AFC coated silica gel, column operation was more difficult as compared to PANI-jute due to less permeability of the column bed. Effort was made to synthesize AFC polymer without any support by increasing the amount of crosslinking agent formaldehyde than aniline and introducing alcohols to create voids. During preliminary study, support less AFC was observed to remove Cr(VI) more than double the amount adsorbed by AFC coated silica gel and PANI-jute. However the synthesis procedure of support less AFC was observed as highly sensitive with respect to temperature and effective size and further studies are required to optimize this. Both AFC with and without support can be stored for six months time without degradation in metal removal capacity whereas PANI-jute showed stability during storage for as long as 40 months time period.

Keywords: Heavy metals; amine; polymer; adsorption; desorption; polyaniline.

Table of Contents

List of Figures

List of Tables

Nomenclatures

%	: percentage
A	: Cross sectional area (m^2)
AER	: Adsorbent exhaustion rate
AFC	: Aniline formaldehyde condensate
b	: Energy (heat) constant of adsorption (L/mg)
b_0	: constant related to entropy
BDST	: Bed depth service time
C	: Concentration of adsorbate at any instance of time t (mg/L)
C_b	: Concentration of adsorbate in effluent at breakthrough concentration (mg/L)
C_{des}	: Final concentration after desorption
C_E	: Concentration of adsorbate in effluent at exhaustion (mg/L)
C_e	: Equilibrium concentration (mg/L)
C_n	: Adsorbate concentration at n^{th} reading (mg/L)
C_{n+1}	: Adsorbate concentration at $(n+1)^{th}$ reading (mg/L)
C_o	: Initial concentration of adsorbate (mg/L)
dh	: Differential depth of column (cm)
EBRT	: Empty bed residence time
ED	: Electrodialysis
EDX	: Electron diffraction X-ray
ESR	: Electromagnetic spin resonance spectrophotometer
FA	: Fly ash
g	: gram
GTA	: Graphite tube atomizer
h	: hour
H_r	: resonance of magnetic field.
h_z	: Height of adsorption zone (cm)
I	: Influent adsorbate loading (mg)
ID	: Internal diameter
JF	: Jute fiber
k_1	: Lagergren's first rate constants
k_2	: Lagergren's second order rate constants
k_{ads}	: Adsorption rate constant (L/mg h)

K_f : Freundlich's empirical constant

Kg : Kilogram

K_o : Overall mass transfer coefficient ($ML^{-2}T^{-1}$)

k_{sp} : Solubility product

k_{TH} : Thomas model rate constant (mL/min mg)

L : Litre

M : Mass of adsorbate not removed (mg)

m : Mass of adsorbent (g)

M1 : Metal 1 in binary system

M2 : Metal 2 in binary system

M_d : Mass of adsorbate desorbed (mg)

mg : milligram

MHz : Mega hertz

min : minute

mmol : milli moles

M_r : Mass of adsorbate removed (mg)

n : Freundlich's empirical constant

NMR : Nuclear magnetic resonance

N_o : Dynamic bed capacity (mg/L)

PANI-jute: Polyaniline synthesized on surface of jute fiber

PEI : polyethyleneimine

pH_{ZPC} : Zero charge potential

Q : Volumetric flow rate (mL/min)

q_e : Amount of adsorbate uptake (mg/g)

$q_{e,col}$: Amount of metal adsorbed per weight of adsorbent in column mode operation

q_{em} : Adsorption capacity at equilibrium calculated using model data

q_m : Langmuir's maximum monolayer coverage (mg/g)

Q_o : Maximum solid phase concentration of solute (mg/g)

R : Universal gas constant

r.p.m : Rotation per minute

R^2 : Correlation coefficent

RH : Rice husk

R_L : Separation factor

RSD : Relative standard deviation percentage

SD : Sawdust

sec : Second

SEM : Scanning electron microscope

T : Temperature (^{o}K)

t : contact time (min)

t_B : Breakthrough time (h)

t_E : Exhaust time (h)

TL : Tea leaves

t_S : Service time (h)

u : Linear flow rate (cm/h)

UV : Ultra viloet

V_{ads} : Volume of sample for adsorption experiment

V_B : Throughput volume at breakthrough (L)

V_{des} : Volume of desorbent

V_E : Throughput volume at exhaust (L)

V_n : Throughput volume at n^{th} reading (L)

V_{n+1} : Throughput volume at $(n+1)^{th}$ reading (L)

V_t : Throughput volume at any instant of time t (L)

w/v : weight/volume

Z : Column depth (cm)

Z_o : Critical bed depth (cm)

α : External surface area

β : Universal constant (9.274×10^{-21} erg/G)

θ : Fraction of complete monolayer coverage that exist

λ_{max} : Maximum wavelength

μm : micrometer

ν : Frequency

Chapter 1

Introduction

Generally heavy metals can be classified based on certain factors — density, atomic number or atomic weight, chemical properties or toxicity etc. From environmental toxicity point of view, heavy metals can be generally defined as group of elements which are toxic even at traces concentrations and that lies on periodic table between chromium and lead with atomic weights of 51.99 and 207.20 respectively and specific gravities greater than 4.0. Examples of heavy metals include mercury (Hg^{2+}), cadmium (Cd^{2+}), arsenic (As^{3+}), chromium (Cr^{6+}), nickel (Ni^{2+}), copper (Cu^{2+}), zinc (Zn^{2+}) and lead (Pb^{2+}). They are very stable and persistent environmental contaminants and cannot be degraded or destroyed and thus tend to accumulate in the soils and sediments. They also accumulate in living tissues and concentrated through food chain. The main anthropogenic sources of heavy metals which are really a concern for environment pollution are effluents from various industries such as electroplating, tanning, wood preservative, textile industry etc. Rapid industrialization and modernization over the years led to an increase and accumulation of heavy metals in environment and have created a major global concern. It was the catastrophe of Minamata in 1952 that led to the public awareness on the toxicity of metals. These episodes prompted the implementation of strict regulations on supply of potable water and discharge of effluents in aquatic environment. Several conventional techniques

such as precipitation, membrane filter technique, ion exchange, adsorption etc. were employed for removal of heavy metals. All these technologies have their inherent advantages and limitations. Production of large amount of sludge from precipitation techniques, inability of ion-exchange for competing with mono and divalent ions such as sodium (Na^{+}) and calcium (Ca^{2+}), high costs and elaborate pretreatment requirement for membrane process are some of the demerits that limits the application of these technologies.

Employment of activated carbon for adsorption of heavy metals though widely used is not suitable due to the high costs associated with the production of activated carbon and generation of spent carbon. Recognizing the economic drawback of activated carbon, many investigators have studied the feasibility of cheaper and abundantly available materials like charcoal cloth, rice husk, saw dust, clays, wood, peat etc. Of lately, biosorbents derived from dead living and dead cells of microorganisms and plants were successfully employed by several researchers for removal of heavy metal ions. However low adsorption capacity and slow kinetics restricts their application. It is established that metal ions can make coordination bond with several functional groups like amine, cyanide, chloride, acetate, phosphate, etc. to form ligand complex ions. Many researchers chemically modified activated carbon and biosorbents with these functional group which can bind metal ions through chemical adsorption and increased the overall efficiency of adsorbent. Synthesis of polymer as adsorbent with functional group and its application to binds metal ions by chelation has emerged as an area of research in recent years. However high cost and complex synthesis techniques of some polymers limits their use. Thus there rise necessities to develop low cost polymer with easy in synthesis procedure. Further, in recent years, emphasis has been given on recovery of metal ions instead of simple disposal. Hence, adsorption when combined with desorption of metal ions from low cost functionalized polymeric adsorbent is really an attractive metal removal option.

Present thesis has been composed with the objective to present an elaborate investigation in the broad area of research undertaken i.e. study on removal of heavy metals ions, to the extent possible, in the specific topic of research i.e Application and evaluation of amine based polymers for heavy metals adsorption and recovery from wastewater. This research work was initiated by synthesizing an amine based functionalized resinous polymer aniline formaldehyde condensate (AFC). In order to granularized the polymer and used as an adsorbent, AFC was coated on support material silica gel. The adsorbent was employed for removal of heavy metal ions such as

hexavalent chromium, trivalent chromium, cadmium and mercury in batch mode and continuous column mode was conducted with mercury. A mixed metal system of cationic metal ions- copper, trivalent chromium, mercury, nickel, cadmium and lead was also investigated to understand the affinity of metal ions towards AFC. Interaction of metal and AFC was studied under various conditions of pH, initial metal concentration, dose of adsorbent, desorption, regeneration and reuse. Understanding the loopholes of AFC coated silica gel, second polymer polyaniline (PANI) was further synthesized on surface of jute fiber and optimized to overcome the drawbacks of AFC coated on silica gel. PANI-jute was then engaged for removal of heavy metal ions and that includes hexavalent chromium, trivalent chromium, mercury, lead, copper and cadmium in batch mode and hexavalent chromium in continuous column mode. Finally, a support less AFC polymer was synthesized after brief study of the two polymers AFC coated on silica gel and PANI-jute. Preliminary study on removal of hexavalent chromium was carried out with this support less AFC.

The entire thesis has been divided into five chapters. Chapter 2 reviews up-to date literature on heavy metal –its definition, source, toxicity and available treatment techniques. Merits and demerits of the conventional treatment techniques had been analyzed and based on literature findings, scope of the study was developed. Chapter 3 consists of materials & methods, where polymer synthesis, adsorbent preparation, experimental protocol and analytical techniques used are discussed. Complete and detailed findings of the research work are presented in Chapter 4 - Results and discussion. The conclusions drawn from the study of interaction of the polymers with metal ions were reported in chapter 5. This chapter also includes certain aspects of this work suggested for future studies.

Chapter 2

Literature Review

2.1 Introduction

Heavy metal pollutants, because of their ubiquity, non destroyability and non biodegradability, continue to be a global concern. Heavy metals ions are highly carcinogenic, teratogenic and mutanogenic even at traces concentration. They are mainly discharged into the environment through various industrial activities. The discharge of heavy metal ions from industries led to several catastrophe- Minamata disaster in Japan due to mercury, Itai-itai in Japan due to cadmium, Sandoz factory leakage of mercury in Switzerland etc. Recent collapse of mine tailings sedimentation basin with billion gallons of zinc, cadmium, arsenic, copper and lead in Spain in 1998 had permanently damaged the Europe's largest bird sanctuary, as well as Spain's agriculture and fisheries. Stringent laws and legislations have been adopted worldwide to control the discharge limit of toxic heavy metal ions from industries. This in turns lead to more efforts of research work in this area, especially in finding better and more efficient technique for separating these contaminants from effluent water.

2.2 Toxicity

Generally a metal can be regarded as toxic if it impairs the growth and metabolism of cells when it is present above a certain concentrations. Almost all heavy metal ions are toxic at high concentrations and a few are severe poisons even at very low concentrations to all forms of life, including microorganisms, higher plants, animals and man. Of greater concern is the continuous exposure to low concentrations of metal as a consequence of widespread environmental contamination resulting in adverse effects. Human exposure to heavy metals has risen dramatically in the last 50 years as a result of an exponential increase in the use of heavy metals in industrial processes and products. In today's industrial society, there is no escaping exposure to toxic chemicals and metals. Details of toxic response on human due to some heavy metals ions which are associated with present study are presented in Table 2.1.

2.3 Sources

Source of heavy metals can be identified as natural and anthropogenic sources. Naturally heavy metals have been often released into sediment and air through chemical and physical weathering of igneous, metamorphic rocks and soils. They are also generally associated with volcanic activities, wind erosion, forest smoke fire and fossil fuels. The level of metals of such natural origin is usually harmless to man and environment. Heavy metals which are released by means of human activities are categorized under anthropogenic source such as from industries. Anthropogenic source of heavy metals are much higher than that of natural source (Goel 1997). For example, the concentration of arsenic in soil and in the earth's crust is in between 0.1-8,000 mg/kg and 1.5-5 mg/kg respectively (Ergican et al. 2005) whereas human activity contributes 80,000 tonnes of arsenic per year. Generally the primary anthropogenic sources of heavy metals are industrial source (point sources) such as mines, foundries, smelters, electroplating, tanneries, coal-burning power plants etc., as well as diffuse sources such as combustion by-products and vehicle emissions. Humans also affect the natural geological and biological redistribution of heavy metals by altering the chemical form of heavy metals released to the environment. Such alterations often affect a heavy metal's toxicity by allowing it to bioaccumulate in plants and animals, bioconcentrate in the food chain, or attack specific organs of the body. Industrial sources of specific metal ions are described in Table 2.2.

Table 2.1: Toxic response of heavy metal ions on human (US Department of Health and Human Services. 1991)

Heavy metal ion	Toxic response
Chromium	Intense gastrointestinal irritation or ulceration, epigastric pain, nausea, vomiting, diarrhea, vertigo, fever, muscle cramps, hemorrhagic diathesis, toxic nephritis, kidney and liver damage, renal failure, intravascular hemolysis, circulatory collapse, acute multisystem organ failure, alteration of genetic material, lung cancer, coma, and even death depending on the dose
Cadmium	Damage to central nervous system and immune system, DNA damage, reduced growth, bone defects (osteomalacia), lung cancer, renal dysfunction osteoporosis, inhibited reproduction, gastrointestinal disturbances such as nausea, vomiting, abdominal cramps, diarrhea, pneumonitis, lung emphysema, and death from pulmonary odema may occur.
Copper	Irritation in eyes, nose and mouth, headaches, dizziness, nausea, diarrhea, vomiting, liver and kidney damage, anemia, stomach and intestinal irritation, Wilson's disease characterized by a hepatic cirrhosis, brain damage and renal disease.
Mercury	Embryocidal, cytochemical and hispathological effects, brain damage, sperm damage, birth defects and miscarriages, sensory impairment, constriction of visual fields, hearing loss, ataxia and speech disturbances, allergic reactions, skin rashes, tiredness, headaches.
Lead	Biochemical effects in the synthesis of hemoglobin, effects on kidneys, joints and gastrointestinal tract, rise in blood pressure, disruption of nervous systems and damage of brain and reproductive system, impairment of liver and thyroid functions, loss of appetite, constipation, abdominal cramps, headache, weakness and fatigue, atrophy of forearm extensor muscles, paralysis of muscles.

Table 2.2: Industrial sources of heavy metal ions

Heavy metal ion	Toxic response	References
Chromium	Electroplating, tanning and leather, textile, pigments, plastic, dye.	Gang et al. 2000; Park et al. 2005a.
Cadmium	Electroplating, batteries, smelting, pigments, plastic, iron and steel, mining and mineral processing, non-ferrous metal industry, printing and photographic, paints.	Aderhold et al. 1996.
Copper	Electroplating, electricals, pipes and tubes, automobile, paper and pulp, paint, textile, fertilizer, petroleum.	Aksu et al. 1991; Figueira et al. 2000.
Mercury	Mining, transporting and processing of mercury ores, combustion of fossil fuels (Hg(II) content of coal is approx. 1 mg/kg), pulp and paper, paints, oil refinery, plastic, battery manufacturing, electrical equipment, leather tanning, metal finishing, petroleum refinery, agriculture, smelters, chlorine and chloroalkali manufacturing processes.	Jeon and Park 2005.
Lead	Battery, paper and pulp, mining, electroplating, lead smelting, metallurgical finishing industries, paints and pigments, metal dye, electricity and petroleum.	Noeline et al. 2005; Ucun et al. 2003.

2.4 Guidelines

The quality of drinking water may be controlled through a combination of protection of water sources, control of treatment processes and management of the distribution and handling of the water. The guidelines are intended to support the development and implementation of risk management strategies that will ensure the safety of drinking water supplies through the control of hazardous constituents of water. For effluents, these standards restrict the quantity of pollutants in the effluents that set the desired degree of treatment. The establishment of minimum standards of quality for wastewater discharge and for public water supply is of fundamental importance in achieving this objective. The Indian standards and the

WHO guidelines for some of the heavy metals for drinking water and the effluents are given in Table 2.3.

Table 2.3: Guidelines of heavy metals for drinking water and effluents (Source: IS: 10500: 1991; WHO 1993)

Heavy Metal	Indian Standards				WHO Guide Lines
	Drinking water		Effluents		Drinking water (mg/L)
	Desirable limit (mg/L)	Permissible limit (mg/L)	Inland surface water (mg/L)	Public sewers (mg/L)	
Chromium	0.05	No relaxation	0.10	2.00	0.05
Cadmium	0.01	No relaxation	2.00	1.00	0.003
Copper	0.05	1.50	3.00	3.00	2.00
Mercury	0.001	No relaxation	0.01	0.01	0.001
Lead	0.05	No relaxation	0.10	1.00	0.01

2.5 Removal techniques of heavy metals

Most of the heavy metals released as industrial effluent are generally soluble in water. The solubility of trace metals in surface waters is predominately controlled by the water pH, the type and concentration of ligands with which the metal ions can form soluble metal ligand complexes and the oxidation state of the mineral components and the redox environment of the system (Connell et al. 1984). The solubility product of metal ions are in order Cd(II) > Pb(II) > Cu(II) > Hg(II) > Cr(III) and their respective values are 5.3×10^{-15}, 1.43×10^{-20}, 4.8×10^{-20}, 3.6×10^{-26} and 6×10^{-31}. Simple physical process like screening, settling and filtration are inadequate to separate metal ions. Since many decades, well known technologies have already been established and practiced for removing heavy metals like chemical precipitation, ion exchange, membrane process, adsorption with activated carbon and bio-adsorbents etc. The brief description of various process and their limitations are presented below.

2.5.1 Chemical precipitation

Chemical precipitation involves the addition of chemicals to alter the physical state of the dissolve and suspended solids and then to facilitate their removal by sedimentation (Metcalf and Eddy 2003). Common precipitants include hydroxides (OH^-), sulphide (S^{-2}) and carbonates (CO_3^{-2}). For hydroxide precipitation of metal ions, every metal has a distinct and different pH at which the optimum precipitation occurs. At a pH at which the solubility of one metal hydroxide may be minimized, the solubility of another may be relatively high. Besides presence of chelating agent such as EDTA, citrates, etc., in electroplating operations poses significant or often impossible challenges for chemical precipitation. Precipitation is also accompanied by formation of large amounts of heavy metal contaminated sludge. Metal-bearing sludge specially metal-hydroxide sludge are inherently susceptible to leaching into ground water when sludges are disposed in landfills, which are heavily hydrated.

2.5.2 Ion exchange

Ion exchange is a unit process in which ions are exchanged between a solution and an ion exchanger, an insoluble solid or gel. Chelating resins, such as amino-phosphonic and iminodiacetic resins have been manufactured with high selectivity for specific metals, such as Cu^{2+}, Pb^{2+}, Ni^{2+}, Cd^{2+} and Zn^{2+}. To date, ion exchange has had limited application because of the extensive pretreatment requirement, less life span of the ion exchange resins and requirement of complex regeneration system. Besides, most of the ion exchange resins are expensive and released other cations such as H^+ or Na^+ in aqueous solution. Process efficiency is strongly pH dependent as most metals bind with the resin at higher pH. Besides, high concentrations of influent total suspended solids can plug the ion exchange beds, and cause high head loss and inefficient operation. Ion exchange waste is highly concentrated and requires careful disposal. Excessive osmotic swelling and shrinking, chemical degradation and structural changes in the resin due to presence of oxidants, solvents and polymers in wastewater are also important factors that limit the useful life and performance of ion exchange resin.

2.5.3 Membrane Process

Various membrane separation processes like reverse osmosis (RO), nanofiltration and electrodialysis are used for removal of heavy metal ions. RO involves an

ionic exclusion process where small particles are rejected by the water layer adsorbed on the surface of the membrane, which is known as dense membrane. Nanofiltration is also a form of filtration that uses membranes to preferentially separate different ions. The membrane use is partially permeable to perform the separation but pores are much larger than that of reverse osmosis. Incase of electrodialysis (ED), ions are transported through semi permeable membrane under the influence of an electric potential. These membrane processes are expensive compared to conventional treatment, as high capital and operating costs are required by the higher energy input to develop pressure needed to operate. Other recognizable limitations include membrane fouling and deterioration with time resulting from deposition of soluble materials, organic materials, suspended and colloidal particles and other contaminants thus requiring high level of pretreatments to prevent it. Presence of common ions such as Ca^{2+} and Mg^{2+} also inhibits this process. Formation of dilute salts due to alternate spacing of cation and anion permeable membranes, formation of metal hydroxides which clog the membrane also limit the application of electrodialysis.

2.5.4 Adsorption

2.5.4.1 Definition

Adsorption can be defined as a process in which atoms or molecules move from a bulk phase (that is, solid, liquid or gas) onto a solid or liquid surface. An example is purification of liquid/gases by adsorption where impurities are filtered by adsorption process onto the surface of a high-surface-area solid such as activated charcoal. Molecules that have been adsorbed onto solid surfaces are referred to as adsorbates, and the surface to which they are adsorbed as the adsorbent. The adsorption process can occur at interface between any two phases, such as, liquid-liquid, gas-liquid, gas-solid or liquid-solid interfaces. In the case of liquid-solid interfaces, three types of adsorption have been distinguished: (a) physical adsorption: due to VanderWaal's attraction, (b) chemical adsorption: due to formation of chemical bond and (c) exchange adsorption: due to electrical attraction of solute to the adsorbent. Chemical adsorption is characterized by high energies (> 40 kJ/mol) which are similar to those found between atoms within a molecule (for example, covalent bonds), strong localized bonds and is generally favoured at higher temperatures. In physisorption, the adsorbed molecule remains intact, but in chemisorption the molecule can be broken into fragments on the surface, in which case the process is called dissociative chemisorption. However adsorbed molecules are considered not to be free to move on the surface or within the interface and are referred to as

"activated" adsorption (Weber 1972) unlike physical adsorption. Most of the adsorption phenomena are combination of the three forms of adsorption and are generally termed as sorption, which includes absorption too while desorption is the reverse process.

The extent of adsorption depends on physical parameters such as temperature, pressure and concentration in the bulk phase, and the surface area of the adsorbent, as well as on chemical parameters such as the elemental nature of the adsorbate and the adsorbent. Low temperatures, high pressures, high surface areas, and highly reactive adsorbate or adsorbents generally favour adsorption.

2.5.4.2 Theoretical background of adsorption

(a) Adsorption Isotherm

Adsorption isotherm is a mathematical model or functional expression to depict the distribution of solute between the solid and liquid phase at equilibrium at a constant fixed temperatures. The isotherm model relates the amount of solute adsorbed per weight of adsorbent (q_e), with amount of solute retain in solvent (C_e) at equilibrium. Commonly, the amount q_e increase with increase in C_e value, but not in direct proportion. Several mathematical model or isotherms were developed based on certain assumptions. Langmuir isotherm, Freundlich isotherm, Langmuir-Freundlich isotherm, BET isotherm, Temkin, Redlich–Peterson etc. are some of the well known models out of which Langmuir and Freundlich isotherm are the commonly and mostly applied models in heavy metal adsorption from aqueous solution.

(i) Langmuir Isotherm

Langmuir isotherm is based on the following assumptions: (a) each surface site can be singly occupied, (b) there are no lateral interactions between adsorbed species, (c) the enthalpy of adsorption is independent of surface coverage and (d) energy of adsorption is constant thus creating homogeneity of energy on the surface (there is dynamic equilibrium between the adsorption and desorption processes). The first assumption implies the validity of Langmuir isotherm for monolayer adsorption. At a given time, the rate of adsorption K_a, is proportional to the solute concentration (C_e) in liquid phase and fraction of free sites or vacant sites (1-θ), where 'θ' represents the fraction of complete monolayer coverage that exist

(Langmuir 1918). Similarly, rate of desorption at the same time can be represented by $K_d\theta$. Equating the rate of adsorption and rate of desorption for equilibrium,

$$K_d\theta = K_a C_e(1-\theta) \tag{2.1}$$

$$\text{or, } \theta = \frac{K_a C_e}{K_d + K_a C_e} = \frac{bC_e}{1+bC_e} \tag{2.2}$$

The adsorption coefficient $b = \frac{K_a}{K_d}$, is related to the enthalpy of adsorption (ΔH) by

$$b = b_0 \exp^{-\Delta H / RT} \tag{2.3}$$

where b_0 is constant related to entropy, R is the universal gas constant, T is the temperature (^oK) (Voice and Weber 1983).

As q_e is proportional to θ, therefore, equation (2.3) can be written as,

$$q_e = \frac{bQ_m C_e}{1+bC_e} \tag{2.4}$$

where q_m is the maximum adsorption for a complete monolayer coverage. Equation (2.4) can be rearranged in variety of linear forms.

$$\frac{C_e}{q_e} = \frac{1}{Q_m b} + \frac{C_e}{Q_m} \tag{2.5}$$

$$\frac{1}{q_e} = \frac{1}{Q_m} + \frac{1}{bQ_m C_e} \tag{2.6}$$

$$q_e = Q_m - \frac{q_e}{bC_e} \tag{2.7}$$

While equation (2.5), (2.6) and (2.7) are equivalent, one particular form may be more desirable than other depending on ranges and spread of data to be described (Voice and

Weber 1983). Another dimensionless parameter named separation factor (R_L) is introduced in Langmuir's model to indicates the favourability of the adsorption and is determined by

$$R_L = \frac{1}{(1 + bC_0)} \tag{2.8}$$

where, b is the Langmuir coefficient, C_0 is the initial liquid phase concentration of adsorbate in equilibrium with the adsorbent and for favourable adsorption, $0 < R_L < 1$ (Hall et al. 1966).

Many researchers had successfully employed Langmuir isotherm model for adsorption of heavy metal ions by various adsorbents. Singh et al. (1998) tested the applicability of the Langmuir isotherm for the Cd(II) adsorption by hematite and monolayer coverage (Q_m) was observed as 0.24, 0.23 and 0.22 mg/g at 20, 30 and 40^{o}C respectively at pH 9.2. Adsorption of Ni(II) and Cd(II) by bagasse fly ash was able to treat by Langmuir's isotherm with monolayer coverage (Q_m) of 1.24, 1.67 and 2.00 mg/g at 30, 40 and 50^{o}C respectively while that of nickel for same condition was 1.12, 1.35 and 1.7 mg/g (Gupta et al. 2003). Adsorption of lead from aqueous solution using agricultural waste maize bran at different temperatures (20, 30 and 40^{o}C) and pH (3.2-8.0) was observed best fitted to Langmuir's model with monolayer coverage values (Q_m) of 142.86, 140.85, 136.98 mg/g respectively (Singh et al. 2006). Inbaraj and Sulochana (2006) employed carbon sorbent derived from fruit shell of terminalia catappa for adsorption of mercury. Data results were best fitted to Langmuir isotherm with monolayer adsorption capacity of 94.43 mg/g at pH 5.0.

(ii) Freundlich isotherm

Freundlich model or van Bemmelon equation has been developed for adsorption system with emphasis on two factors, namely the lateral interaction between the adsorbed molecules and the energetic surface heterogeneity. The equation has the general form (Freundlich 1906)

$$q_e = K_f C_e^{\frac{1}{n}} \tag{2.9}$$

but it is well cited in logarithmic form as

$$\log q_e = \log K_f + \frac{1}{n}\log C_e \quad (2.10)$$

where K_f and n are empirical constant. Here, K_f α RT nb exp(ΔH/RT). The Freundlich constant 'n' indicates the degree of favourability of adsorption and its value should be lying in the range of 1 to 10 for classification as favorable adsorption. A smaller value of (1/n) indicates a stronger bond between adsorbate and adsorbent, while a higher value for K_f indicates higher rate of adsorption. Equation (2.9) suggests that with increase in C_e, adsorption capacity (q_e) would increase without restriction, which is practically impossible. The model may simulate concentrations far outside the range of the defining batch experiment. Extrapolating equation (2.9) into such concentration regions hence may give results of unknown, but potentially very large error. For example, it is likely that there is a limiting value to the partition coefficient at lower concentrations, possibly reflecting sorption on only the most active sites as concentrations approach zero. This limits the application of Freundlich model at higher C_e values. However in practical situation, adsorption process are sufficiently dilute and one never encounters the region where Freundlich equation breaks down for this region and Freundlich isotherm equation implies that the energy distribution of adsorption site is of exponential (Cooney 1999).

Several researchers reported employment of Freundlich isotherm model for heavy metal adsorption. Ajmal et al. (1998) employed both Freundlich and Langmuir isotherm for investigating the adsorption nature of Cu(II) by sawdust. They observed Freundlich K_f value of 0.58, 0.10 and 0.11 at 30, 40 and 500 g/mg respectively with regression value of almost above 0.99 for all the varied temperatures as to Langmuir model with regression coefficient of 0.97-0.98 under same condition. This suggest that the surface of sawdust is made up of small heterogeneous adsorption patches, which are very much similar to each other in respect of adsorption phenomenon as assumed by Freundlich.

(b) Adsorption kinetics

Adsorption kinetics is the rate of adsorption of adsorbate towards adsorbent. Slow kinetics will require more time to remove adsorbate effectively. Therefore to achieve large amount of adsorbate removal in short time, reactor volume needs to be increased. Chemical adsorption however displayed rapid kinetics due to formation of chemical bond. The adsorption kinetics of metal can be well treated and explained by Lagergren's first and second order kinetic models (Ho 2006).

(i) Pseudo first order adsorption model

Lagergren's Pseudo first order kinetic model for removal of metal ion was successfully employed by various researchers during removal of copper and cadmium by peanut hull carbon (Periasamy and Namasivayam 1996), activated carbon from coconut coir pith (Kadirvelu and Namasivayam 2003) and waste Fe^{2+}/Cr^{3+} hydroxide (Namasivayam and Ranganathan 1995). The pseudo first order adsorption kinetic rate equation is given as

$$\frac{dq_t}{dt} = k_1 (q_e - q_t) \tag{2.11}$$

where, q_e and q_t are the amounts of metal ions adsorbed on adsorbent (mg/g) at equilibrium and at time t, respectively, and k_1 is the rate constant of pseudo first order adsorption (min^{-1}). After integrating Equation (2.11) for the boundary conditions t = 0 to t= t and $q_t = 0$ to $q_t = q_e$,

$$log(q_e - q_t) = log\ q_e - \frac{k_1}{2.303} t \tag{2.12}$$

Further, Equation (2.12) can be expressed as a function of time as

$$q_t = q_e \left(1 - e^{-k_1 t}\right) \tag{2.13}$$

(ii) Pseudo second order adsorption model

The second order adsorption kinetic rate equation was used by various authors for removal of chromium (Khezami and Capart 2005; Karthikeyan et al. 2005) and mercury (Yardim et al. 2003) and given as

$$\frac{dq_t}{dt} = k_2 (q_e - q_t)^2 \tag{2.14}$$

where, q_e and q_t are the amounts of metal ions adsorbed on adsorbent (mg/g) at equilibrium and at time t, and k_2 (g/mg.min) is the rate constant of the second order adsorption. Integrating Equation 2.14 for the boundary conditions t = 0 to t = t and $q_t = 0$ to $q_t = q_e$, leads to

$$\frac{1}{q_e - q_t} - \frac{1}{q_e} = k_2 t \tag{2.15}$$

or,

$$q_t = q_e \frac{q_e k_2 t}{1 + q_e k_2 t} \tag{2.16}$$

$$\text{or, } \frac{t}{q_t} = \frac{1}{k_2 q_e^2} + \frac{t}{q_e} \tag{2.17}$$

In order to select the best bit isotherm or kinetic model, Chi-square test was done (Equation 2.18) (Ho et al. 2005).

$$\chi^2 = \Sigma \frac{(q_e - q_{em})^2}{q_{em}} \tag{2.18}$$

where, q_e and q_{em} (mg/g) are metal adsorption capacity at equilibrium calculated using experimental data and model respectively

(c) Column performance

Batch process data has several limitations to predict the performances in practical situation such as actual industrial wastewater treatment plant where continuous reactors replaced batch operation. Besides, in batch mode adsorption process, adsorption equilibrium is achieved and the adsorption characteristics were analyzed by isotherms. However, in fixed-bed column, the adsorption zone or mass transfer zone keeps moving through the bed and the fluid and solid phase in that zone are never able to achieve equilibrium. Adsorption efficiency by column mode depends on flow rate, bed height and influent adsorbate initial concentration. (Deepa et al. 2008).Generally the performance of the continuous column mode operation is usually described through the concept of breakthrough curve which is the typical 'S' shape profile of exit concentration (C) as a function of lapse time (t) or throughput volume (V_t) reacted. Throughput volume was calculated using Equation 2.19.

$$V_t = Q.t \tag{2.19}$$

where, Q is the volumetric flow rate (mL/min).

Usually breakthrough is defined as phenomenon when concentration of adsorbate from column is about 3-5% (Chen et al. 2003; Malkoc et al. 2006). However breakthrough at 1% was also considered and reported on basis of effluent discharge limit for specific metal adsorbate (Vijayaraghavan et al. 2005). Employment of breakthrough of 50% was also reported for removal of Pb(II) using treated granular activated carbon (Goel et al. 2005). For our study, the breakthrough time was obtained for effluent metal concentration of 0.1 mg/L considering the factor of effluent permissible limit concentration. Exhaustion is generally considered when the effluent concentration remains same for long period close to influent concentration. Vijayagarvan et al. (2005) considered exhaustion at 99% of influent concentration for removal of copper by brown marine alga *Turbinaria ornata*. Adak and Pal (2006) considered exhaustion when effluent reached 90% of influent on removing phenols by SDS-modified alumina. Exhaustion for the present studies was considered when effluent metal ion reached 95% of influent concentration (Benefield et al. 1982). The area below breakthrough curve represents mass of metal ions which is not removed (M) and was calculated using Equation (2.17) (Sincero and Sincero 2003):

$$M = \sum[(V_{n+1} - V_n)\,(C_{n+1} + C_n)/2] \qquad (2.20)$$

where, V_n = throughput volume at n^{th} reading (L), V_{n+1} = throughput volume at $(n+1)^{th}$ reading (L), C_n = effluent adsorbate concentration at n^{th} reading (mg/L) and C_{n+1} = effluent adsorbate concentration at $(n+1)^{th}$ reading (mg/L).

Influent adsorbate load (I) was calculated from throughput volume (V_E) at column exhaustion and influent adsorbate concentration (C_o) according to equation 2.21.

$$\text{Influent adsorbate load (mg)} = I = (V_E * C_o) \qquad (2.21)$$

Mass of adsorbate removed was calculated from difference of influent adsorbate load (I) and mass of adsorbate not removed (M) from equation 2.22

$$\text{Mass of adsorbate removed} = M_r\ (\text{mg}) = (I-M) \qquad (2.22)$$

Adsorbate uptake by adsorbent was calculated using equation 2.23.

$$\text{Adsorbate uptake by adsorbent } (q_e) = M_r\ (\text{mg})/\ \text{weight of adsorbent (g)} \qquad (2.23)$$

(d) Models on column performance

Optimization of parameters in the continuous adsorption process by experimental methods is an expensive and time-consuming. It would be much cheaper and faster to use mathematical modeling to predict the duration of the column bed before regeneration becomes necessary (Warchol and Petrus 2006). Moreover, it is hard to generalize operational design parameters, therefore, theoretical models taking into account of chemical and physical conditions become important (Chen et al. 2003). Some of the well known mathematical models applied for column mode operation are Bed Depth Service time (BDST) model, Thomas model, theoretical breakthrough curve etc.

(i) Bed Depth Service Time (BDST) model

The Bohart-Adams equation can be represented as (Bohart and Adams 1920):

$$Ln(\frac{C_o}{C_b}-1) = Ln(e^{k_{ads}N_o(Z/u)}-1) - k_{ads}C_o t_S \quad (2.24)$$

Further, Hutchins (1973) modified the Bohart–Adams equation and presented a linear relationship between the bed depth and service time (equation 2.25) which requires only three fixed bed tests to collect the necessary data.

$$t_S = \frac{N_o Z}{C_o u} - \frac{1}{k_{ads}C_o} Ln(\frac{C_o}{C_b}-1) \quad (2.25)$$

where, t_s is the service time at breakthrough point (h), N_o the dynamic bed capacity (mg L^{-1}), Z the packed-bed column depth (cm), u the linear flow rate (cm/h) defined as the ratio of the volumetric flow rate Q (cm^3/h) to the cross-sectional area of the bed A (cm^2), C_o and C_b are respectively the influent and the breakthrough adsorbate concentration (mg/L) and k_{ads} the adsorption rate constant (L/mg.h). Plotting service time (t_s) versus bed depth (Z) will generate a straight line equation having slope of ($N_o/C_o.u$) and intercept of $(-)\frac{1}{k_{ads}C_o} Ln(\frac{C_o}{C_b}-1)$. Critical bed depth ($Z_o$) represents the theoretical minimum depth of column that would be able to prevent the adsorbate concentration from exceeding C_b. It is obtained when breakthrough is immediate and it can be calculated by substituting $t_S = 0$ in equation 2.25 as shown below:

$$Z_0 = \frac{u}{k_{ads} N}\left(\frac{C_0}{C_b} - 1\right) \quad (2.26)$$

According to BDST model equation (2.25), the data collected from one flow rate experiment can predict the system with different flow rate. When an experiment conducted at flow rate Q_1, yields an equation of the form

$$t_s = a_1 Z + b_1 \quad (2.27)$$

the predicted equation for new flow rate Q_2, is given by:

$$t_s = a_2 Z + b_1 \text{ and} \quad (2.28)$$

$$a_2 = a_1\left(\frac{Q_1}{Q_2}\right) \quad (2.29)$$

where, a_1 and a_2 are the slopes at flow rate Q_1 and Q_2 respectively. However the intercept b_1 remained same since it is independent of flow rate in linearized BDST equation (2.25). BDST model can also be used to design systems for treating other influent solute concentrations using the data of a previous laboratory experiment of one influent solute concentration. When an experiment conducted at initial concentration C_1, yields an equation of the form

$$t = r_1 X + s_1 \quad (2.30)$$

the predicted equation for new flow rate Q_2, is given by:

$$t = r_2 X + s_2 \text{ and} \quad (2.31)$$

The new slope and intercept values can be determined as:

$$r_2 = r_1\left(\frac{C_1}{C_2}\right) \quad (2.32)$$

$$s_2 = s_1 \frac{C_1}{C_2}\left(\frac{\mathrm{Ln}[C_2/C_F)-1]}{\mathrm{Ln}[C_1/C_b)-1]}\right) \tag{2.33}$$

where, r_1 and r_2 is slopes at influent concentration C_1 and C_2 respectively, s_1 and s_2 are intercepts at influent concentration C_1 and C_2 respectively, C_F is effluent concentration at influent concentration C_2 and C_b is effluent concentration at influent concentration C_1.

(ii) Thomas model

Thomas model assumes Langmuir kinetics of adsorption-desorption and no axial dispersion. It is derived with the adsorption that the rate driving force obeys pseudo second order reversible reaction kinetics. Thomas equation is given by (Thomas 1994)

$$\frac{C_o}{C} = 1 + \exp\left((\frac{k_{TH}}{Q}(Q_o M - C_o V_t)\right) \tag{2.34}$$

where, C_o is the initial adsorbate concentration (mg/L), C is the effluent adsorbate concentration (mg/L), k_{TH} is the Thomas model rate constant (mL min^{-1} mg^{-1}), Q_o the maximum solid-phase concentration of the solute (mg/g), V_t the throughput volume. Linearized form of Thomas Model is as follows:

$$ln\left(\frac{C}{C_o}-1\right) = \frac{k_{TH}Q_o M}{Q} - \frac{k_{TH}C_o}{Q}V_t \tag{2.35}$$

(iii) Theoretical breakthrough curve

The breakthrough curve of a continuous fixed bed operation mode can be evaluated using the data obtained from the batch isotherm studies. Thus column operation can be designed from batch experiment data without running the column experiment and the procedure is given below.

(i) An operating line needs to be drawn passing through the origin and intersecting the equilibrium curve (C_e versus q_e of batch data) at C_o (designed influent adsorbate concentration of column bed experiment to be conducted). The significance of this operating line was that the data of continuously mixed batch reactor and the data of fixed bed reactor are identical at

these two points, first at the initiation and other at the exhaustion of the reaction (Michaels 1952).

(ii) The rate of transfer of the adsorbate from the solution over a differential depth of column d*h* is given by

$$QdC = K^o\alpha(C - C_e)dh \tag{2.36}$$

where Q is the flow rate, K^o the overall mass transfer coefficient ($ML^{-2}T^{-1}$), α the external surface area, C_e is the equilibrium concentration of the adsorbate in the solution corresponding to a adsorbed concentration q_e and C is the concentration of the adsorbate at a given instant of time t (Weber 1972).

(iii) The term ($C - C_e$) is the driving force for adsorption and is equal to the difference between the operating line and equilibrium curve at any given q_e value. Integrating the Equation 2.36 and solving for the height of adsorption zone (h_z) at saturation yields

$$h_z = \frac{Q}{K^o\alpha}\int_{C_B}^{C_E}\frac{dc}{(C - C_e)} \tag{2.37}$$

where C_B and C_E are the concentrations of adsorbate in effluent at breakthrough and at exhaustion point respectively.

(iv) The area under the curve of C versus $(C - C_e)^{-1}$ represented the value of the above integration. Since $(C - C_e)^{-1}$ approaches infinity as C approaches C_o, it is necessary to terminate the plot of C at a value somewhat less than C_o or at C = 0.95 C_o (exhaustion for adsorption beds). For any value of h less than h_z corresponding to a concentration $C_B < C < C_E$, Equation 2.37 can be written as

$$h = \frac{Q}{k_o\alpha}\int_{C_B}^{C}\frac{dc}{(C - C_e)} \tag{2.38}$$

Dividing Equation 2.38 by equation 2.37 results in

$$\frac{h}{h_z} = \frac{\int_{C_B}^{C} dC/(C - C_e)}{\int_{C_B}^{C_E} dC/(C - C_e)} = \frac{V_t - V_B}{V_E - V_B} \tag{2.39}$$

h/h_z is equal to the ratio $(V_t - V_B)/(V_E - V_B)$ where V_B and V_E are throughput volumes at breakthrough and exhaustion respectively and V_t is the throughput volume within V_E for an effluent concentration C within C_E (or throughput volume at any instant of time t within exhaustion point). It should be noted that equation (2.39) is valid only if the transfer term $K_o\alpha$ is constant within the adsorption zone for changing concentrations. For most practical applications, this term is sufficiently constant to permit use of the relationship for evaluation of the breakthrough curve (Weber 1972).

(v) Finally the theoretical breakthrough curves were generated by plotting $(V_t - V_B)/(V_E - V_B)$ versus (C/C_o).

2.5.4.3 Types of adsorbents used for removal of heavy metals

Various types of adsorbents used for metal removal are activated carbon, micro and plant biomass, silica based adsorbents, synthetic polymeric adsorbent etc. Performance of various adsorbents for heavy metal removal is described in following sections.

(a) Activated Carbon

Activated carbon is a form of carbon that has been processed to make it extremely porous and thus to have a very large surface area available for adsorption. Due to its high degree of micro porosity, just one gram of activated carbon has a surface area of approximately 1500 m², as determined typically by nitrogen gas adsorption. Usually activated carbon is derived from charcoal. The use of activated carbon for removal and recovery of heavy metal ion has been receiving a great attention for decades. In recent years a variety of carbon-based materials, like coal, wood, lignite, coconut shells etc. are used for preparation of activated carbon. Table 2.4 presents heavy metal adsorption by activated carbon prepared from different base materials and their metal adsorption capacities. Preparation techniques for these varieties of activated carbon though slightly different; the main principle is still the same with carbonization of raw materials at high temperature and grinding to granules or powders. Activated carbon derived from comingled waste, coconut, *Hevea Brasilinesis* and fruit shell of *Terminalia catappa* took high equilibrium time of 500 minutes, 5 days, 300

minutes and 720 minutes respectively for removal of Cr(III), Cr(VI), Cr(VI) and Hg(II) (Table 2.4). For such high equilibrium time, volume of the reactor needs to be increased to facilitate treatment of higher concentration of metal ions which in turns will increase the over all cost. Though adsorption equilibrium were achieved within 120 minutes by coconut shell (Sekar et al. 2004), baggase fly ash (Gupta et al. 2003) and herbaceous peat (Gündogan et al. 2004) on removal of Cu(II), Pb(II) and Cd(II) respectively, maximum corresponding removal were reported 26.51, 1.18 and 4.8 mg/g which are less as compared to other reported adsorbents. Activated carbon derived from sago waste (Kadirvelu et al. 2004) and tree fern (Ho 2003) though achieved adsorption equilibrium within 120 minutes also on removal of Hg(II) and Cu(II) respectively, their smaller particle size of 125–250 μm and 74–88 μm will caused clogging in column mode operation. Waste tyre sawdust showed high Cr(VI) removal of 58.47 mg/g (Hamadi et al. 2001) and wheat bran removed maximum Cr(III), Hg(II), Hg(II), Cd(II) and Cu(II) of 93, 70, 62, 21 and 15 mg/g (Farajzadeh et al. 2004) respectively within adsorption equilibrium of 120 minutes. Such wide ranges of metal removal by different activated carbon are due to degree of micro porosity present in it. As such, creation of micro pores due to pyrolysis was responsible for metal removal by waste tyre sawdust. Generally, modes of adsorption for all activated carbon are similar by physical adsorption due to van der Walls force of attraction which usually took longer time to achieve adsorption equilibrium. However several activated carbons contained functionalized group that also bind metal through chemical bond formation and thus achieved adsorption equilibrium in less time.

In Table 2.4, it can be observed that phenolic, hydroxyl, carbonyl and lactone groups are the functional group responsible for rapid uptake of Cd(II) and Pb(II) by activated carbon prepared from peanut husk (Ricordel et al. 2001) and Hg(II) by furfural (Ekinci et al. 2002; Yardim et al. 2003). Therefore several researchers have modified activated carbon by treating with chemicals to accomplish chemical adsorption and increase the reaction kinetics and removal capacity of metal ions adsorption. Chemically treated activated carbon derived from fertilizer waste with CS_2 was reported to achieved a maximum Hg(II) uptake of 798.00 mg/g in comparison to 357.05 mg/g by the untreated activated carbon (Mohan et al. 2001). Activated carbon treated with H_2SO_4, H_3PO_4 and $ZnCl_2$ achieved Hg(II) adsorption capacities of 57.60, 95.80 and 128.00 mg/g as against 43.90 mg/g by untreated activated carbon derived from organic sewage sludge (Zhang et al. 2005). $ZnCl_2$ and H_3PO_4 were used to chemically activate granular activated carbon prepared from different raw materials like leather, almond shell, olive stone, peat etc. for removal of Cr(VI) (Manuel et al. 1995). Zinc chloride activated carbons prepared from *Terminalia arjuna* nuts showed 99.5% removal of Cr(VI) with an initial Cr(VI) concentration of 10 mg/L at adsorbent dose of 2g/L (Mohanty et al. 2005).

Activated carbon was enriched with sulphur by impregnating with Na_2S and reported a lead uptake of 29.4 mg/g against 21.9 mg/g by the untreated one (Goel et al. 2005). From the industrial point of view, for significant quantity of industrial wastewater flow, activated carbon adsorption is a proven reliable technology to remove dissolved organics and metals. Due to less space requirements, activated adsorption can be easily incorporated into an existing wastewater treatment facility. However, even after chemically modified, equilibrium time for activated carbon is very long due to presence of micro pores where slow diffusion controls the reaction. Equilibrium time for Cr(VI) uptake by granular activated carbon prepared from different raw materials (leather, almond shell, olive stone, and peat) was reported as 300 hours (Manuel et al. 1995). Lorenzen et al. (1995) found the equilibrium time for adsorption of arsenic species on activated carbon prepared from coconut shell as 24 hours. Such high equilibrium time suggests requirement of large reactor volume. Generation of spent carbon which leads to problem of solid waste disposal also remained one of the major drawbacks of activated carbon which limits its application. These reported literatures also reflect the importance of chemicals or functional group that can bind the metal ions much more effectively than simple activated carbon.

Table 2.4: Performance of activated carbon prepared from different materials in removing of heavy metal ions

Activated Carbon	Heavy metal	pH	Equilibrium time	Adsorption capacity (mg/g)	Reference
Comingled waste Commercial Norit	Cr(III)	-	500 mins (8 hour) for initial Cr(III) of 200 mg/L	1.09 1.02	Lyubchik et al. 2004
Coconut Commercial FS-100	Cr(VI)	3	5 days	73.90 50.30	Hu et al. 2003
Waste tyre Sawdust	Cr(VI)	2	120 mins for initial Cr(VI) of 40-100 mg/L	58.47 24.65	Hamadi et al. 2001
Hevea Brasilinesis	Cr(VI)	2	300 mins for initial Cr(VI) of 50-200 mg/L	44.05	Karthikeyan et al. 2005
Tree fern	Cu(II)		120 mins	11.7	Ho 2003

Activated Carbon	Heavy metal	pH	Equilibrium time	Adsorption capacity (mg/g)	Reference
Herbaceous peat	Cu(II)	5.5	150 min for initial concentration of Cu(II) 6×10^{-4} M	4.8	Gündogan et al. 2004
Bagasse fly ash	Cd(II)	6	60 mins for initial Cd(II) of 14 mg/L	1.18	Gupta et al. 2003
Peanut husk	Cd(II) Pb(II)		2 hour for initial Cd(II) and Pb(II) of 0.15 mmol	50.58 113.96	Ricordel et al. 2001
Coconut shell	Pb(II)	4.5	2 hour for initial Pb(II) of 10- 50 mg/L	26.51	Sekar et al. 2004
Coal (Mengen) Coal (Seyitomer) Coal (Some) Coal (Bolluca) Apricot stones Furfural	Hg(II)	5.5	60 mins for initial Hg(II) of 10–40 mg/L	92.00 56.00 105.00 37.00 153.00 174.00	Ekinci et al. 2002
Furfural	Hg(II)	5.5	60 mins	174.00	Yardim et al. 2003
Sago waste	Hg(II)	5	120 mins for initial Hg(II) of 50 mg/L	55.60	Kadirvelu et al. 2004
Fruit shell of *terminalia catappa*	Hg(II)	5–6	720 mins	94.43	Inbaraj and Sulochana 2006
Grafted silica	Pb(II) Cu(II)	5.5-6	90 mins	38 16.40	Chiron et al. 2003
Cellulose grafted copolymers	Cu(II) Cd(II)	-	2 hours	12.96 13.26	Okieimen et al. 2005
Wheat bran	Cr(III) Hg(II) Pb(II) Cd(II) Cu(II)	6	10 mins	93 70 62 21 15	Farajzadeh et al. 2004

(b) Micro and plant biomass adsorbents

Adsorption process by various naturally available biomaterials, dead and living cells of microorganisms, plants etc is generally termed as biosorption. Biosorption of heavy metals occurred through metabolically mediated or physico-chemical pathways of uptake (Fourest et al. 1992). Algae, bacteria, fungi and yeasts have proved to be potential metal biosorbents (Volesky 2001). Generally non-toxic and highly efficient microbial biomass functions as an ion exchanger by virtue of various reactive groups available on the cell surface such as carboxyl, amine, phosphate, sulfate and hydroxyl (Vasudevan et al. 2001). Biosorption by living organisms mainly comprises of two steps. Firstly, the metals are bound to the cell walls (metabolism independent binding) and secondly, metal ions are transported across the cell membrane (metabolism dependent intracellular uptake) (Huang and Huang 1996). During non-metabolism dependent biosorption, metal uptake is governed by physico-chemical interaction between the metal and the functional groups present on the microbial cell surface. Such type of biosorption is relatively rapid and reversible (Kuyucak and Volesky 1988).

Recent biosorption experiments have focused attention on waste materials with functional groups, which are by-products or the waste materials. Some of the reported successful investigations are on removals of Pb(II) and Cd(II) from aqueous solutions using grape stalk waste (a by product of wine production) (Martinez et al. 2006), adsorption of arsenate and arsenite by orange waste (Kedar et al. 2003), cadmium and zinc adsorption by cassava waste biomass (Horsfall and Abia 2003), biosorption of copper, lead and cadmium by apple residues (Lee et al. 1998), lead removal by coffee grounds (Tokimoto et al. 2005) etc. During the last decade, many researchers have reported the use of fungal and bacterium biomass for uptaking heavy metals. These include fungi (Fourest et al. 1994) and marine algae (Matheickal et al. 1999) etc. Table 2.5 presents a summary of the biosorbents with responsible functional group for binding metal ions. Presence of chitin and chitosan which are rich in amines in biomass of *Rhizopus arrhizus* (Prakasham et al. 1999) and amines, hydroxyl, carboxylate anions, carbonyl groups and phosphate group in fungal biomass *Neurospora crassa* (Tunali et al. 2005) are observed responsible for binding Cr(VI). During binding of Cd(II), carboxyl group was found as the responsible functional group in both marine algae (Matheickal et al. 1999) and dead sargassum (Cruz et al. 2004). It can be seen in Table 2.5 also that, for removal of Cu(II), Cd(II) and Zn(II) by papaya wood (Saeed et al. 2005), Cu(II) by sugar beet pulp (Aksu and Isoglu 2005), peat (Ho and McKay 2003) and grape stalks (Villaescusa et al. 2004), protein, lignin,cellulose, carboxylate and some weaker acidic groups and pentose were observed as responsible functional group. Presence of various functional

group in cell wall of algae were also reported responsible for high uptake of Hg(II) with 149.25 mg/g by *Ulva lactuva* (Zeroual et al. 2003) and 178 mg/g by Macroalga *Cystoseira baccata* (Herrero et al. 2005).

Survey of biosorption studies reveals certain advantages of biosorption over conventional treatment methods including low cost, high efficiency, minimization of chemical and biological sludge, no additional nutrient requirement, regeneration of biosorbent and possibility of recovery of metal ions (Kratochvil and Volesky 1998). Generally, biosorptive processes can reduce capital costs by 20%, operational costs by 36% and total treatment costs by 28%, when compared with conventional treatment systems (Volesky 2001). Managing the solid waste by utilizing as adsorbent adds another advantages on it. However, metal biosorption from wastewater has several major limitations. Biosorption is found to be strongly influenced by physico-chemical parameters such as ionic strength and the concentration of competing organic and inorganic compounds. Also biosorption is highly influenced by solution pH as can be seen in Table 2.5. Biosorption of copper(II) from aqueous solutions by pre-treated biomass of marine algae *Padina sp.* was reported inhibited by 10% due to presence of Ca^{2+}, K^{+} and Mg^{+2} (Kaewsarn 2002). Besides, presence of metal ions inhibits the other metal removal activity of some microorganisms. Veenstra et al. (1999) observed that a 3 mg/L copper dose had no effect on microorganism behavior, but doses of 47 and 56 mg/L significantly reduced performance of biological systems. Biosorption of lead, cadmium and mercury by immobilized *Microcystis aeruginosa* was reported as highly effective but it was unable to achieve the effluent below permissible limit even in column mode (Chen et al. 2005). Some biosorbents also exhibit long adsorption equilibrium. A complete removal of Cr(VI) was observed by dead fungal biomass of *Aspergillus niger* within contact time of 30 h and 400 h for initial Cr(VI) 25 and 200 mg/L (Park et al. 2005a). Such high adsorption kinetics are not favorable for practical application in industries. Presence of high COD in wastewater is another major drawback for employing biosorbents. As such 2 g/L biosorbent, *Platanus orientalis* leaves and its ash caused 110 mg/L and 76 mg/L COD increase in deionizd water after 120 min. Thus further chemical treatment is necessary for industrial wastewater treatment. A further disadvantage of the known generic biosorbents is their low mechanical stability. At high flow rates there may be compaction of the adsorbent packing, which may lead to complete blockage of the exchange or purification process.

Table 2.5: Biosorbents used for removal of heavy metals

Biosorbent	Heavy metals	pH	Adsorption capacity (mg/g)	Functional group	Reference
Biomass of *Rhizopus arrhizus* (Immobilized)	Cr(VI)	2	23.88	Chitin and chitosan takes more than 8 h to achived equlibrium	Prakasham et al. 1999
Fungal biomass *Neurospora crassa*	Cr(VI)	1	15.85	–NH, hydroxyl, carboxylate anions, carbonyl groups and phosphate group	Tunali et al. 2005
Marine algae	Cd(II)	5	112.4	Carboxylic	Matheickal et al. 1999
Dead Sargassum	Cd(II)	3- 6	120	Carboxyl and guluronic acids	Cruz et al. 2004
Papaya wood	Cd(II) Cu(II) Zn(II)	5	17.35 19.99 14.44	Protein, lignin and cellulose	Saeed et al. 2005
Sugar beet pulp	Cu(II)	4	28.5	Carboxylate and some weaker acidic groups	Aksu and Isoglu 2005
Peat	Cu(II)	2	14.3	Cellulose, pentose and lignin	Ho and McKay 2003
Grape stalks	Cu(II)	5- 6	10	Lignin and C–O bond	Villaescusa et al. 2004
Maize bran	Pb(II)	6.5	98.4	Metal oxides	Singh et al. 2006
Ulva lactuca	Hg(II)	7	149.25	Algal cell sites	Zeroual et al. 2003
Macroalga *Cystoseira baccata*	Hg(II)	7	178	Acid algal sites	Herrero et al. 2005

During heavy metal removal by various biosorbents, many researchers have observed that the functional group on the surface of adsorbents was responsible for uptake of heavy metal ions by chemical adsorption. Bai and Abraham (2002) also reported that the carboxyl and amino groups on the surface of fungal biomass *Rhizopus nigricans* was responsible for effective adsorption of chromium ions. Dakiky et al. (2002) concluded that presence of higher amount of amine groups in wool was responsible for large uptake of chromium as compared to other adsorbents like sawdust, olive cake, pine needle, coal, cactus leaves and almond shell etc. Polysaccharides bound to mucilaginous seeds of *Ocimum basilicum* was observed responsible for binding chromium (Melo and D'Souza 2004). Understanding the importance of functional group for binding metal ions, researchers further impregnated or chemically modified the biosorbents to improve the metal removal efficiency. In order to increase the removal of lead, marine brown algae *Laminaria japonica* was chemically-modified by crosslinking with epichlorohydrin (Luo et al. 2006). Maximum lead removal of 348.09 mg/g was obtained as against 250.71 mg/g by biomass simply washed with distilled water. Jeon and Holl (2003) also modified chitosan with ethylenediamine and observed higher adsorption capacities of 453.33 mg Hg(II)/g as compared to chemically modified xanthated chitosan, phosphorylated chitosan, carboxylated chitosan and cross-linked chitosan with 369.09, 310.19, 302.89 and 294.87 mg/g respectively. Amine group was found responsible for highest mercury ion uptake capacity for aminated chitosan beads in comparison with other functional group. Microbial biomass functions as an ion exchanger by virtue of various reactive groups available on the cell surface such as carboxyl, amine, phosphate, sulfate and hydroxyl (Vasudevan et al. 2001). Presence of carboxyl and phenolic groups in apple was detected responsible for binding of copper, lead and cadmium (Lee et al. 1999). All these findings detect the importance of functional groups on binding metal ions and evoke the synthesis of adsorbent based purely on these functional groups.

(c) Functionalized polymer

It is well known that metal ions form chemical bonds with several ligands and yield complexes. Some of the responsible functional groups that bind metal ions include amines, carboxylate, ether, hydroxyl, sulphate, phenolic, cyanide, chloride, acetate etc. Considerable studies were performed in the recent years for the preparation of novel polymeric adsorbents with high adsorption capacity with these functional groups to remove heavy metal ions from aqueous medium. High surface area, excellent ion-exchange properties, easy synthesis and flexibility for use in batch and continuous systems allow them to find a great application in wastewater treatment. Prado and Airoldi (2001) studied the adsorption of Ni(II), Zn(II) and

Cd(II) from aqueous solutions by herbicide 2,4-dichlorophenoxyacetic acid (2,4-D), chemically anchored on a silica gel surface. However, adsorption capacity were less with 27.06, 18.78, 17.65 and 15.73 mg/g for Cu(II), Ni(II), Zn(II) and Cd(II) respectively. Removal of Cu(II) and Pb(II) ions using commercial silica grafted with an ethylediamine derivative, N-[3-(trimethoxysilyl) propyl-ethylenediamine], was studied and observed with maximum Cu(II) and Pb(II) removal of 16.57 mg/g and 38.07 mg/g respectively (Chiron et al. 2003). Despite the presence of functional group ethylediamine, such less removal may be probably due to location site of functional group in the polymer matrix where metal ions were not able to penetrate. Similar process of polyethyleneimine coated on silica gel was also reported for removal of uranium compounds with 75% efficiency from initial uranium of 0.1-0.4 mmol (Chanda and Rempel 1995). Silica was replaced with porous cellulose as base material for coating polyethyleneimine (PEI) and observed mercury uptake of 288 mg/g along with Hg-ligand stability constant of approximately 12.9 mg/g (Navarro et al. 1996). Lighter cellulose enabled more uptake value than corresponding silica based functionalized adsorbents. However porous cellulose size polymer will be difficult for employing in column bed mode operation for industrial practice.

A thiol-compound cysteine which is rich in sulphur and hydrogen was grafted onto the chitosan beads whose main functional group are amines to improve the adsorption affinity of Hg(II) (Merrifield et al. 2004). The synthesis procedure however was complex consuming long time with one week shaking of highly viscous mixture of chitosan, acetic acid and deionized water to ensure dissolution of the chitosan and to reduce the viscosity. On addition to it, the beads were rinsed to a neutral pH with deionized water for a minimum of 16 h in the 0.5 M NaOH solution. Viel et al. (2003) synthesized films of poly-4-vinylpyridine having high chelating properties due to presence of pyridine functional group and employed for removal of copper. Copper contaminated wastewater of 20 liters at 20 mg/L was treated on a pilot plant scale and final effluent of less than 0.3 mg/L (equal or lower than drinking water) was achieved with flow rates of 60–80 L/h retaining more than 98% of the initial copper. But synthesis technique was complex requiring grafting of the polymer under stringent experimental conditions (no oxygen, aprotic and anhydrous medium) working under glove boxes kept in an argon atmosphere. Besides, expulsion of copper ions was done with electrical control increasing the overall cost of the system. A polymer poly(glycidylmethacrylate-co-methylmethacrylate) with Cr(VI) removal capacity of only 2.28 mg/g was increased to 22.93 mg/g by incorporating ethylenediamine on polymer (Bayramoglu and Arica 2008). Even though introduction of amine groups increased the removal capacity of the polymer, over all effectivity of ethylenediamine incorporated polymer

was very less compared to other functionalized polymers. Mathew and Pillai (1993) also highlighted the metal binding capability of amino functions by complexation it with polyacrylamides and divinylbenzene and found the uptakes of Co(II), Ni(II), Cu(II), Zn(II) and Hg(II) as 47, 38, 173, 130 and 797 mg/g respectively. Using amine based polymer aminated polyacrylonitrile fibers, Deng and Bai (2004) reported achievement of 20.7 mg/g uptake of Cr(VI) within one hour and two hours for Cr(VI) and Cr(III) respectively. However, lower removal capacity of aminated polyacrylonitrile fibers was the major limitation.

2.6 Scope and objective of the present study

Literature review highlighted succesful employment of various functionalized polymer with their inherent advantages of high metal removal capacities, rapid kinetics, reusability etc. over activated carbons and biosorbents. Functional groups responsible for binding metal ions include phenolic, sulpahtes, carboxylate, ethers, amines etc and amongst the functional groups, amine was observed responsible for highest mercury ion uptake. Such moderate to high metal removal by amine is due to presence of unpaired electron in *sp3* orbital of nitrogen of amine that makes bond with positive charge of metal ions. Many researchers synthesized amine base polymer such as polyacrylonitrile fibers, polyacrylamides, polyethyleneimine, polyvinylpyridine etc. and successfully employed for removal of heavy metal ions with rapid adsorption from aqueous solution. However, the synthesis procedures of many of these functionalized polymers are complex and involved high cost. Thus there exists a need for synthesis of low cost functionalized polymer with easy synthesis technique and acquiring the properties of rapid metal removal kinetics, moderate to high metal removal efficiency and stability for long term use. Nowadays, emphasis has been given on metal recovery rather than disposals to avoid management of metal contaminated adsorbents. Therefore, though amine exhibited moderate to high metal removal with rapid kinetics, the possibility of recovery of metal by desorption and reuse of polymer made amine group an attractive alternative for effective removal of metal ions.

Very recently, an amine based resinous functionalized polymer, aniline formaldehyde condensate (AFC) coated on silica gel was successfully used for removal of copper from aqueous solution (Kumar et al. 2007). Amine group present in the AFC replaced one or more of water molecules from Cu(II) molecules and formed coordination bonds with metal ions and again released back copper upon addition of acid. However, some of the heavy metal ion like chromium exists in aqueous solution in anionic forms like chromate (CrO_4^{2-} / $HCrO_4^-$) and

effectiveness of AFC for removal of these anionic metals is still unknown. Various cationic metal ions such as mercury, trivalent chromium, lead etc also possess different chemical binding properties towards amines. As such, trivalent chromium [Cr(III)] are hard acid and immobile whereas mercury and lead are categorized as soft acid and hence the affinity of these cationic metal ions towards hard base amine of AFC will be different. Besides, for effective treatment of metal contaminated wastewater in real applications, data base needs to be generated for each single metal ion to design the treatment plant and therefore studies on interaction of AFC with single metal ions are very vital. It was observed during removal of copper that the weight of silica gel throws hurdles to AFC on its effective removal. Therefore replacement of silica gel by low cost and easily available support materials also needs to be investigated.

Recently, another amine based functionalized polymer, polyaniline, was synthesized for the purpose of electrical conductivity (Yang et al. 2004). Unlike AFC with amines throughout the chain of polymer, amines are available only at terminal end of polyaniline. Very recently, Olad and Nabavi (2007) used polyaniline as reducing agent for Cr(VI) to Cr(III). However reported literatures on removal of metal ions by polyaniline are very scanty and hence effectivity of polyaniline on removal of metal ions still needs to be explored.

In practical situation such as industrial wastewater, several metal ions exist together and presence of one metal may hindered or enhanced the adsorption of another metal. Therefore, detail studies are necessary for both AFC and polyaniline polymers to explore the affinity of metal ions in mixed metal system towards the polymers. Further, batch mode operation is hardly practiced in real situation such as in industrial wastewater treatment and is replaced by column mode operation. As such in batch mode operation, adsorption characteristics were analyzed by isotherms after adsorption equilibrium is achieved. However, in fixed-bed column mode operation, the fluid and solid phase in the adsorption zone or mass transfer zone never achieved equilibrium and the zone keeps moving through the bed. Adsorption characteristics in column mode are generally characterized by the concept of breakthrough curve. Thus investigation on effectivity of AFC and polyaniline for removal of metal ions in column mode operations are very vital.

Thorough literature review and defining the scope of this present work led to development of several objectives. The main objective of this research work is to advance the state-of-the-art of synthesizing of amine based functionalized polymer and employed for

removal of heavy metal ions from aqueous solution. The lists of objectives are elaborately presented.

a) standardization of amine based polymer synthesis technique and optimization to achieved low cost polymer with maximum metal removal capacity with rapid kinetics.
b) conduct detailed laboratory scale studies by employing polymers for removal of metal ions in both batch and column mode operation as well as mono and mixed metal system
c) Identify optimum operating condition such as solution pH, initial concentration of metals ions, dose of adsorbents, desorption, recycle and reuse, identification of binding and unbinding mechanism etc.
d) develope base line design data and criteria to enable design for higher scale metal wastewater treatment plant with the polymers.

In order to execute the planned objectives sequentially, list of experimental methodologies were developed. The methodologies were approached and adopted for the complete research.

1. Optimization of synthesis procedure of polymer through source of amine, support materials, ratio of polymer ingredients.
2. Characterization of polymer to identify surface charge, chain length of polymer and surface morphology of the polymer before and after metal adsorption.
3. Employment of polymers for removal of heavy metal ions in batch mode operation considering various conditions such as solution pH, reaction time, initial concentrations of metal ions, dose of adsorbent, desorption, regeneration and reuse of polymer etc.
4. Generation of base line design data by validating experimental data with available mathematical models.
5. Adsorption of metal ions in mixed system to investigate competition of metal ions and evaluate the affinity of metal towards polymer.
6. Study on removal of metal ions in column mode operation considering various parameters which includes initial metal concentration, flow rate, depth of column bed and identify appropriate mathematical models.
7. Analyzing the loop holes of the polymer and synthesizing another new polymer overcoming the demerits and similar investigation on removal of heavy metal ions.

Chapter 3

Materials and methods

This study was conducted with synthetic wastewater prepared from distilled water containing the desired concentration of heavy metal ions. All chemicals used were of analytical grade and distilled water was used for preparation of solutions. This chapter is divided into four sections - materials, synthesis of polymer and adsorbent preparation, studies with metal ions and analytical techniques were explained in brief.

3.1 Materials

Commercial grade aniline ($C_6H_5NH_2$) was purified by distilling over KOH/NaOH pellets. Column chromatographic grade silica gel (60-120 mesh size), methanol (CH_3OH) and formaldehyde (37% HCHO) for synthesis of aniline formaldehyde condensate polymer were used as received. Ammonium peroxydisulfate [$(NH_4)_2S_2O_8$] and 1,4-phenylenediamine [$C_6H_8N_2$] required for synthesis of polyaniline were also used as received. Source of heavy

metal ions — mercury, lead, copper, cadmium and nickel were prepared from their respective salts of mercuric chloride [$HgCl_2$], lead nitrate [$Pb(NO_3)_2$], cupric chloride [$CuCl_2$], cadmium chloride [$CdCl_2$] and nickel chloride [$NiCl_2$] procured from Merck, India. Solution of potassium dichromate [$K_2Cr_2O_7$] salt purchased from Merck, India, was used as the source of hexavalent chromium and that of chromic chloride [$CrCl_3.6H_2O$] procured from Central drug house, India, as trivalent chromium. Standard metal solution for calibration of metal concentration was procured from Merck, Darmstadt, Germany. Initial concentration of all received metal standard solution were 1000 mg/L. Thus lower metal concentrations for calibration were obtained by series dilution of standard solution using dilution factor of 10. Mineral acids such as hydrochloric acid, sulphuric acid and nitric acid procured from Merck, India, were used as received. All chemicals and reagents used were of analytical grade purity and distilled water prepared in laboratory was used for all dilutions and reagents preparations. Used tea leaves and sugarcane baggase as support material for AFC and PANI were collected from canteen of Siang hostel, Indian Institute of Technology Guwahati, India. Sawdust and rice husk were collected from respective saw mills and rice mills. Waste jute bags were purchased from local market and washed with detergents to remove dirts. Then these were dried and chopped into fibers of 0.5-1.0 cm length and used in the present work. Fly ash was obtained from Farakka thermal power plant, West Bengal India. Fly ash was used as received.

Stock solutions for metal ions, acid/base of different strength and buffers were prepared at regular intervals. All experimental apparatus and analytical aids involving metals were soaked overnight in chromic acid followed by washing with tap water and several time rinsing with distilled water.

3.2 Polymer synthesis and adsorbent preparation

In this study, three polymers were employed for removal of heavy metal ions from aqueous solution. Aniline formaldehyde condensate (AFC) and polyaniline (PANI) were synthesized on solid support and finally, a support less AFC was synthesized.

3.2.1 Synthesis of aniline formaldehyde condensate (AFC) coated on silica gel

3.2.1.1 Synthesis of aniline formaldehyde condensate (AFC) polymer

Aniline formaldehyde condensate (AFC) was synthesized by reacting formaldehyde (HCHO) with aniline ($C_6H_5NH_2$) as per Liu and Freund (1997) and the reaction scheme is shown in Figure 3.1. In a 100 mL beaker, 10 mL of 37% formaldehyde (123 mmoles) was added slowly to a mixture of 18.6 g of aniline (200 mmoles) and 6 mL of concentrated HCl and kept in the water bath at 80^{o}C for 2 h with intermittent stirring. Then it was neutralized with 8 mL of 30% NaOH and kept in the water bath for another one h at 60 ^{o}C temperature. Thereafter it was removed from the water bath and kept at room temperature for 12 hour, then washed for three to four times with warm water to remove unreacted aniline and formaldehyde and dried by applying vacuum in a vacuum desiccator. AFC synthesized was of yellow color resinous material and its photograph is shown in Figure 3.2(a)

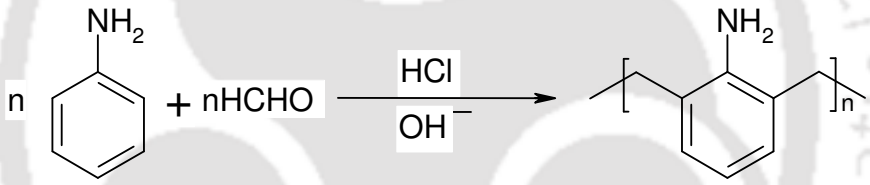

Figure 3.1: Synthesis scheme of Aniline formaldehyde condensate (AFC)

3.2.1.2 Coating of AFC on silica gel

In 25 mL methanol (CH_3OH) solution, 25- 30 g resinous AFC polymer was dissolved at 40- 45 ^{o}C with stirring. Experimentally it was observed that maximum 25 g of silica could be added in methanol-AFC solution to completely soak the silica gel and permit mixing. After addition of 25 g silica gel in methanol-AFC mixture, manual stirring was applied for five minutes. Then excess liquid was removed by filtering and AFC coated on silica gel was air dried for 6 hour. This AFC coated silica gel was used as the adsorbent in the present work. The photograph of silica gel and AFC coated silica gel are shown in Figures 3.2(b & c).

3.2.1.3 Regeneration and reuse of AFC polymer

During desorption experiment it was observed that in mineral acid along with metal ion, significant amount of polymer also released from surface of silica gel (solution became yellow). This polymer from mineral acid solution was extracted out and silica gel was recoated using this polymer. Initially 25 g of the adsorbent was employed for adsorption experiment with metal ions followed by desorption in 250 mL HCl solution. Then HCl-AFC-metal containing supernatant and settled silica gel were separated. HCl-AFC-metal containing supernatant solution was neutralized to pH to 7- 8 by adding 1 M NaOH solution. Then 10 mL chloroform (as extracting agent) was added to this neutralized solution forming two distinct layers of one with chloroform and resin and another of aqueous layer (Figure 3.3). Using separation funnel, chloroform-resin mixture was separated from the aqueous solution and 1.0 g of anhydrous sodium sulfite was then added and mixed thoroughly to remove moisture. Sodium sulfite settled at the bottom and moisture free chloroform-resin solution was separated and mixed with the silica gel (collected after desorption experiment) and thereafter dried as usual to obtain a new set of polymer.

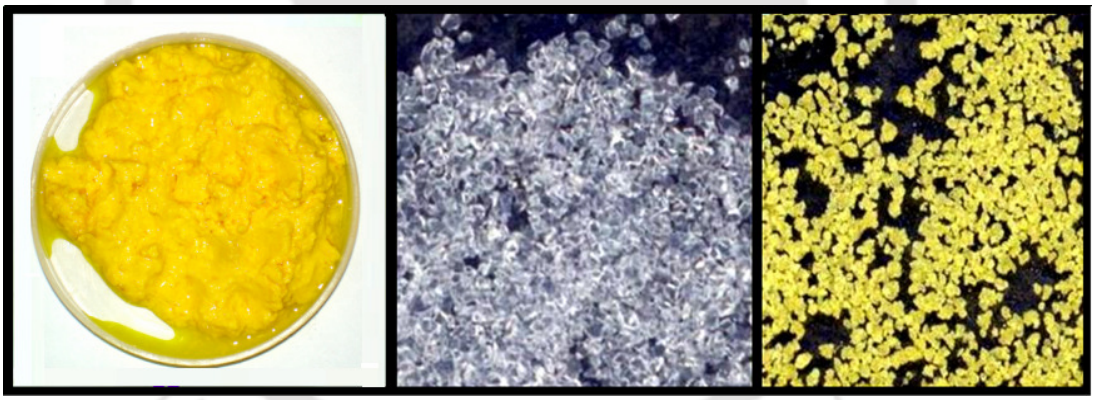

Figure 3.2(a): AFC polymer resin; Figure 3.2(b): Silica gel and
Figure 3.2(c):AFC coated silica gel

3.2.2 Synthesis of short chain polyaniline polymer on surface of jute fibers

Polyaniline was synthesized by oxidation of aniline ($C_6H_5NH_2$) in presence of 1,4-phenylenediamine, a chain terminator in acidic aqueous medium in presence of an oxidant, ammonium peroxydisulfate [$(NH_4)_2S_2O_8$]. The synthesis scheme of PANI is shown in Figure 3.4 (Yang et al., 2004). Aniline (2.00 g, 21.5 mmol) and 1,4-phenylenediamine (0.330 g, 3.05 mmol) were dissolved in 66 mL of 1 M HCl (aq.). The mixture was cooled in iced bath to 0- 5 °C followed by addition of 5 g jute fibers and stirred for 5 min. The polymerization reaction

started after introduction of pre-cooled (5 °C) solution containing ammonium peroxydisulfate (1.62 g, 7.10 mmol) and 16 mL of 1 M HCl (aq.). The reaction mixture was maintained at 5 °C for 65 min and then kept for overnight at room temperature (25°C). Then the liquid was decanted from PANI-jute fiber. To ensure complete deprotonation of PANI-jute, alkali treatment was given by soaking PANI-jute in 1 M NH_4OH for 5 min. The products were then washed with distilled water to adjust the solution to neutral pH. Finally, the blue black colored PANI-jute fiber was dried at 40 °C in the oven. The photographs of raw jute fibers and PANI-jute are shown in Figures 3.5 (a and b).

Figure 3.3: Separation of chloroform-AFC resin mixture from aqueous solution

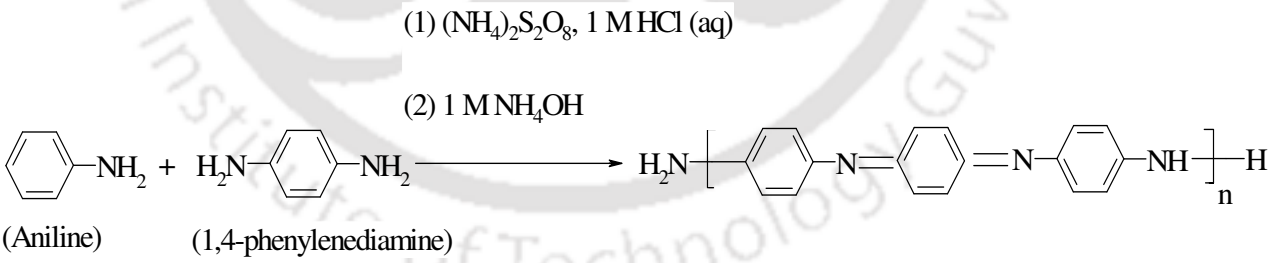

Figure 3.4: Synthesis scheme of short chain polyaniline

3.2.3 Synthesis of support less AFC modified with alcohols

In a typical synthesis, alcoholic solution of aniline and conc. HCl was precooled to 0–5 ^oC before mixing. Upon addition of a cold mixture solution of alcohol and formaldehyde to the unstirred aniline solution, the solution turned turbid and slowly thickened over few minutes, changing from white to pale yellow color [Figure 3.6 (a)]. Over time the polymer

solidified and turned light yellow. When this reaction was performed at room temperature, the exothermic reaction resulted in a fragile, dark red polymer and not uniform in texture [Figure 3.6 (b)]. The solid polymers formed in shape of the reaction vessel were washed sequentially with 1M HCl, 1 M NaOH, and distilled water to remove unreacted reagents and to form the polymers in the amine form. The light yellow polymers were dried in vacuum desiccator for 1– 3 days (depending on alcohol used) over anhydrous calcium chloride to remove water and any traces of alcohols remain trapped in the polymer. A quantitative detail of one synthesis (t-butanol) is described here. Aniline (9 g, 0.096 mol) and t-butanol (3.5 mL) were dissolved in 2.25 mL of conc. HCl (0.025 mol). The solution was cooled to below 5 ^{o}C with an ice bath arrangement. A solution of 37% (w/v) formaldehyde (7.5 mL, 0.094 mol) in 3.5 mL of precooled t-butanol was added drop wise into the aniline-acid solution with vigorous stirring to obtain a uniform homogeneous solution. The temperature was maintained at 0–5 ^{o}C for 25 min and then allowed to warm up to the room temperature. The solid polymer was cut into pieces by sharp clean blade and washed with 1 M HCl solution followed by 1 M NaOH solution and finally with distilled water and dried under vacuum desiccator. The dried polymer is shown in Figure 3.6 (c).

Figures 3.5(a): Photographs of jute fiber

Figures 3.5(b): polyaniline synthesized on jute fiber

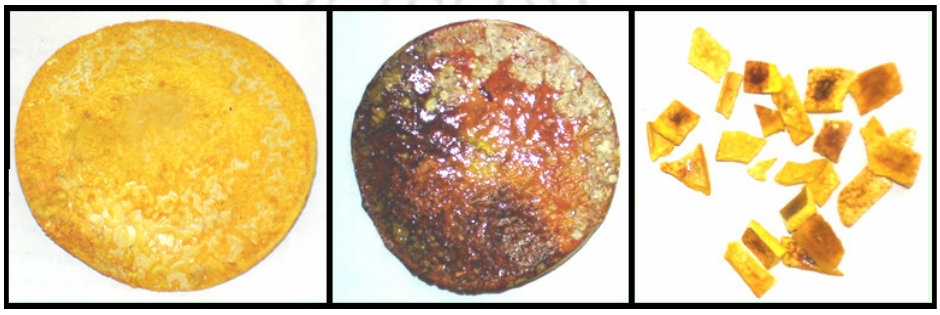

Figures 3.6(a): Support less AFC polymer synthesized at low temperature (5 ^{0}C);

Figures 3.6(b): Support less AFC polymer synthesized at room temperature (20 ^{0}C)

Figure 3.6(c): Support less AFC polymer synthesized dried cube polymer.

3.3 Studies with metal ions

Adsorption studies with heavy metals by polymers have been conducted in two manners- batch mode and continuous column mode adsorption. This study was carried out using synthetic wastewater containing heavy metal ions.

3.3.1 Batch mode experiments

3.3.1.1 Adsorption experiments

Batch mode adsorption experiments were conducted at room temperature (23- 25 ^{o}C) except where mentioned. All batch studies were carried out with 1000 mL of metal solution in 2 L (two-liter) beaker to prevent the spill off of the solution during experiment. Predetermined quantities of adsorbent were added in the beaker and to achieve the degree of mixing and adsorption equilibrium, a magnetic stirrer was employed with speed adjusted at 100 rpm. A paddle stirrer was also employed with speed adjusted at 1000 rpm to check the difference in metal removal due to different mode of physical mixing. Cr(VI) solution ranging from pH 3-7 were well adjusted by using 0.1 N of H_2SO_4 and NaOH whereas extreme pH were adjusted using 1 N acid/base solution. Other metal solution of Cr(III), Cu(II), Cd(II), Pb(II) and Hg(II) were adjusted with HCl and NaOH. Acid/base were preferred than buffer as it was observed more economical when adsorption experiments were conducted in large scale. However for experiment with higher dose of adsorbent exhibiting high fluctuation in pHs, buffer prepared from potassium hydrogen orthophosphate was used to minimize the fluctuation. Addition of acid/base solution to adjust the pH never exceeded 1% of the total volume of the reactor.

Aliquots were drawn at predetermined time intervals and were filtered through Whatman filter paper No. 42 and filtrate was used for estimation of metal ion concentrations. Another alternative for filtering sample was made by sample centrifuged for 10 minutes at 10000 rpm and concentration of metal ion was analyzed. The total drawn aliquot volumes were less than 2.5% of total sample volume. All experiments were carried out in two sets and average values were considered for data analysis. A blank solution experiment was run in each set to confirm the inability of plastic reactor vessel to adsorb metal ions and to check the precipitation of metal ions. The amount of metal ion adsorbed by adsorbent was calculated based on the difference of metal ion concentration in aqueous solution before and after adsorption according to the following equation:

$$q_t = \frac{(C_0 - C_t)V}{m} \quad (3.1)$$

where, q_t is the amount of metal ions adsorbed per unit weight of adsorbent (mg/g) at time t, C_0 and C_t are the concentrations of metal ions (mg/L) at initial time and at time t respectively, V is the initial volume of metal ions sample (L) and m is mass of adsorbent (g). When t is equal to the equilibrium contact time, $C_t = C_e$, $q_t = q_e$, then the amount of metal ions adsorbed at equilibrium, q_e was calculated using equation (3.1).

3.3.1.2 Desorption experiments

For desorption experiment, 50 mL desorbent was added in a specimen tube along with metal ion containing adsorbent. This was subjected to end over rotatory shaker (20-30 rpm) for 3 hours. Then it was again centrifuged and desorbed concentrations of metal ions were determined in the filtrate. Amount of desorption (%) was calculated using Equation 3.2.

$$Desorption\,(\%) = \frac{C_{des}V_{des}}{(C_o - C_e)V_{ads}} X100 \quad (3.2)$$

where C_o is the initial concentration of metal ions for adsorption, C_e the final metal ions concentration after adsorption, V_{ads} the volume of sample for adsorption experiment, C_{des} the final concentration after desorption and V_{des} the volume of desorbent employed.

3.3.2 Continuous column mode operation

3.3.2.1 Experimental set up

The fixed bed column studies with PANI-jute were conducted using a laboratory-scale glass column of 1- 3 cm ID and 70 cm length. Column was packed with known quantity of adsorbents to obtain a particular bed depth. A cotton plug was provided at the bottom to support the adsorbent bed as well as to prevent wash out of adsorbent. Another cotton plug was also provided on top of the bed to prevent floating up of adsorbents. The schematic arrangement of the column set up is shown in Figure. 3.7. The presence of air pockets within the packed adsorbent caused channeling of influent chromium contaminated solution and lowered the adsorption efficiency of the bed (Ko et al. 2000). To ensure expulsions of the trapped air, adsorbent packed columns were fully wetted by filling with deionised water for 5

hour prior to starting of the experiments. In a typical experiment metal ion containing influent was pumped in the column at a constant flow rate using a peristaltic pump. Flow rate was cross checked at the exit of the column at regular intervals of 2 hour to prevent and minimize the flow rate fluctuations if occurred inside the column bed.

3.3.2.2 Column experiment

In order to study the behavior of metal ion removal in fixed bed column mode, column experiments were conducted with varying pH, influent concentration, flow rate and bed depth. Treated solution samples were collected from the exit of column at predetermined time intervals. These samples were then centrifuged at 10,000 rpm for 10 min and analyzed for metal ions concentration. pH values of the effluent samples were also monitored and recorded along. In order to prevent any leakage of toxic metal ions into the sewer line, a polishing column of ID 3 cm by 5 cm length packed with adsorbent was introduced after exit point of column as further polishing unit (Figure 3.7).

Generally the performance of the column bed is described through the concept of breakthrough curve, which is obtained by plotting throughput volume (V_t) at any time (t) versus effluent chromium concentration (C). Throughput volume was calculated using equation (3.3).

$$V_t = Q.t \tag{3.3}$$

where Q is the volumetric flow rate (mL/min).

3.3.3 Experimental protocol

Studies on metal ion- adsorbent interaction were studied under various conditions by conducting several set of experiments. Metal stock solutions of 1000 mL volume with concentration of 1000 mg/L were prepared for all metal ions by dissolving their respective metal salts. Details of salts and amount used to prepare the metal stock solution are given in Table 3.1.

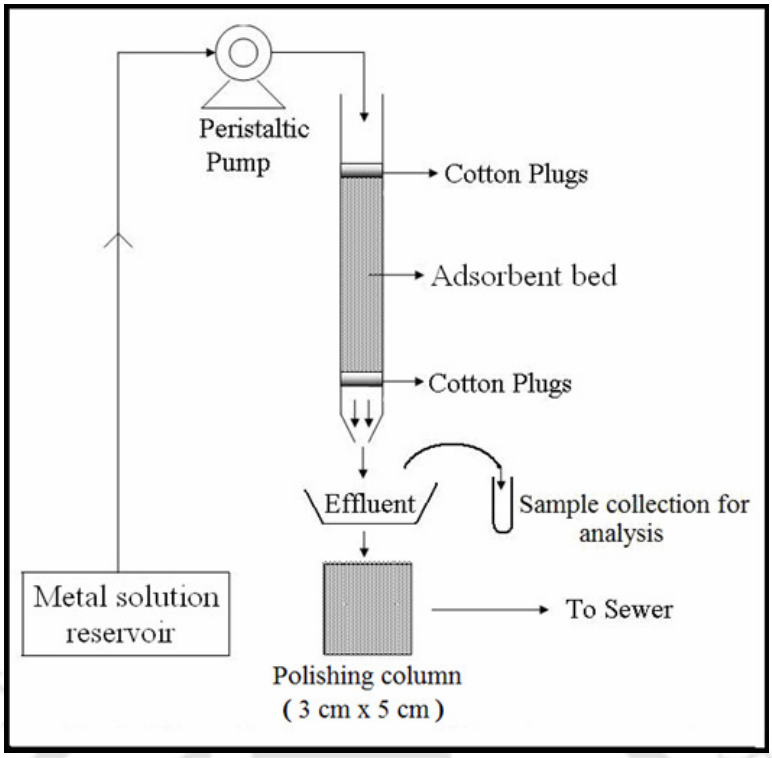

Figure 3.7: Schematic arrangement of experimental set up for column study

Table 3.1: Detail of metal salts and amount to prepared stock solution of 1000 mg/L

Metal ions	Amount (g)	Salt	Chemical formula
Cr(VI)	2.828	Potassium dichromate	$K_2Cr_2O_7$
Cr(III)	5.124	Chromic chloride	$CrCl_3.6H_2O$
Cd(II)	1.631	Cadmium chloride	$CdCl_2$
Cu(II)	2.682	Cupric chloride	$CuCl_2.2H_2O$
Pb(II)	1.598	Lead nitrate	$Pb(NO_3)_2$
Hg(II)	1.353	Mercuric chloride	$HgCl_2$
Ni(II)	4.049	Nickel chloride	$NiCl_2.6H_2O$

3.3.3.1 Experimental protocol with AFC coated silica gel

Metals considered for adsorption study with AFC coated silica gel in batch mode includes hexavalent chromium, trivalent chromium, mercury and cadmium and mixed metal system of trivalent chromium, copper, mercury, nickel, cadmium and lead. For continuous column mode study, mercury was considered as the model metal ion. Details of set of experiments for each metal ion- interaction with AFC coated silica gel in batch mode were described and presented sequentially in Table 3.2- 3.5.

Table 3.2: Experimental design for batch studies with hexavalent chromium and AFC coated silica gel

Experimental set	Variable parameter	Controlled parameter	Purpose
1	Uncontrolled pH: Initial pH 2.1	Initial Cr(VI): 100 mg/L; AFC dose: 8 g/L.	Effect of pH
2	Controlled pH: 2, 3, 4, 5, 6	Initial Cr(VI): 40 and 100 mg/L; AFC dose: 8 g/L; reaction time: 3 h.	
3	Strength of desorbent (N): 0.2, 0.5	Desorption time: 3 h, desorbents: NaOH, NH_4OH, EDTA, H_2SO_4, HNO_3, HCl	Desorption
4	Initial Cr(VI) (mg/L): 10, 40, 60, 100 and 200	Reaction pH controlled at 3; AFC dose: 8 g/L.	Effect of initial Cr(VI) concentration
5	AFC dose (g/L): 0.5, 1.0, 1.5, 2.0, 2.5, 3.0, 3.5, 4.0, 6.0, 8.0	Reaction pH controlled at 3; Initial Cr(VI): 50, 100, 150, 200 mg/L; reaction time: 3 h.	Effect of AFC dose and isotherm studies

Table 3.3: Experimental design for batch studies with trivalent chromium and AFC coated silica gel

Experimental set	Variable parameter	Controlled parameter	Purpose
1	Controlled pH: 1, 2, 3, 4, 5, 6, 7, 8, 9, 10, 11	Initial Cr(III): 0 (control) and 50 mg/L; AFC dose: 4 g/L.	Effect of pH
2	AFC dose (g/L): 1, 2, 4, 6, 8, 10	Initial Cr(III): 100 mg/L; reaction pH: 6; reaction time: 3 h.	Effect of AFC dose
3	Initial Cr(III) (mg/L): 15, 30 and 45	Reaction pH controlled at 5 and 6; AFC dose: 4 g/L; reaction time: 3 h.	Effect of initial Cr(III) concentration
4	Initial Cr(III) (mg/L): 15, 30 45, 100, 150, 200, 250 and 500	Reaction pH controlled at 6; AFC dose: 4 g/L; reaction time: 3 h.	Isotherm studies
5	Desorbents: HCl, HNO_3, H_2SO_4 and EDTA	Desorbent strength: 0.5 M (HCl, HNO_3, H_2SO_4) and 0.1 M (EDTA)	Desorption

Table 3.4: Experimental design for batch studies with cadmium and AFC coated silica gel

Experimental set	Variable parameter	Controlled parameter	Purpose
1	Controlled pH: 2, 3, 4, 5, 6, 6.5, 7, 8, 9, 10, 11	Initial Cd(II): 50 and 100 mg/L; Adsorbent dose: 5 g/L.	Effect of pH

Table 3.5: Experimental design for batch studies with mercury and AFC coated silica gel

Experimental set	Variable parameter	Controlled parameter	Purpose
1	Controlled pH: 2, 3, 4, 5, 6, 6.5, 7, 8, 9, 10, 11	Initial Hg(II): 50 and 80 mg/L; adsorbent dose: 2 g/L.	Effect of pH
2	Initial Hg(II) (mg/L): 5, 10, 20, 50, 100, 200, 380, 425 and 1000	Adsorbent dose: 2 g/L; reaction pH 9.5; agitation time: 3 h.	Effect of initial Hg(II) concentration
3	Initial Hg(II) concentration (mg/L): 4, 7, 14, 56, 90, 100, 182, 200, 300, 450, 750, 800 and 900	Reaction pH: 9.5; AFC dose 2 g/L	Isotherm studies
4	Desorbent strength (N): 0.005, 0.01, 0.05, 0.1, 0.5, 1 and 2	Desorbents: HCl, H_2SO_4, HNO_3; desorption time: 3 h	Desorption

Detail study of Hg(II) adsorption by AFC in column mode continuous study was carried out considering various parameters. For different bed depth study, three columns of bed depth 10, 20 and 30 cm filled with 50, 100 and 150 g of AFC coated silica gel were considered. Initial concentration effect of influent Hg(II) was studied with concentration of 25 mg/L and 50 mg/L Hg(II) ions. All column studies were carried out at optimum pH 6.5 which was obtained earlier from batch study. Constant flow rate for influent fed was maintained at 5 mL/min.

3.3.3.2 Experimental protocol with PANI-jute

Metals considered for adsorption study with PANI-jute in batch mode single metal system includes hexavalent chromium, trivalent chromium, mercury, copper, cadmium and lead and mixed metal system of trivalent chromium, copper, mercury, nickel, cadmium and lead. Continuous column mode study was carried out with hexavalent chromium and trivalent

chromium. Details of set of experiments for each metal ion- interaction with PANI-jute were described are presented sequentially in Table 3.6- 3.13.

Table 3.6: Experimental design for batch studies with Cr(VI) and PANI-jute

Experimental Set	Variable parameters	Control parameters	Purpose
1	Solution pH: 1, 2, 3, 4, 5, 6, 7, 8, 9, 10	Initial Cr(VI): 10 and 50 mg/L; PANI-jute: 2 g/L; agitation time: 24 h	Effect of pH on Cr(VI) removal
2	Initial Cr(VI) (mg/L): 5, 10, 20, 50, 100, 300, 500	PANI-jute: 2 g/L; agitation time: 4 h; Solution pH: 3, 4	Adsorption isotherm and effect of initial Cr(VI) concentration
3	PANI-jute (g/L): 0.2, 0.5, 0.8, 1, 1.5, 2, 3, 4, 5, 6, 8, 10, 12, 16, 18, 20, 25, 30	Initial Cr(VI): 20, 50, 100; pH: 3; agitation time: 3 h	Effect of PANI-jute dose
4	Desorbent strength (N): 0.5, 1.0, 2	Initial Cr(VI): 50 mg/L; PANI-jute dose: 2 g/L Desorbent: NaOH, NH_3OH	Desorption

Table 3.7: Experimental design for batch studies with Cr(III) and PANI-jute

Experimental Set	Variable parameters	Control parameters	Purpose
1	Solution pH: 1, 2, 3, 4, 5, 6, 7, 8, 9, 10, 11	Initial Cr(III): 50 mg/L; PANI-jute: 2 g/L; agitation time: 24 h	Effect of pH Cr(III) removal

Table 3.8: Experimental design for batch studies with Hg(II) and PANI-jute

Experimental Set	Variable parameters	Control parameters	Purpose
1	Solution pH: 1, 2, 3, 4, 5, 6, 7, 8, 9, 10, 11, 12	Initial Hg(II): 50 and 100 mg/L; PANI-jute: 2 g/L; agitation time: 24 h	Effect of pH
2	Initial Hg(II) (mg/L): 10, 25, 50, 75 and 100	PANI-jute dose: 2 g/L; reaction pH: 7	Effect of initial Hg(II) concentration
3	PANI-jute dose (g/L): 0.2, 0.4, 0.6, 0.8, 1.0, 1.2, 1.4, 1.6, 1.8, 2.0, 3, 4, 6, 8, 10, 12, 15, 20	Initial Hg(II): 100 mg/L; reaction pH: 7	Effect of PANI-jute dose and isotherm study
4	Desorbent strength (N): 0.005, 0.05, 0.5 and 1	Initial Hg(II): 70 mg/L; PANI-jute dose: 2 g/L; desorbent: HCl, H_2SO_4, HNO_3, KI	Desorption
5	-	Initial Hg(II): 80 mg/L; PANI-jute dose: 10 g/L; desorbent (H_2SO_4): 1 N	Reuse

Table 3.9: Experimental design for batch studies with Cu(II) and PANI-jute

Experimental Set	Variable parameters	Control parameters	Purpose
1	Solution pH: 1, 2, 3, 4, 5, 6	Initial Cu(II): 20 and 50 mg/L; PANI-jute: 10 g/L; agitation time: 3 h	Effect of pH
2	Initial Cu(II) (mg/L): 10, 20 and 50	PANI-jute dose: 5 g/L; reaction pH: 6	Effect of initial Cu(II) concentration
3	PANI-jute dose (g/L): 2, 5, 10, 15, 20, 50, 100	Initial Cu(II): 50 mg/L; reaction pH: 6	Effect of PANI-jute dose
4	PANI-jute dose (g/L): 0.2, 0.4, 0.6, 0.8, 1.0, 1.5, 2.0, 3, 4, 5, 10, 8, 15, 20, 30	Initial Cu(II): 20 and 50 mg/L; reaction pH: 6	Isotherms study
5	-	Initial Cu(II): 40 mg/L; PANI-jute dose: 10 g/L; desorbent (H_2SO_4): 1 N	Reuse

Table 3.10: Experimental design for batch studies with Cd(II) and PANI-jute

Experimental Set	Variable parameters	Control parameters	Purpose
1	Solution pH: 1, 2, 3, 4, 5, 6, 7, 8, 9	Initial Cd(II): 36 and 90 mg/L; PANI-jute: 10 g/L; agitation time: 3 h	Effect of pH
2	Initial Cd(II) (mg/L): 18, 36 and 90	PANI-jute dose: 5 g/L; reaction pH: 6	Effect of initial Cd(II) concentration
3	PANI-jute dose (g/L): 0.2, 0.4, 0.6, 0.8, 1.0, 1.5, 2.0, 3, 4, 5, 10, 8, 15, 20, 30	Initial Cd(II): 36 and 90 mg/L; reaction pH: 6	Isotherm study
4	-	Initial Cd(II): 90 mg/L; PANI-jute dose: 10 g/L; desorbent (H_2SO_4):1N	Reuse

Table 3.11: Experimental design for batch studies with Pb(II) and PANI-jute

Experimental Set	Variable parameters	Control parameters	Purpose
1	Solution pH: 1, 2, 3, 4, 5, 6, 7, 8, 9	Initial Pb(II): 64 and 166 mg/L; PANI-jute: 10 g/L; agitation time: 3 h	Effect of pH
2	Initial Pb(II) (mg/L): 32, 64 and 166	PANI-jute dose: 5 g/L; reaction pH: 6	Effect of initial Pb(II) concentration
3	PANI-jute dose (g/L): 0.2, 0.4, 0.6, 0.8, 1.0, 1.5, 2.0, 3, 4, 5, 10, 8, 15, 20, 30	Initial Pb(II): 64 and 166 mg/L	Isotherm study
4	-	Initial Cu(II): 187 mg/L; PANI-jute dose: 10 g/L; desorbent (H_2SO_4):1N	Reuse

Table 3.12: Experimental design for adsorption studies of mixed metals with PANI-jute

Experimental Set	Variable parameters	Control parameters	Purpose
1	Binary metal system [Metal 1 (mmol)+ Metal 2 (mmol)]: 0.15+ 0.15, 1.15+ 0.3, 0.15+ 0.8, 0.3+ 0.15, 0.8+ 0.3, 0.3+ 0.3	PANI-jute dose: 5 g/L; reaction pH: 6; agitation time: 3 h	Competition of metal ions towards adsorption on PANI-jute
2	Dose of PANI-jute (g/L): 0.2, 0.4, 0.6, 0.8, 1.0, 1.5, 2.0, 3, 4, 5, 10, 8, 15, 20, 30, 40	Ternary metal system (Cu+Cd+Pb): 0.3 mmol each; reaction pH: 6; agitation time: 3 h	Isotherm study

Table 3.13: Experimental design for continuous studies with Cr(VI) and PANI-jute

Experimental Set	Variable parameters	Control parameters	Purpose
1	Influent pH; 2, 3, 4, 5, 6	Column bed depth: 30 cm (7.05 g PANI-jute); flow rate: 2 mL/min	Effect of pH
2	Bed depth (cm): 40, 50 and 60 (9.4, 11.75 and 14.1 g of PANI-jute respectively)	Influent Cr(VI): 10 mg/L; pH: 3; flow rate: 2 mL/min	Effect of bed depth
3	Flow rate (mL/min): 1.5 and 2.5	Bed depth: 40 cm; influent Cr(VI): 10 mg/L; pH: 3	Effect of flow rate
4	Influent Cr(VI) concentration (mg/L): 5 and 15	Bed depth: 40 cm; flow rate: 2 mL/min; pH: 3	Effect of influent Cr(VI) concentration
5	Column bed depth (cm): 20, 30 and 40	Desorbent: 1 M NaOH; desorption flow rate: 1 mL/min.	Desorption

3.3.3.3 Experimental protocol with support less AFC

Preliminary adsorption experiment was conducted with support less AFC synthesized by introduction of alcohols. Introduced alcohols include methanol, isopropanol, t-butanol, n-octanol and glycerine. In order to investigate the degradation of polymer in acidic condition, metal ion whose optimum pH is at acidic pH needs to be considered. Maximum removal of anionic metal ion Cr(VI) was observed at acidic pH 3 by both polymer AFC coated on silica gel and PANI-jute. Thus Cr(VI) was considered as model metal ions for investigation on metal interaction with support less AFC.

Table 3.14: Experimental design for adsorption study of Cr(VI) with support less AFC in batch mode

Experimental Set	Variable parameters	Control parameters	Purpose
1	Initial Cr(VI) concentration (mg/L): 50, 100	Dose of support less AFC: 1 g/L; pH: 3, agitation time: 3 h	To evaluate binding capacity
2	Initial Cr(VI) concentration (mg/L): 9	Dose of support less AFC: 2 g/L; pH: 3, agitation time: 3 h	

Set 1. experiment was conducted twice (first set with grinded polymer and second set with large particles of polymers ~ 100 mm^3 cubic blocks)

3.4 Analytical techniques

All analyses were carried out according to APHA (1998). Drying and ignition of polymer was done using a drying oven and a muffle furnace respectively. During adsorption experiment, degree of mixing was provided by employing magnetic stirrer or end over rotatory shaker with 100- 1000 r.p.m. Solution pH was measured by a digital pH meter. All weighing of reagents and adsorbents was carried out in an analytical weighing balance. For conducting continuous column operation, influent metal ions feed at a particular flow rate was supplied and maintained throughout the experiments by use of peristaltic pump. Particle size of silica gel and AFC coated silica gel was estimated by using particle size analyzer.

Degradation of AFC polymer after subjected in acidic condition was studied using NMR spectra. UV Spectrophotometer was used for scanning PANI-jute dissolve in DMF solvent at dual beam mode for characterization of PANI-jute. Change in surface morphology of adsorbent after adsorption of metal ions was recorded by SEM photographs and confirmation of presence of metal ions on surface of adsorbent by analyzing electron diffraction X-ray (EDX) using a Leo-1430 VP Scanning electron microscope instrument with Energy Dispersive X-ray (EDAX) analysis attachment. The polymer samples were coated with gold vapor before measurements to reduce charging. Presence of adsorbed Cu(II) and Cr(II) on adsorbent were also examined by employing Electromagnetic Spin Resonance Spectrophotometer (ESR).

Concentration of Cr(III), Hg(II), Cu(II), Cd(II), Ni(II) and Pb(II) were estimated using atomic absorption spectrophotometer using air-acetylene flame at wavelength of 429, 253.7, 218.2, 326.1, 341.5 and 283.3 nm respectively at slit width of 0.2 nm for Cu(II) and Ni(II) and 0.5 nm for Cr(III), Hg(II), Cd(II) and Pb(II). Working condition of lamp current for estimating Cr(III) and Pb(II) are 7 mA and 5 mA whereas that of Hg(II), Cu(II), Cd(II) and Ni(II) are all same at 4 mA. Sensitivities of atomic absorption spectrophotometer varies with wavelength and slit width. At respective wavelength of metal ions, the detection limit of Cr(III), Cd(II), Cu(II), Pb(II), Hg(II) and Ni(II) are 1-100 mg/L, 20-1000 mg/L, 0.3- 80 mg/L, 0.5-50 mg/L, 2-400 mg/L and 1-100 mg/L respectively. Concentration of Cr(VI) was measured by diphenyl carbazide colorimetric method at 540 nm wavelength using U.V. Spectrophotometer according to APHA (1998). To further cross checked of concentration of Cr(VI), estimation was also done in visible spectrophotometer at 540 nm. Hg(II) concentration below 5 mg/L was estimated on Graphite tube atomizer (GTA). Standards for calibration on GTA were prepared with Hg(II) concentration of 50, 100 and 200 ppb. All calibration of metal concentration were carried out with 7 (seven) standards to achieved a better accuracy during estimation of unknown metal ion concentrations. Calibration were considered for estimating samples only when regression coefficient (R^2) > 0.99. The details of instrument(s) and equipment(s) used in this work are presented in Table 3.15.

Table 3.15: Details of analytical instruments used in the present work

Instrument /Equipment	Manufacturer
Analytical balance	Model: AB304S, M/S Mettler Instrument AG, Switzerland
Digital pH meter	Model: µpH System 361, M/S Systronics India Ltd., India
Water bath	International commercial traders, kolkata, India.
Mechanical Stirrer	Model: LS04B, Eltek motors, electrocarfts, Goregaon (east) Mumbai.
End over end rotary shaker	Model: Wagner's shaking machine, HS, M/S Reico Pvt. Ltd., Kolkata
Peristaltic Pump	Model: PA-SF Control , IKA-WERKE, Germany Model: PP-10 EX, Miclins India, Chennai
Centrifuge	Model: R24, M/S REMI Instruments Ltd., Mumbai, India
Digital spectrophotometer	Model: 166, M/S Systronics India Ltd., India
Drying oven	Model: PSI, M/S Mahindra Scientific Instrument Co., India
Muffle furnace	ICI, International Commercial Traders, Kolkata.
Scanning electron microscope with EDX	Model: LEO 1430 VP, M/S Carl Zeiss, Germany
Particle size analyzer (Hydro 2000 MU)	Model: AWM 2000, Malvern instruments, Worcestershire, UK.
Atomic Adsorption Spectrophotometer	Model: Spectra Duo, Varian BV, The Netherlands (Spectra AA Varian, model 55B)
Graphite Tube Atomizer	Graphite tube atomizer 120 (Spectra AA, Varian Model).
Fourier Trasnformation Infra Red (FTIR)	Perkin–Elmer Spectrum one spectrophotometer
Nuclear magnetic resonance (NMR)	400 MHz FT NMR spectrometer system (BG-M4, BNML-01, Varian, Switzerland).
Microwave Digestor	(Microwave digestion system, Model: 7295, OI Analytical, Texas).
Electron Spin Resonance	(Model: JES-FA 200 ESR System, JEOL, Ltd. Japan).
UV-Visible spectrophotometer	Varian, model Cary 50 (Netherland)

Chapter 4

Results and discussion

Present study on removal and recovery of heavy metal was conducted with two polymers namely aniline formaldehyde condensate coated on silica gel (AFC) and short chain polyaniline synthesized on jute fiber (PANI-jute). Heavy metals that were considered for the studies include hexavalent chromium, trivalent chromium, copper, mercury, cadmium and lead. Studies on metal removal were carried out in batch & column mode using single and multi-metal system. Some preliminary investigation on metal removal was also carried out using a third polymer, support less AFC. The performance of these polymers on metal removal is discussed in this chapter.

4.1 Studies with AFC

4.1.1 Synthesis and characterization of AFC coated on support materials

AFC polymer was synthesized by cross-linking of aniline and formaldehyde to obtain a polymer with amine group. Various synthesis parameters were modified to determine the optimum synthesis condition for the adsorbent such as source of amine and proportion of aniline and formaldehyde. The obtained AFC being resinous required support material to granularize the polymer adsorbent. Screening and optimization of amount of support material was carried out with various support materials like cellulose, jute fiber, rice husk, fly ash, tea leaves, saw dust, silica gel and sugarcane baggase.

4.1.1.1 Synthesis with different source of amine

Besides aniline, several other amine compounds such as chloro aniline, para nitro aniline and para toluedine were reacted with formaldehyde in a similar way like synthesis of AFC. Preparations of polymers with different amine source were carried out separately in parallel manner. It was observed that polymers synthesized with chloro aniline, para nitro aniline and para toluedine doesn't yield any isolable polymer. Hence they were not considered. Polymer synthesized with aniline only yielded resinous substances which were completely soluble in methanol thus providing the possibility to coat on supporting materials. AFC prepared with aniline was opted for further research on metal adsorption.

4.1.1.2 Screening of supporting materials for coating AFC

Since AFC polymer obtained is resinous, granularization of the polymer is also vital to improve the rigidity of the polymer and to facilitate separation of metal ion after metal-polymer interaction. Thus addition of support material in polymer matrix was necessary. Selection criteria of supporting material include inertness so as to avoid reaction with AFC polymer, uniformity shape and size, cost effectivity and also accounted with stability in aqueous environment. Cellulose, jute fibre, rice husk, tea leaves, fly ash, saw dust, silica gel and sugarcane baggase were considered to coat the resinous AFC. Varying quantities of these support materials were mixed with resinous AFC polymer matrix. It was observed that the obtained AFC coated on cellulose, jute fibre, rice husk, tea leaves, saw dust and sugarcane baggase were lumped together due to its stickiness and were difficult to segregate and unable

to obtain a granularized adsorbent. Only AFC coated on silica gel showed a granular adsorbent probably due to inertness of silica gel and was thus chosen as support for AFC for present research work. The stability of the coating was another important parameter that we monitored by dissolving AFC coated silica gel in distilled water, methanol and chloroform solution separately for 24 hours. It was observed that the coating was insoluble and stable in distilled water. In methanol and chloroform solution, coating were partially soluble within initial ten minutes and methanol/chloroform solution turned to yellow. This result suggested that the coating of silica gel with AFC polymer though stable in water is unstable in organic solvent and the coating was a physical one. Further experiments were also carried out to determine metal removal potential of plain silica gel with Cr(VI), Cr(III), Hg(II), Cr(VI) and Cd(II) at varying pH of 2- 10. When initial metal concentration of 50 mg/L were contacted with 4 g/L silica gel, maximum removal for all metal ions were not more than 4%. Since silica gel showed poor adsorption property, considering it as support material was justified to reveal the amount of metal ions removed by lone AFC polymer.

4.1.1.3 Optimization of silica gel amount for coating AFC

To achieve the uniform and maximum coating of AFC polymer on the surface of silica gel, amount of silica gel needs to be optimized. Therefore amount of AFC polymer synthesized (section 3.2.1.1) was coated on various amount of silica gel. Initial Cr(III) of 40 mg/L and 100 mg/L were contacted with 4 g/L of different AFC coated on varying amount of silica gel. The finding is shown in Figure 4.1 and can be seen that for both the initial Cr(III) of 40 mg/L and 100 mg/L, AFC removed a maximum of 60% when amount of AFC was approximately 25 g. With further increase in the amount of silica gel (more than 25 g), removal of Cr(III) decreased possibly due to excess silica gel with incomplete and non uniform polymer coating. Considering the economical point of view, 25 g of silica gel was fixed for coating AFC synthesized with 200 mmol aniline and 123 mmol formaldehyde.

4.1.1.4 Characterization and optimization of AFC coated on silica gel

(a) Optimization of aniline: formaldehyde ratio

The molar ratio of aniline to formaldehyde ratio was set at 1.6:1 by Liu and Freund (1997) and further possibility of changing the molar ratios of formaldehyde to aniline was

suggested to control the molecular weight of AFC polymer (Zheng 2002). In the present work, aniline to formaldehyde ratio was varied at 0.5:1, 1.6:1, 2:1 and 3:1 to synthesize polymer with highest metal removal capacity. Resinous polymer was obtained at aniline formaldehyde ratio of 1.6:1 and 2:1 and were employed for Cr(VI) removal and results are shown in Figure 4.2. Aniline to formaldehyde ratio of 1.6:1 had Cr(VI) adsorption capability of 10% to 29% times higher than that of ratio of 2:1. This result shows that aniline to formaldehyde ratio of 1.6:1 was the optimum in terms of Cr(VI) removal from aqueous solution. Probably at aniline to formaldehyde ratio of 2:1, more diamines were formed as shown in Figure 4.3(a). At higher aniline formaldehyde ratio of 3:1, amount of polymer formation were very less with more unreacted aniline. However at lesser ratio of 0.5: 1, a very rigid and hard material was formed instead of a resinous polymer. It was suggested that formaldehyde when used in excess as compared to aniline was responsible for more cross-linking (Zheng 2002) as shown in Figure 4.3(b). Excessive cross linking makes the polymer brittle, insoluble and unsuitable for use.

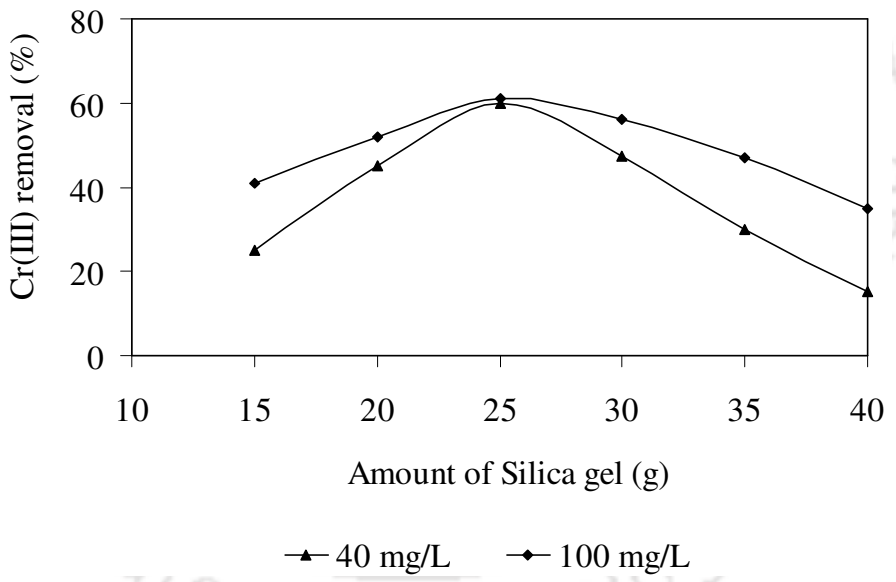

Figure 4.1: Optimization of silica gel amount for coating AFC [Cr(III): 40, 100 mg/L; silica gel dose: 4 g/L; pH: 6; agitation time: 4 h]

(b) pH of zero point charge (pH_{ZPC})

pH of zero point charge (pH_{ZPC}) is defined as pH of the adsorbent where surface charge is zero. Generally, at pH below pH_{ZPC}, surface of adsorbent will be positive in nature due to hydrogen ions and will favour adsorption of anions by electrostatic attraction. Above pH_{ZPC}, surface of adsorbent will becomes negative and favored for adsorbing cations. It is

well known that solubility and species distribution (cation or anion) of metal ions depend on pH of the solution. Therefore it is necessary to know the surface charge of adsorbent to assess the mechanism of metal binding at a particular pH. The pH of zero point charge (pH_{ZPC}) of AFC coated silica gel was determined by fast alkalimetric titration method (Huang and Ostovic 1978). From Figure 4.4, it can be clearly seen that pH_{ZPC} for AFC coated silica gel was 6.2. Therefore cationic species will be favoured for adsorption by AFC coated silica gel at pH > 6.2 by coordination bond and anionic species at pH < 6.2 by electrostatic attraction.

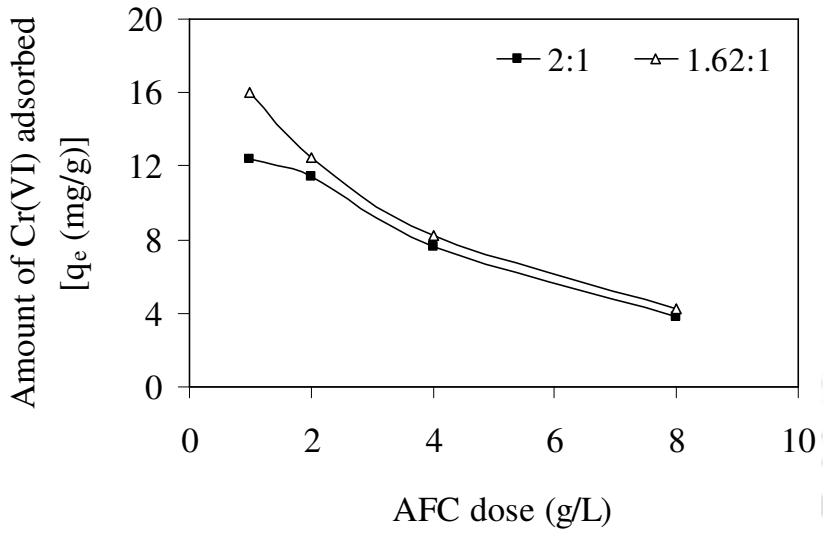

Figure 4.2: Effects of Cr(VI) uptake due to different aniline- formaldehyde ratios [initial Cr(VI) 50 mg/L ; pH 3]

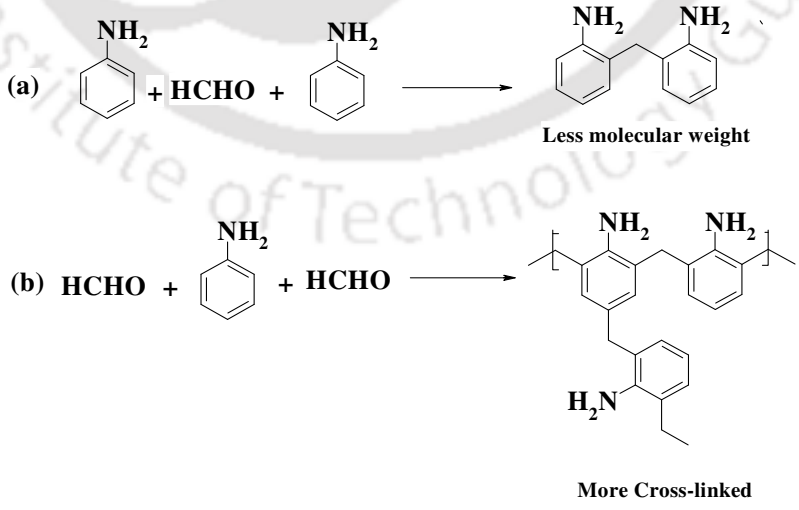

Figure 4.3: Plausible mechanism of forming polymer at different aniline formaldehyde ratio

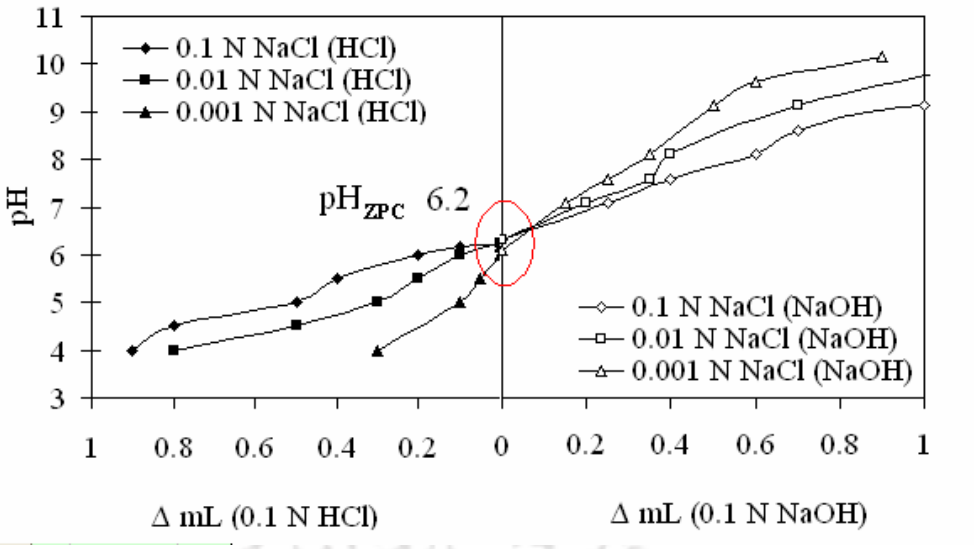

Figure 4.4: pH of zero point charge (pH_{ZPC}) of AFC coated silica gel

(c) Size of AFC coated silica gel

It was observed that the particle diameters for plain silica gel were more uniform (68% in the range of 200-600 μm) with mean particle diameter of 251 μm. After coating with AFC resin, small increase in particle size of plain silica gel was observed, with mean particle diameter of 353 μm. Probably the increase in the average size of the coated silica gel was due to coating effect. After adsorption of metal ion, mean particle size of the AFC coated silica gel decreased slightly to 303 μm. It may be due to some coatings removed from silica particles.

(d) Surface characteristics of AFC coated silica gel

Surface morphology, shape and size of silica gel and AFC coated silica gel were characterized by comparing between them. Surface characterization was carried out by scanning electron microscope (SEM) and electron diffraction X-ray (EDX) investigation. It can be seen from the Figures 4.5(a) that the uncoated silica gel particles were segregated particles with sharp edges and irregular in shape. EDX images [Figure 4.5(b)] showed presence of only silicon and oxygen in silica gel. SEM images of AFC coated silica gel [Figure 4.6(a)] showed more aggregated particles. The surface of AFC coated silica gel was smooth with resinous layer. The edges of the coated silica gel particles were less sharp as compared to uncoated silica gel particles which might be due to coating effect. EDX spectrum of AFC coated silica gel showed silicon, carbon, oxygen and chloride atoms [Figure 4.6(b)]. Chloride peak was present due to addition of hydrochloric acid during AFC synthesis.

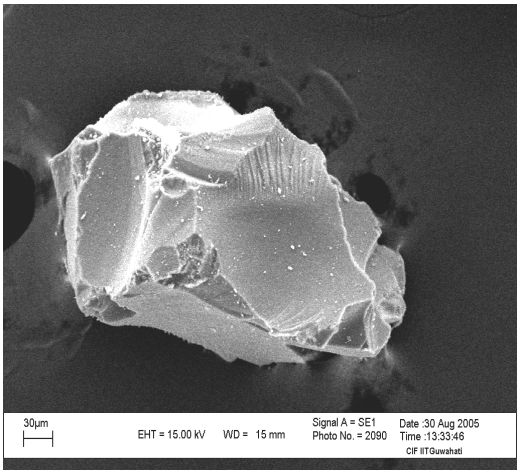

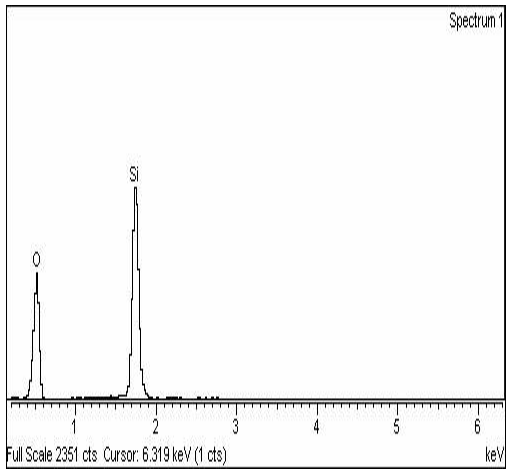

Figure 4.5(a): SEM image of silica gel & Figure 4.5(b): EDX spectra of silica gel

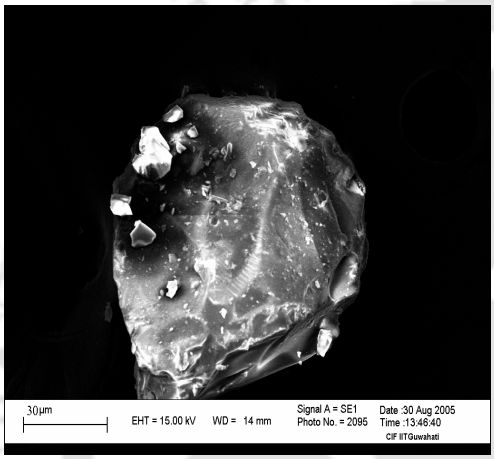

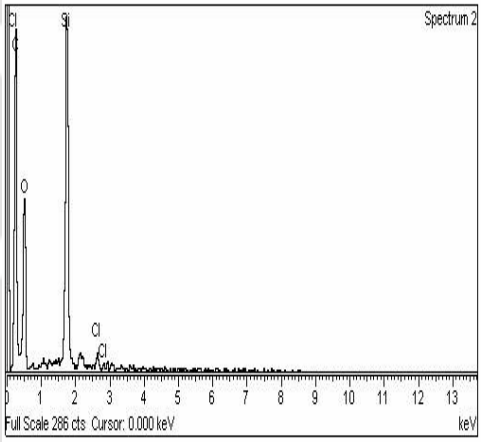

Figure 4.6(a): SEM image of AFC coated silica gel &
Figure 4.6: EDX spectra of AFC coated silica gel

4.1.2 Performance of AFC polymer in heavy metal removal

Study with AFC polymer in batch mode was conducted with hexavalent chromium, trivalent chromium, cadmium and mercury. Study parameter includes solution pH, initial metal concentration, dose of AFC coated silica gel and desorption.

4.1.2.1 Hexavalent chromium [Cr(VI)]

(a) Effect of solution pH

Effect of reaction pH on adsorption of chromium ion by AFC coated on silica gel was studied by conducting experiments with initial Cr(VI) 100 mg/L with 8 g/L AFC coated silica gel at pH 2 without controlling pH. Profiles of pH, Cr(VI) and total chromium

[Σ{Cr(VI)+Cr(III)}] are shown in Figure 4.7 (a). Cr(VI) concentration decreased rapidly from 100 to 20 mg/L within 30 minutes. However total chromium removal was quite less than Cr(VI) with total chromium final concentration of 68 mg/L after 60 min suggesting the reduction of Cr(VI) to Cr(III). Cr(VI) removal was associated with increase in solution pH from 2.17 to 3.5 in 30 minutes. Proton disappearance was proportional (with R^2 0.99) to Cr(VI) removal with 4.26 mmol of protons consumption for each mole of Cr(VI) removal [Figure 4.7 (b)]. Similarly consumptions of 3.99 mmol and 2.7 mmole of protons for each mole of Cr(VI) removal were observed by dead biomass *Aspergillus niger* and *Rhizopus oryzae* respectively (Park et al. 2005a; Park et al. 2005b).

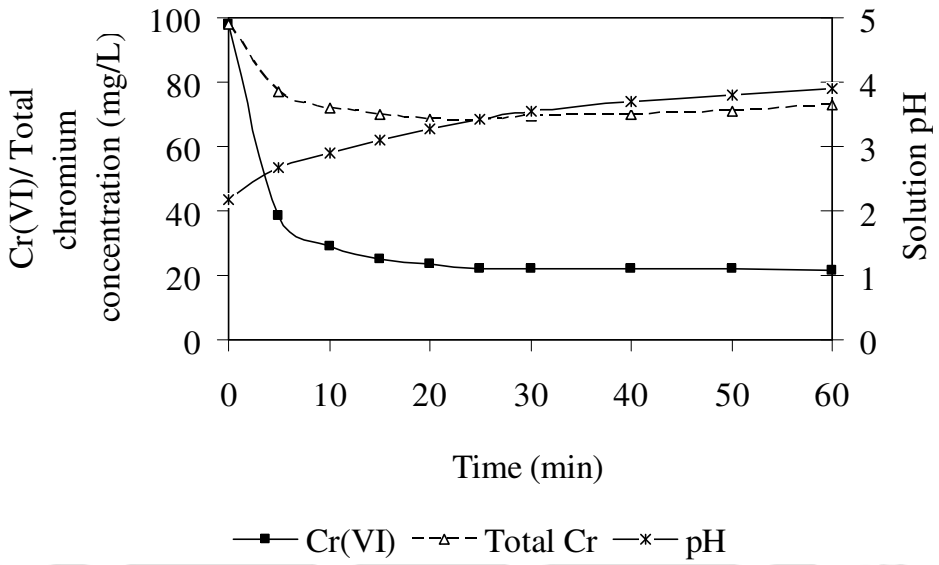

Figure 4.7 (a): Profiles of Cr(VI), total chromium and solution pH during uncontrolled reaction pH condition [Initial Cr(VI) 100 mg/L, AFC dose 8 g/L]

Experiments were conducted at controlled pH and results are shown in Figure 4.8. Concentrations of Cr(VI) and total chromium [Σ{Cr(VI)+Cr(III)}] were measured and removals (%) of Cr(VI) and total chromium and amount of initial Cr(VI) present in solution as Cr(III) (%) were calculated as shown below:

$$\text{Cr(VI) removal (\%)} = \frac{\left(\{Initial\ Cr(VI)(mg/L) - Final\ Cr(VI)(mg/L)\}x100\right)}{\{Initial\ Cr(VI)(mg/L)\}} \quad (4.1)$$

Total chromium removal (%) =

$$\frac{[\{Initial\ Cr(VI)\,(mg/L)\ -\ Final\,Total\,Chromium\,(mg/L)\}x100]}{\{Initial\,Cr(VI)\,(mg/L)\}} \quad (4.2)$$

Cr(III) in solution (%) =

$$\frac{[\{Final\,Total\,chromium\,(mg/L)\ -\ Final\ Cr(VI)\,(mg/L)\}x100]}{\{Initial\,Cr(VI)\,(mg/L)\}} \quad (4.3)$$

In equation (4.3), substituting values of final Cr(VI) and final total chromium from equations (4.1) and (4.2) respectively, it can be written as

Cr(III) in solution (%) = {Cr(VI) removal (%) – Total chromium removal (%)} (4.4)

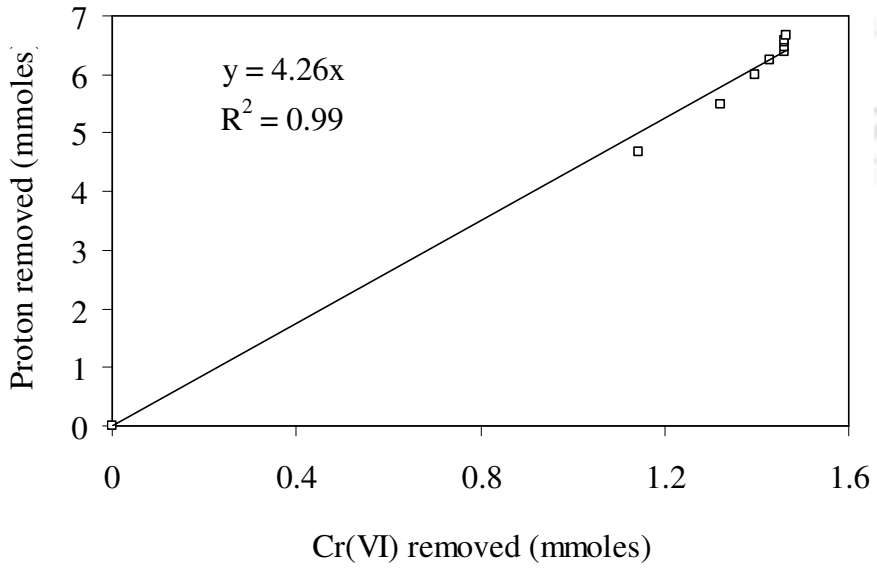

Figure 4.7 (b): Proton disappearance due to Cr(VI) removal

Figure 4.8 shows that removal of Cr(VI) was very high (92- 96%) at pH of 2 and thereafter it decreased with increase in pH (only 13- 16% at pH 5). However removal of total chromium was relatively less (12- 38%) than that of Cr(VI) at pH 2. Maximum amount of total chromium removal achieved at pH 3 which were 58- 61%. Removal of total chromium again decreased drastically at pH 4 (15- 36%) and above pH 5, it was negligible. It can be observed in Figure 4.8 also that 58% and 80% of initial Cr(VI) (40 and 100 mg/L

respectively) were present in solution as Cr(III) at controlled reaction pH 2. With increase in reaction pH, Cr(III) fraction in solution decreased steadily and became negligible at pH of 4 and above.

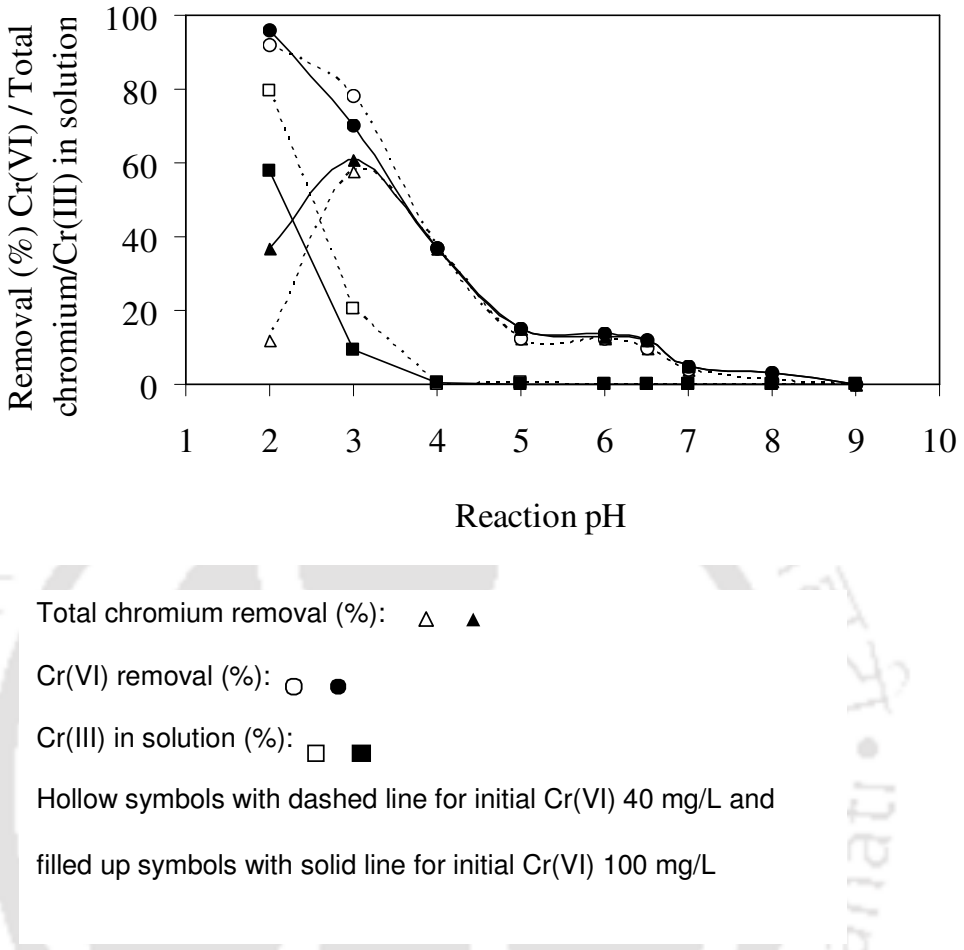

Figure 4.8: Effect of controlled reaction pH on chromium removal by AFC coated silica gel.

Within the studied pH range (2-6) used in the present work, the predominating form of Cr(VI) in solution is acid chromate ion ($HCrO_4^-$) (Benefield et al. 1982). In acidic medium amine group ($-NH_2$) of AFC exists as protonated ammonium ($-NH_3^+$) form and electrostatic attraction between protonated ammonium ion and negative chromate ion [$HCrO_4^-$] is expected for removal of Cr(VI) from solution. With increase in pH, this electrostatic attraction was less due to decrease in the positive charge of the amine group. Removal mechanism of Cr(VI) by AFC is shown in Figure 4.9.

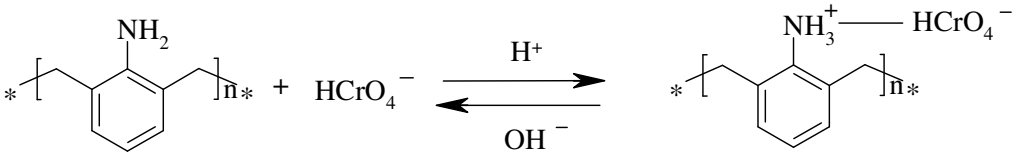

Acidic form works
like anion exchanger

Figure 4.9: Binding and unbinding mechanism of Cr(VI) with AFC

Literatures reported that under acidic environment, Cr(VI) spontaneously reduces to Cr(III) ion due to high redox potential (1.3 V at standard state) as shown below (Cimino et al. 2000; Altundogan 2005; Deng and Bai 2004).

$$HCrO_4^- + 7H^+ + 3e^- \rightarrow Cr^{3+} + 4H_2O \quad (4.5)$$

Equation (4.5) suggests that lower the solution pH, reaction will be favoured to right side with higher reduction of Cr(VI) to Cr(III). In the present work when solution pH was controlled at 2, chemical reduction of Cr(VI) to Cr(III) ion was the predominating step and very few $HCrO_4^-$ ion was available in solution for electrostatic bond formation with the protonated amine group. Further, charge repulsion between cation Cr(III) and highly protonated AFC was very high and maximum fraction of Cr(III) remained in solution at pH 2. Thus total chromium removal was low. When reaction pH was increased by one unit at pH 3, reduction of Cr(VI) was less and more $HCrO_4^-$ ion was available for electrostatic interaction with AFC. When solution pH was increased above 3, protonation of amine group decreased and so less total chromium was achieved. Present study can be summarized as maximum removal of Cr(VI) observed at pH 3 by electrostatic attraction of acid chromate ion with protonated amine group of AFC and interaction of Cr(VI) and AFC ion was largely pH dependent reaction. EDX spectra showed presence of chromium ion on surface of AFC after adsorption (Figures 4.10). Sulphur peak was present due to addition of sulfuric acid for pH adjustment during adsorption experiment.

Desorption study was conducted using five types of desorption agents and results are given in Table 4.1. When alkalis like NaOH and NH_4OH were used for desorption, $HCrO_4^-$ ion attached to protonated amine group by electrostatic attraction, were released from AFC as Cr(VI). When 0.2 N EDTA was used for desorption, almost 40% of adsorbed total chromium

was released in the form of Cr(III) ion. EDTA is known to make multidentate coordination bonds with various metal ions and was able to recover Cr(III) ions attached with nitrogen atom of AFC by coordination bond. Using mineral acids of 0.2N strength, 84%, 81% and 76% of adsorbed chromium were released in solution as Cr(III) ion by H_2SO_4, HNO_3 and HCl respectively. Probably $HCrO_4^-$ adsorbed by AFC, was reduced to Cr(III) ion during desorption by mineral acids and this Cr(III) ions were released into solution due to repulsion by protonated nitrogen atom. Desorption results also support previously stated mechanism of chromium removal by AFC coated silica gel. Similar phenomenon were observed during desorption of chromium from *Aspergillus niger* fungi and seaweed by mineral acids (Kratochvil et al. 1998, Park et al. 2005a).

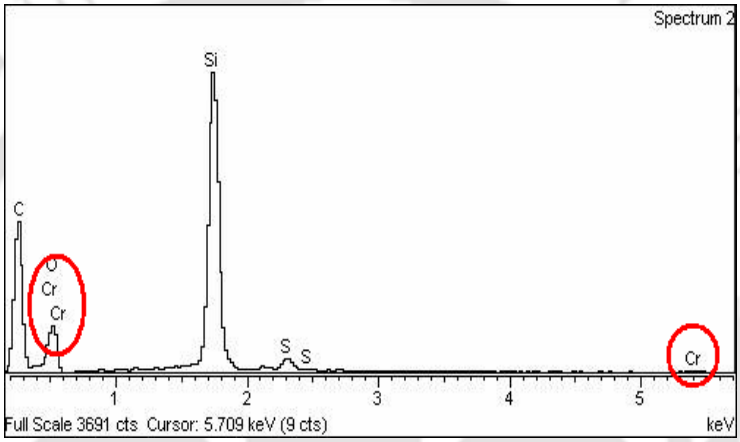

Figure 4.10: EDX spectra of AFC coated silica gel after chromium binding

Table 4.1: Desorption of chromium from AFC coated silica gel by various desorption agents

Desorption agents	Desorption time (hours)	Desorption efficiency (%)	
		Cr(VI) (%)	Cr(III) (%)
0.5 N NaOH	3	56.62	0
0.5 N NH_4OH	3	32.82	0
0.2N H_2SO_4	3	0	83.91
0.2 N HNO_3	3	0	81.05
0.2 N HCl	3	0	76.18
0.2N EDTA	3	0	37.14

(b) Degradation of AFC after interaction with metal ion

During interaction of chromium–AFC, slight brown color effluent was generated probably due to degradation of AFC in strong acidic environment. Degradation of AFC after interacting with metal ions in acidic condition was studied by comparing ^{1}H NMR spectra of AFC extracted from AFC coated silica gel before and after adsorption of Cr(VI) at pH 3. The spectra are shown in Figures 4.11 (a & b). Silica gel does not interfere in ^{1}H NMR spectrum. The ^{1}H NMR spectrum of AFC coated silica gel before metal binding showed multiple peaks in the aromatic region 6-7 ppm and at 3.5 ppm which was consistent with aromatic ring and methylene (-CH_2- group connecting between aromatic rings of AFC) groups present in the AFC. The position or shape of the peaks remained unchanged after chromium binding, which clearly indicates very insignificant degradation of AFC during interaction with Cr(VI) ion.

(c) Removal kinetics

Chromium removal kinetics was studied with varying initial Cr(VI) concentrations (10-200 mg/L) at optimum pH 3. Total chromium removals (%) with time are presented in Figure 4.12. Almost 30% to 65% removal of total chromium was observed within initial 20 minutes and equilibrium was achieved within 90-120 minutes. Total chromium adsorption by AFC coated gel increased from 43% to 70% with increase in initial Cr(VI) concentration from 10 to 200 mg/L. Adsorption equilibrium time of 50-350 hours was observed from initial Cr(VI) 25-200 mg/L by fungal biomass *Aspergillus niger* (Park et al. 2005a) whereas HNO_3 pre-treated seaweed biomass *Ecklonia* required 9 hours for complete removal from initial concentration of 200 mg/L (Park et al. 2005c). Equilibrium times of 2 hours and 5 hours were reported for total chromium removal (initial concentrations 3 mg/L and 10 mg/L) by iron hydroxide loaded sugar beet pulp and PVP coated silica gel respectively (Altundogan 2005; Gang et al. 2000). In terms of total chromium removal kinetics, AFC coated silica gel showed fairly good results.

The kinetics of total chromium adsorption by AFC coated silica gel was tested with pseudo first order and pseudo second order Lagergren kinetic model. The results is shown in Table 4.2. Lagergren pseudo first order model showed lesser correlation coefficient (R^2) in compared to the second order kinetic model suggesting the chromium adsorption following pseudo second order model. Less χ^2 value for second order model further confirmed the pseudo second order kinetics behavior of Cr(VI) adsorption on AFC. Pseudo Second order

chromium removal kinetics were also reported by previous researchers with various adsorbents like used tyres, saw dust, activated carbon prepared from rubber wood saw dust, KOH activated wood carbon etc. (Khezami and Capart 2005; Dakiky et al. 2002; Karthikeyan et al. 2005).

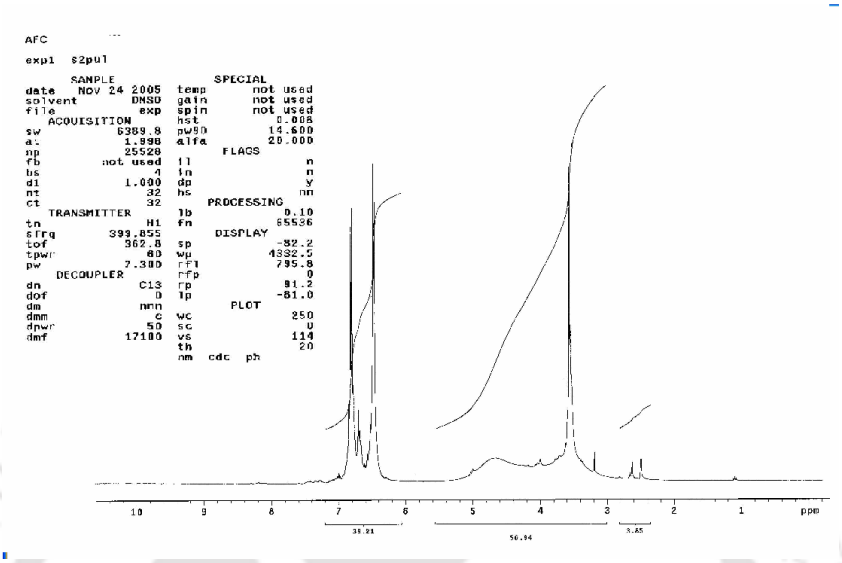

Figure 4.11(a): NMR spectrum of AFC coated silica gel before chromium adsorption

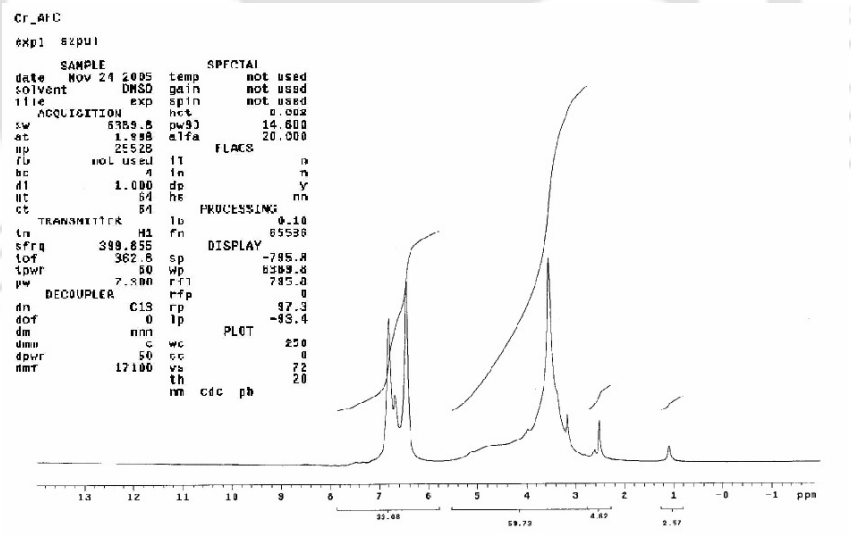

Figure 4.11(b): NMR spectra of AFC coated silica gel after chromium adsorption

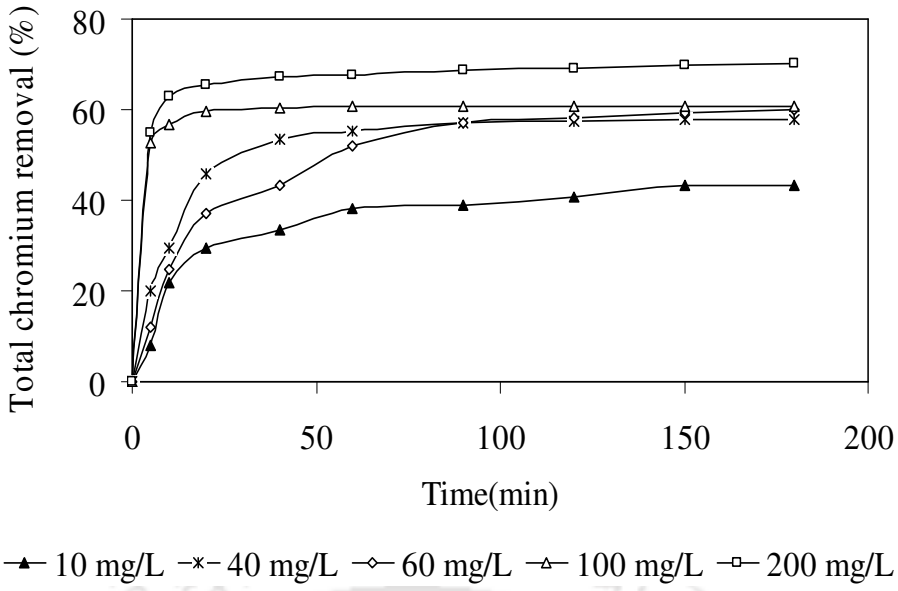

Figure 4.12: Total chromium removal with time by AFC coated silica gel at varying initial Cr(VI) concentration [AFC dose 8 g/L; reaction pH controlled at 3]

Table 4.2: Comparison of pseudo first and pseudo second order kinetic model for total chromium adsorption

Initial Cr(VI) (mg/L)	First order kinetic model			Second order kinetic model		
	k_1 (L/min)	R^2	χ^2	k_2 (g. mg^{-1}. min^{-1})	R^2	χ^2
10	0.034	0.92	0.19	0.09	0.99	0.02
40	0.029	0.98	20.78	0.07	0.99	0.07
60	0.041	0.90	1.58	0.06	0.99	0.06
100	0.054	0.86	456.14	0.04	1.00	0.01
200	0.004	0.38	2365.00	0.03	0.99	0.18

(d) Effect of adsorbent (AFC) dose and adsorption isotherm

Effect of adsorbent dose on adsorption was carried out with AFC dose varied from 0.5-8 g/L. Initially with increase in AFC dose up to 4 g/L, total chromium removal increased and remained constant beyond that (Figure 4.13). At AFC dose of 4 g/L, total chromium removal varied from 60- 70% from initial Cr(VI) of 50- 200 mg/L. As compared to AFC, 4 g/L pyrite removed only 30% total chromium from initial Cr(VI) of 100 mg/L (Zouboulis et al. 1995)

and iron hydroxide loaded sugar beet pulp required 10 g/L dose to achieve 70% removal from initial Cr(VI) 10 mg/L (Park et al. 2005c).

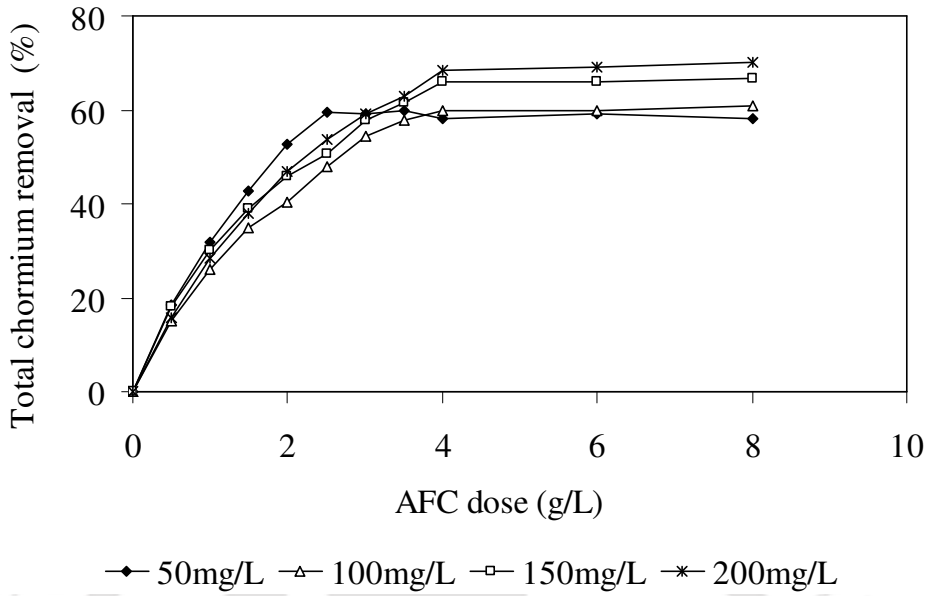

Figure 4.13: Effect of adsorbent dose on total chromium removal [Reaction pH controlled at 3; Adsorption time 3 hours; Initial Cr(VI) 50-200 mg/L]

Langmuir and Freundlich isotherm models were used to determine appropriate isotherm for total chromium adsorption by AFC coated silica gel. From Table 4.3, higher correlation coefficient (R^2) and less χ^2 values suggests that total chromium adsorption by AFC coated silica gel can be best described by Freundlich's isotherm. Freundlich's constant n value of 1.31 > 1 clearly indicates total chromium adsorption by AFC coated silica gel as a favourable process.

Table 4.3: Isotherm constants for total chromium adsorption by AFC coated silica gel

Freundlich isotherm				Langmuir isotherm				
K_f (mg/g)	n	R^2	χ^2	Q_m (mg/g)	b (L/mg)	R^2	R_L	χ^2
2.39	1.56	0.99	0.07	140.8	0.005	0.98	0.50	0.30

A comparison of the chromium adsorption capacity of AFC coated silica gel with various adsorbents in Table 4.4 shows that chromium adsorption capacity varied in wide range. However, in many of the reported studies chromium adsorption was estimated only on the removal of Cr(VI) from solution instead of removal of total chromium [Cr(VI) and

Cr(III)]. Adsorption capacity observed with AFC coated silica gel (17- 65 mg/g) compared well with most of the adsorbents, except few materials like tamarind hull and nanocrystalline akaganeite which exhibited very high adsorption capacity of 95 mg/g and 80 mg/g, probably due to basic morphology of the raw material and very high surface area of nanosized particles. AFC coated silica gel can be considered a viable adsorbent for removal of chromium from aqueous solution.

Table 4.4: Comparison of adsorption capacity of chromium with other adsorbents

Adsorbent	Adsorption capacity (mg/g)	Initial Cr(VI) (mg/L)	pH	Reference
KOH treated AC prepared from wood[a]	160.0	5-200	3.0	Khezami and R. Capart 2005
Zinc chloride AC from *Terminalia arjuna* nuts[a]	28.4	10-30	1.0	Mohanty et al. 2005
Activated carbon from *Hevea Brasilinesis* saw dust[a]	44.1	200	2.0	Karthikeyan et al. 2005
Nanocrystalline akaganeite[a]	80.0	10-50	5.5	Lazaridis et al. 2005
Polyacrylamide grafted sawdust[a]	45.0	100	3.0	Raji and Anirudhan 1998
PVP coated silica gel[b]	3.0	10	5.0	Gang et al. 2000
Polyacrylonitrile fibers[b]	35.0	50	5.0	Deng and Bai 2004
Hazelnut shell[b]	3.9	-	3.0	Cimino et al. 2000
Iron hydroxide loaded sugar beet pulp[b]	4.9	5-200	4.4	Altundogan 2005
Soya cake[b]	0.3	48	1.0	Daneshvar et al. 2002
Tamarind hull[b]	95.0	50-150	2.0	Verma et al. 2006
AFC[b]	17.0- 65.0	50-200	3.0	Present study

[a] Chromium removal based on only estimation of Cr(VI) concentration.

[b] Chromium adsorption based on total chromium removal.

4.1.2.2 Trivalent chromium [Cr(III)]

(a) Effect of solution pH

Effect of pH on adsorption of Cr(III) by AFC was studied at pH range of 1- 11. Initial Cr(III) of 50 mg/L was contacted with 4 g/L AFC dose. A control experiment without any adsorbent was also run in parallel to checked the precipitation of Cr(III) or adsorption by the rector vessel. Control experiment suggest precipitation of Cr(III) above pH 6 hence removal of Cr(III) below pH 6 was considered due to adsorption by AFC. Figure 4.14 shows that removal of Cr(III) increased with increase in pH obtaining maximum removal of 80% at pH 6. Within pH range of 1 to 4, removal of Cr(III) was almost negligible (only 0.2- 7%) and increased to 20% and 80% at pH of 5 and 6 respectively. The distribution of different species of Cr(III) at different pH was studied using equations of complexation between Cr(III) and OH^- ligand using logarithmic constant k_1, k_2, k_3 and k_4 value were 10, 8.3, 5.7 and 4.6 respectively with solubility product k_{sp} of 6 x 10^{-31} (Sawyer et al. 2003). Species distribution diagram of Cr(III) is shown in Figure 4.15.

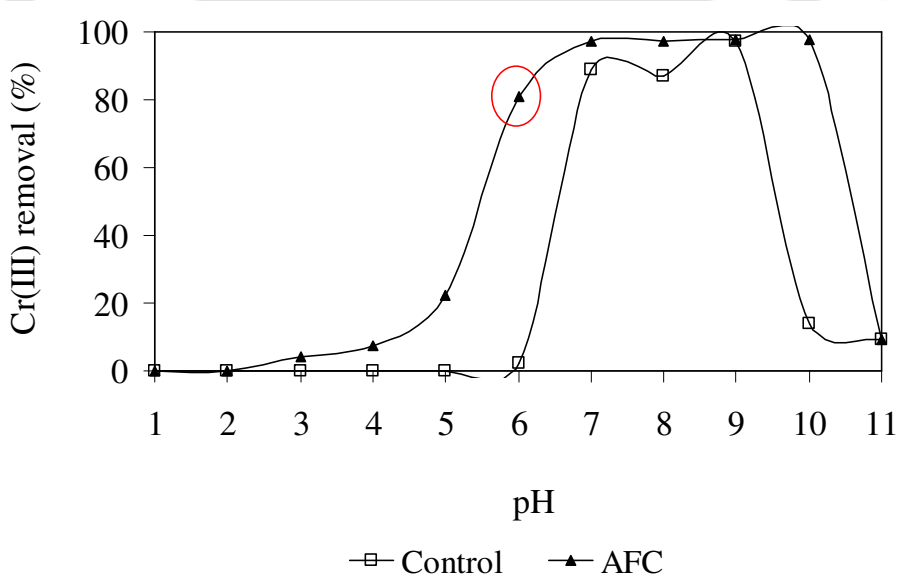

Figure 4.14: Removal of Cr(III) at different pH. [Initial Cr(III): 50 mg/L; AFC dose: 4 g/L; agitation time: 4 h]

In acidic pH of 1- pH 4, trivalent Cr^{3+} is the dominant species followed by divalent $Cr(OH)^{2+}$ from pH 4 to almost pH 5.5. In acidic pH range, surface of AFC was highly protonated as NH_3^+ form and this repulsed Cr^{3+} and $Cr(OH)^{2+}$ ions thus yielding very less

removal of Cr(III). At neutral pH range (pH 5.5 and above), the dominant species of Cr(III) are monovalent $Cr(OH)_2^+$ and divalent $Cr(OH)^{2+}$ which are octahedral geometry (six-coordinate) (Cotton and Wilkinson 1998) with one or two hydroxide ligand. Thus in neutral pH range where amine of AFC deprotonates, $Cr(OH)_2^+$ and $Cr(OH)^{2+}$ were bound to the polymer through at least two or three amine group of the polymer with rest of the coordination sites filled up with chloride (starting material is $CrCl_3$) and water molecules (Figure 4.16). The binding of amines occurred presumably due to the multidentate (multiple point binding) nature of the polymer compared to monodentate (single point binding) water or halide ion (Type I in Figure 4.16). With increase in pH, the bound water molecules got deprotonated generating more and more $[CrOH]^{2+}$ and $[Cr(OH)_2]^{1+}$ species and formed bond with amine group of AFC [Type II in Figure 4.16], thus Cr(III) removal by AFC increased with increase in pH from 5.5 to 6. At very high pH (above 10), Cr(III) hydroxides are known to act as bridging ligands forming multinuclear species in the basic medium (eg. $[(H_2O)_4Cr(OH)_2Cr(H_2O)_4]^{4+}$) which are shown as type (III) in Figure 4.16. Thus above pH of 10, large amount of Cr(III) ions formed this bridge structure and adsorption by AFC decreased. Similar observations were also reported during removal of Cr(III) by aminated polyacrylonitrile fibers, where removal of Cr(III) was negligible at pH 2 and started only from solution pH of 3 due to charge repulsion of amine group and Cr(III) ion (Deng and Bai 2004).

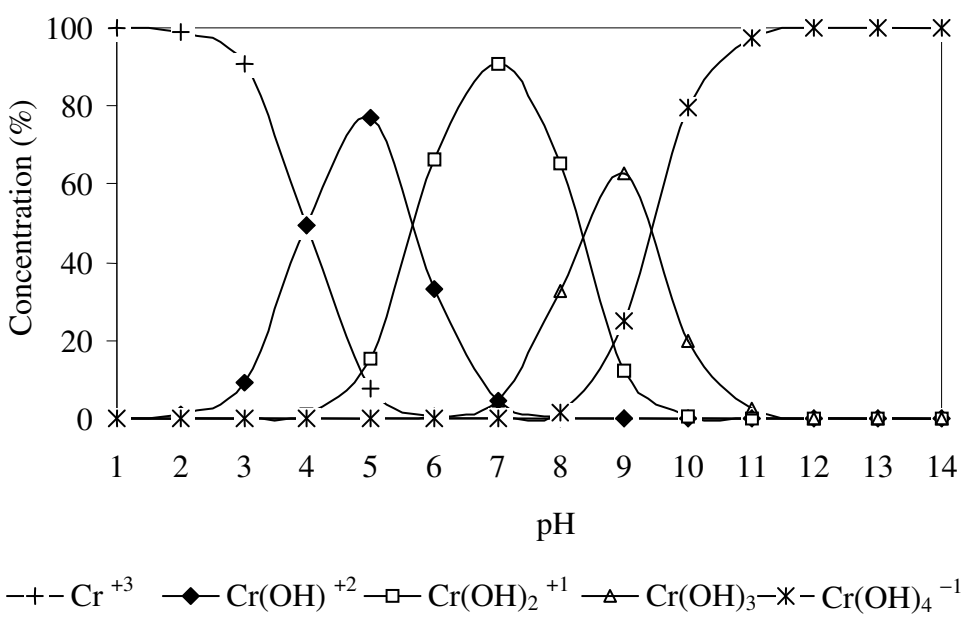

Figure 4.15: Concentration distribution diagram of Cr(III) at different pH

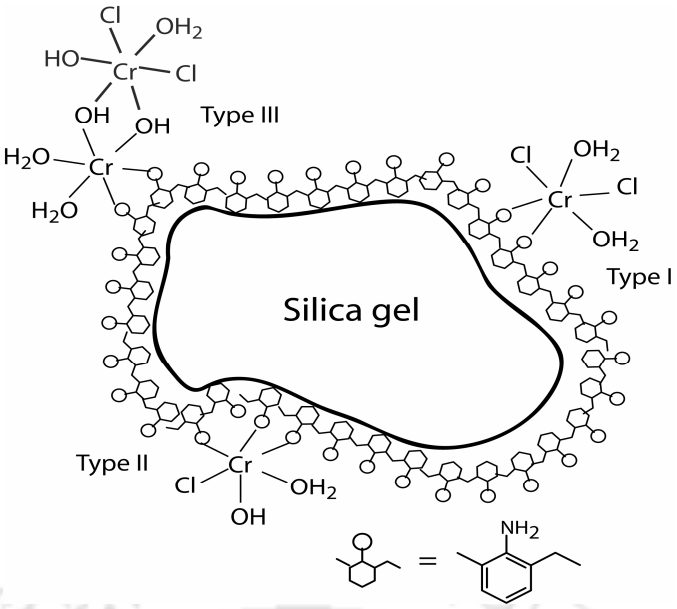

Figure 4.16: Proposed mechanism of Cr(III) adsorption by AFC coated silica gel

(b) Effect of adsorbent dose

Effect of adsorbent dose on Cr(III) removal is shown in Figure 4.17. Cr(III) removals increased from 46% to 95% with increased in adsorbent dose from 1- 10 g/L. With increase in AFC dose more active surface area were available for Cr(III) bindings thus achieving an increase in removal (%). However reverse trend was observed with adsorbed Cr(III) by unit amount of AFC (q_e) which decreased from 23 mg/g at AFC dose of 1 g/L to 4.75 mg/g at AFC dose of 10 g/L. Once the interaction of Cr(III)-AFC reached equilibrium, the addition of extra adsorbent were probably left unutilised or unsaturated. These unutilised mass of AFC were accounted however during the calculation of removal capacity, leading to decrease in value of q_e.

(c) Initial concentration effect and adsorption kinetics

The effect of initial concentration of Cr(III) on adsorption is illustrated in Figure 4.18. Almost 30- 70% removals of Cr(III) was observed within initial 20 min and equilibrium was achieved within 90- 120 min. Such rapid adsorption suggest chemisorptions and high adsorption rate of Cr(III) ion by AFC. Hexavalent chromium equilibrium was also achieved within 120- 150 minutes. With increase in initial Cr(III) concentration from 15 to 45 mg/L, adsorption increased from 32- 37% and 78- 90% at pH 5 and 6 respectively. Similar phenomenon was observed during chromium removal by polyvinylpyridine-coated silica gel

(Gang et al. 2000). This finding clearly suggests the dependence of initial concentration of adsorbate on adsorption. The kinetics of Cr(III) adsorption by AFC coated silica gel was tested with Lagergren first order and second order kinetic model. Lagergren's first order model showed less correlation coefficient (R^2) than second order kinetic model at different initial concentration of Cr(III) and at pH 5 and 6. It can be seen from Table 4.5 also that χ^2 value for second order is much lesser than first order kinetic model suggesting Cr(III) adsorption on AFC followed second order kinetic model.

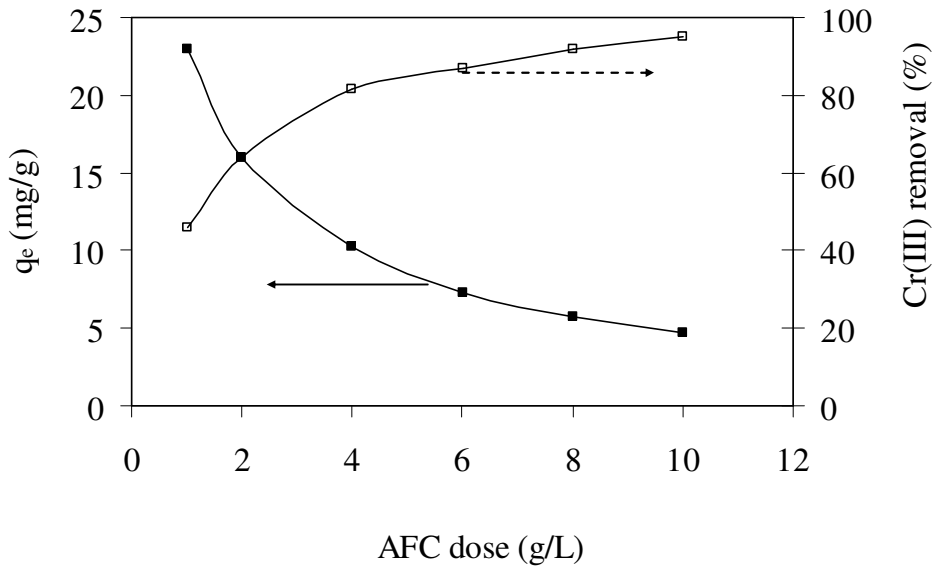

Figure 4.17: Effect of adsorbent dose on Cr(III) adsorption [Initial Cr(III) 50 mg/L, solution pH 6]

(d) Adsorption Isotherm

Adsorption isotherm was studied by conducting experiment with varying initial concentration of Cr(III) from 15- 500 mg/L at pH of 6 and AFC dose of 4 g/L. The isothermal data were treated with Langmuir and Freundlich equation and the results are shown in Table 4.6. Lanmuir's correlation coefficient (R^2) showed higher value than that of Freundlich's and lesser χ^2 value for Langmuir suggest the adsorption of Cr(III) on AFC coated silica gel can be well explained by Langmuir isotherm. Comparison of Cr(III) removal of capacity of AFC coated silica with reported literature is presented in Table 4.7.

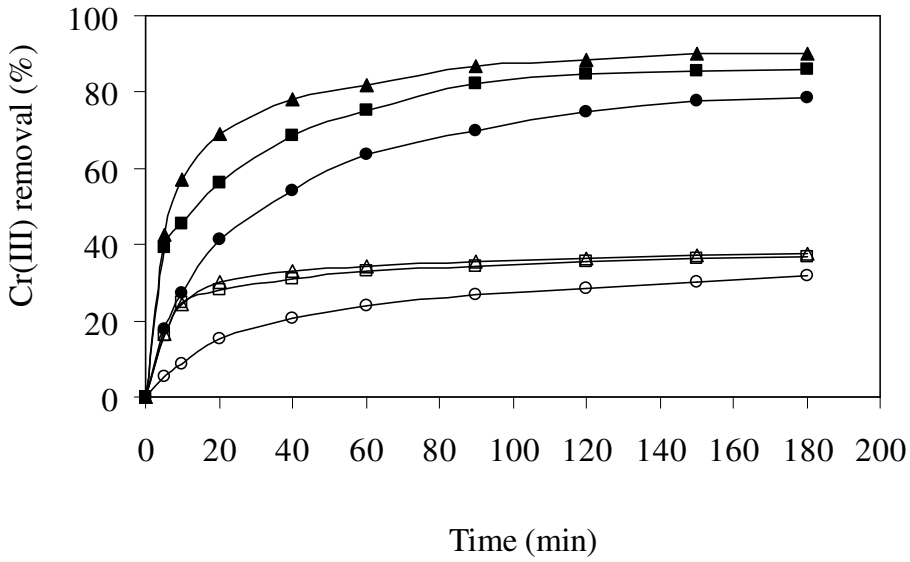

Figure 4.18: Cr(III) removal kinetics by AFC coated on silica gel [Circle, square and triangle denotes initial Cr(III) of 15, 30 and 45 mg/L respectively. Hollow symbols signify reaction pH 5 and filled signifies reaction pH 6]

Table 4.5: Comparison of first and second order kinetic model for Cr(III) adsorption

pH	Initial Cr(III) (mg/L)	Pseudo first order kinetic model			Pseudo second order kinetic model		
		k_1	R^2	χ^2	k_2	R^2	χ^2
5	15	0.018	0.98	0.58	0.024	0.99	0.01
	30	0.027	0.96	6.51	0.047	0.99	0.04
	45	0.027	0.95	9.83	0.034	0.99	0.01
6	15	0.028	0.98	0.33	0.014	0.99	0.11
	30	0.034	0.98	5.33	0.014	0.99	0.22
	45	0.033	0.96	15.8	0.015	0.99	0.05

Table 4.6: Isotherm constants for Cr(III) adsorption by AFC coated silica gel

Langmuir's isotherm					Freundlich's isotherm			
Q_m (mg/g)	b (L/mg)	R^2	R_L	χ^2	K_f	n	R^2	χ^2
25.31	0.08	0.98	0.45	2.5	3.34	2.36	0.92	7.47

Table 4.7: Removal capacity of Cr(III) by various adsorbents

Adsorbent	Cr(III) removal capacity (mg/g)	Reference
Palm flower (*Borassus aethiopum*) Acid treated palm flower (*Borassus aethiopum*)	6.24 1.410	Elangovan et al. 2008
Lignin	17.97	Wu et al. 2008
Wine processing waste sludge	26.79	Li et al. 2004
Agricultural waste coir pith	11.52	Parab et al. 2004
Ion-exchange resins Chelex-100 Ion-exchange resins Lewatit TP 207	14.97 17.73	Gode and Pehlivan 2003
Agave lechuguilla biomass	14.20	Gonza´le et al. 2006
Low cost natural diatomite	28.0	Guru et al. 2008
Lignite based humic acid	15.08	Arslan and Pehlivan 2008
Composite alginate–goethite beads	30.37	Lazaridis and Charalambous 2005
AFC	25.31	Present Study

(e) Desorption

Study of desorption was carried out by employing three mineral acids and chelating agent EDTA as desorbents. Maximum desorption obtained were 33.3%, 41.7% and 41.7% by 0.5 M HCl, H_2SO_4 and HNO_3 respectively whereas EDTA recovered only 5.8%. Irrespective of desorbents type, all desorption process was however observed to complete in 10 min and no further desorption observed within 10 min- 4 hours. Such less desorption for Cr(III) may be probably due to the high kinetic immobility of Cr(III).

(f) Characterization of AFC coated silica gel after Cr(III) adsorption

EDX analysis was employed to confirm the presence of chromium ions on AFC coated silica gel. EDX spectra in Figure 4.19(a) show presence of chromium peak after adsorption. The presence of potassium (K) and phosphorous (P) peak after adsorption experiment were

contributed from buffering agent potassium hydrogen ortho phosphate. Confirmation of presence of Cr(III) on surface of AFC was also investigated by employing ESR (electronic paramagnetic resonance) also. The ESR spectrum is shown in Figure 4.19(b). The resonance signal appears at a magnetic field position corresponding to g value of 1.975, confirming the presence of Cr(III) whose standard signal g value is 1.98 (Ravi et al. 2006). Here, $g = \frac{h\nu}{\beta Hr}$, where, h is the Planck constant ($6.626 \times 10{-}27$ erg/s); β is Universal constant (9.274×10^{-21} erg/G); ν is frequency (9.707×10^{9} Hz) and H_r is resonance of magnetic field (G).

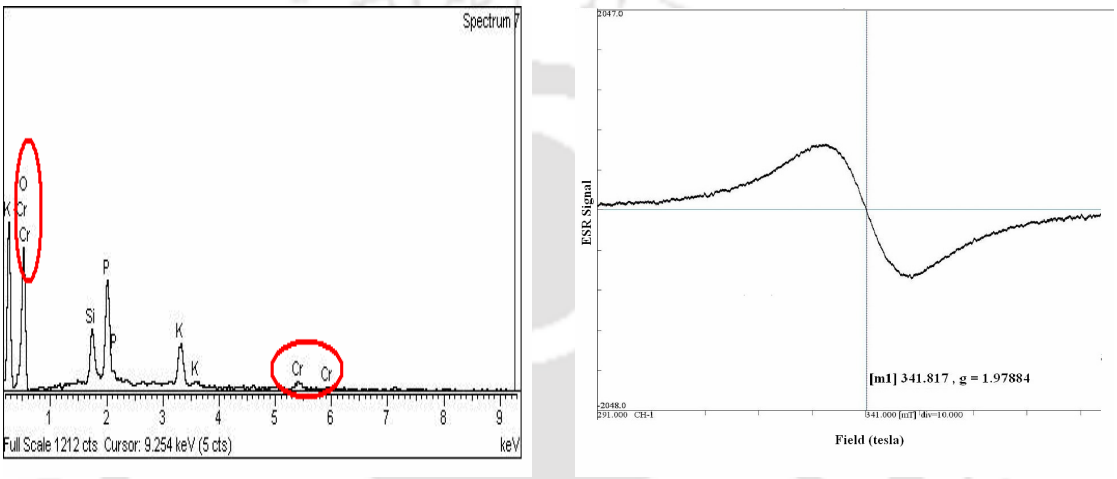

Figure 4.19(a & b): EDX and ESR spectra of AFC coated silica gel after Cr(III) binding

4.1.2.3 Cadmium [Cd(II)]

Removal of cadmium ions by AFC was conducted initially at different pH by contacting 100 mg/L of Cd(II) with 2 g/L and 10 g/L AFC coated silica gel. However it was observed that uptake of Cd(II) at various condition were almost negligible. To confirm the negligible binding of Cd(II), higher initial Cd(II) concentration of 500 mg/L was contacted with 20 g/L AFC coated silica at pH 2 to pH 6. Even at higher concentration there were no uptake of Cd(II) removal by AFC coated silica gel. According to Pearson's theory, Cd(II) behaved as a soft acid and unable to bind any bond with hard base of amine (Pearson 1963). EDX investigation of AFC coated silica gel after adsorption experiment with Cd(II) also showed no presence of Cd(II) confirming no affinity for Cd(II) to bind towards the amines of AFC coated silica gel.

4.1.2.4 Mercury [Hg(II)]

(a) Effect of solution pH

Effect of pH on Hg(II) adsorption is presented in Figure 4.20. The optimum pH for Hg(II) removal was 7- 9. At pH 2, very less removals (8- 12%) of Hg(II) were achieved. Maximum removal of Hg(II) was achieved at pH 6.5 with 88% and 85% for initial Hg(II) 50 mg/L and 80 mg/L respectively and remained almost constant till pH 9. With every set of experiment, control experiment without any adsorbent were run in parallel to checked the precipitation of Hg(II). Within the experimental condition of initial 80 mg/L at pH 9 control experiment showed no precipitation suggesting whatever amount of Hg(II) removed from the solution is solely due to adsorption by AFC coated silica gel. Similar maximum Hg(II) removal trend at pH 5– 8 were also reported by different authors with activated carbon derived from furfural (Yardim et al. 2003), activated carbon obtained from coal and biomass (Ekinci et al. 2002) and fruit shell of *Terminalia catappa* (Inbaraj and Sulochana 2006). EDX spectra (Figure 4.21) of AFC coated silica gel after adsorption of Hg(II) showed peak of Hg(II) confirming the adsorption Hg(II) on surface of AFC.

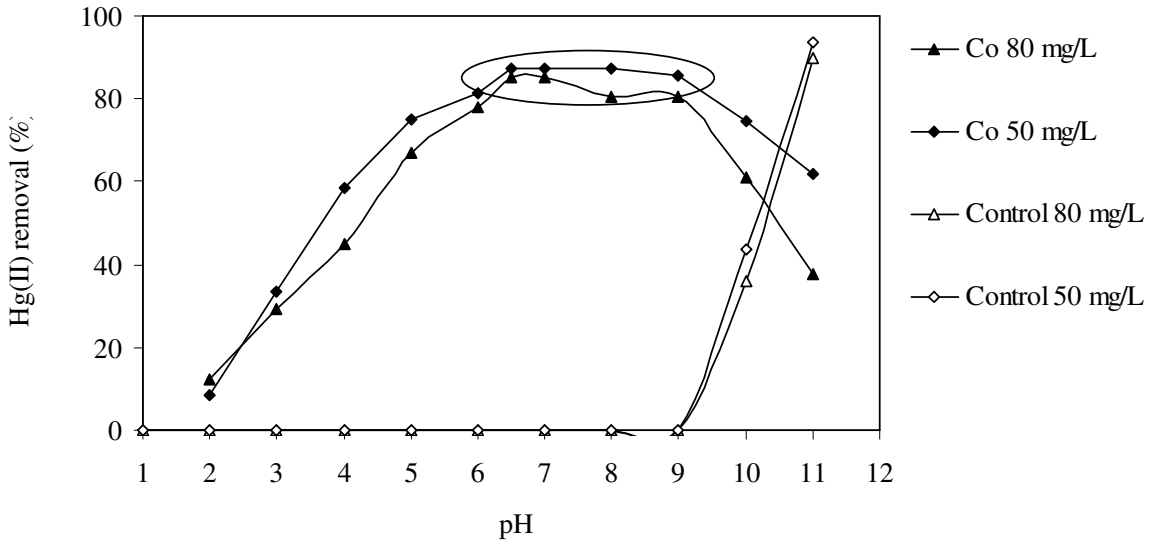

Figure 4.20: Profile of Hg(II) removal at various solution pH

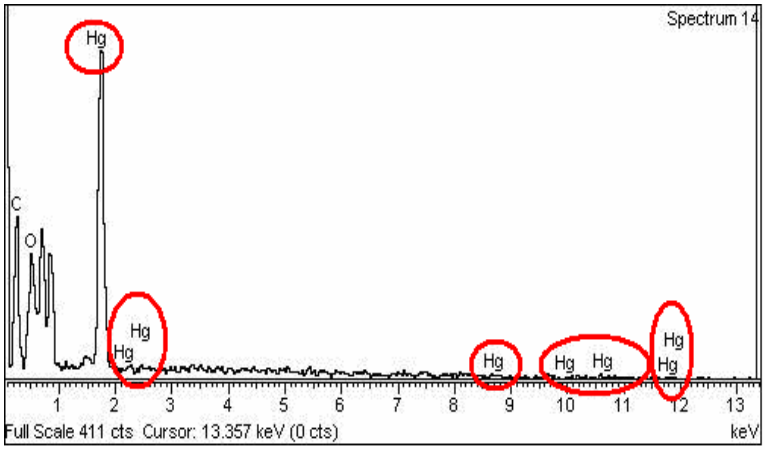

Figure 4.21: EDX spectra of AFC coated silica gel after Hg(II) adsorption

In the present work, source of Hg(II) was $HgCl_2$. It is known that Hg(II) exist in different anionic and cationic aqueous forms when combined with chloride ions in water like $Hg^{2+}_{(aq)}$, $HgCl^{+}_{(aq)}$, $HgCl_{2(aq)}$, $HgCl_3^{-}{}_{(aq)}$, $HgCl_4^{2-}{}_{(aq)}$, $HgOH^{+}_{(aq)}$, $Hg(OH)_{2(aq)}$ and $Hg(OH)_3^{-}{}_{(aq)}$. Hence, it is first of all necessary to identify the species of Hg(II) at different pH to understand the mechanism of interaction of Hg(II) and its complexes with amine group of AFC. The distribution of different species of Hg(II) at different pH was studied using equations of complexation between Hg(II), Cl^- and OH^- ligand using logarithmic constant k_1, k_2, k_3, k_4, k_5, k_6 and k_7 value of 6.72, 6.51, 1, 0.97, 10.3, 11.4 and -0.9 respectively with solubility product k_{sp} of 10^{23} (Sawyer et al. 2003). Logarithmic constant $k_1=[HgCl^+]/\{[Hg][Cl^-]\}$; $k_2=[HgCl_2]/\{[HgCl^+][Cl^-]\}$; $k_3=[HgCl_3^-]/\{[HgCl_2][Cl^-]\}$; $k_4=[HgCl_4^{2-}]/\{[HgCl_3^-][Cl^-]\}$; $k_5=[Hg(OH)^+]/\{[Hg][OH^-]\}$; $k_6=[Hg(OH)_2]/\{[Hg(OH)^+][Cl^-]\}$ and $k_7=[Hg(OH)_3^-]/\{[Hg(OH)_2][OH^-]\}$. Species distribution diagram of Hg(II) is shown in Figure 4.22.

From Figure 4.22, it can be seen that at pH range of pH 1 to 4, the most dominating specie is neutral $HgCl_2$ followed by anionic species $HgCl_3^-$, $HgCl_4^{2-}$ and cationic specie $HgCl^+$. At acidic pH, less dominating species $HgCl_3^-$, $HgCl_4^{2-}$ are attached with $-NH_3^+$ group of AFC by electrostatic attraction whereas the most dominating specie $HgCl_2$ is unbounded. Hence removal of Hg(II) was less at acidic pH. At pH of 5 to 9.5, $Hg(OH)_{2(aq)}$ is the main specie followed by $HgCl_{2(aq)}$, followed by $HgOH^+_{(aq)}$ and $HgCl_3^-{}_{(aq)}$. $HgOH^+$ and $Hg(OH)_2$ can undergo complexation with amine groups (Baes and Mesmer 1976), where binding of $Hg(OH)_{2(aq)}$ actually involve a ligand exchange process where one of the OH^- group is replaced by the amine group (Walcarius et al. 2004). Hence from pH 5-9, the main plausible

mechanism of mercury removal is the binding of $Hg(OH)_2$ with amine group of AFC by ligand exchange process. The pH_{ZPC} of AFC coated silica gel was 6.2, suggesting AFC surface has negative charge above pH 6.2. Therefore, some removal with positive specie $Hg(OH)^+$ with the deprotonated amine group of AFC could also be responsible for some mercury removal from pH 6.2- 9.5. From pH 9.5- 14, though $Hg(OH)_{2(aq)}$ is the predominating specie, it is followed by $HgOH_3^-{}_{(aq)}$. This anionic specie $Hg(OH)_3^-$ got repelled by deprotonated AFC causing decrease in total mercury removal above pH 9.5 and this caused decrease in total mercury adsorption by AFC. From Figure 4.22 it can also be seen that at pH range of pH 5- 14, when $HgCl_2$ salt was used, precipitation of Hg(II) as $Hg(OH)_2$ (s) started when initial Hg(II) is higher than log(-1.3) which equals to 0.05 M Hg(II) [10073 mg/L]. Atia et al. (2005) observed precipitation of Hg(II) ion at pH 5 and above at initial concentration of 4040 mg/L (0.02 M). It can hereby suggest that the removal of Hg(II) by AFC coated silica gel within the experimental condition was solely due to adsorbent and not by precipitation. Therefore the main mechanisms of Hg(II) removal by AFC coated silica gel were: (i) the electrostatic attraction of anionic Hg(II) which is in the form of $HgCl_4^{2-}$ and $HgCl_3^-$ at lower pH and (ii) formation of coordinate bond between cationic specie $Hg(OH)_2$ and amine ($-NH_2$) of AFC by ligand exchange process at pH 5- 9.5 and is shown in Figure 4.23.

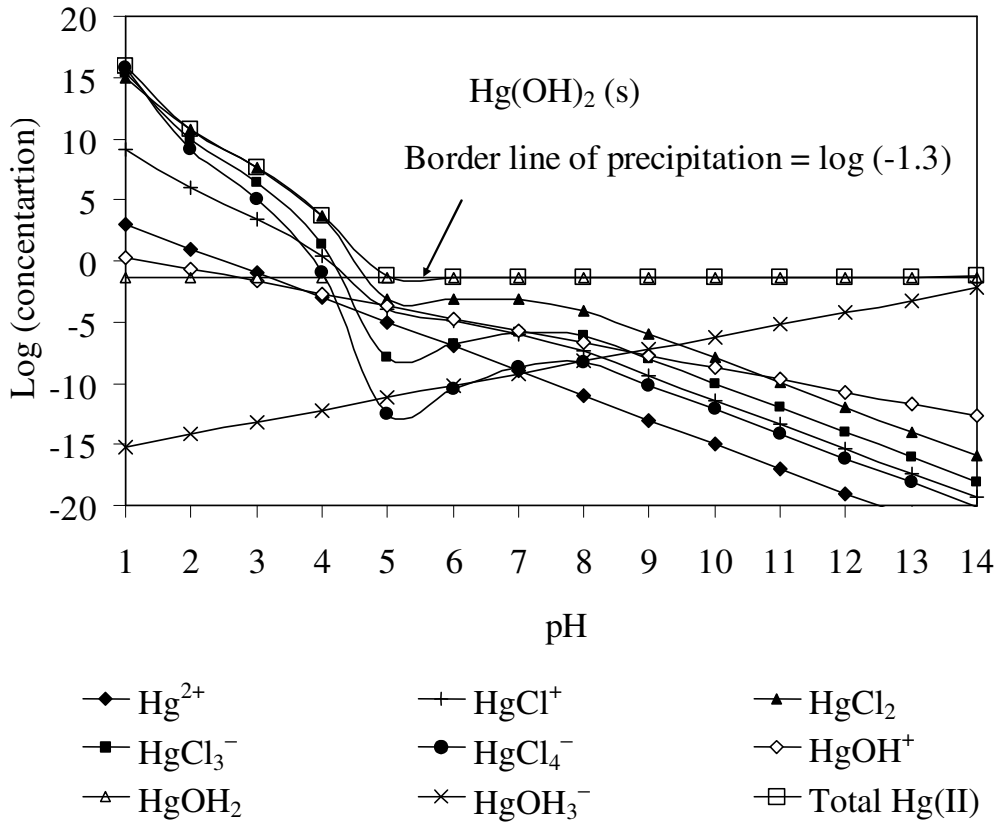

Figure 4.22: Log concentration diagram for different specie of Hg(II) at different pH

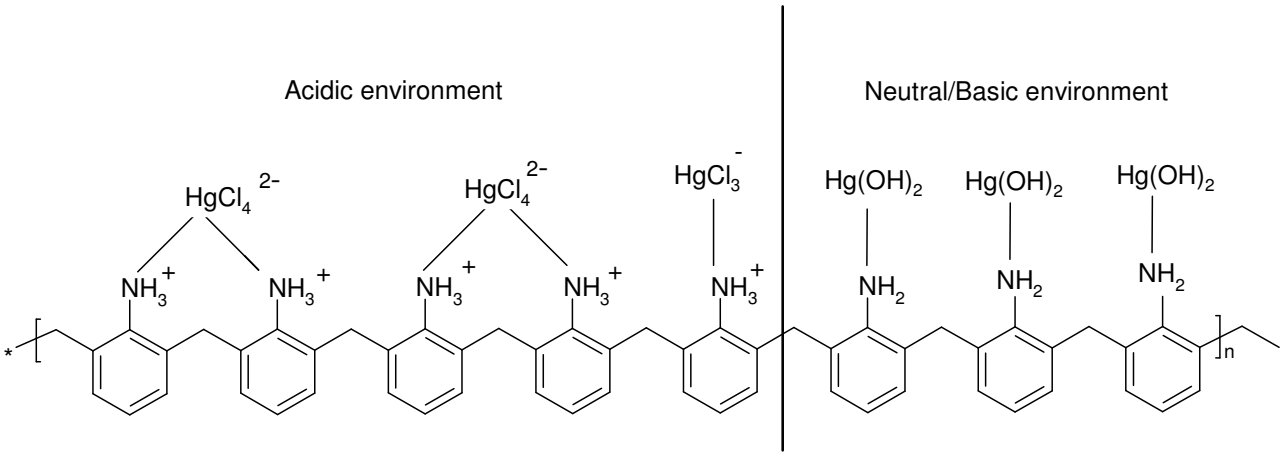

Figure 4.23: Removal mechanism of Hg(II) at acidic and neutral/basic pH

(b) Effect of initial concentration on Hg(II) removal

Hg(II) adsorption by AFC was studied in a wide range of 5- 1000 mg/L. From initial Hg(II) concentration of 5- 20 mg/L, complete removal was achieved within 20 min. At higher initial concentration, equilibrium time increased to 240 min. Difference of only 60 min between the initial concentration of Hg(II) below 100 mg/L and above up to 1000 mg/L signify the rapid adsorption of Hg(II) by AFC coated silica gel. This may be probably due to chemical adsorption on the surface of AFC rather than physical adsorption by diffusion. Equilibrium times of 24 hour were reported for the adsorption by chemically modified chitosan (Jeon and Ho¨ ll 2003), pinus pinaster bark (Va´ zquez et al. 2002) or ion exchange resins (Chiarle et al. 2002) during removal of Hg(II). Even longer equilibrium times were reported from 80 to 120 h for carbonaceous materials (Cox et al. 2000).

Hg(II) removal and q_e Vs initial Hg(II) are plotted in Fig. 4.25. Opposite trend was observed between Hg(II) removal (%) and the amount removed (q_e). It can be observed that with increase in initial Hg(II) from 5 to 1000 mg/L, removal (%) decreased from 100 to 31% whereas q_e increased from 2.4- 174 mg/g. For a fixed AFC dose, the total available adsorption sites are limited thereby adsorbing almost the same amount of Hg(II). This was responsible for decrease in the percentage removal of the Hg(II) corresponding to an increase in initial Hg(II) concentration. However at higher initial concentrations, the ratio of initial number of moles of Hg(II) to the available surface area is high. This enables more chances of interaction between Hg(II) and active sites of AFC at higher initial concentration thus q_e increased with increased in initial Hg(II) concentration.

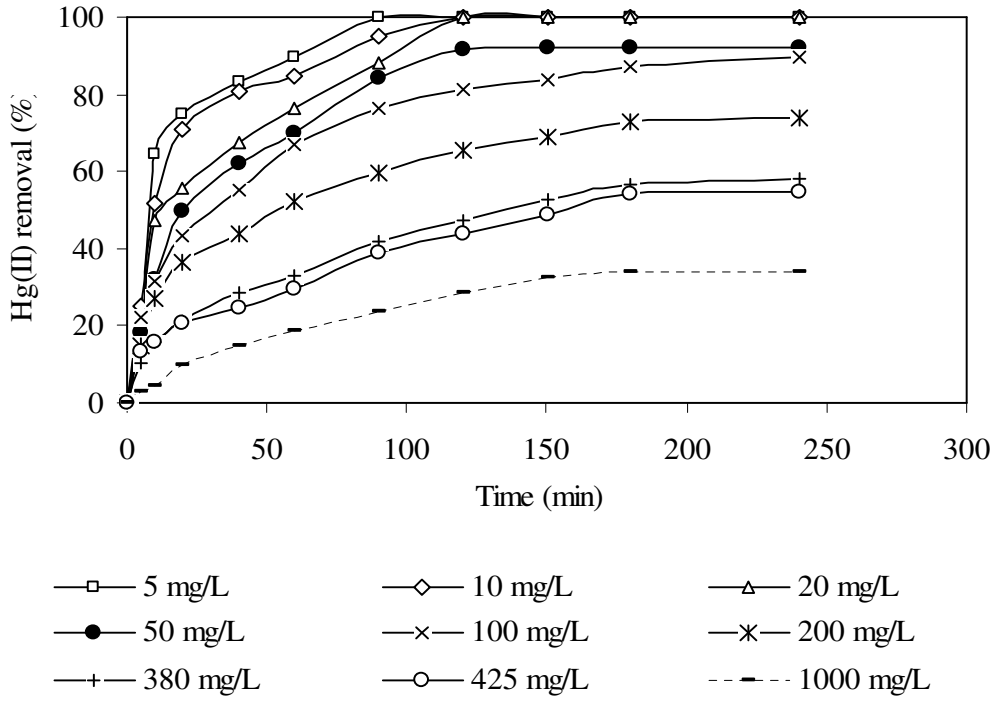

Figure 4.24: Effect of time on removal of Hg(II) by AFC coated silica gel

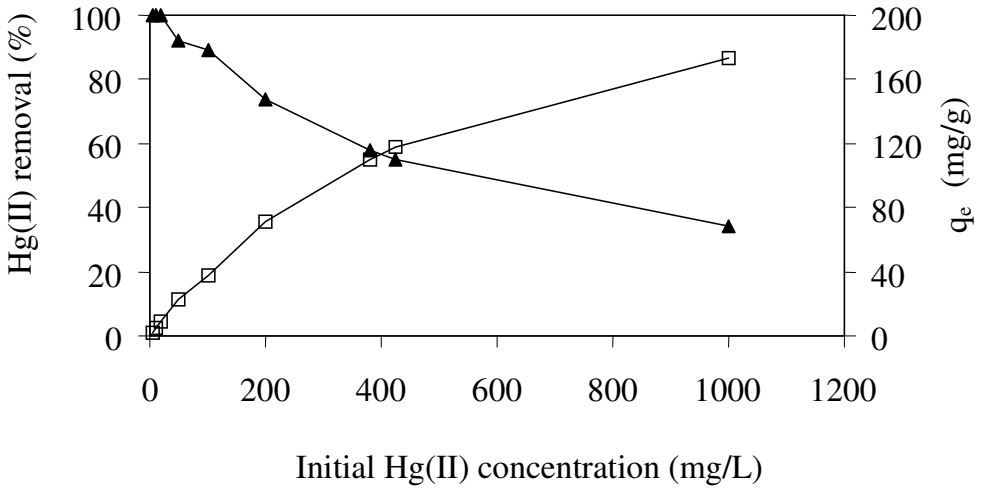

Figure 4.25: Effect of Hg(II) initial concentration on adsorption on AFC coated silica gel

(c) Adsorption Isotherm

Isotherm study was carried out by contacting varied concentration of Hg(II) (5- 1000 mg/L) with 2 g/L AFC coated silica gel at pH 7. Isothermal data were treated with Langmuir's and Freundlich's isotherm model equation and the obtained isotherm parameters are shown in

Table 4.8. Based on higher correlation coefficient (R^2) and lesser χ^2, isotherm data is better fitted to Langmuir model supported by Langmuir's R_L value less than 1. However high regression coefficient of Freundlich's equation along with intensity factor 'n' > 2.1 suggests the applicability of Freundlich equation on adsorption of Hg(II) by AFC coated silica gel. Similar isothermal nature of fixing on both Langmuir and Freundlich's isotherm was also observed on removal of Hg(II) by activated carbon derived from fertilizer waste (Mohan et al. 2001), sago waste (Kadirvelu et al. 2004), microalgae *Chlamydomonas reinhardtii* immobilized in alginate beads (Bayramoğlu et al. 2006).

Table 4.8: Comparison of Freundlich's and Langmuir's isotherm coefficient for Hg(II) adsorption on AFC

Freundlich's				Langmuir's				
K_f (mg/g)	n	R^2	χ^2	Q_{max} (mg/g)	b (L/mg)	R^2	R_L	χ^2
8.9	2.1	0.95	10.8	175.4	0.01	0.98	0.94	3.6

In Table 4.9, Removal capacity of Hg(II) by several adsorbents was compared. Removal capacity of AFC coated silica was bit comparable to furfural only with other adsorbents exhibiting higher removal. Contribution of weight of support material silica gel to the AFC polymer is one of the reason for lesser competition by AFC coated silica gel.

Table 4.9: Comparison of removal capacity of Hg(II) by various adsorbents with different functional group.

Adsorbent	Functional Group	Maximum removal capacity of Hg(II) (mg/g)	Reference
Furfural	C_xSO_3H	174	Yardim et al. 2003
Chitosan	Amines with ethylenediamine	462	Jeon and Ho¨ll 2003
Synthetic resin	Amine and mercaptan	621.8	Atia et al. 2005
White rot fungus *Lentinus edodes*		336	Bayramoğlu and Arıca 2008

(d) Desorption

Study of desorption was carried out by employing various desorbents like HCl, H_2SO_4, HNO_3, KI and EDTA of varied strength. The result is shown in Figure 4.26. At strength of 0.005 M, desorption was low (53- 68%) with all desorbents. However, almost 88- 100% desorption was achieved at higher desorbent strength (0.2 M EDTA & 2 M mineral acid). Iodine present in KI is known to form relatively strong complexes of Hg(II) (Kadirvelu et al. 2004) and thus behaved better desorbents than others. However for practical use in wastewater treatment, mineral acid though little less efficient than KI, might prove as cost-effective. Irrespective of desorption (%), all desorbing agents however completed desorption within 10 mins and is shown in Figure 4.27. Such rapid desorption indicates surface adsorption of Hg(II) on amines of AFC coated silica gel.

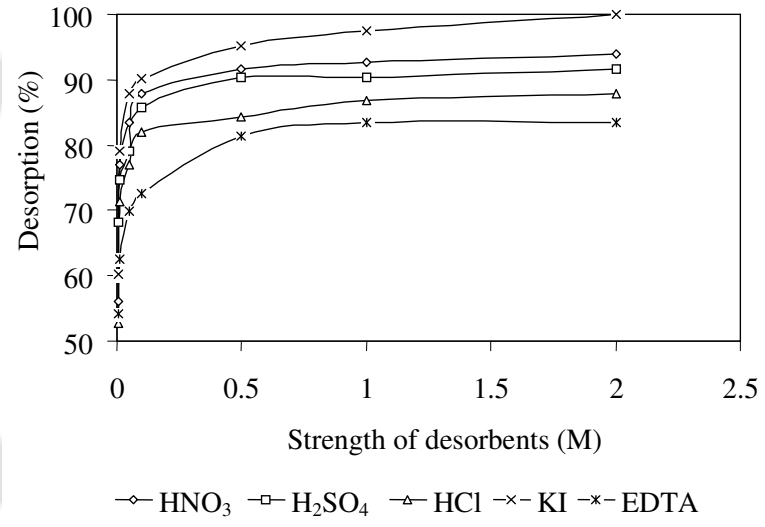

Figure 4.26: Desorption of Hg(II) by different strength of desorbents

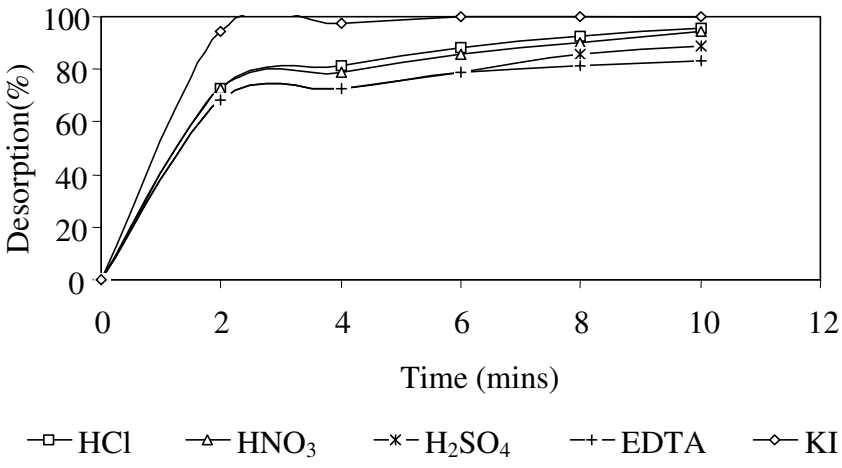

Figure 4.27: Effect of different desorbent strength

4.1.2.5 Removal of metal ions from mixed metal system

In natural wastewaters, toxic metallic species rarely exist singly and coexist with various other metal ions. Hence the presence of those metals produces interactive effects that could influence the removal of the desired metal ion. In order to investigate the affinity of metal ions towards the active sites of AFC coated silica gel, solution containing mixtures of Cu(II), Ni(II), Cr(III), Pb(II), Cd(II) and Hg(II) each of 0.5 mmol was contacted with 2 g/L of AFC coated silica gel (Figure 4.28). Cu(II) showed maximum adsorption with q_e value of 0.218 mmol/g, followed by Ni(II) of slight lesser q_e value of 0.211 mmol/g and Cr(III) with 0.192 mmol/g. Hg(II) and Pb(II) showed similar q_e value upto initial 60 min. Above that time, Hg(II) removal increased than removal of Pb(II) with q_e of 0.15 mmol/g for Hg(II) and 0.09 mmol/g for Pb(II). Cd(II) showed the lowest preference for amine with negligible q_e value of 0.008 mmol/g. Binding of metal ions by amine ligand can be explained by hard-soft theory of acids and bases as suggested by Pearson (Pearson 1963). According to the classification of metal ions (hard or soft acids), Cr(III) is hard acid, Cu(II) and Ni(II) are "borderline hard acids" whereas Pb(II) is "borderline soft acid" and Hg(II) and Cd(II) are "soft acids". Hence hard base amine ($-NH_2$) of AFC formed strong and stable complex with hard acid Cr(III) and borderline acids Cu(II) and Ni(II) as compared to soft acids Hg(II), Pb(II) and Cd(II). It is reported that ligand exchange rates are faster for the divalent metal ions as compared to trivalent metals (Lippard and Berg 1994). Exchange rates for water molecules from the first coordination sphere of Cu(II) and Ni(II) and Cr(III) at 25 ºC are reported as: Cu(II): 1×10^9 sec^{-1}; Ni(II): 4×10^4 sec^{-1} and Cr(III): 2×10^{-6} sec^{-1} (Lippard and Berg 1994) suggesting Cu(II) having higher exchange rate compared to Ni(II) and Cr(III) is kinetically almost immobile compared to Cu(II) and Ni(II). Due to higher ligand exchange rate Cu(II) adsorption was higher than Ni(II), whereas kinetically inert Cr(III) was slow and sluggish to react with AFC. Even though the bond between "hard acid" Cr(III) and "hard base" amine is thermodynamically favored, due to kinetic limitation, Cr(III) removal was less compared to Cu(II) and Ni(II) ions. Higher binding constant ("b" of Langmuir's model) was observed for Cr(III) as compared to Cu(II) in single metal-AFC studies (Kumar et al. 2007) [4.160 L/mmol for Cr(III) and 1.386 L/mmol for Cu(II)], suggesting that Cr(III) adsorption by AFC was thermodynamically favoured than Cu(II).

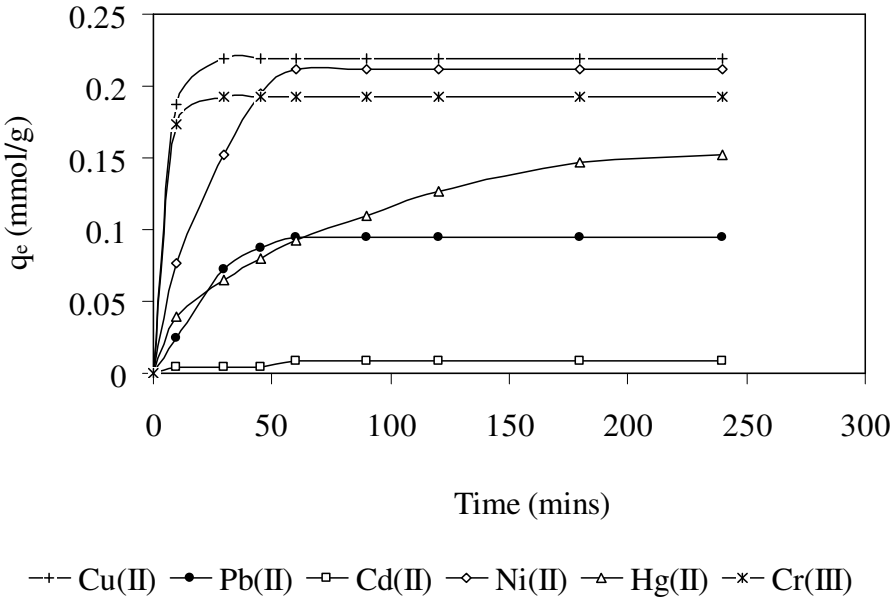

Figure 4.28: Competition on removal of metal ions by AFC from a mixed solution

4.1.2.6 Regeneration of AFC

During desorption experiment it was observed that in various desorbing agents, along with cationic metal ions, significant amount of polymer also released from surface of silica gel (as solution turn yellow). This polymer from mineral acid solution was extracted out and silica gel was recoated using this polymer. As such regeneration of adsorbent reduced the overall cost of adsorbent. The regeneration of AFC was conducted for several cycles using Hg(II) as the heavy metal ion and the results are presented in Table 4.10.

Table 4.10: Performance of AFC in removing Hg(II) in several cycles after regeneration

No of experiment cycle	C_o (mg/L)	C_e (mg/L)	AFC dose (g)	Removal (%)
Original	80	2	25	97.5
1st	85	11	14	87.0
2nd	83	11	7	86.7
3rd	85	17	4.5	80

As expected, the removal (%) for original experiment when fresh AFC was used more than 97%. At 1st cycle 87% removal of Hg(II) was achieved and efficiency of AFC still remained same for 2nd cycle and that decreased to 80% after 3rd cycle. Since adsorbed Hg(II) were not recovered back completely by desorption using mineral acids, some amount of Hg(II) were left in the adsorbent matrix occupying the active sites of amine. Thus amount of

available active sites were decreased with every regeneration cycle obtaining a decrease in removal of Hg(II). Above this, it was also observed that the amount of AFC coated silica gel decrease gradually from 25 g to 4.5 g with number of cycle increased till the 3rd cycle. Probably some polymers as well as silica gel were washed out while decanting, filtering, and shifting of polymers from one vessel to another during the course of regeneration as mentioned in material and method section. This is also one of the reason for decrease in removal (%) of Hg(II) as regeneration cycle increase.

4.1.3 Continuous column mode operation study

In batch process, adsorption equilibrium is achieved and adsorption characteristics are analyzed using isotherms. However batch data has several limitations to predict the performances in practical situation such as actual industrial wastewater treatment plant, where batch operation is replaced by continuous reactors. In fixed-bed column, the adsorption zone or mass transfer zone keeps moving through the bed and the liquid and solid phase in that zone are never able to achieve equilibrium. Therefore obtaining a correlation between batch and column operation is necessary. In the present work the suitability of AFC in column mode was studied using Hg(II) as the metal ion.

4.1.3.1 Mercury [Hg(II)]

(a) Effect of bed depth

Effect of bed depth in column mode adsorption of Hg(II) was carried out by employing three columns of bed depth 10, 20 and 30 cm filled with 50, 100 and 150 g of AFC coated silica gel respectively. Influent Hg(II) concentration of 25 mg/L and 50 mg/L with optimum pH 6.5 were fed at constant flow rate of 5 mL/min and results are illustrated in Figure 4.29. Before the column operation starts with Hg(II) solution, the column bed was fed with distilled water adjusted at pH 6 to minimize pH fluctuations during mercury-AFC interaction. The breakthrough times (corresponding to $C/C_o = 5\%$) were found to be 31- 127 hour for column bed depth of 10- 30 cm respectively when initial Hg(II) was 25 mg/L. The corresponding breakthrough times at initial Hg(II) 50 mg/L were 21- 84 hour respectively. It is obvious that with increase in bed depth (10- 30 cm), there were more contact time between Hg(II) and AFC resulting more Hg(II) to adsorb and delayed the breakthrough time. However with increase in initial Hg(II) from that 25 mg/L Hg(II) to 50 mg/L, loading rate of Hg(II)

increased, and saturated the AFC more quickly thereby decreasing the breakthrough time. Besides it can be observed that slopes (dc/dt) of the breakthrough curve increased from 1.34 to 3.33 mg/Lh with increased in initial Hg(II) from 25 mg/L to 50 mg/L (Table 4.11).

These findings infact clearly indicate early saturation of column bed for higher initial concentration. The exhaustion time for 10- 30 cm bed depth also increased from 53- 150 hour for initial Hg(II) 25 mg/L but consequently less corresponding depth for Hg(II) 50 mg/L (37-105 hour). Even though breakthrough and exhaust time decreased with increase in initial Hg(II), the uptake of Hg(II) was observed to follow opposite trend. With increase in bed depth from 10- 30 cm, Hg(II) removal till exhaust time increased from 295- 987 mg (calculate using equation 2.22) for initial Hg(II) 25 mg/L where corresponding removals at Hg(II) 50 mg/L were higher with 356- 1383 mg Hg(II). However the uptake of Hg(II) ($q_{e,col}$) by AFC coated silica gel increased from 5.89 to 6.58 mg/g AFC with increased in bed depth from 10 to 30 cm at initial Hg(II) 25 mg/L. At lower bed depth, predominant mass transfer phenomenon was the axial dispersion and reduced the diffusion of Hg(II) ions effectively (Taty-Costodes et al. 2005). Also with increase in bed depth, mass transfer zone got broadened as well as more binding sites for adsorption of Hg(II) ions were available. At initial Hg(II) 50 mg/L, $q_{e,col}$ further increased from 7.11 to 9.22 mg/g with increase in bed depth from 10 to 30 cm. However such low $q_{e,col}$ value as compared to q_e value of batch process of 174 mg Hg(II)/g probably may be due to less contact time (residence time) between adsorbate and adsorbent for column mode operation. Similar observation was reported on removal of Pb(II) ions by immobilized *Pinus sylvestris* sawdust with q_e of 7.14 mg/g in batch process as compared to 1.7, 1.6 and 2.2 mg/g at inlet concentrations of 3, 5 and 10 mg/L respectively in continuous fixed bed column (Taty-Costodes et al. 2005). Since fixed bed needs to be changed once the discharge limit or breakthrough is reached, utilization of full bed capacity of column is not the main criteria in treating industrial wastewater. However running till the exhaustion experimentally is necessary to understand the mechanism and nature of metal adsorbent interaction and to analyze the application of mathematical models. Interestingly it was observed that irrespective of initial Hg(II), the removal (%) for both Hg(II) 25 and 50 mg/L were almost similar with 86- 87% unlike different removal (%) at different initial Hg(II) concentration at batch process. In fact these findings depict the difference in mechanism between batch and column mode operations.

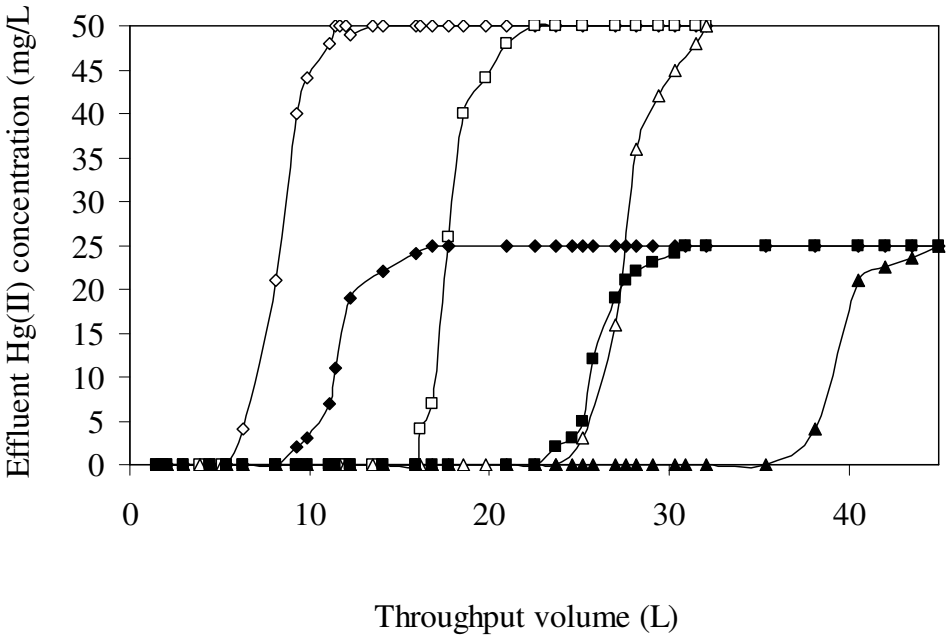

Diamond, square and triangle represent bed depth of 10, 20 and 30 cm respectively

Hollow symbol represents initial Hg(II) 50 mg/L;

Filled symbol represents initial Hg(II) 25 mg/L

Figure 4.29: Effect of bed depth on removal of Hg(II) by AFC[Initial Hg(II) 25 and 50 mg/L]

Table 4.11: Breakthrough time, exhaust time, breakthrough volume, exhaustion volume, total Hg(II) removed, Hg(II) uptake and removal (%) of Hg(II) (flow rate 5 mL/min)

Initial Hg(II) (mg/L)	Depth (cm)	t_b (h)	t_E (h)	V_b (L)	V_E (L)	dc/dt (mg/L h)	Mr (mg)	q_e (mg/g)	Removal (%)
25	10	31	53	9.3	15.9	1.35	294.8	5.89	26.2
	20	82	101	24.6	30.3	1.34	654.9	6.55	58.1
	30	127	150	38.1	45	1.35	986.9	6.58	87.7
50	10	21	37	6.3	11.1	3.33	355.7	7.11	22.2
	20	56	70	16.8	21	3.25	897.5	8.98	55.9
	30	89	105	25.2	31.5	3.33	1383.3	9.22	86.2

(b) Theoretical breakthrough curve

The theoretical breakthrough was generated with the initial Hg(II) concentration of 25 and 50 mg/L Hg(II). The equilibrium line was prepared using Langmuir's adsorption

isotherm of batch work of $q_e = \frac{175.4\,x\,0.01C_e}{1+0.01C_e}$. An operating line was drawn passing through the origin and intersecting the equilibrium curve at C_o of 25 mg/L and 50 mg/L yielding respective q_e values of 35.08 mg/g and 58.46 mg/g and is shown in Figure 4.30.

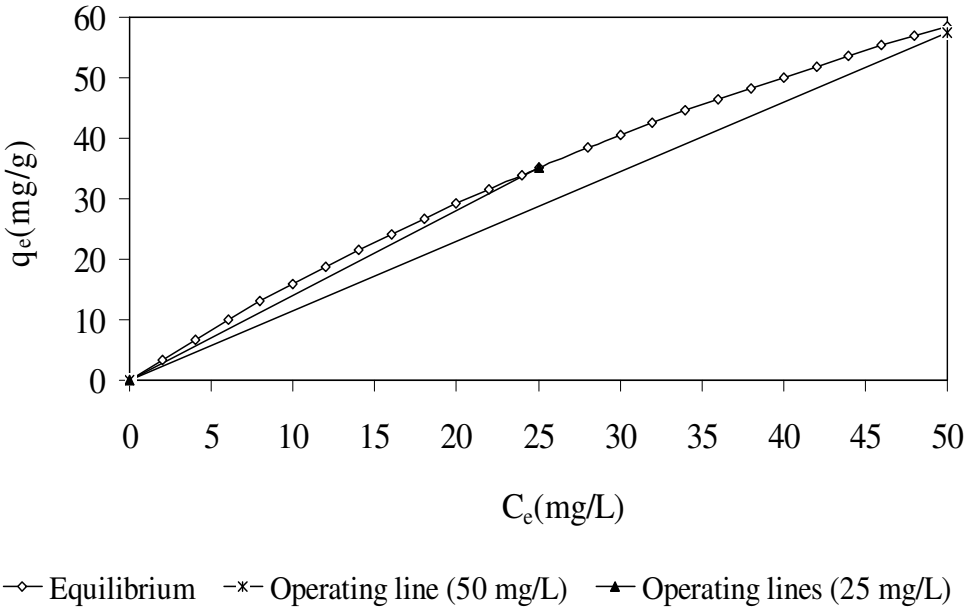

Figure 4.30: Equilibrium and operating lines to predict breakthrough curve

A graph of C versus $(C - C_e)^{-1}$ was plotted where the area under the curve of $(C - C_e)^{-1}$ represented the value of the integration of Equation 2.37 and is shown in Figure 4.31. For initial Hg(II) of 25 mg/L and 50 mg/L, 105.42 and 49.71 sq. units were obtained respectively. The theoretical breakthrough curves were generated by plotting $(V_t - V_B)/(V_E - V_B)$ versus (C/C_o). It can be seen in Figure 4.32 that for both the initial Hg(II) of 25 mg/L and 50 mg/L, the experimental and theoretical breakthrough curves followed the same trend.

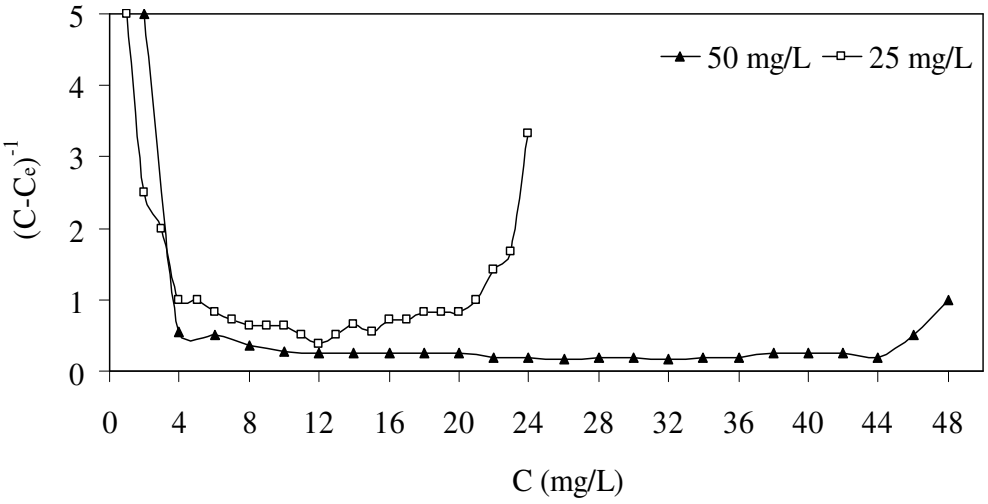

Area under Curve of 25 mg/L = 105.42 sq. units
Area under Curve of 50 mg/L = 49.71 sq. units

Figure 4.31: Curve area to evaluate for determination of theoretical breakthrough curve of Hg(II)

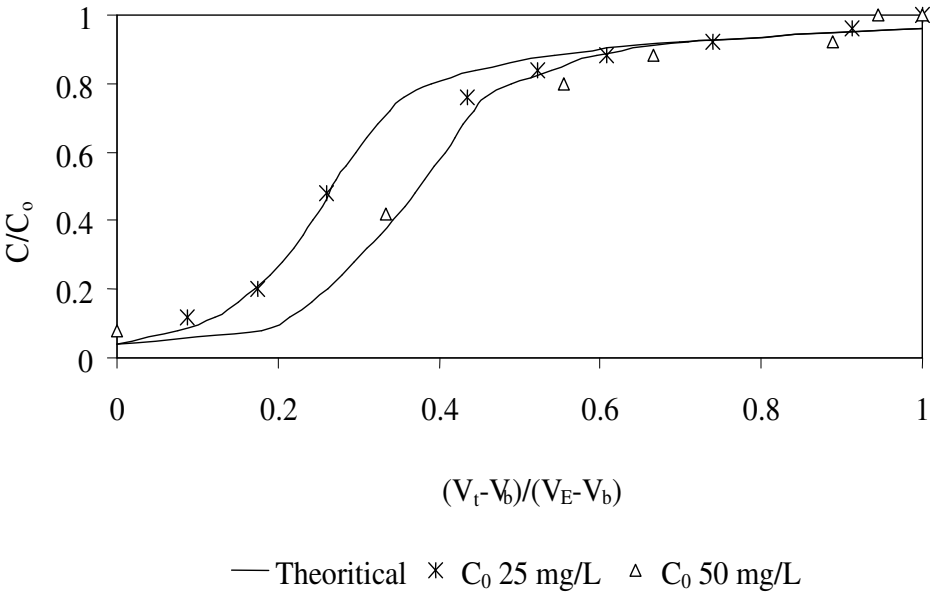

Figure 4.32: Theoretical and experimental breakthrough curve of Hg(II)

4.2 Studies with PANI-jute

4.2.1 Synthesis and characterization of PANI synthesized on support materials

Metal removal was studied using another amine based polymer, polyaniline (PANI). Instead of coating this polymer on support medium, it was directly synthesized on the support medium itself to improve the stability. To yield polymer with maximum metal removal capacity, synthesis of polyaniline was optimized with respect to chain length. Selection of supporting material and optimization of amount of support material for PANI was also studied. Metal ions considered for the study in batch mode were Cr(VI), Cr(III), Cu(II), Cd(II), Pb(II) and Hg(II). Removal of Hg(II) was also studied in continuous column mode.

4.2.1.1 Screening of supporting materials

Previous work was carried out on AFC coated on silica gel. For the support for PANI, an attempt was made for waste biomaterials such as saw dust (SD), tea leaves (TL), fly ash (FA), jute fiber (JF) and rice husk (RH). Such waste biomaterials are combustible and thus can be ignited after metal binding by PANI synthesized on it which in turns will minimize the problem of solid waste disposal. It is already known that at acidic pH Cr(VI) is converted to Cr(III) by various biomaterials. Therefore various biomaterials were subjected to Cr(VI) solution at strong acidic pH and degree of reduction to Cr(III) was checked. For the study, initial Cr(VI) of 50 mg/L was contacted with 2 g/L dose of different SD, TL, FA, JF and RH separately at varying pH. The findings are presented in Figure 4.33. Optimum pH for TL, SD and RH were observed at pH 2 whereas that of FA and JF at pH 3. Within pH 1 and 3, reduction of Cr(VI) were 64- 74%, 36- 58%, 86- 96%, 10%- 20% and 8- 12% by SD, TL, FA, JF and RH respectively. During experimentation, RH remained floating on surface making it difficult to mix uniformly with metal solution. FA and SD were difficult to separate from the solution after metal adsorption due to its smaller size. From workability point of view, only TL and JF were the better alternatives. However total chromium removal and reduction was much higher with TL as compared to JF. Therefore JF was selected as the supporting material for PANI for removal of metal.

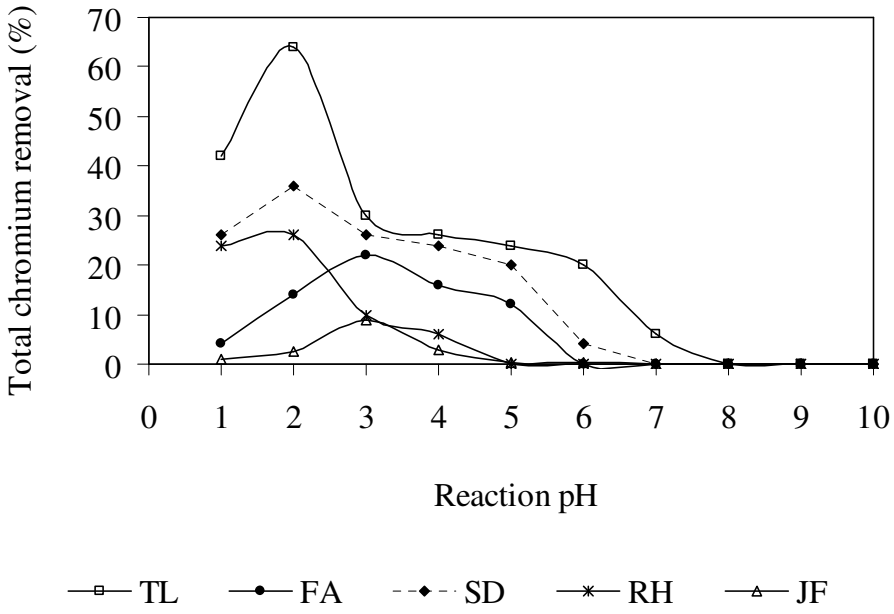

Figure 4.33: Removal of Cr(VI) at different pH by various support materials [Initial Cr(VI) 50 mg/L; dose 2g/L; agitation time 24 h]

4.2.1.2 Optimization of amount of base support (jute fiber)

In our previous work with AFC coated on silica gel, it was observed that coating was a physical one with moderate stability as it was unstable in organic solvent. In order to improve the stability we directly synthesized the PANI on JF. The amount of jute fiber for PANI synthesis was determined by varying JF (1– 10 g) and contacted with initial Cr(VI) of 50 mg/L at solution pH 3. From Figure 4.34, it can be seen that PANI-jute exhibited a maximum removal of almost 40% when amount of jute fiber support base was 1 to 5 g. With increase in the amount of jute more than 5 g, removal of total chromium decreased. Probably excess amount of support medium resulted less and non-uniform amount of polymer on the surface of jute fiber. The maximum 5 g of JF was considered for PANI-jute synthesis (with 21.5 mmol aniline and 3.05 mmol chain terminator agent 1,4-phenylenediamine) for further investigations.

4.2.1.3 Characterization and optimization of PANI-jute

(a) Optimization of ratio of aniline and chain terminating agent 1,4-phenylenediamine

The molar ratio of amine source (aniline) to chain inhibitor (1,4-phenylenediamine) was varied to control the chain length of PANI-jute with fixed aniline of 21.5 mmol with

varied 1,4-phenylenediamine of 2- 4 mmol. Results are shown in Table 4.12. With 2 mmol of 1,4-phenylenediamine, amount of total chromium adsorbed were 7.5 mg/g and 20 mg/g from initial Cr(VI) concentration of 50 and 120 mg/L respectively. With increase in 1,4-phenylenediamine amount to 3.05 mmol, amount of total chromium adsorbed increased to 12 and 29.5 mg/g respectively. However, these decreased to 10.5 mg/g and 22 mg/g with further increase in amount of 1,4-phenylenediamine to 4 mmol. When amount of chain length inhibitor (1,4-phenylenediamine) was increased, chain length of PANI decreased yielding an increase in number of terminal NH_2 groups per gram of polymer due to reduction in formula weight of chain of PANI, and this was responsible for increase in amount of total chromium adsorbed. With further increase of quantity of chain inhibitor, the solubility of PANI also increased and washed out from jute fiber surface and chromium adsorption decreased due to availability of fewer polymers. Therefore optimum 1,4-phenylenediamine of 3.05 mmol was fixed and used for preparation of PANI-jute for further investigation on removal of metal ions.

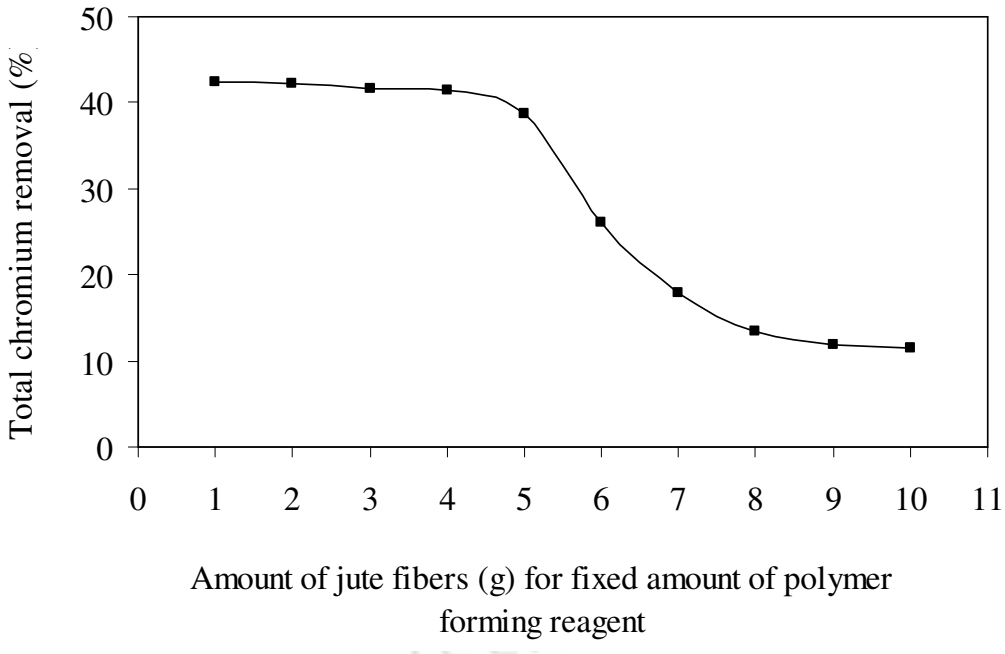

Figure 4.34: Optimization of support materials (jute) for synthesizing PANI on it [initial Cr(VI) 50 mg/L; pH 3; dose 2 g/L]

(b) Chain length of PANI-jute

From structure of PANI, it can be understood that higher the chain length of the PANI, molecular weight of PANI will increase but removal of metal ions will be lesser due to

presence of amines at terminal end only. However shorter the chain length will unable the polymer to remain insoluble. To characterize the polymer, polyaniline coated on jute fiber was dissolve in N,N′-dimethylformamide (DMF) solvent and investigate by UV spectra and is shown in Figure 4.35. Literatures mentioned that polyaniline of shorter chain length shows maximum absorbance at 572 nm (Wei et al. 1996) and higher chain length shows maximum absorbance at 635 nm (Huber 2003). With maximum peak λ_{max} at 561 nm, the synthesized PANI-jute is short chain polyaniline (oligoaniline).

Table 4.12: Optimization of chain length of PANI synthesized on jute fiber

Amount of 1,4-phenylenediamine during PANI synthesis (mmol)	Amount of total chromium adsorbed (mg/g) by PANI-jute	
	Initial Cr(VI) 50 mg/L	Initial Cr(VI) 120 (mg/L)
2.00	7.5	20
2.50	10	27.5
3.05	12	29.5
3.50	11	24
4.00	10.5	22

Solution pH 3; initial Cr(VI) 50 and 120 mg/L; PANI-jute 2 g/L

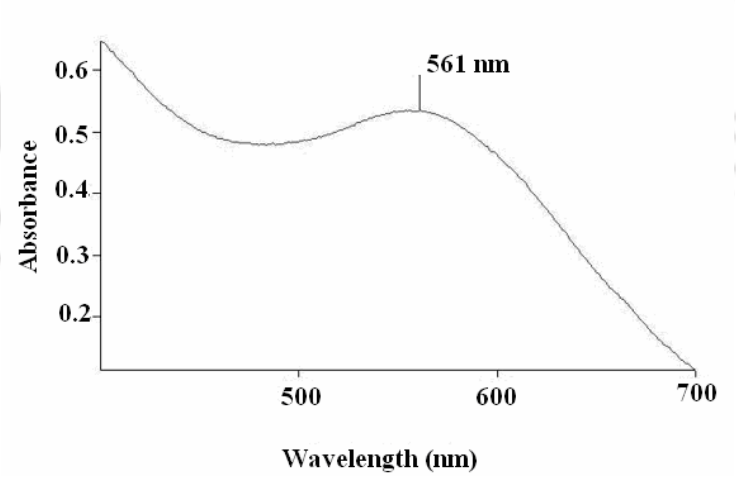

Figure 4.35: UV spectra of PANI-jute

(c) pH of zero point charge (pH_{ZPC})

To know the surface charge of adsorbent to assess the mechanism of metal binding at a particular pH, pH of zero point charge (pH_{ZPC}) of PANI-jute was determined. From Figure

4.36, it can be clearly seen that pH_{ZPC} for PANI-jute was 6.6. Therefore below pH 6.6, the acidic water will donate more proton than hydroxide groups, and so the PANI-jute surface will be positively charged. Conversely, above pH 6.6, the surface of PANI-jute will be negatively charged. pH_{ZPC} of PANI-jute is about the same as AFC (section 4.1.1.4) reflecting similarity (amine in the surface) of the adsorbent.

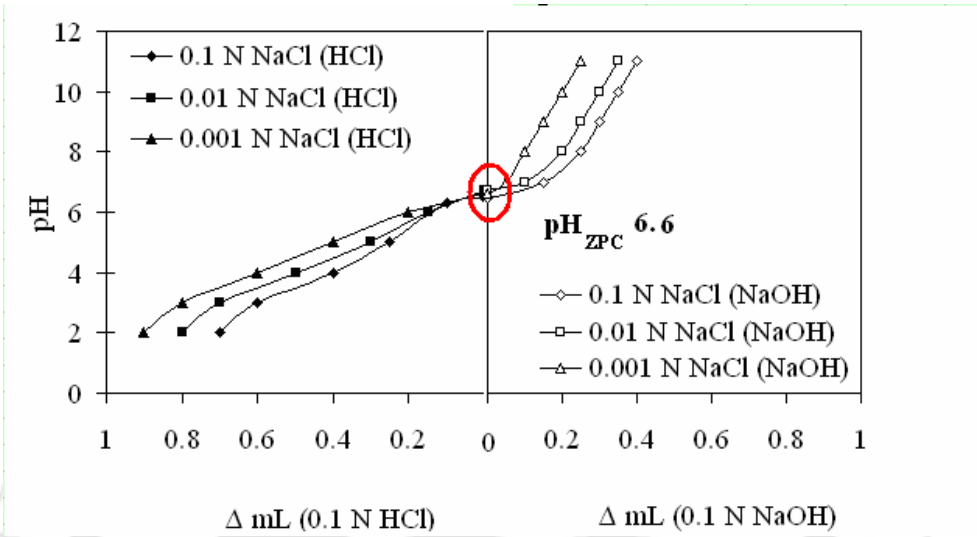

Figure 4.36: pH of zero point charge (pH_{ZPC}) of PANI-jute

(d) Surface characteristics of PANI-jute

SEM images were investigated to analyze the surface morphology of PANI-jute. It can be seen from the Figure 4.37(a) that the surface of PANI-jute was smooth and even. EDX analysis was employed to further check the elements present in the polymer. Only carbon and oxygen were visible on PANI-jute suggesting the absence of impurities in PANI-jute [Figure 4.37(b)].

4.2.2 Removal of metal ions by PANI-jute in batch mode

4.2.2.1 Hexavalent chromium [Cr(VI)]

Investigation on removal of Cr(VI) was conducted in batch mode and study parameters include reaction pH, initial concentration of Cr(VI), dose of adsorbent and temperature. Chromium adsorption kinetics, isotherm, desorption, recovery of the adsorbed chromium from PANI-jute were also investigated.

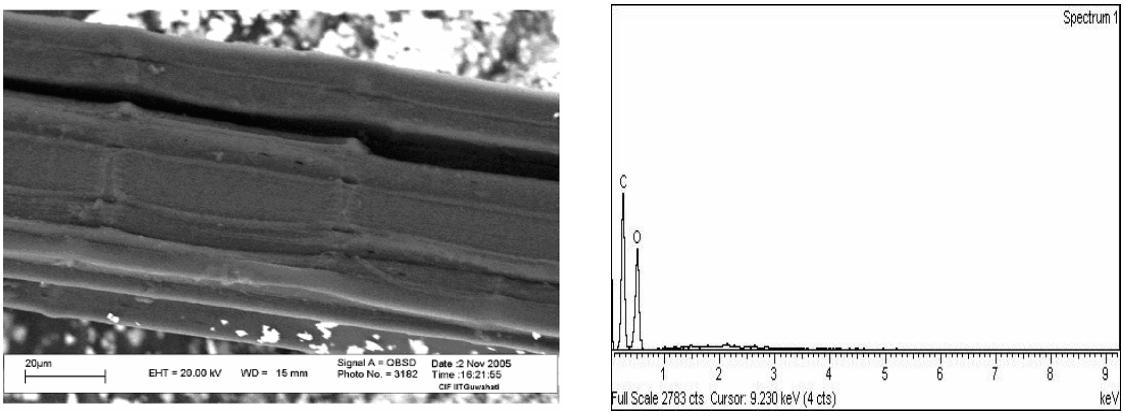

Figures 4.37(a): SEM images & Figure 4.37(b): EDX spectra of PANI-jute

(a) Effect of pH and mechanism of Cr(VI) removal

To study the effect of pH on removal of Cr(VI) by PANI-jute fiber, initial Cr(VI) concentration of 10 mg/L and 50 mg/L were contacted with 2 g/L of PANI-jute at various pH from pH 1- 10 and results are shown in Figure 4.38. It can be seen that, with the increase in solution pH from 1 to 3, total chromium removal increased from 47 to 72% and 35 to 48% for initial Cr(VI) concentrations of 10 and 50 mg/L respectively approaching a plateau at pH 3. However with further increase in pH above 3, removal of total chromium decreased significantly with sharp drop at pH 5 and negligible removal at pH 8 and above. It is known from our previous studies with AFC that Cr(VI) remained soluble in all solution pH suggesting no precipitation of Cr(VI). Similar pH trend with plateau formation on removal of chromium were also observed by various adsorbents like wool, olive cake, sawdust, pine needles, almond, coal and cactus with optimum pH 2 as well as by modified PVP-coated silica gel at pH 5.5 (Dakiky et al. 2002; Gang et al. 2000) and also by AFC coated silica gel at pH 3. Such plateau formation with chromium adsorption decreasing on both sides of optimum pH 3 suggests different mechanisms of interaction of Cr(VI) and PANI-jute.

As we know that Cr(VI) was easily reduced to Cr(III) at acidic pH, distributions of Cr(VI) (%) and Cr(III) (%) in solution at various pH levels were estimated and values are given in Table 4.13 in columns E and F respectively for both initial Cr(VI) of 10 and 50 mg/L. Estimation was also crosschecked on the solid phase adsorbent by digesting PANI-jute loaded chromium in a microwave digester in presence of nitric acid (0.2 N) and then chromium concentration was measured in digested solution. In our previous study, AFC coated on silica gel after adsorption of metal ions metal could not be digested as it requires higher pressure than that of jute fiber. Besides, estimating amount of Cr(VI) in effluent after

adsorption (column A, Table 4.13), chromium bounded PANI-jute was also digested in 0.2 nitric acid and total chromium was estimated in digested solution (Column B, Table 4.13) to cross check the estimation. A difference of 0.47- 3.9% indicate a minimum error between the two different types of analysis.

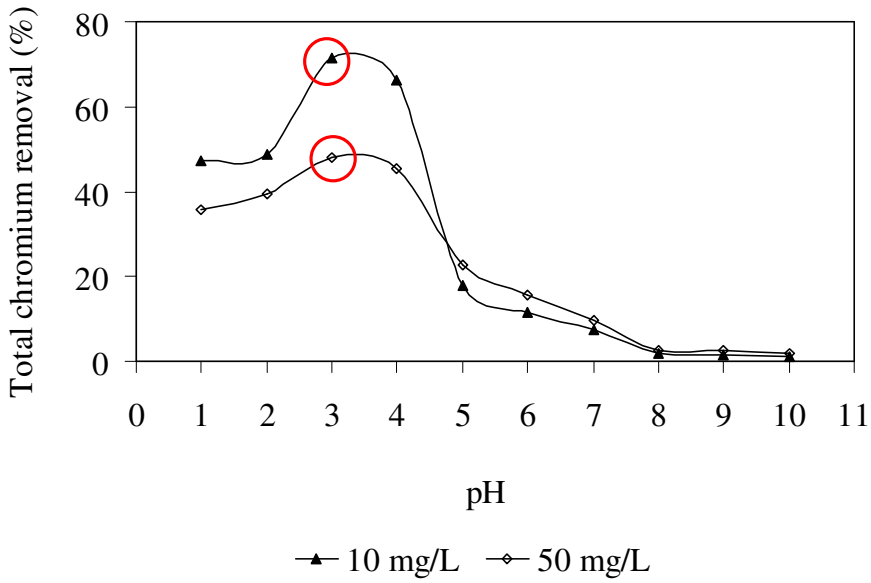

Figure 4.38: Effect of pH on total chromium removal [dose: 2g/L; agitation time: 24 hours].

In the acidic pH range of 1 and 2, almost 66 to 73% of total chromium in the treated solution was in the form of reduced Cr(III) for both initial Cr(VI) concentration of 10 and 50 mg/L (column F, Table 4.13). However the corresponding Cr(III) amount in solution at pH 3 were only 3.9% and 6.6% of treated effluent with 72% and 48% of initial Cr(VI) adsorbed (Figure 4.38). At pH above 3, amount of Cr(III) in solution was almost negligible (column D, Table 4.13). Such insignificant amounts of Cr(III) in the treated solution at pH 3 and above indicates the possibility of either less reduction of Cr(VI) to Cr(III) or adsorption of reduced Cr(III) by PANI-jute. Therefore, the possibility of Cr(III)- PANI-jute interaction was checked with initial Cr(III) 50 mg/L and with 2 g/L PANI-jute at pH 1– pH 4 and observed insignificant removal of Cr(III). One of the most possible reason may be that at acidic pH, -NH_2 sites of PANI-jute was highly protonated and this was responsible for repulsion of Cr(III) ions. However, even though adsorption of whatever reduced Cr(III) by PANI-jute can be ruled out, Cr(VI) after adsorption may reduce to Cr(III) on the surface of PANI-jute itself. ESR (Electro spin resonance) technique was used to verify the presence of Cr(III) on PANI-jute surface. After adsorption experiment with Cr(VI) at pH of 2- 4, effluent solution and PANI-jute adsorbent were examined by ESR technique. The resonance signal of the effluent

solution after adsorption experiment at pH 2 appears at a magnetic field position corresponding to g value of 1.975 [Figure 4.39], confirming the presence of Cr(III) whose standard signal g value is 1.98 (Bryson 1980). When ESR was employed on effluent solution after adsorption experiment at pH 3 and 4, no spectra was observed indicating insignificant amount of Cr(III) in solution after adsorption experiment at pH 3 and 4. After ESR examination of PANI-jute adsorbent (after adsorption experiment at pH 2- 4), no spectrum was observed indicating absence of Cr(III) on solid PANI-jute surface after adsorption. This confirms that total chromium bounded on PANI-jute was predominantly Cr(VI) form with negligible or insignificant amount of Cr(III).

Table 4.13: Distribution of Cr(VI) and reduced Cr(III) in treated solution

pH	Initial Cr(VI) 10 mg/L						Initial Cr(VI) 50 mg/L					
	A	B	C	D	E	F	A	B	C	D	E	F
1	5.8	6.0	1.6	4.2	27.6	72.4	31.2	32.0	8.3	22.9	26.5	73.4
2	5.5	5.7	1.7	3.8	31.2	68.8	28.6	29.2	9.62	18.9	33.6	66.3
3	2.8	2.7	2.7	0.1	96.1	3.91	23.9	24.3	22.3	1.58	93.3	6.61
4	3.3	3.4	3.3	0.1	98.5	1.48	25.0	24.6	24.3	0.66	97.	2.63
5	8.4	8.3	8.4	0	99.8	0.23	37.5	38.0	36.9	0.53	98.5	1.41
6	9.0	9.2	9.1	0	100	0	41.5	41.8	41.5	0.02	99.9	0.05
7	9.2	9.4	9.2	0	100	0	46.3	46.2	46.3	0	100	0

A: Effluent total Cr (mg/L) after adsorption (Estimation based on filtrate solution)

B: Effluent total Cr (mg/L) after adsorption (Estimation based on digestion of PANI-jute)

C: Cr(VI) concentration (mg/L) in solution after adsorption

D: Cr(III) concentration (mg/L) in solution after adsorption (Subtracting values of column C from column A)

E: Cr(VI) in solution (%) with respect to effluent total chromium after adsorption

F: Cr(III) in solution (%) with respect to effluent total chromium after adsorption

During our studies of Cr(VI) removal by AFC coated silica gel, consumption of protons was observed during the reduction of Cr(VI) supported by Equation 4.5. To cross check the consumption of proton, adsorption of Cr(VI) experiment were further carried out without controlling the reaction pH and it was observed that solution pH increased from initial value of 2.2 to 2.5 on removal of 40 mg/L of Cr(VI) suggesting the consumption of 4 mmol of proton for removal of 1 mmol of Cr(VI). However, no shifting of pH was observed when experiment was conducted at pH 3 and above suggesting negligible reduction. In our previous

investigation, consumptions of 4.26 mmol of protons for each mmol of Cr(VI) removal by aniline formaldehyde condensate was observed at pH 2.5, while consumption of 3.99 and 2.7 mmol of protons for each mmol of Cr(VI) removal by dead biomass *Aspergillus niger* and *Rhizopus oryzae* were reported (Park et al. 2005a, Park et al. 2005b).

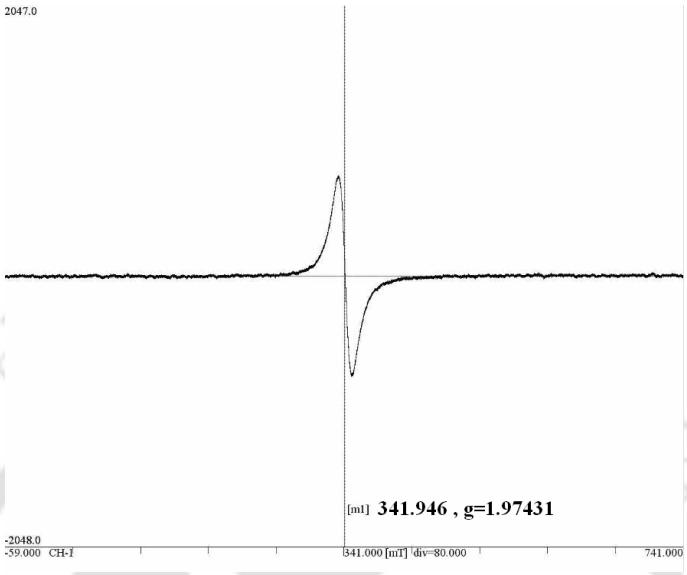

Figure 4.39: ESR spectra of Cr(III) on PANI-jute at pH 2

Based on the results of study on effect of pH on removals of Cr(VI) and Cr(III)] and ESR study with PANI-jute, it can be hereby concluded that, adsorption of total chromium on PANI-jute was only in the form of Cr(VI). A fate of Cr(VI) when interacted with PANI-jute at pH range of 1 to 7 is shown in Figure 4.40. At pH 1 to 4, Cr(VI) exists in solution as $HCrO_4^-$ (acid chromate) ions. In this acidic pH, $-NH_2$ of PANI exists in protonated form ($-NH_3^+$) and can form bond with acid chromate ion by electrostatic attraction. With pH increase from 4 to 6, amount of protonation on PANI-jute surface decreased yielding a decrease in total chromium adsorbed from 66- 7% and 45- 9% at initial Cr(VI) of 10 and 50 mg/L respectively. The optimum pH of 3-4 were also reported during removal of Cr(VI) by biomaterials like *Ecklonia* biomass (Park et al. 2004; Park et al. 2006). The main mechanism was reported as reduction coupled adsorption, where Cr(VI) was first completely reduced to Cr(III) at pH 3-4 and reduced Cr(III) formed complex with biomaterials (Park et al. 2006; Park et al. 2008), whereas in the present work the main mechanism of Cr(VI) removal by polymer at optimum pH 3 was anionic adsorption. The difference in behaviour between AFC and PANI shows despite the similarity in functional group present, difference in redox stability of PANI polymer backbone, significantly prevents Cr(III) oxidation.

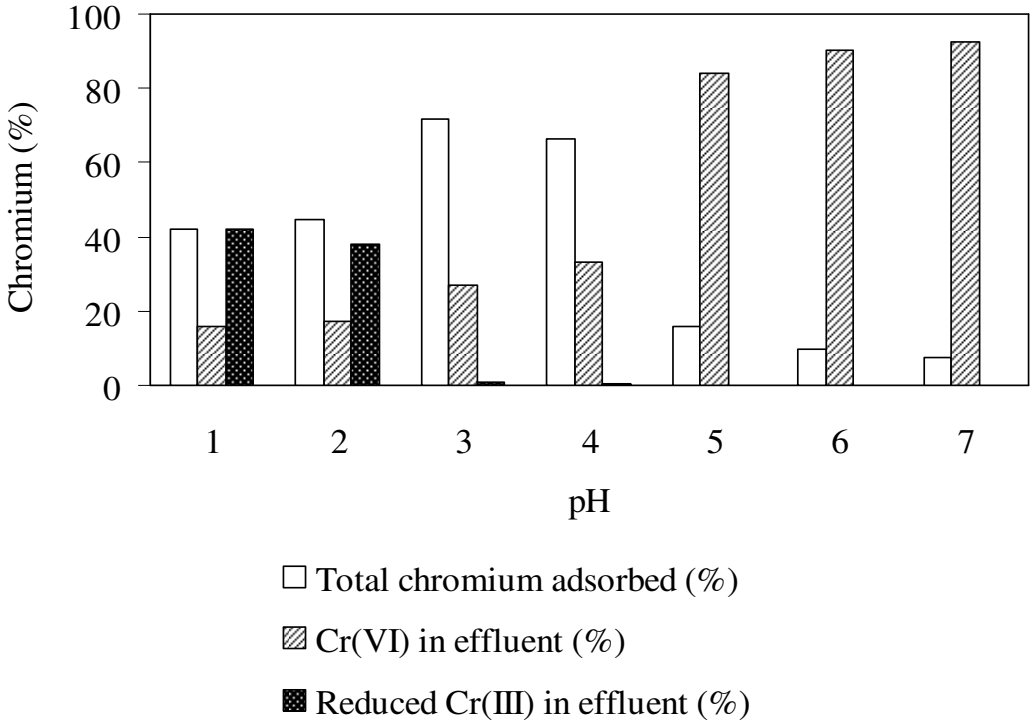

Figure 4.40: Fate of Cr(VI) after interaction with PANI at different pH range [Initial Cr(VI) 10 mg/L; effluent Cr(VI) and Cr(III) (%) shown are evaluated with respect to initial Cr(VI)]

(b) Adsorption isotherm

To identify the functional relationship between the amount of Cr(VI) in the bulk solution and adsorbed on PANI-jute, isotherm study was carried out. The regression data of Langmuir's and Freundlich's linear isotherm model are shown in Table 4.14. The regressions coefficient (R^2) for both the isotherms at reaction pH of 3 and 4 were much above 0.98 suggesting the data well fitted on both the isotherms. Lesser χ^2 value for Langmuir suggest the adsorption of chromium by PANI-jute can be described better by Langmuir's isotherm models. A polymer polyacrylamide grafted sawdust exhibited an adsorption capacity of 45 mg/g from initial chromium concentration of 100 mg/L at pH 3 (Raji and Anirudhan 1998) as compared to 62.9 mg/g of PANI-jute in the present study. Another amine based adsorbent polyacrylonitrile fibers was reported to remove a maximum of 35 mg/g from initial chromium of 50 mg/L at pH 5 (Deng and Bai 2004). Also, PVP coated on silica gel showed a maximum removal of 3 mg/g from initial chromium of 10 mg/L at pH 5 (Gang et al. 2000). Based on total chromium removal capacity, PANI-jute showed a better option.

Table 4.14: Regression data of Freundlich and Langmuir isotherm models for Cr(VI) adsorption by PANI-jute

Solution pH	Frendlich's isotherm				Langmuir's isotherm				
	K_f (mg/g)	n	R^2	χ^2	Q_{max} (mg/g)	b (L/mg)	R^2	R_L	χ^2
3	1.74	1.60	0.98	8.89	62.8	0.02	0.99	0.90	4.82
4	1.10	1.50	0.98	6.75	62.5	0.01	0.99	0.95	2.62

(c) Adsorption kinetics

Adsorption kinetics of chromium removal was studied and result is shown in Figure 4.41. Adsorption of total chromium increased from 1.43 to 61.65 mg/g with increase in initial Cr(VI) concentrations from 5 to 500 mg/L. With the increase in Cr(VI) concentrations, chances of interaction between chromate ions and PANI-jute increased and fractional removal of total chromium increased. Adsorption equilibrium was almost achieved within 40 min of agitation time for Cr(VI) of 50 mg/L and 2 h for initial Cr(VI) concentration of 500 mg/L. Such a rapid adsorption suggests a readily available, large surface area and smaller diffusion path of PANI-jute for chromium ions adsorption. Data were further treated with Lagergren's first order model and second order kinetics models. Correlation coefficient of well above 0.99 (Table 4.15) along with less error between calculated and experimental q_t values for second order model (with much less χ^2 value) suggest chromium adsorption following second order kinetics.

(d) PANI-jute dose effects on adsorption

Study on effect of dose on Cr(VI) and total chromium removal by PANI-jute was carried out and the result is shown in Figure 4.42. The rate of removal of Cr(VI) increased with increase in initial Cr(VI) concentration. Probably higher concentration of Cr(VI) allowed quicker and more bindings than lower initial Cr(VI) concentration for same dose of adsorbent. With increase in PANI-jute dose from 0.2- 30 g/L removal of total chromium were increased for all different initial concentration of Cr(VI) (Figure 4.42). The trend was as expected since more active sites of adsorbent were exposed when dose of PANI-jute increased. However, after rapid increase of adsorption of chromate ions with increase in PANI-jute dose up to 10 g/L, total chromium removal attained an asymptotic value for larger dose of PANI-jute. Such slow increase in removal beyond an optimum dose may attribute to the attainment of equilibrium between adsorbate and adsorbent at the operating conditions. This effect had been

termed as ‘‘solid concentration effect’’ i.e. overcrowding of particles, by Mehrotra (Mehrotra et al. 1999). From the economical point of view, 10 g/L would be suggested for the adsorption of total chromium for initial concentration of Cr(VI) of 20- 100 mg/L.

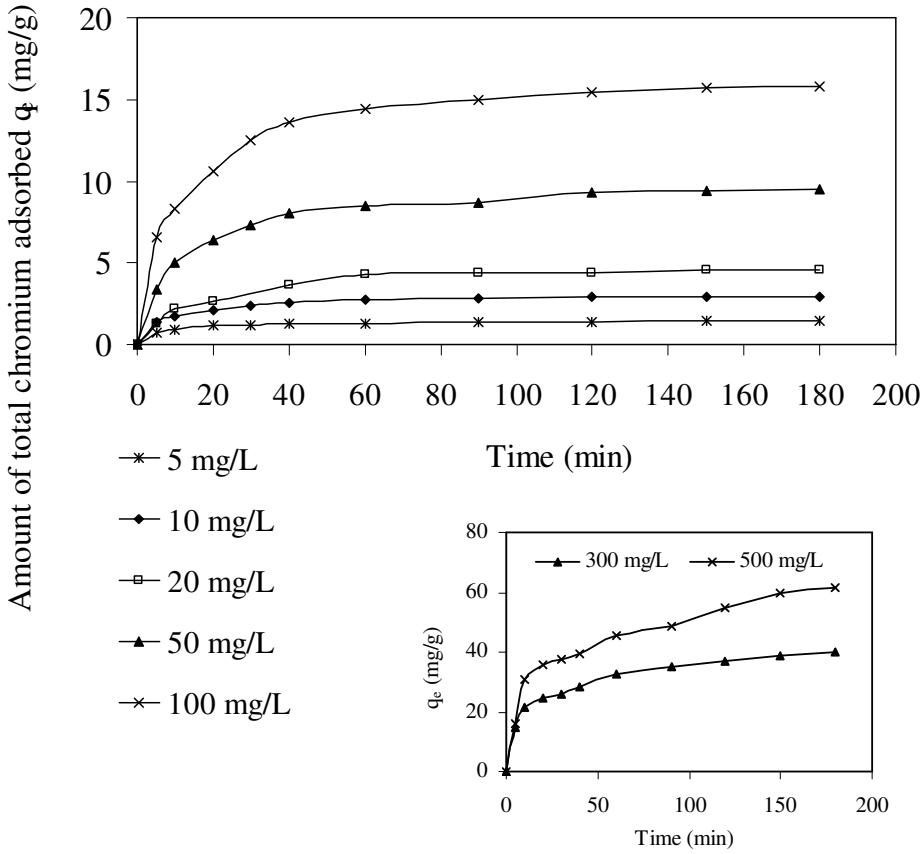

Figure 4.41: Effect of initial concentration of Cr(VI) on total chromium adsorption [PANI-jute dose 2 g/L; pH 3]

Table 4.15: Comparison of kinetic model for total chromium adsorption

Initial Cr(VI) (mg/L)	Pseudo first order kinetics			Pseudo second order kinetics		
	k_1 (L min^{-1})	R^2	χ^2	k_2 (g mg^{-1} min^{-1})	R^2	χ^2
5	0.03	0.92	4.75	0.11	0.99	0.02
10	0.04	0.99	4.44	0.04	0.99	0.03
20	0.03	0.96	4.51	0.02	0.99	0.06
50	0.03	0.97	16.28	0.01	0.99	0.05
100	0.04	0.96	17.22	0.01	0.99	0.19
300	0.02	0.97	68.57	0.01	0.99	2.54
500	0.02	0.93	63.71	0.01	0.99	6.69

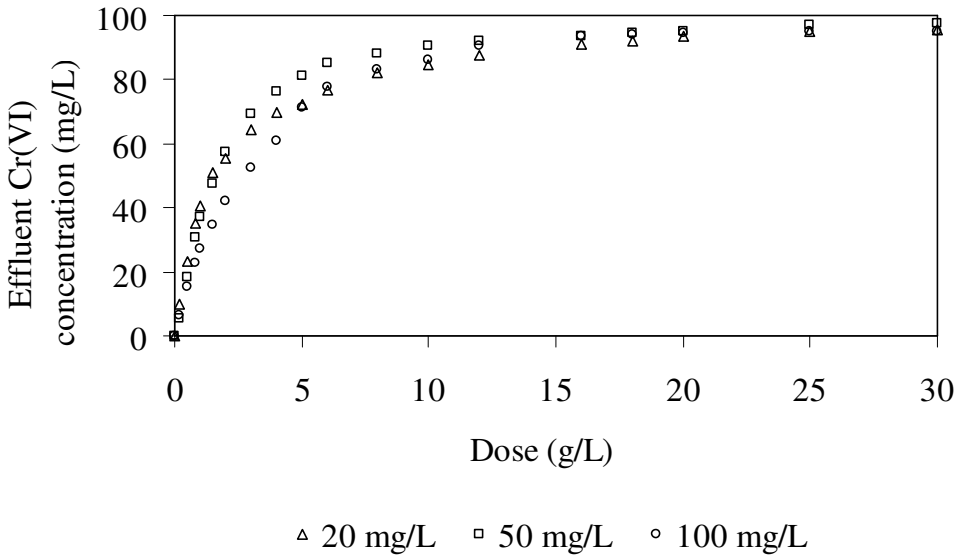

Figure 4.42: Effect of PANI-jute dose on total chromium adsorption (pH 3; agitation time 3 h)

(e) Desorption and recovery of adsorbed chromate ions

To understand the nature of bonding of Cr(VI) on PANI-jute, desorption experiment was conducted. As Cr(VI) was attached as $HCrO_4^-$ on $-NH_3^+$ site, hydroxides with higher affinity may replace $HCrO_4^-$ from PANI-jute sites. Hence different strength of NaOH and NH_3OH were employed as desorbents. It can be seen in Table 4.16 that desorption of Cr(VI) by NaOH at different strength were higher than that of NH_3OH. NaOH being the stronger base was responsible for more desorption of chromate ions than NH_4OH. However, even with the strong base like 2 M NaOH, desorption of chromate ions was incomplete. During adsorption, along with the binding of $HCrO_4^-$ with $-NH_3^+$, there is a possibility of formation of chemical bond between the Cr(VI) species and the nitrogen atoms of polyaniline (other than amine) as observed by Deng and Bai (Deng and Bai 2004). This factor may be responsible for incomplete desorption of Cr(VI). However, maximum desorption occurs in equilibrium time of 10 min indicating adsorption of Cr(VI) mostly on surface of PANI-jute and less of internal diffusion in nature.

Table 4.16 : Desorption of Cr(VI) (%) by different desorbents

Desorbent	Strength of desorbents (M)		
	0.5	1	2
NaOH	17	63	83
NH_3OH	11	21	38

The main advantage of desorption of metal ions is the reusability of adsorbent. Since the desorption of Cr(VI) from PANI-jute was not complete even by desorbents strength of 2 M, attempt were made to recover the Cr(VI) in its salt form by igniting the Cr(VI) contaminated PANI-jute. To investigate the degree of recovery of chromate ions bound on PANI-jute fibers after adsorption, 4 g of PANI-jute was employed for adsorption of chromium ion Cr(VI) concentrations 46 and 120 mg/L. It was observed that weight of PANI-jute increased from 4 g to 4.2 g after adsorption experiment probably due to chromate ions binding. After ignition at 550 ^{o}C in muffle furnace, the weight of PANI-jute-chromium decreased to only 0.2 g reducing the weight by 95% (Figure 4.43). This PANI-jute-chromium after dissolving in HNO_3, almost 94% of the Cr(VI) adsorbed were recovered back in solution in the form of non toxic Cr(III) ion. Adsorbed Cr(VI) from PANI-jute was converted to Cr(III) in presence of strong mineral acids and released. Thus ignition of PANI-jute recovers the Cr(VI) and also minimized the problem of solid waste disposal of metal contaminated adsorbents. Similar phenomenon was also tried for AFC coated silica gel but obtained an ash of metal oxides and silica gel.

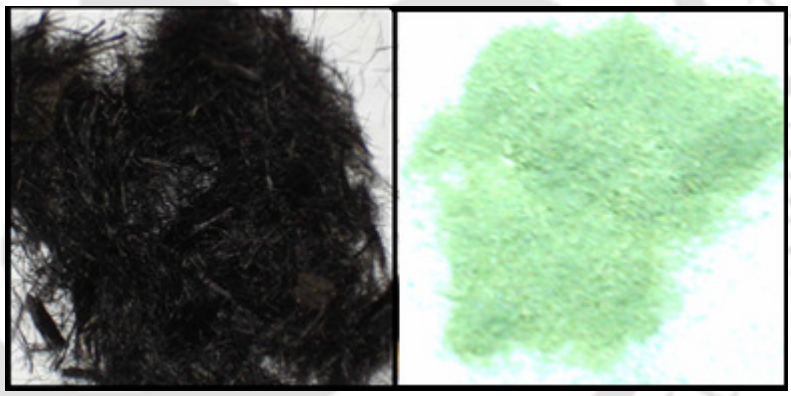

Figure 4.43 (a): Cr(VI) contaminated PANI-jute and Figure 4.43(b) Oxides of chromium after ignition of Cr(VI) contaminated PANI-jute

4.2.2.2 Removal of trivalent chromium ions [Cr(III)] by PANI-jute

Removal of Cr(IIII) by PANI-jute was studied with main emphasis given on mechanism of binding. Experiments were conducted with varying pH and the results are presented in Figure 4.44. Removal of Cr(III) increased with increase in pH with maximum removal at basic pH. At pH of 6- 9, almost 70% removal of Cr(III) was achieved by PANI-jute. Since Cr(III) precipitates at pH > 6, maximum removal of Cr(III) through adsorption is at pH 6. Removal trend of Cr(III) by PANI-jute is similar to that of AFC coated silica gel. At acidic pH, amines of PANI-jute gets protonated and repel the Cr(III) which exist as Cr^{3+} and

$Cr(OH)^{2+}$ ions thus yielding very less removal of Cr(III). At pH 5.5 and above, amines of PANI-jute get deprotonated acquiring surface negative charge and decrease the repulsion of dominant species of Cr(III) monovalent $Cr(OH)_2^+$ and divalent $Cr(OH)^{2+}$. Thus cationic Cr(III) bind with sites of amines by coordinate bond yielding higher removal with increase in pH. However at pH > 9, removal of Cr(III) in this strong basic region was almost negligible. At pH values above 7, neutral $Cr(OH)_3$ and anionic $Cr(OH)_4^-$ species begin to appear, and were not able to bind with deprotonated amines of PANI. Besides, formation of multi metal species $H_2O_4Cr(OH)_2Cr(H_2O)_4)^{4+}$ by OH^- ligand bridging is also responsible for less removal at pH > 9 (Rivera-Utrilla and Sanchez-Polo 2003).

4.2.2.3 Removal of mercury ions [Hg(II)] by PANI-jute

(a) Effect of pH

The removal trend of Hg(II) at different pH is shown in Figure 4.45 and can be observed that the removal of Hg(II) increase with increased in pH of the solution. At pH 2, removal (%) was negligible with only 2.5- 5%. At pH 6, 65- 71% Hg(II) removals were achieved. These increased to maximum removal of 74- 75% at pH 7 and remained constant till pH 9 thus achieving amount of Hg(II) adsorbed (q_e) value of 18.85 mg/g and 35 mg/g respectively. Similar trend of maximum Hg(II) removal at pH 6- 7 was also observed with AFC coated silica gel also. Presence of Hg(II) was investigated by EDX analysis of PANI-jute after adsorption process and are shown in Figure 4.46. Presence of Hg(II) peak on EDX after adsorption confirms the presence of Hg(II) on AFC which was absent before adsorption.

(b) Mechanism of Hg(II) removal by PANI-jute

Removal trend of Hg(II) at different pH by PANI-jute is very much similar to that Hg(II) removal by AFC coated silica gel. Amine group is responsible in both the polymers for binding Hg(II) ion. At pH < 4, the major dominant specie $HgCl_2$ was not removed by protonated PANI-jute. Less dominating anionic species $HgCl_3^-$ and $HgCl_4^{2-}$ were removed by protonated amine group of PANI-jute due to electrostatic attraction. It is already known that at pH 5- 9.5, $Hg(OH)_{2(aq)}$ is the main specie followed by $HgCl_{2(aq)}$, $HgOH^+_{(aq)}$ and $HgCl_3^-{}_{(aq)}$. Similar to AFC coated silica gel at pH 5- 9.5, the main specie $Hg(OH)_2$ formed complexes with amine group (Baes and Mesmer 1976). Also above pH 6.6, less dominating specie $HgOH^+$ formed electrostatic bond with negatively charged surface of PANI-jute (pH_{ZPC} of

PANI-jute 6.6). From pH 9.5- 14, though $Hg(OH)_{2(aq)}$ is the predominating specie, it is followed by anionic specie $Hg(OH_3)^-_{(aq)}$ which got repelled by deprotonated PANI-jute causing decrease in total mercury removal above pH 9.5 and this caused decrease in total mercury adsorption by PANI-jute.

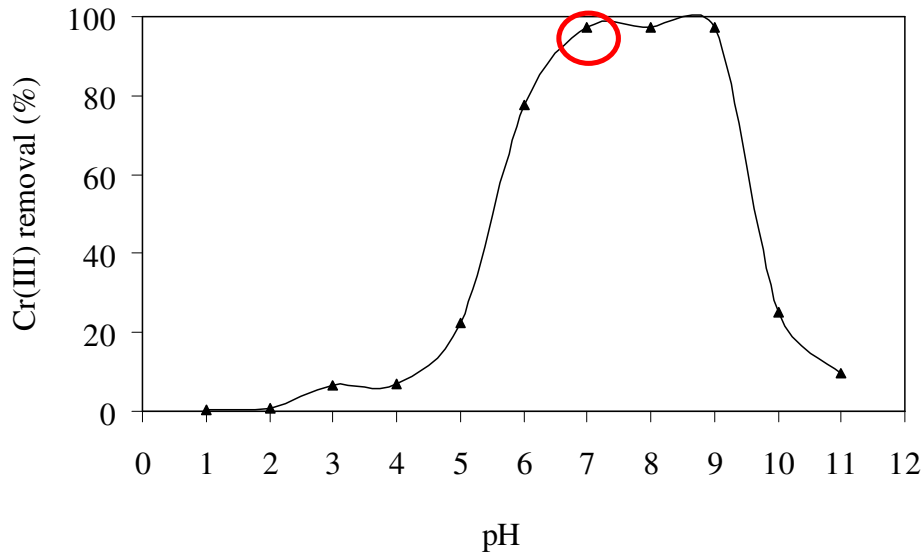

Figure 4.44: Effect of pH on removal of Cr(III) [Initial Cr(III) 50 mg/L; dose 2 g/L; agitation time 24 h; control experiments without adsorbent]

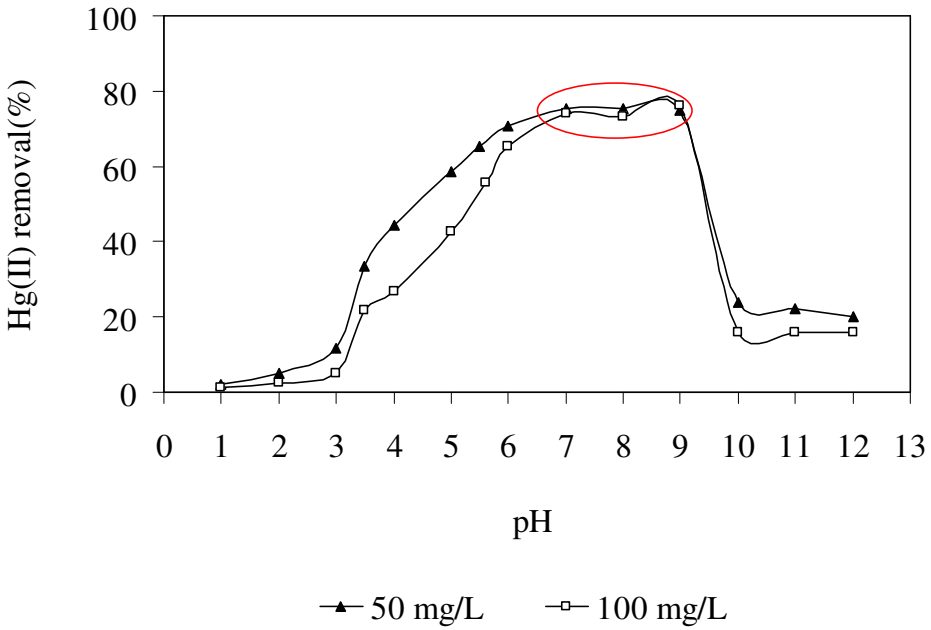

Figure 4.45: Effect of solution pH on removal of Hg(II) by PANI-jute

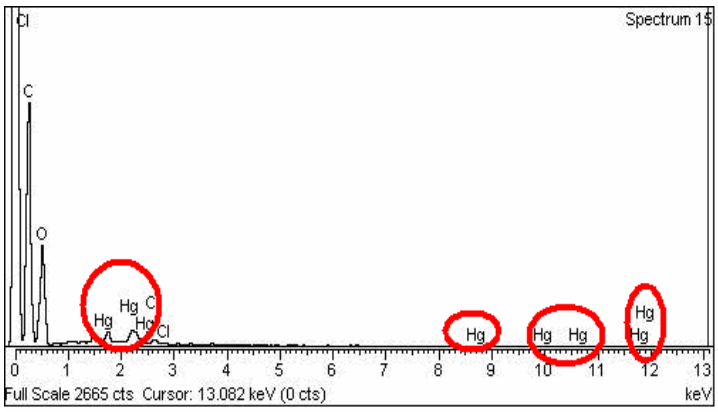

Figure 4.46: EDX spectra of PANI-jute after Hg(II) adsorption

(c) Effect of initial Hg(II) concentration and adsorption kinetics

Adsorption kinetic studies of Hg(II) by PANI-jute is shown in Figure 4.47. Adsorption equilibrium was achieved almost within 120 min for all varied initial concentrations suggesting rapid adsorption of Hg(II). Such rapid adsorption even at higher initial concentration of Hg(II) suggests that nature of adsorption was probably chemical in nature, rather than physical one. Identification of kinetic model was also tried and comparison between Lagergren's first order and second order model predicted values were incorporated in Table 4.17. Higher correlation coefficient (R^2) and less χ^2 were achieved for second order. This suggest adsorption of Hg(II) by PANI-jute following second order kinetic model. With the increase in initial Hg(II) from 10 mg/L to 100 mg/L, rate of adsorption for second order (k_2) decreased from 0.053 to 0.005 g $mg^{-1}min^{-1}$. This decrease is due to the saturation of the available adsorption sites (Yardim et al. 2003).

(d) Adsorption Isotherm

Adsorption isotherm studies of Hg(II) removal by PANI-jute was studied and the evaluated coefficient of Langmuir's and Freundlich's isotherm are presented in Table. 4.18 Higher R^2 and lower χ^2 value for Freundlich's model suggest the adsorption of Hg(II) on PANI-jute obeying Freundlich's isotherm.

(e) Desorption

Desorption study was carried out with certain desorbents like HCl, H_2SO_4, HNO_3 and KI of varied strength and result is shown in Table 4.19. Complete desorption was achieved

with KI as Hg(II) form stronger complexes with iodine than amine. However with mineral acid also, higher desorption was achieved at higher strength of desorbent.

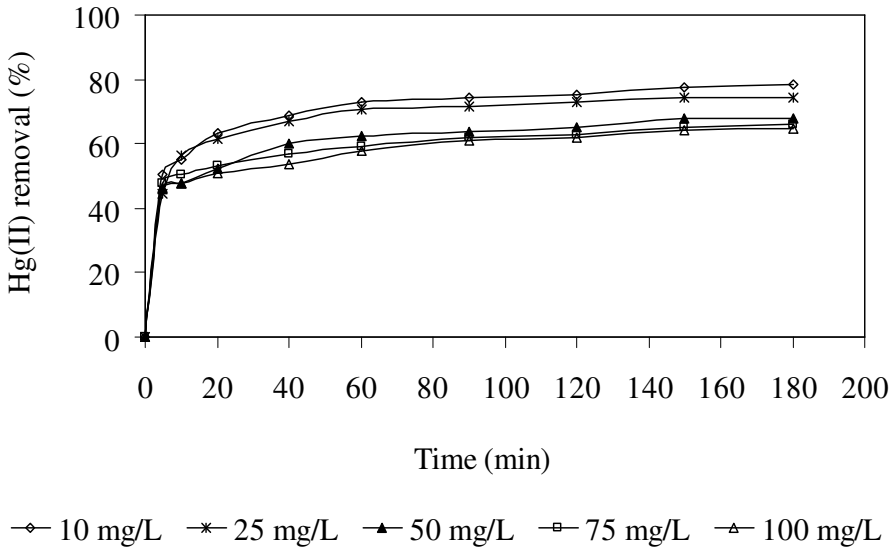

Figure 4.47: Effect of initial concentration of Hg(II) on adsorption and adsorption kinetics [Initial Hg(II) 10- 100 mg/L; adsorbent dose 2 g/L; pH 6.5]

Table 4.17: Comparison of Lagergren's first and second order kinetic model

	Pseudo first order kinetics				Pseudo second order kinetics			
C_o(mg/L)	k_1 (min^{-1})	q_e (mg/g)	R^2	χ^2	k_2 (g.min/mg)	q_e (mg/g)	R^2	χ^2
10	0.023	1.534	0.90	14	0.053	3.71	0.99	0.12
25	0.029	4.56	0.94	37	0.021	10.57	0.99	0.10
50	0.024	5.24	0.61	74	0.011	16.56	0.99	1.02
75	0.017	9.76	0.84	110	0.008	24.94	0.99	2.10
100	0.019	13.68	0.89	121	0.005	31.45	0.99	3.20

Table 4.18: Comparison of Langmuir's and Freundlich's isotherm on removal of Hg(II) by PANI-jute

Langmuir					Freundlich			
Q_m (mg/g)	b (L/mg)	R^2	χ^2	R_L	K_f (mg/g)	n	R^2	χ^2
113.63	0.018	0.98	19.50	0.35	2.35	1.17	0.99	2.08

Table 4.19: Desorption of Hg(II) by mineral acids of different strength

Strength of desorbents	Desorption (%)			
	HCl	H_2SO_4	HNO_3	KI
0.05	54.54	90.90	47.27	90
0.50	69.09	94.54	54.54	100
1.00	80.00	100	72.72	100

(f) Reuse of PANI-jute

Reuse of adsorbent will increase the removal capacity of adsorbent and decrease overall cost effective of adsorbent. All together 5 (five) cycles of adsorption was conducted [fresh PANI-jute + 4 (four) cycles] and the results are presented in Table 4.20. Desorption was carried out with mineral acids. At first cycle, 75% Hg(II) removal was achieved and till 4^{th} (fourth) cycle, removal capacity of PANI-jute remained same. After 4^{th} cycle desorption (%) was reduced from 75% to 70% and this probably leads to decrease in removal of Hg(II) at 5^{th} cycle with 71%.

Table 4.20: Reuse of PANI-jute in removal of Hg(II)

Adsorption-desorption-adsorption cycle					
	1^{st}	2^{nd}	3^{rd}	4^{th}	5^{th}
Adsorbed (%)	75.22	73.75	75.12	76.25	71.25
Desorbed (%)	75.25	76.27	76.66	70.49	68.42

4.2.2.4 Removal of Cu(II) by PANI-jute

(a) Effect of solution pH

Effect of reaction pH on copper removal by PANI-jute was studied at varying pH and result is presented in Figure 4.48(a). Negligible removal of copper ion was observed till pH 2 with gradual increase in removal as pH increase. A control experiment without adsorbent suggest precipitation of Cu(II) at pH > 6 thus obtaining maximum adsorption at pH 6. Logarithmic speciation diagram of various soluble copper species against pH was also studied using equations of complexation between Cu(II) and OH^- ligand using logarithmic constant $k_1= 10^6$, $k_2= 1.5x10^7$, $k_3=17.37$ and $k_4=1.38$ with solubility product k_{sp} of $2x10^{-19}$ (Sawyer et al. 2003). Here, $k_1= [CuOH^+]/[Cu^{2+}][OH^-]$; $k_2= [Cu(OH)_2]/[CuOH^+][OH^-]$; $k_3= [Cu(OH)_3^-]/$

$[Cu(OH)_2][OH^-]$ and $k_4 = [Cu(OH)_4^{2-}]/ [Cu(OH)_3^-][OH^-]$. Species distribution diagram of Cu(II) is shown in Figure 4.48(b) and can be seen clearly that pH values for maximum soluble concentration of copper of 50 mg/L (7.9×10^{-4} moles/L with logC = –3.1) is 6.25. Thus adsorption was considered till pH 6. ESR (electronic spin paramagnetic resonance) spectrum was used to confirm presence of Cu(II) ion on surface of PANI-jute and ESR spectrum is shown in Figure 4.49(a). In ESR spectrum g value of 2.0- 2.1 suggests presence of Cu(II) ion on PANI-jute. The rhombic nature of the spectra indicates distorted geometry of Cu(II) bound on PANI-jute (Jezierska et al. 1991; Justi et al. 2004). Presence of Cu(II) on surface of PANI-jute was further confirmed by employing EDX. EDX spectra of PANI-jute after adsorption of Cu(II) showed peaks of Cu(II) [Figure 4.49(b)] suggesting the presence of Cu(II) ions on PANI-jute surface.

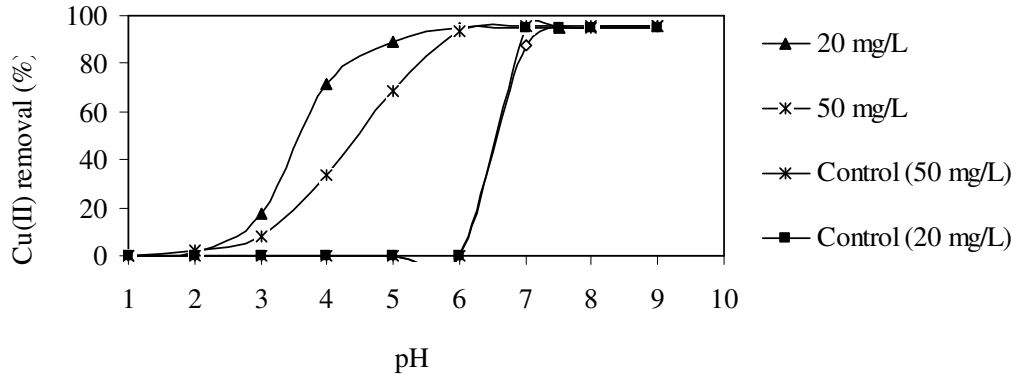

Figure 4.48(a): Removal of Cu(II) by PANI-jute at different pH. [PANI-jute dose 10 g/L, agitation time 3 h].

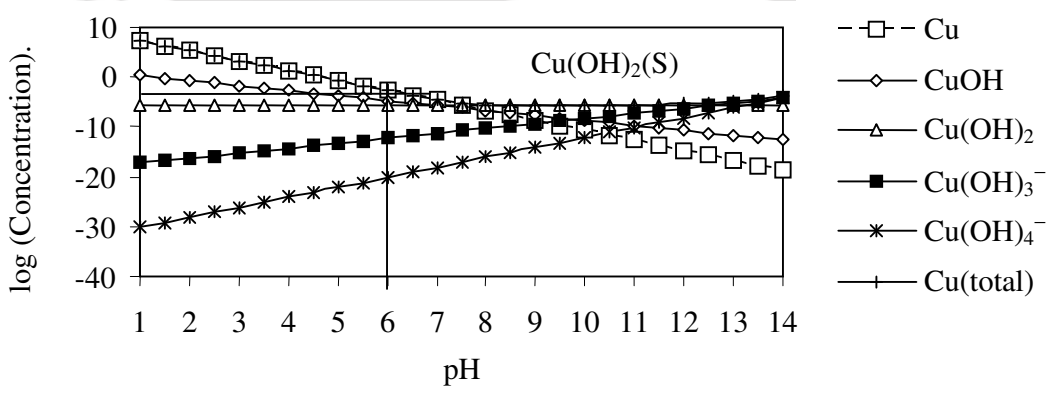

Figure 4.48(b): Logarithmic plot of soluble copper species against solution pH

(b) Mechanism of copper removal

It is well known that copper ion (Kumar et al. 2007) exists in aqueous medium as

square pyramidal form coordinated by water molecules. In acidic medium affinity of protonated ammonium (-NH_3^+) towards Cu(II) ion was negligible and due to charge repulsion. Hence very low removal of copper ion was achieved in acidic pH. With increase in solution pH, deprotonated -NH_2 replaced one or more of water molecules from the coordination sphere of Cu(II) as shown in Figure 4.50(a). During desorption studies, it was observed that 52- 92% of adsorbed Cu(II) ions released into the solution in presence of 1 N strength of mineral acids HCl, H_2SO_4 and HNO_3 with EDTA released 76 % adsorbed Cu(II) ions. During desorption by acids, amine group were protonated and caused release of copper ion in solution [Figure 4.50(b)] whereas with EDTA, being a hexadentate chelating ligand, it forms stronger complex with Cu(II) ion compared to amine group in PANI (Jeffery 1989).

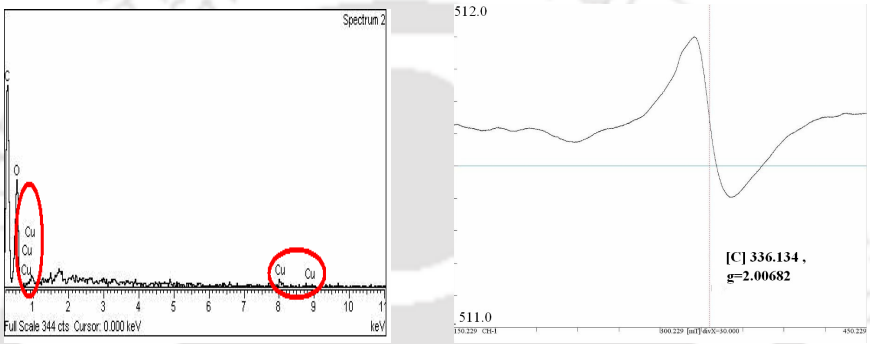

Figure 4.49(a): ESR spectra of PANI-jute after Cu(II) adsorption and

Figure 4.49(b) EDX spectra of PANI-jute after Cu(II) adsorption

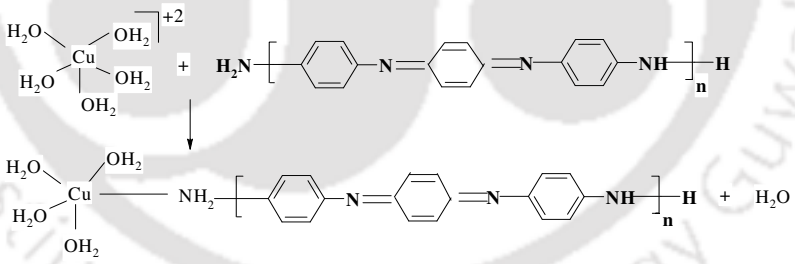

Figure 4.50(a): Proposed mechanism of copper adsorption by PANI-jute

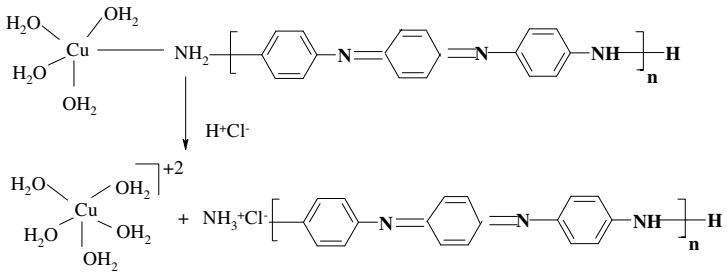

Figure 4.50(b): Proposed mechanism of copper desorption in presence of acid

(c) Effect of initial concentration of Cu(II) and adsorption kinetics

Initial concentrations of copper ion were varied from 10- 50 mg/L at a constant pH 6 using an adsorbent dose of 5 g/L. The adsorbent-copper ion interaction reached equilibrium within 90- 120 min (Figure 4.51). The shape of the curve representing copper uptake versus time suggests that a two-step process involved. The first portion indicates rapid adsorption during initial 20- 30 min after which equilibrium was achieved slowly in 90- 120 min. From Table 4.21, it is clear that adsorption kinetics can be well explained by Lagergren second order model with higher correlation coefficient (R^2) and lesser χ^2 that that of first order. Second order copper removal kinetics were also postulated for adsorption of copper on various adsorbents like grafted silica, tree fern, H_3PO_4- activated rubber wood sawdust, peat, chitin, papaya wood etc (Chiron et al. 2003; Ho, 2003; Gündogan et al. 2004; Kalavathy et al. 2005; Rengaraj et al. 2004).

(d) Effect of PANI-jute dose and adsorption isotherm

Effect of PANI-jute dose on Cu(II) adsorption and identification of isotherm model was studied. With the increase in adsorbent dose, removal (%) of Cu(II) increase due to availability of more sites to bind Cu(II) ions with complete removal at dose of 20 g/L (Figure 4.52). As expected, opposite trend was observed with decreased in amount of Cu(II) adsorbed (q_e) with increase in dose of PANI-jute. At higher dose of adsorbent, some amount of PANI-jute were left unutilized which are however accounted on calculation on amount of Cu(II) adsorbed (q_e) per weight of adsorbent. Isothermal data were treated on Langmuir and Freundlich isotherm model. The evaluated coefficients of the models were presented in Table 4.22. Both the isotherm model correlation coefficient was very high and close to unity. However lesser χ^2 value for Freundlich's isotherm suggest the adsorption of Cu(II) by PANI-jute can be better explained by Freundlich's isotherm than Langmuir's isotherm.

A comparison of the Cu(II) uptake by PANI-jute with various adsorbents based on the isotherm constants is presented in Table 4.23. Copper uptake varied in a wide range from 0.5 mg/g on goethite to 147 mg/g on marine algae *Turbinaria ornata* within studied pH range of 4 to 6. It can be seen that copper uptake by PANI-jute is comparable with other adsorbents.

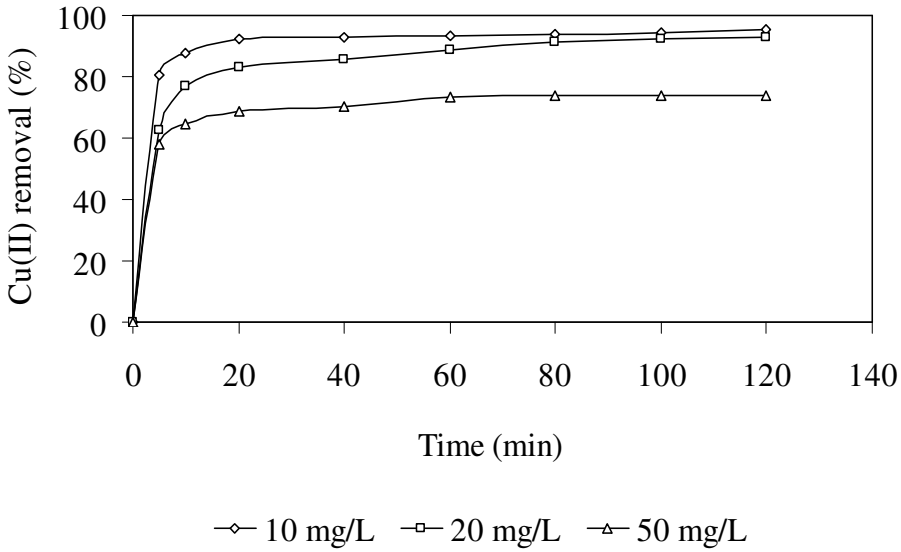

Figure 4.51: Effect of agitation time and initial concentration of Cu(II) [PANI-jute dose: 5 g/L; pH 6]

Table 4.21: Comparison of pseudo first and pseudo second order kinetic model for copper adsorption by PANI-jute

Initial Cu(II) (mg/L)	Pseudo first order kinetics			Pseudo second order kinetics		
	R^2	k_1 (min^{-1})	χ^2	R^2	k_2 (g/mg.min)	χ^2
10	0.68	0.03	13.51	0.99	0.39	0.01
20	0.93	0.04	12.10	0.99	0.07	0.02
50	0.92	0.05	28.93	0.99	0.07	0.02

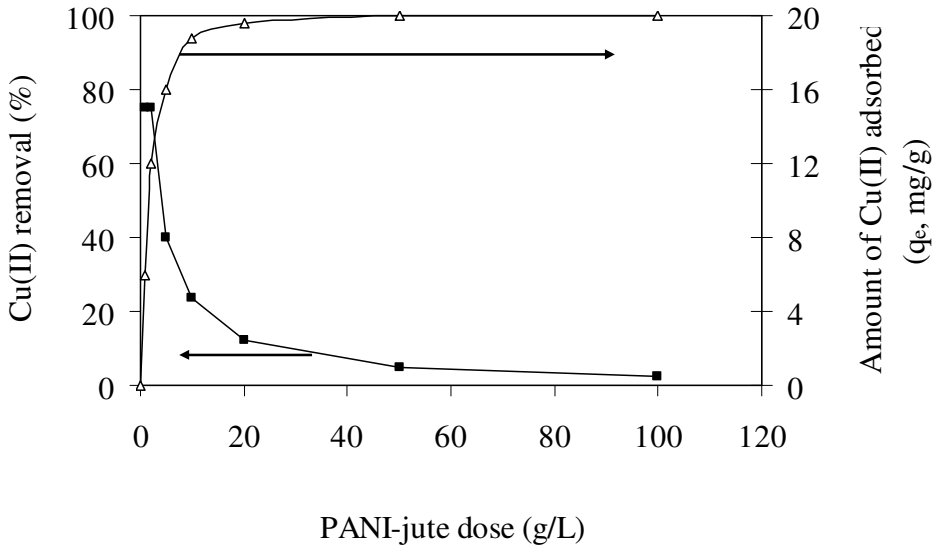

Figure 4.52: Effect of dose of PANI-jute on removal of Cu(II) [pH 6; agitation time: 3 hour]

Table 4.22: Comparision between Langmuir and Freundlich's isotherm for removal of Cu(II) by PANI-jute

Freundlich's isotherm				Langmuir's isotherm			
k_f (mg/g)	n	R^2	χ^2	Q_m (mg/g)	b (L/mg)	R^2	χ^2
1.3	1.4	0.98	0.55	16.5	0.08	0.99	1.14

Table 4.23: Comparison of copper adsorption capacity of various adsorbents

Adsorbent	Copper uptake (mg/g)	pH	Reference
Marine algae *Turbinaria ornata*	147.0	6.0	Vijayaraghavan et al. 2005
Grafted silica	16.5	5.5-6.0	Chiron et al. 2003
Tree fern	11.7	-	Ho 2003
Herbaceous peat	4.8	5.5	Gündogan 2004
H_3PO_4 activated rubber wood sawdust	5.7	6.0	Kalavathy 2005
Goethite	0.5	6.0	Christophi and Axe 2000
Green algae *Spirogyra*	133.3	5.0	Gupta et al. 2006
Cellulose grafted copolymers	12.9	-	Okieimen et al. 2005
Wheat bran	15.0	5.0	Farajzadeh and Monji 2004
Kraft lignin	93.8	4.5	Mohan et al. 2006
PANI-jute	24.5	6	Present work

(e) Reuse of PANI-jute

Reuse of PANI-jute after adsorption-desorption-adsorption of Cu(II) was studied. All together 6 (six) cycles of adsorption was conducted [fresh PANI-jute + 5 (five) cycles] and the results are presented in Table 4.24. With 80% Cu(II) removal at 6th cycle as compared to 85% of 1st cycle, PANI-jute is still good enough to run for more cycles. Similarly efficiency of Cu(II) desorption was almost same through out all cycles with 85- 88%. PANI-jute exhibits

highly reusable property without much decrease in its removal and desorption efficiency. This impacts the overall cost effectiveness of the adsorbent. On addition to it Cu(II) contaminated PANI-jute was able to achieve in reduction of weight of the polymer by more than 98% by ignition as similar to that of Cr(VI)-PANI-jute.

Table 4.24: Reuse of PANI-jute in removal of Cu(II)

Adsorption-desorption-adsorption cycle						
	1st	2nd	3rd	4th	5th	6th
Adsorbed (%)	85.71	83.33	83.72	83.25	83.72	80.95
Desorbed (%)	88.57	88.57	88.55	85.29	88.42	85.29

4.2.2.5 Removal of Cd(II) by PANI-jute

Removal of Cd(II) by AFC-silica el in our previous study was observed as insignificant. An attempt was made to investigate the performance of PANI-jute for removal of Cd(II).

(a) Effect of pH on removal of Cd(II) by PANI-jute

Preliminary investigation showed lesser removal of Cd(II) by PANI-jute dose of 2- 5 g/L. Therefore to reflect better adsorption and to study the effect of pH on Cd(II) adsorption, initial Cd(II) of 36 and 90 mg/L were employed with PANI-jute 10 g/L. The results are presented in Figure 4.53(a). Removal of Cd(II) was insignificant till pH 3 and gradually increase in removal with increase in pH. Control experiment showed precipitation of Cd(II) at pH > 9.5. To cross checked the precipitation of Cd(II) through species diagram of Cd(II) at different pH, logarithmic speciation diagram of various soluble cadmium species against pH was also studied. For complexation between Cd(II) and OH^- ligand, logarithmic constant k_1= $1.2x10^6$, k_2= $4.16x10^2$, k_3=$4.78x10^{-1}$ and k_4=1.09 with solubility product k_{sp} of $7.2x10^{-15}$ (Sawyer et al. 2003) were used. Here, k_1= $[CdOH^+]/[Cd^{2+}][OH^-]$; k_2= $[Cd(OH)_2]/[CdOH^+][OH^-]$; k_3= $[Cd(OH)_3^-]/[Cd(OH)_2][OH^-]$ and k_4= $[Cd(OH)_4^{2-}]/[Cd(OH)_3^-][OH^-]$. In Figure 4.53(b), pH values for maximum soluble concentration of cadmium of 90 mg/L ($4.38 x10^{-4}$ moles/L with logC = –3.36) is 9.5. Thus optimum pH was considered as pH 9.5 with 94% and 99% removal from initial Cd(II) of 36 and 90 mg/L respectively. Removal trend of Cd(II) is also very much similar to other cationic metal ions [Hg(II), Cr(III) and Cu(II)] with

removal increase as pH increase. Similar mechanisms can therefore be postulated for Cd(II) removal by PANI-jute as coordinate bond formation between amines and Cd(II) ions. Insignificant removal at lower pH was due to repulsion of cationic Cd(II) by protonated surface of PANI-jute. EDX spectra of PANI-jute after Cd(II) adsorption (Figure 4.54) showed presence of Cd(II) ions confirming the adsorption of Cd(II) on surface of PANI-jute. During desorption, mineral acids (H_2SO_4, HCl and HNO_3) of 1 N strength were able to recovered back complete 100% adsorbed Cd(II) whereas EDTA recovered 76% Cd(II). Since binding of soft acid Cd(II) with hard amines of PANI-jute was not held stronger as compared to that of border line acid Cu(II), mineral acid were probably able to replaced Cd(II) and recover back almost completely.

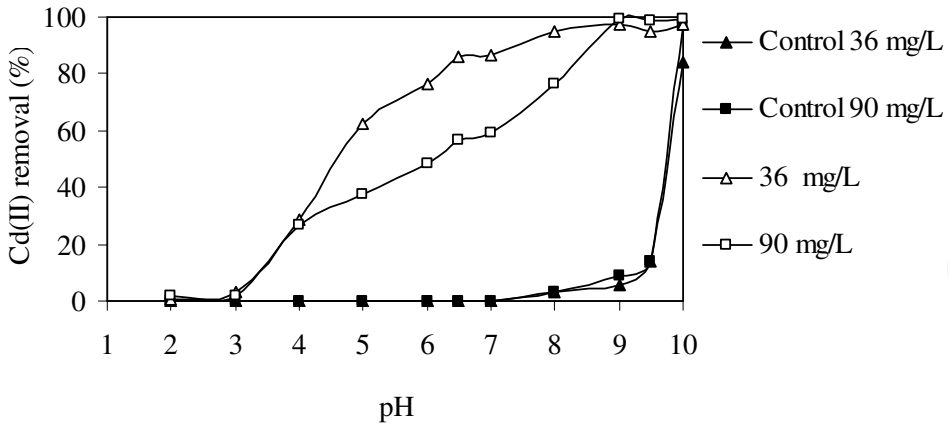

Figure 4.53(a): Effect of pH on removal of Cd(II) by PANI-jute

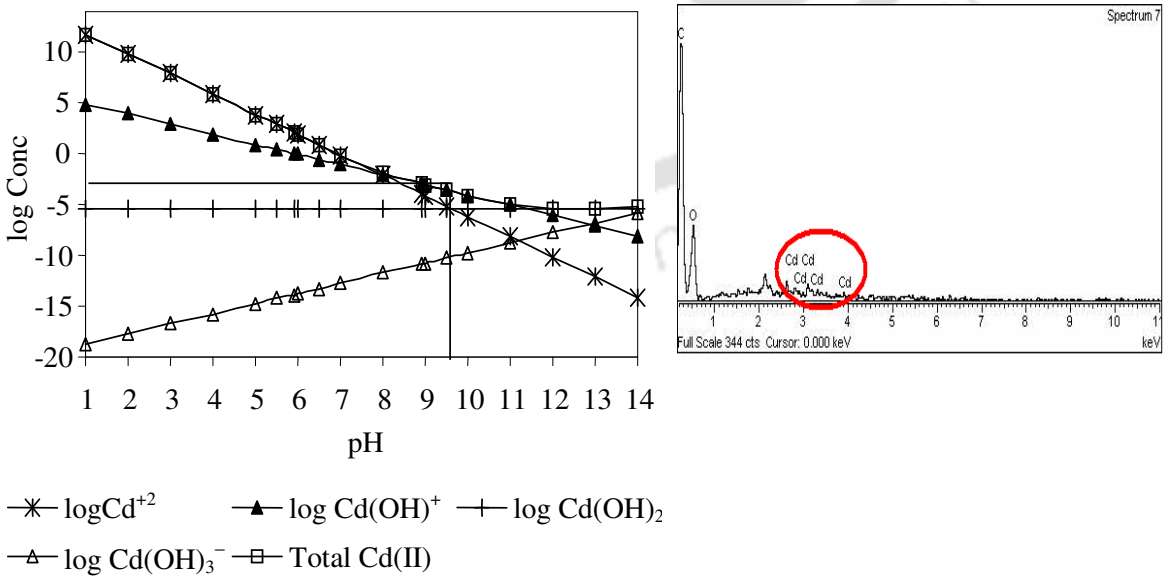

Figure 4.53(b): Logarithmic plot of soluble cadmium species against solution pH

Figure 4.54: EDX spectra of PANI-jute after Cd(II) adsorption

(b) Adsorption kinetics of Cd(II) adsorption by PANI-jute

Cd(II) removal kinetics by PANI-jute is shown in Figure 4.55. Adsorption of Cd(II) was rapid with equilibrium achieved within 20- 60 min suggesting easily available active amine sites on surface of PANI-jute. The data were further treated with Lagergren's first and second order kinetic models and evaluated kinetic coefficients are shown in Table 4.25. Higher correlation coefficient (R^2) and lesser χ^2 value for second order for all different initial concentrations of Cd(II) confirms applicability of second order kinetic model for Cd(II) adsorption on PANI-jute.

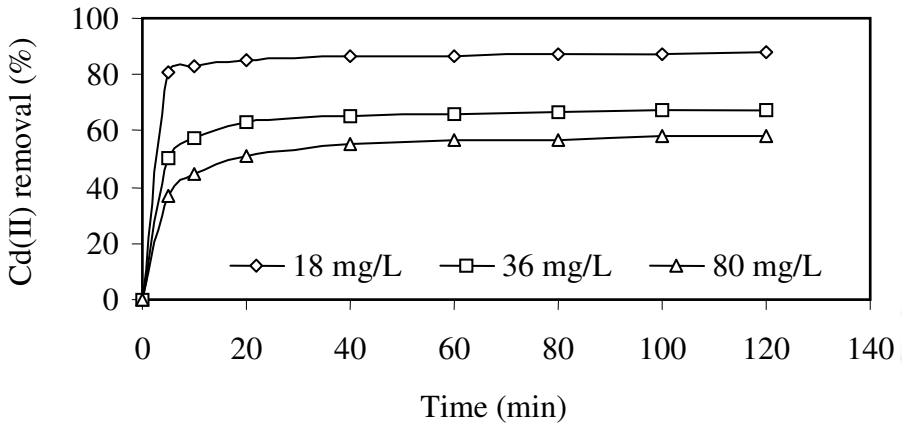

Figure 4.55: Effect of time on removal of Cd(II) by PANI-jute

Table 4.25: Comparison between pseudo first order and pseudo second order kinetic model for adsorption of Cd(II) by PANI-jute

Initial Cd(II) (mg/L)	Pseudo first order kinetics			Pseudo second order kinetics		
	R^2	k_1 (min^{-1})	χ^2	R^2	k_2 (g/mg.min)	χ^2
18	0.63	0.03	18.5	0.99	0.49	0.01
36	0.84	-0.01	36.8	0.99	0.07	0.09
80	0.18	0.01	61.1	0.99	0.02	0.18

(c) Effect of PANI-jute dose and adsorption isotherm

Results of PANI-jute dose effect was studied and presented in Figure 4.56. With increase in dose of PANI-jute, removal (%) of Cd(II) also increase with complete removal achieved at dose 10 g/L and 30 g/L from initial Cd(II) of 36 and 90 mg/L respectively with q_e value of 1.8 and 3.0 mg/g. Such less removal of Cd(II) by PANI-jute suggest non selectivity of soft metal Cd(II) by amine based polymer.

Adsorption isotherm was carried out with initial Cd(II) of 36 mg/L and contacting with PANI-jute dose of 0.2- 30 g/L. Correlation regression coefficient (R^2) for Freundlich and Langmuir were 0.98 and 0.96 respectively with maximum Langmuir monolayer coverage of 18.79 mg/g, 'b' value of 0.03 l/mg. Freundlich's 'n' value of 1.3 further suggest the favorable adsorption of Cd(II) by PANI-jute. The predicted q_e (mg/g) isothermal values were compared with experimental value and observed less χ^2 of 0.44 and 0.13 for Langmuir and Freundlich isotherm respectively suggesting that the data can be well explained by both the isotherm model. The experimental and predicted values of q_e for Langmuir and Freundlich isotherm were plotted and are shown in Figure 4.57.

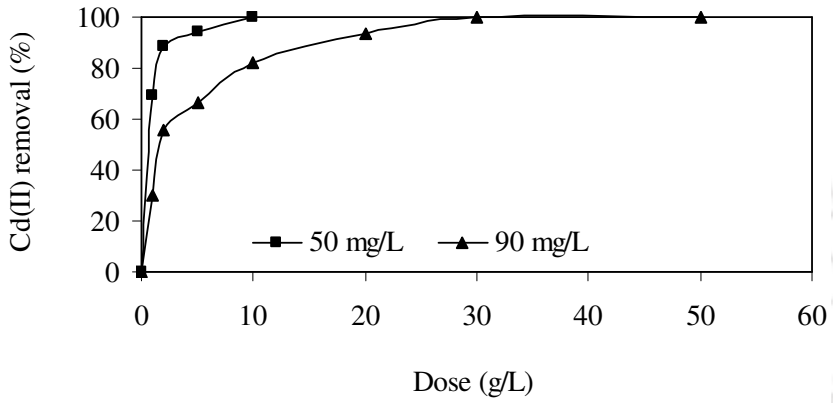

Figure 4.56: Effect of PANI-jute dose on removal of Cd(II) [pH 9.5; agitation time 3 h]

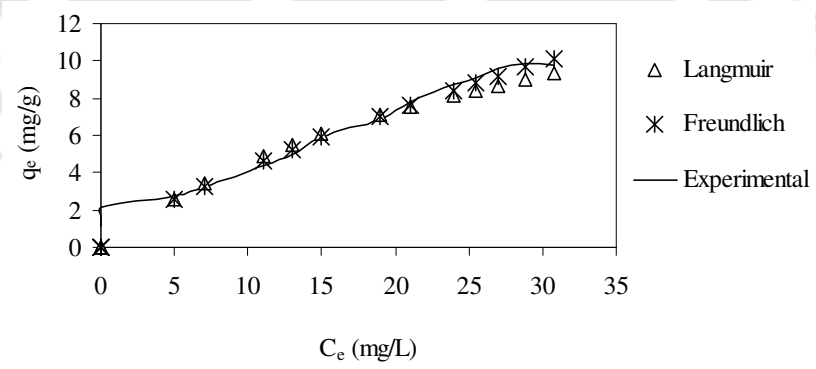

Figure 4.57: Comparison of Langmuir and Freundlich predicted isotherm values with experimental value for Cd(II) adsorption by PANI-jute

(d) Reuse of PANI-jute

Reuse of PANI-jute on removal of Cd(II) was studied by contacting 1 g/L of PANI-jute with Cd(II) of initial concentration of 90 mg/L. Less PANI-jute was preferred for reuse to

saturate the adsorbent to use effectively. Adsorption efficiency was only 26% with 75% desorption efficiency in 1st (first) cycle. However the efficiency was still same till the 6th (sixth) cycle (Table 4.26) with no degradation of PANI-jute. The reusability of PANI-jute justify its use to remove Cd(II) effectively thus giving an impact on the overall cost effectiveness of the adsorbent.

Table 4.26: Regeneration of PANI-jute in removal of Cd(II)

	Adsorption-desorption-adsorption cycle					
	1st	2nd	3rd	4th	5th	6th
Adsorbed (%)	26.6	27.2	26.8	24.5	25.8	24. 5
Desorbed (%)	75	76	78.9	75.4	78.3	77.3

4.2.2.6 Removal of Pb(II) by PANI-jute

(a) Effect of pH on removal of Pb(II)

During study on removal of Pb(II) at varying pH, control experiment [Figure 4.58(a)] and species diagram of Pb(II) [Figure 4.58(b)] at different pH suggest precipitation of Pb(II) after pH 6. Logarithmic constants used for complexation between Pb(II) and OH^- are k_1= $6.6x10^7$, k_2= $1.14x10^3$ and k_3=$1.14x10^3$ with solubility product k_{sp} of $1.43x10^{-20}$ (Sawyer et al. 2003). Here, $k_1=[PbOH^+]/[Pb^{2+}][OH^-]$; $k_2=[Pb(OH)_2]/[PbOH^+][OH^-]$ and $k_3= [Pb(OH)_3^-]/[Pb(OH)_2][OH^-]$. Therefore adsorption of Pb(II) was accounted till pH 6 and observed removal increase with increase in pH. Adsorption/complexation by NH_2 group present in PANI-jute was the main mechanism for removal of cationic metal ions, and removal trend of Pb(II) was similar to other cationic metals [Cr(III), Cu(II), Hg(II) and Cd(II)]. Therefore similar hypothesis for removal of Pb(II) by PANI-jute can also be suggested. At lower pH value, H^+ ions competed with Pb^{2+} ion for the adsorption sites in the system and this was responsible for insignificant lead removal at pH 2. However with increase in solution pH, this competition weakened and Pb^{2+} ion replaced H^+ ion bound to the adsorbent. Presence of Pb(II) was confirmed by EDX spectrum and is shown in Figure 4.59.

(b) Adsorption kinetics

Adsorption kinetics study was conducted at optimum pH 6. Lagergren's pseudo first and second order kinetic model coefficients were shown in Table 4.27. Higher correlation

coefficient (R^2) and less χ^2 suggest that the kinetic data can be well treated by pseudo second order kinetic model. The pseudo second order equation has been reported in explaining adsorption kinetics for removal of Pb(II) by fungus *Mucor rouxxi*, Azadirachta indica (Neem) leaf powder, Syzygium cumini biomass and Palygorskite clay (Yan and Viraraghavan 2003; Bhattacharyya and Sharma 2004; King et al. 2007; Chen and Wang 2007).

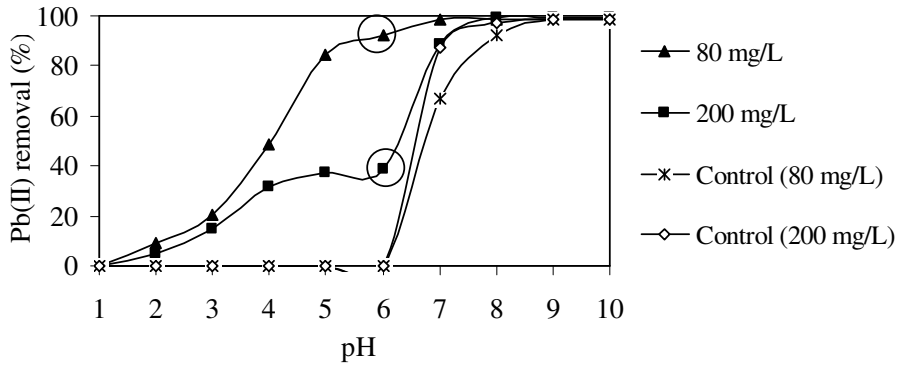

Figure 4.58(a): Effect of pH on removal of Pb(II) by PANI-jute

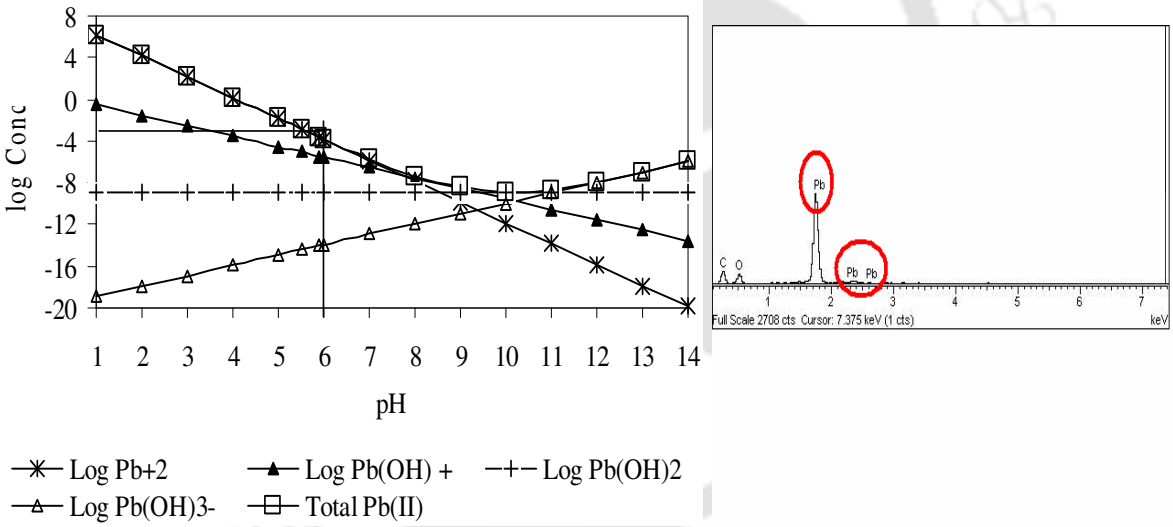

Figure 4.58(b): Logarithmic plot of soluble lead species against solution pH

Figure 4.59: EDX spectra of PANI-jute after Pb(II) adsorption

Table 4.27: Comparison of Lagergren's pseudo first and second order kinetic model for removal of Pb(II) by PANI-jute

Initial Pb(II) (mg/L)	Pseudo first order kinetics			Pseudo second order kinetics		
	R^2	k_1 (min^{-1})	χ^2	R^2	k_2 (g/mg.min)	χ^2
64	0.79	0.016	13.07	0.99	0.009	0.17
200	0.80	0.014	16.37	0.99	0.005	0.48

(c) Adsorption isotherm

Adsorption isotherm was studied with initial Pb(II) of 164 mg/L contacting with varied PANI-dose of 1- 50 g/L. The data were treated on Langmuir and Freundlich isotherm model and coefficients were evaluated. Correlation coefficient (R^2) of 0.97 was observed for both the isotherm with χ^2 of 0.43 and 0.75 for Freundlich and Langmuir respectively. Such less χ^2 suggest the applicability of both the isotherm. Langmuir's 'b' value was observed as 0.044 L/mg and Freundlich's 'n' was 1.71 >1 further suggest the favorability of adsorption of Pb(II) on PANI-jute. Maximum monolayer coverage was obtained as 21.33 mg/g. The comparison between the experimental and isotherm predicted plots of C_e Vs q_e are shown in Figure 4.60. A comparison of the maximum capacity Q_m of PANI-jute with other unconventional adsorbents reported in literature is given in Table 4.28.

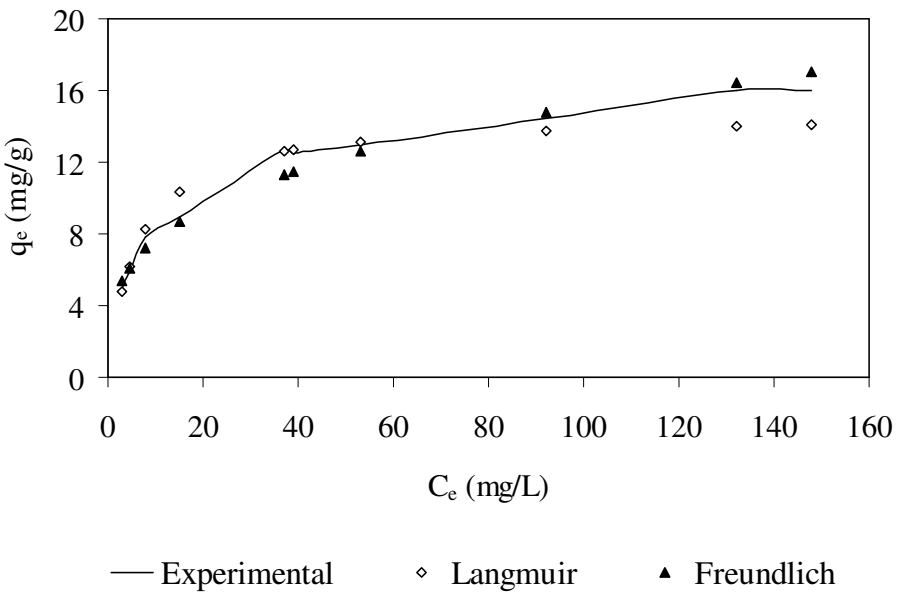

Figure 4.60: Comparison between experimental and Langmuir and Freundlich isotherm predicted values for Pb(II) adsorption by PANI-jute

(d) Desorption of Pb(II) ions and reuse of PANI-jute

Desorption of Pb(II) ions by 1 N of HCl, H_2SO_4 and EDTA recover 78%, 73% and 85% respectively. To improve the efficiency of PANI-jute, possibility of reuse of PANI-jute was evaluated and the findings of the adsorption-desorption-adsorption recycle are shown in Table 4.29. Similar to the case of Cu(II) and Cd(II), adsorption–desorption–adsorption performance of PANI-jute were also carried out till 6th (sixth) cycle. Also with Pb(II), PANI-jute showed same removal efficiency of 30- 33% till 6th (sixth) cycle as virgin PANI-jute.

Table 4.28: Monolayer adsorption capacity for adsorption of Pb(II) on various adsorbents (Namasivayam and Periasamy, 1994)

Materials	Maximum monolayer capacity (mg/g)
Waste slurry	1380
Amberlite IR 120	1039
Focus Vesiculosus	600
Peat	150
Tea-leaves	78.7
Montmorillonite	71.8
Sphagnum moss peat	61.9
Coke	19.1
Kaolinite	9.37
Wollastonites	1.68
China clay	0.411
Fly ash	0.368
PANI-jute	18.34

Table 4.29: Reuse of PANI-jute for removal and recovery of Pb(II) ions.

	Adsorption-desorption-adsorption cycle					
	1st	2nd	3rd	4th	5th	6th
Adsorbed (%)	33.15	30.48	31.55	30.48	31.55	30.48
Desorbed (%)	75.80	78.94	79.66	80.70	74.57	82.45

4.2.2.7 Competition between metal ions

(a) Evaluation of metal competitions

In adsorption, compounds in mixtures may mutually enhance their respective adsorptions, may act relatively independently, or may interfere with one another. Competition between the different metal ions for surface sites occurs and depends on the ion's characteristics. To have a better insight on competitions of metal ions, Cu(II), Cd(II) and Pb(II) were considered as model metal ions. All the three metal exhibit their optimum pH near to pH 6 and thus several sets of experiment in binary and mixed system were carried out with

different combinations of initial concentration at pH 6. The results are shown in Table 4.30. When metals concentrations exceed their saturation, both precipitation and adsorption may have occurred and adsorption effects cannot be distinguished from surface precipitation. Thus lower initial concentrations below metal's saturation limit were considered for mixed metal system study.

At binary system of initial Cu(II) and Cd(II) concentration of 0.15 and 0.30 mmol each, complete Cu(II) removal was achieved. Increased in initial Cd(II) to 0.8 mmol shows a slight decrease in removal of Cu(II) to 0.14 mmol which was replaced by 0.18 mmol of Cd(II) suggesting a slight competition of Cu(II) binding on PANI-jute by Cd(II). On the other hand, Cd(II) removal decrease from 0.08 mmol to 0.02 mmol with increase in initial Cu(II) from 0.15- 0.30 mmol. Complete inhibition of Cd(II) removal was observed when initial Cu(II) further increase to 0.8 mmol indicating suppression of Cd(II) removal by Cu(II). Ligand exchange rate for Cu(II) with 1 x 10^9 was much higher than that of Cd(II) with 3 x 10^8 (Stumm and Morgan 1996) and also their electronegativity. Thus borderline acid Cu(II) which is more preferable by hard base amine than soft acid Cd(II) will exchange its hydroxyls ligands with amine ligands of PANI-jute more stronger than Cd(II). Besides binding constant ("b" of Langmuir's model) of Cu(II) was 0.083 L/mmol as compared to 0.037 L/mmol for Cd(II) suggesting thermodynamically favoured for Cu(II) adsorption on PANI-jute than Cd(II).

In binary system of Cu(II) and Pb(II), complete removal of Cu(II) at equimolar concentration of 0.15 mmol decrease to 0.08 mmol when initial Pb(II) increased to 0.8 mmol. On the other hand, removal of Pb(II) decreased from 0.08 to 0.02 mmol with initial Cu(II) increased from 0.15 mmol to 0.80 mmol and at constant initial Pb(II) of 0.15 mmol. In this binary system of Cu(II) and Pb(II), both the metal ions inhibits the adsorption of each other towards amine of PANI-jute. However Cu(II) showed better competitor than Pb(II) with higher removal as also evidence from their mono metal removal studies too. Ligand transfer rate of Pb(II) was higher with 7 x 10^9 than that of Cu(II) with 1 x 10^9 and hydrated radii of Pb(II) [0.401 nm] is also less than that of Cu(II)[0.409 nm]. This suggest higher preference of Pb(II) to replace its hydroxyl ligands with other ligand than that of Cu(II). However Pb(II) being soft metal is less preferred by amine than borderline acid Cu(II). Also electronegativity of Cu(II) is higher than Pb(II) thus having more affinity for Cu(II) to bind amines of PANI-jute. Thermodynamically, Cu(II) adsorption is more favourable with Langmuir's 'b' value of 0.083 L/mg than that of 0.031 L/mg for Pb(II).

Within binary system of Cd(II) and Pb(II), removal of Cd(II) decreased from 0.09 mmol to 0.02 mmol due to suppression by presence of Pb(II) with initial concentration increased from 0.15 mmol to 0.8 mmol. Therefore presence of Pb(II) suppress adsorption of Cd(II) significantly similar to Cu(II). It was however observed that for fixed initial Pb(II) concentration of 0.15 mmol and with initial Cd(II) concentration increased from 0.15 mmol to 0.8 mmol, removal of Pb(II) increase from 0.11 mmol to 0.15 mmol. This observation suggest specific interactions between Cd(II) and Pb(II) to enhance removal of Pb(II). Similar observation on enhancement of Pb(II) removal by presence of Cd(II) was also reported using fly ash as adsorbent (Cho et al. 2005)

Table 4.30: Binary system of Cu(II), Cd(II) and Pb(II) removal by PANI-jute

Experiment Set no.	Initial metal concentration (M1 + M2)	Removal of metal ions (mmol/g)					
		Cu(II) + Cd(II)		Cu(II) + Pb(II)		Cd(II) + Pb(II)	
		Cu(II)	Cd(II)	Cu(II)	Pb (II)	Cd(II)	Pb (II)
1	0.15 + 0.15	0.15	0.08	0.15	0.08	0.09	0.11
2	0.15 + 0.30	0.15	0.13	0.14	0.06	0.04	0.23
3	0.15 + 0.80	0.14	0.18	0.08	0.24	0.02	0.39
4	0.30 + 0.15	0.26	0.02	0.27	0.05	0.18	0.15
5	0.80 + 0.15	0.55	0	0.56	0.02	0.31	0.15

M1: Metal 1 in binary system
M2: Metal 2 in binary system

Based on ligand exchange rate, Pb(II) has higher affinity for PANI-jute than Cu(II) followed by Cd(II) whereas hydrated radii which is inversely proportional to binding affinity is of order Cd(II)> Cu(II)> Pb(II). Therefore competitions between these metal ions were not in agreement with neither ligand exchange rate nor hydrated radii completely. However the adsorption capacity which is of order Cu(II) > Pb(II) > Cd(II) is in agreement with metal electro negativity. Thus, the relative ionic property orders are not good quantitative indicators of the relative adsorption capacities of single and multi-component metal ion systems. Similar results was also reported by Schwertmann and Taylor (1989) with affinity of heavy metals for goethite followed Cu > Pb > Zn > Cd > Co > Ni > Mn order, which is fairly consistent with electro negativity being an important factor. Predictability of mutual inhibition of adsorption capacity suggest confinement of adsorption to a single or few molecular layers and also adsorption affinities of the solutes do not differ by several orders of magnitude.

(b) Adsorption isotherm

To predict the adsorption behavior of metal ions in a multi-component system, Langmuir competitive model (Equation 4.6) can be applied. The extent of adsorption, $q_{e,i}$ of the *i*th solute from an *n*-solute mixture is given by (Weber and Digiano 1995)

$$q_{e,i} = Q_{m,i} b_i C_{e,i} (1 + \sum_{i=1}^{n} b_j C_{e,j})^{-1} \quad (4.6)$$

For a two-solute mixture of substances A and B, Equation 4.6 can be written as

$$q_{e,A} = \frac{Q_{m,A} b_A C_{e,A}}{1 + b_A C_{e,A} + b_b C_{e,B}} \quad (4.7)$$

and for a three-solute mixture of substances A, B and C, Equation 4.7 can be written as

$$q_{e,A} = \frac{Q_{m,A} b_A C_{e,A}}{1 + b_A C_{e,A} + b_b C_{e,B} + b_C C_{e,C}} \quad (4.8)$$

where $Q_{m,A}$, b_A, b_B, b_C are Langmuir constant determined from adsorption measurements in solutions containing each single solutes, and $C_{e,A}$, $C_{e,B}$ and $C_{e,C}$ are equilibrium concentration in the mixture of the solutes. From our previous experiments, Q_m values for Cu(II), Cd(II) and Pb(II) in mono system were 16.5, 16.61 and 13.21 mg/g respectively and corresponding b values are 0.083, 0.037 and 0.15 L/mg. As such, Langmuir competitive model is much applicable for mixed metal ions system where maximum monolayer coverage of each metal in mono system is near to each other. Using equations (4.7 and 4.8), theoretical value of q_e for Cu(II), Cd(II) and Pb(II) were evaluated for both binary and ternary system. Experimental values were obtain by conducting experiment in binary and ternary metal system of Cu(II), Cd(II) and Pb(II) with equimolar concentration of 0.3 mmol and contacted with varied PANI-jute dose of 0.2– 40 g/L. It was observed that χ^2 value for all metal ions between experimental and predicted in binary and ternary system were in range of 0.44- 1.80 with maximum χ^2 of 2.20 obtained for Cd(II) in binary system of Cd(II)- Pb(II). Such low χ^2 suggests the applicability of competitive Langmuir isotherm in mixed system.

4.2.2.8 Removal of metal ions from mixed metal system

Affinities of metal ions from mixed metal system towards PANI-jute was studied with Cu(II), Ni(II), Cr(III), Pb(II), Cd(II) and Hg(II). The result is presented in Figure 4.61 and can be seen that the adsorption affinity followed Cu(II) > Ni(II) > Cr(III) > Hg(II) > Pb(II) > Cd(II). Similar affinity trend was observed in our previous study with AFC coated silica gel. Since both the polymer have same responsible functional group amine ($-NH_2$) for binding the metal ions, the preference of metal ions by PANI-jute can also be explained based on Pearson hard-soft acid-base theory, ligand exchange rate and Langmuir's binding constant 'b' factor.

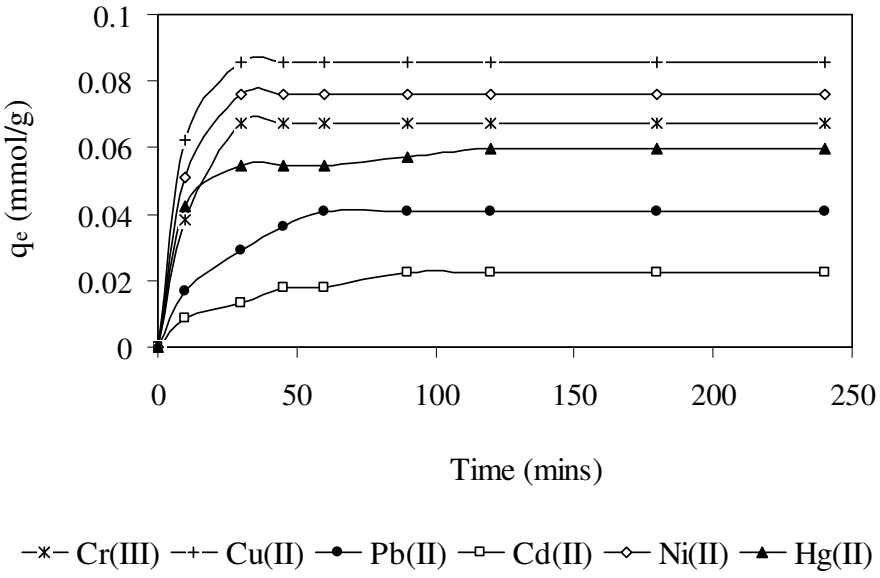

Figure 4.61: Competition of metal ions towards PANI-jute [Metal ion concentration 0.5 mmol; PANI-jute 5 g/L; pH 6]

4.2.3 Continuous column mode operation study

Batch data has several limitations to predict the performances in practical situation such as actual industrial wastewater treatment plant, where continuous reactors replace batch operation. It was also observed that literatures on chromium ion removal by polymers in fixed-bed mode are very scanty. In the present work, short chain polymer PANI-jute fiber was used for removal of chromium ion in continuous mode. Influent pH, column bed depth, influent Cr(VI) concentrations, influent flow rates and recovery of chromium were selected as variable factors for the present work.

(a) Effect of influent pH

During batch experiment work, to achieved maximum removal of Cr(VI) by PANI-jute, optimum pH of 3 was maintained throughout by addition of acid /base. However during continuous column mode experiment as well as in real practical situation, the solution pH was not controlled and the pH of effluent solution fluctuates. Therefore effects of influent pH on Cr(VI) removal by PANI-jute in column mode operation was studied by running five columns of 30 cm bed depth (7.05 g PANI-jute) at influent pH 2, 3, 4, 5, and 6. Empty bed residence time (EBRT) was calculated using Equation 4.9.

$$\text{EBRT (min)} = \frac{Empty\ bed\ column\ volume\ (m^3)}{Volumetric\ flowrate\ (m^3/\text{min})} \qquad (4.9)$$

Empty bed column volume was calculated from column ID (1 cm) and height of column bed (30 cm) and EBRT was 11.78 min. From batch studies on removal of Cr(VI) by PANI-jute, it was observed that Cr(VI) was highly reduced to Cr(III) at acidic pH. Perusals of literature had also reported the reduction of Cr(VI) to Cr(III) at acidic pH along with protons been consumed. Hence throughout the study in column effluent, both Cr(VI) and total chromium were analyzed and Cr(III) was estimated. Also amount of total chromium and Cr(VI) removed till exhaust were calculated separately. Breakthrough curve of Cr(VI) is presented as throughput volume versus effluent Cr(VI) concentration in Figure 4.62. The column bed exhaustion time (t_E), throughput volume at exhaustion (V_E) of Cr(VI) were evaluated with respect to Cr(VI) exhaustion point [effluent Cr(VI) 19 mg/L] and presented in Table 4.31

Amount of Cr(VI) removed (M_r) was evaluated from the area above the curve of throughput volume versus effluent Cr(VI) using Equations (2.18- 2.20) and shown in Table 4.31. It can be seen that with the increase in pH, mass of Cr(VI) removed decreased. With decreased in pH from pH 6 to pH 3, respective exhaust time and throughput volume increased from 23 h and 2.76 L to 46 h and 5.52 L with corresponding Cr(VI) removal increased from 4.17 mg to 33.2 mg. At pH 2, column bed was not exhausted even after 102 h of operation time with 12.24 L volume treated and effluent concentration Cr(VI) of only 7.66 mg/L (38.3% C_o) and column operation was stopped at this point. Breakthrough curve for total chromium is shown in Figure 4.63.

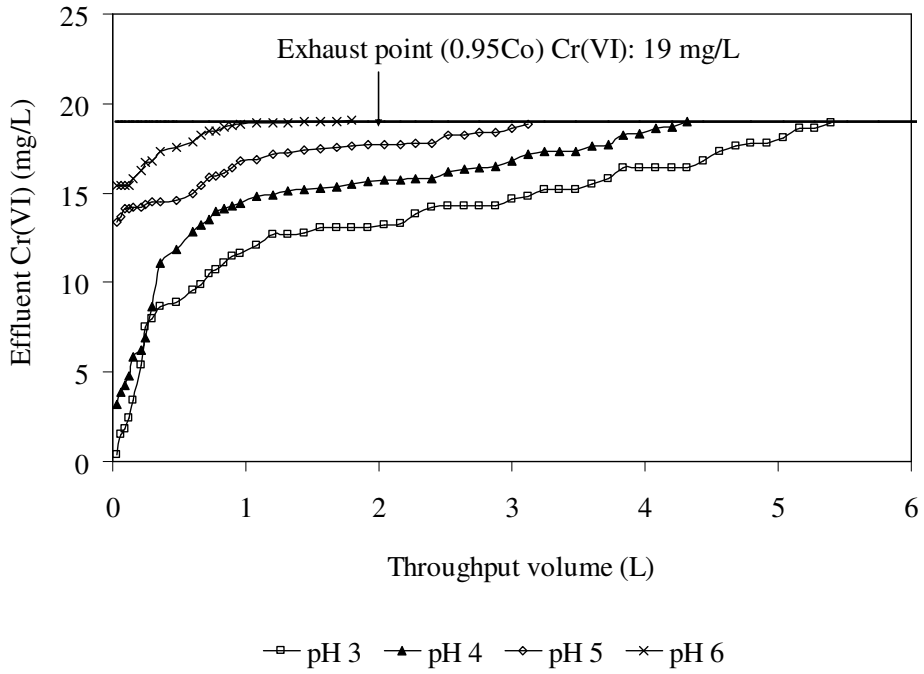

Figure 4.62: Effluent Cr(VI) removal by PANI-jute at varying influent pH [Influent pH: 2, 3, 4, 5 and 6; Initial Cr(VI): 20 mg/L; flow rate: 2 mL/min; column bed depth: 30 cm]

Table 4.31: Exhaust time, throughput volume and total uptake of total chromium and Cr(VI) at different pH by PANI-jute

Influent pH	Cr(VI)			Total chromium			Cr(III)
	t_E (h)	V_E (L)	M_r (mg)	t_E (h)	V_E (L)	M_r (mg)	M (mg)[a]
2	102[b]	12.24[b]	35.26[b]	37	4.44	16.57	62.65[b]
3	46	5.52	33.20	45	5.40	26.74	6.29
4	39	4.68	21.26	39	4.68	20.66	0.53
5	28	3.36	9.84	28	3.36	9.81	0
6	23	2.76	4.17	23	2.76	4.17	0

[a] Mass of Cr(III) in the effluent was calculated theoretically as difference of total chromium and Cr(VI) of same solution.

[b] Effluent Cr(VI) concentration was 7.66 mg/L at 102 h and column bed was not exhausted, though column bed was exhausted with respect to total chromium.

Throughput volume and mass of chromium removed at exhaustion with respect to total chromium values evaluated using Equations (2.17- 2.20) are incorporated in Table 4.31. From

the breakthrough curve of total chromium [Cr(VI) + Cr(III)] [Figure 4.62], it can be observed that maximum removal of total chromium was obtained at pH 3 unlike that of pH 2 for Cr(VI). With increase in pH from 2 to pH 3, exhaust time and throughput volume increased from 37-45 hour and 4.4- 5.4 L respectively with corresponding mass of total chromium removed increased from 16.57 mg to maximum of 26.74 mg. However with further increase in pH, exhaust time and throughput volume decreased to 23 hour and 2.76 L respectively at pH 6 with 4.17 mg of total chromium was removed. These findings of maximum Cr(VI) removal at pH 2 but simultaneously less removal for total chromium suggest the reduction of Cr(VI) to Cr(III) at pH 2. Similar trend of maximum total chromium removal at pH 3 by electrostatic attraction of anionic Cr(VI) along with maximum reduction at strong acidic pH 2 was also observed.

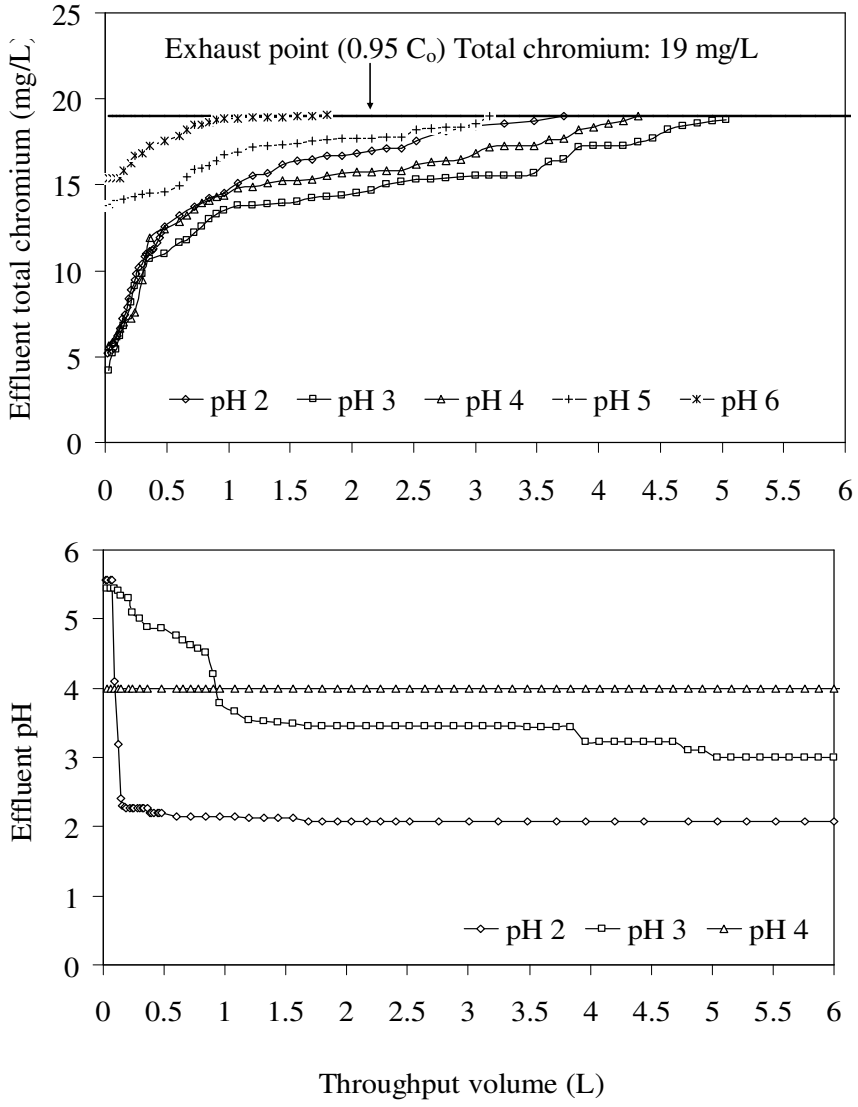

Figure 4.63: Effluent total chromium breakthrough profile and effluent pH at different influent pH (Influent pH: 2, 3, 4, 5 and 6; Initial Cr(VI): 20 mg/L; flow rate: 2 mL/min; column bed depth: 30 cm)

In order to understand the reduction nature of Cr(VI) to Cr(III) in column mode, concentration of reduced Cr(III) appeared in effluent solution calculated from difference of total chromium and Cr(VI) was plotted against throughput volume along with effluent pH and is shown in Figure 4.64. At pH 2, maximum concentration of Cr(III) in the effluent was 15 mg/L at a throughput volume of 1.5 L and remained same throughout. However at pH 3, maximum Cr(III) concentration in effluent was only 3.8 mg/L and decreased thereafter with almost no Cr(III) in effluent after throughput volume of 5.5 L. At pH 4, Cr(III) were untraceable after throughput volume of 0.6 L. The total amount of Cr(III) appeared in the effluent till exhaustion was evaluated from the curve of Cr(III) versus throughput volume using Equation (2.17- 2.20) as area below Figure 4.64 and incorporated in Table 4.31 (as M). Total amount of Cr(III) in effluent that appeared till the exhaustion with respect to total chromium (effluent total chromium 19 mg/L) decreased with increase in pH. At pH 2, mass of Cr(III) in the effluent solution was 62.65 mg and decreased to 6.29 mg at pH 3 followed by insignificant Cr(III) in the effluent at pH 4 and above.

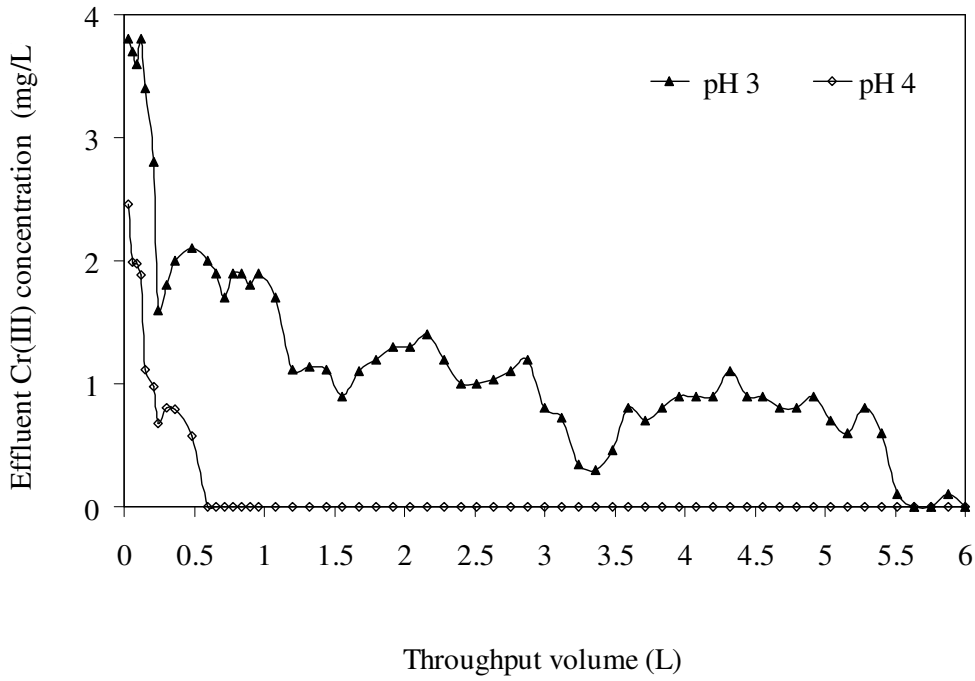

Figure 4.64: Profile of reduced Cr(III) and pH in the treated effluent [Influent pH: 2, 3, 4, 5 and 6; Initial Cr(VI): 20 mg/L; flow rate: 2 mL/min; column bed depth: 30 cm]

Studies on removal of Cr(VI) by PANI-jute in batch mode already reveals that electrostatic attraction between the protonated ammonium and the negative chromate ions is the plausible mechanism for removal of Cr(VI) from solution along with reduction of Cr(VI) to Cr(III). To confirm the presence of reduced Cr(III) on surface of PANI-jute at pH 2 and pH

3, experiment was carried out using columns with initial Cr(III) of 20 mg/L of influent pH 2 and 3. No removal of Cr(III) were observed confirming the repulsion of reduced Cr(III) by protonated PANI-jute at pH 2 and pH 3. Interestingly it was also observed that removal of total chromium was associated with increase of effluent pH from pH 2 to pH 5.57 and pH 3 to 5.54 with insignificant increase when influent pH was 4 and above (Figure 4.63). This result shows that at lower influent pH, higher was proton consumption during chromium removal by PANI-jute. Similar observation was also observed with AFC and PANI-jute in batch mode and also in reported literatures, where an increase in pH from 2 to 5 was observed during Cr(VI) adsorption by waste acorn in the fixed bed study (Malkoc et al. 2006). An effort was made to correlate proton consumption (mmol), removal of total chromium (mg/L), appearance of Cr(III) in effluent (mg/L) and throughput volume (L) when column was operated at influent pH of 3 and results are shown in Figure 4.65. Till throughput volume of 0.12 L, 13 to 15 mg/L of total chromium has been adsorbed on PANI-jute from influent Cr(VI) 20 mg/L with remaining 5 mg/L to 7 mg/L Cr(III) appeared in solution. This observation suggest the adsorption of total chromium predominated over Cr(VI) reduction at initial phase. During this period (up to throughput volume of 0.12 L), 9.9 mmol of protons were consumed. Thereafter with increase in throughput volume (from 0.12- 1 L) adsorption of total chromium decreased gradually (from 12- 5 mg/L of total chromium adsorbed). On the other hand reduction of Cr(VI) gradually increased with 15 mg/L Cr(III) generated in the effluent at throughput of 1 L and consumed 2.75 mmol protons. Probably with time elapsed and total chromium being adsorbed, active sites of PANI-jute (NH_2) got exhausted and the available protons in the solution were probably utilized for reduction of Cr(VI) to Cr(III). However these findings of more proton consumption at initial period when adsorption predominated over reduction process and vice versa may be due to requirement of more protons for surface protonation of active sites of PANI-jute than that of protons requirement for reduction process.

(b) Effect of column bed depth

To study the effect of bed depth, experiment were conducted with three columns filled with 9.4, 11.75 and 14.1 g of PANI-jute to yield respective bed depth of 40, 50 and 60 cm and results are shown in Figure 4.66. Influent Cr(VI) of 10 mg/L with pH 3 was fed at constant flow rate of 2 mL/min. Details of breakthrough time, exhaustion time, breakthrough volume, exhaustion volume along with amount of total chromium removed and uptake is presented in Table 4.32.

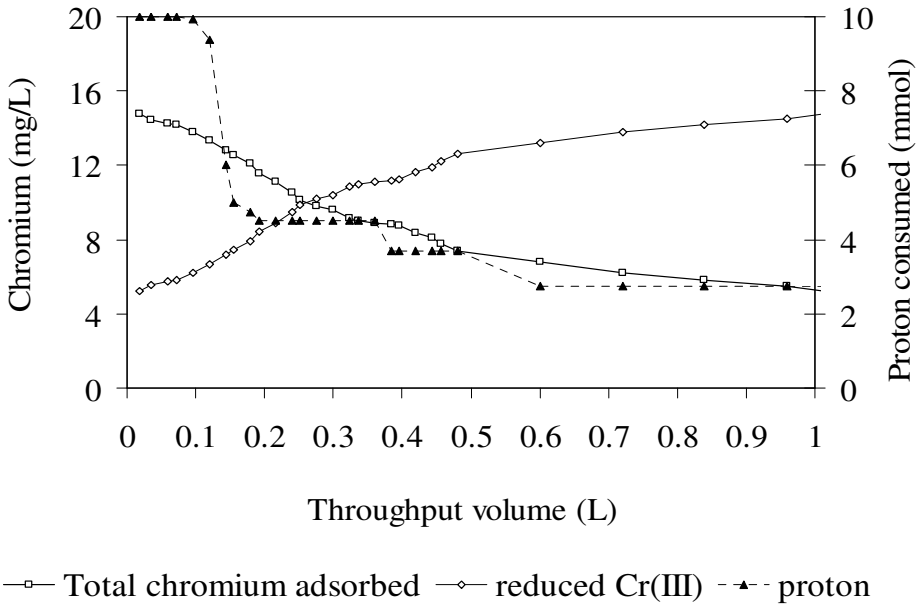

Figure 4.65: Profiles of proton consumption and effluent pH against total chromium adsorbed and Cr(VI) reduced at reaction pH 3 [Influent pH: 3; Initial Cr(VI) 20 mg/L; flow rate 2 mL/min; column bed depth 30 cm]

Table 4.32: Effect of column bed depth on total chromium removal by PANI-jute

Bed depth (cm)	PANI-jute amount (g)	t_B (h)	t_E (h)	V_B (L)[a]	V_E (L)	Amount of total chromium removed [M_r] (mg)	Total chromium uptake [q_e] (mg/g)	EBRT (min)	AER (g/L)[a]
40	9.40	8	82	0.96	9.84	38.87	4.14	15.7	9.79
50	11.75	11	105	1.32	12.6	50.71	4.32	19.65	8.90
60	14.10	20	120	2.40	14.4	65.72	4.66	23.55	5.88

[a] Calculated at 1% breakthrough values

The throughput volumes of total chromium obtained for 40, 50 and 60 cm bed depth at breakthrough point were 0.96, 1.32 and 2.40 L respectively and their corresponding exhaust volumes were 9.84, 12.6 and 14.4 L respectively. At lower bed depth, predominant mass transfer phenomenon was the axial dispersion and reduced the diffusion of chromate ions effectively (Taty-Costodes et al. 2005). Also with increase in bed depth mass transfer zone got broadened as well as more binding sites for adsorption of chromate ions were available. Thus total chromium mass removed (M_r) were evaluated using Equations (2.18- 2.20) for

column depth of 40, 50 and 60 cm were observed as 38.87, 50.71 and 65.72 mg respectively. Table 4.32 shows that EBRT were 15.7 min, 19.6 min and 23.5 min (at column heights of 40, 50 and 60 cm respectively). Adsorbent exhaustion rate (AER) was calculated using Equation 4.10 for 1% breakthrough.

$$\text{AER (g/L)} = \frac{Mass\ of\ adsorbent\ in\ column(g)}{Throughput\ volume\ at\ breakthrough(L)} \tag{4.10}$$

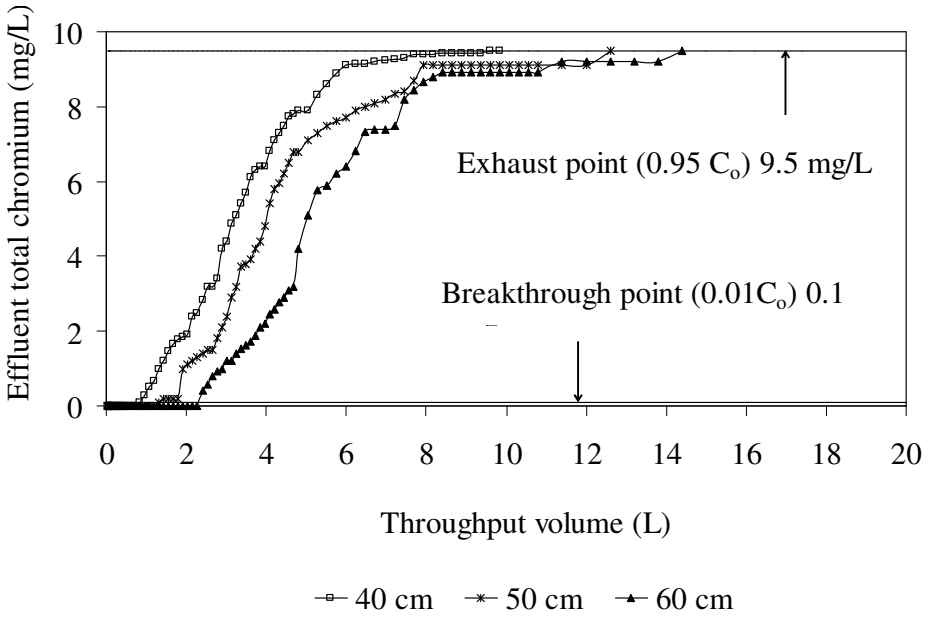

Figure 4.66: Breakthrough curves on total chromium removal at various column bed depth (Column bed depth (cm): 40, 50 and 60; Initial Cr(VI): 10 mg/L; flow rate: 2 mL/min; pH: 3)

Table 4.32 shows that when EBRT increased from 15.7 min to 19.65 min (25% increase) AER decreased from 9.79 g/L to 8.90 g/L (only 9% decrease). However, when EBRT was further increased to 23.5 min (19.8% increase), AER decreased to 5.88 g/L (33% decrease). Higher EBRT suggests longer residence time i.e. larger column at the same flow rate, thus indicating more capital cost. Less adsorbent exhaustion rate indicates lower operational cost. From the present experimental observations optimum column bed height is observed as 60 cm, where with small increase in capital cost caused maximum beneficial effect on lowering operational cost.

Table 4.32 also shows that total chromium uptake by PANI-jute (q_e) for bed depth of 40, 50 and 60 cm were 4.14, 4.32 and 4.66 mg/g respectively. With the increased in bed depth, contact time between the adsorbate and adsorbent increased resulting increase in q_e value. However uptake (q_e) value obtained from batch study process showed 62.9 mg/g

(Kumar et al. 2007), much higher than uptake value observed in column work. Similar observation was noted in removal of Hg(II) by AFC. Less contact time (residence time) between adsorbate and adsorbent for column mode operation is one of the main reasons for such decrease in uptake value.

(c) Bed depth service tome (BDST) model

In order to correlate data with BDST model, service time (t_s) and bed depth results are plotted in Figure 4.67 according to Equation 2.25 for 1%, 50% and 90% breakthrough (calculated from Figure 4.66) at column bed depth of 40, 50 and 60 cm. At other breakthrough values also, slope, intercepts and correlation coefficients were calculated in a similar way plotting service time and bed depth and results are shown in Table 4.33.

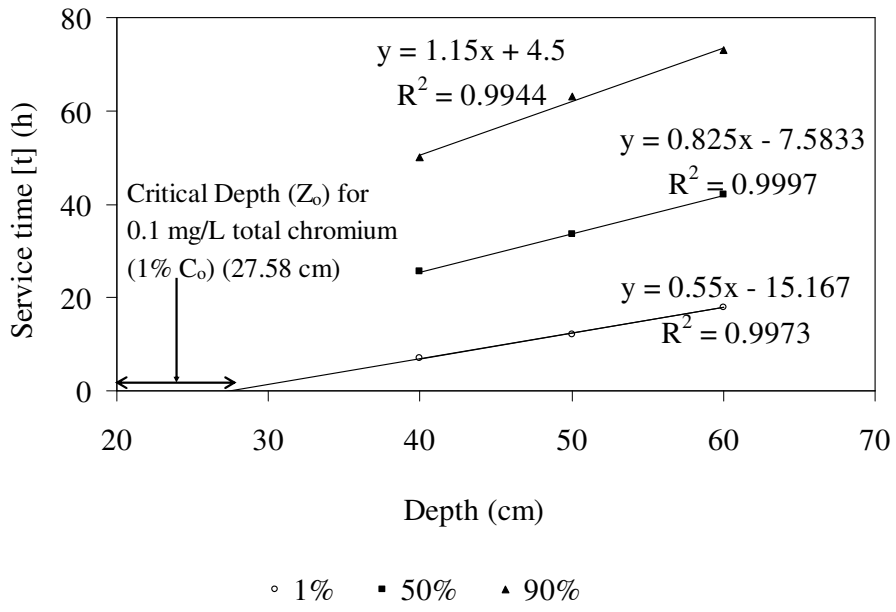

Figure 4.67: BDST plot for total chromium adsorption at various breakthrough (Figure 4.63 data was used)

From Table 4.33 it can be seen that correlation coefficient values are all above 0.99 suggesting the data fixing on BDST model. There was also a consistent rise in slopes from 0.55 to 1.15 from breakthrough of 1% to 90% and subsequent increase in corresponding dynamic adsorption capacity N_o from 840.29 mg/L to 1756.97 mg/L. At lower breakthrough value, there are some active sites of the polymer still unoccupied by metal ions and thus the adsorbent remained unsaturated. The dynamic adsorption capacity in such low breakthrough condition was therefore bound to be lower than the full bed capacity of the adsorbent. An increased in slope by 4.72 folds from a breakthrough of 30 to 70% was reported on removal

of Cr(VI) by activated carbon (Sharma and Forster 1996). Similar fact was also observed during removal of lead by granular activated carbon with the slope increase from 12.5 to 35 at breakthrough values of 20 to 60% (Goel et al. 2005). However Bohart and Adams equation BDST theory assumes a rectangular isotherm having constant dynamic adsorption capacity. Kumar and Bandyopadhyay (2006) observed same slopes and constant adsorption capacity N_o for both 10% and 90% breakthrough on removal of Cd(II) by treated rice husk. Constant slope of 0.355 was also reported on removal of phenols by surfactant modified alumina, thus validating the assumption of constant dynamic adsorption capacity N_o by BDST model (Adak and Pal 2006).

Table 4.33: Coefficients of BDST equation at different breakthrough

Breakthrough (%)	Slopes	Intercepts	N_o (mg/L)	K (L/mg.h)	Coefficient correlation (R^2)
1[a]	0.55	-15.16	840.29	0.03	0.99
10	0.70	-18.33	1069.46	0.01	0.99
20	0.72	-12.25	1107.65	0.01	0.98
30	0.82	-13.41	1260.43	0.01	0.99
40	0.82	-9.91	1260.43	0.004	0.98
50[a]	0.82	-7.58	1260.43	0	0.95
60	0.95	-9.50	1451.41	-0.004	0.97
70	0.95	-4.50	1451.41	-0.02	0.98
80	0.96	3.79	1466.68	0.04	0.99
90[a]	1.15	4.50	1756.97	0.05	0.99

[a] BDST plots for these breakthroughs were also plotted and is shown in Figure 4.67

Another way to examine the application of BDST model is to check the 50% breakthrough curve. At 50% breakthrough, $C_o/C_b = 2$, thus reducing the logarithmic term of BDST equation to zero. Thus 50% breakthrough curve bounds to pass the origin. Contrastingly, intercept of -7.58 (Table 4.33) was obtained at 50% breakthrough concluding the nonconformity of BDST models with adsorption of total chromium by PANI-jute. Similar case of non conformity of Cr(VI) on BDST with respect to 50% breakthrough on removal of Cr(VI) by leaf mould and activated carbon was also reported (Sharma and Forster 2006). All

these experimental and literature findings suggest that BDST model cannot be validated only by analyzing the correlation coefficient (R^2). Also the findings suggest that it is not necessary for BDST model to be validated for all breakthrough percentage. Therefore BDST coefficients of lower breakthrough below 50% can still be utilized for evaluating other parameters such as critical bed depth. Also lower breakthrough below 50% can be fixed on BDST model to design column with different scale process for other flow rates and initial adsorbate concentration without further experimental run (Vijayaraghavan et al. 2005). Using Equation 2.26, calculated critical bed depth for breakthrough of 1% (0.1 mg/L total chromium) was 27.58 cm. Graphical solution of critical bed depth can also be obtained by extending the best fit linearized line of BDST Equation 2.25 to intersect the bed depth axis at t = 0 resulting same critical value of 27.58 cm as shown in Figure 4.67.

(d) Design of columns for different flow rates

To investigate the validity of BDST model for prediction of different flow rates, two new columns of different flow rates of 1.5 mL/min and 2.5 mL/min were operated with same bed depth of 40 cm. Theoretical breakthrough time was obtained by applying data of previous column study at flow rate 2 mL/min using Equation 2.27- 2.29. The comparison between theoretical or predicted and experimental values is shown in Table 4.34.

The predicted values were much in well agreement with experimental value with RSD values of 0.84% and 1.89% for breakthrough of 1% and 10% respectively for initial flow rate of 1.5 mL/min. At higher breakthrough, RSD values increased (32% at 90% breakthrough). Similarly predicted breakthrough times for initial flow rate of 2.5 mL/min were also in well agreement with experimental breakthrough for 1% and 10% breakthrough with RSD values of 1.92% and 1.17% respectively. However, after 10% breakthrough, RSD values also increased to 32- 44%. These finding suggest the well conformity of BDST model for total chromium removal by PANI-jute for lower breakthrough till 10%. Inverse relationship has been observed between flow rates and throughput volume for total chromium uptake by PANI-jute. Increase in flow rate from 1.5 to 2.5 mL/min for 1% breakthrough resulted a decreased in contact time from 13 - 2.5 hour yielding a decreased in throughput volume from 1170 to 375 mL. Along with, the amount of total chromium uptake (q_e) was evaluated using Equation 2.23 and observed that q_e also decreased from 4.45- 3.26 mg/g with increased in flow rate from 1.5 mL/min to 2.5 mL/min. At higher flow rate, contact time between PANI-jute and chromate ions decreased resulting lesser intra-particular diffusion of metal ions on PANI-jute. This led to an early breakthrough and early saturation of column bed yielding less adsorption.

Table 4.34: Comparison of experimental and theoretical breakthrough time using BDST model for total chromium adsorption using PANI-jute

Break-through (%)	Flow rate (mL/min)						Initial Cr(VI) (mg/L)					
	1.5			2.5			5			15		
	t_{exp} (h)[a]	t_{theo} (h)[b]	RSD (%)[c]	t_{exp} (h)[a]	t_{theo} (h)[b]	RSD (%)[c]	t_{exp} (h)[a]	t_{theo} (h)[b]	RSD (%)[c]	t_{exp} (h)[a]	t_{theo} (h)[b]	RSD (%)[c]
1	13	14.2	0.84	2.5	2.4	1.92	19	19.4	1.82	3.5	3.4	1.67
10	18.5	19.0	1.89	3	4.1	1.17	26	26.8	1.03	5	5.1	0.98
50	26	36.4	23.60	9.8	18.8	44.56	30	53.7	40.1	20	16.4	14.08
90	105	65.8	32.42	66	41.3	32.55	160	99.2	33.1	47	34	22.68

[a] t_{exp}: Experimental breakthrough time (h)

[b] t_{theo}: Theoretical breakthrough time (h)

[c] RSD: Relative standard deviation percentage (Standard deviation x 100/average)

(e) Design of columns for different initial concentrations

Degree of predictability for different scale initial concentration of Cr(VI) by BDST model was checked by conducting running two columns with different influent Cr(VI) of 5 and 15 mg/L at flow rate of 2 mL/min and column bed depth 40 cm. Theoretical breakthrough time were obtained from previous column study conducted at same flow rate 2 mL/min, depth 40 cm and influent Cr(VI) 10 mg/L. Using Equations (2.30- 2.33), theoretical slopes and intercepts were calculated and breakthrough times for both 5 and 15 mg/L initial Cr(VI) concentration were evaluated (Table 4.34).

Predicted breakthrough time were much in agreements with the experimental breakthrough time with RSD value of 1.82% and 1.03% at breakthrough of 1% and 10% respectively for initial Cr(VI) 5 mg/L. Similarly for Cr(VI) 15 mg/L, RSD value of 1.67% and 0.98% for breakthrough of 1% and 10% respectively were obtained. However RSD value of 5– 40.1% for both initial Cr(VI) concentration of 5 and 15 mg/L suggest the conformity of BDST model till 10% breakthrough. With the increase in influent Cr(VI) from 5 to 15 mg/L corresponding 1% breakthrough time decreased from 19-3.5 hour with the subsequent decrease of throughput volume from 2.28 L to 0.42 L. At higher influent Cr(VI), fixed bed got

saturated with chromate ions more quickly thereby decreasing the breakthrough and exhaustion time. However q_e value increased from 4.14 to 5.02 mg/g total chromium with increase in influent concentration from 5 to 15 mg/L. Probably at higher concentration of chromate, loading rate increased even though contact time decreased and the net effect was an appreciable increase in adsorption capacity. These suggest that initial concentration of adsorbate effects the diffusion of adsorbate in adsorbent.

(f) Theoretical break through curve

The theoretical breakthrough was generated with the initial concentration of 10 and 20 mg/L. The equilibrium line was prepared using Langmuir's adsorption isotherm of batch work of total chromium removal by PANI-jute, $q_e = \frac{162.89 \text{ X } 0.02 C_e}{1 + 0.02 C_e}$. An operating line was drawn passing through the origin and intersecting the equilibrium curve at C_o of 10 mg/L and 20 mg/L yielding respective q_e values of 10.48 mg/g and 17.96 mg/g (Figure 4.68).

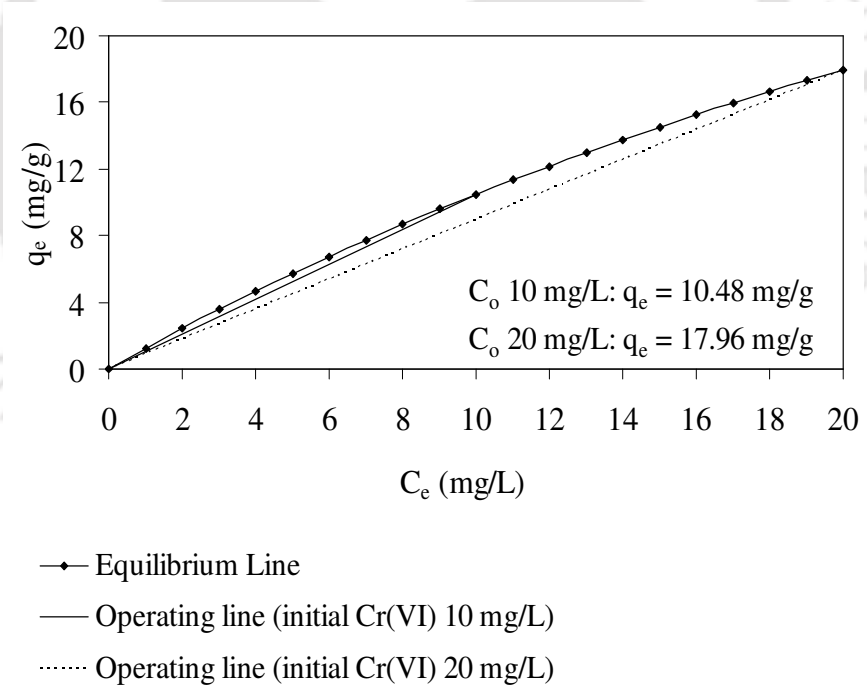

Figure 4.68: Equilibrium and operating lines to predict breakthrough curve

A graph of C versus $(C - C_e)^{-1}$ was plotted where the area under the curve of $(C - C_e)^{-1}$ represented the value of the integration of Equation 2.37 and is shown in Figure 4.69. For initial Cr(VI) of 10 mg/L and 20 mg/L, 41.48 and 17.48 sq. units were obtained respectively.

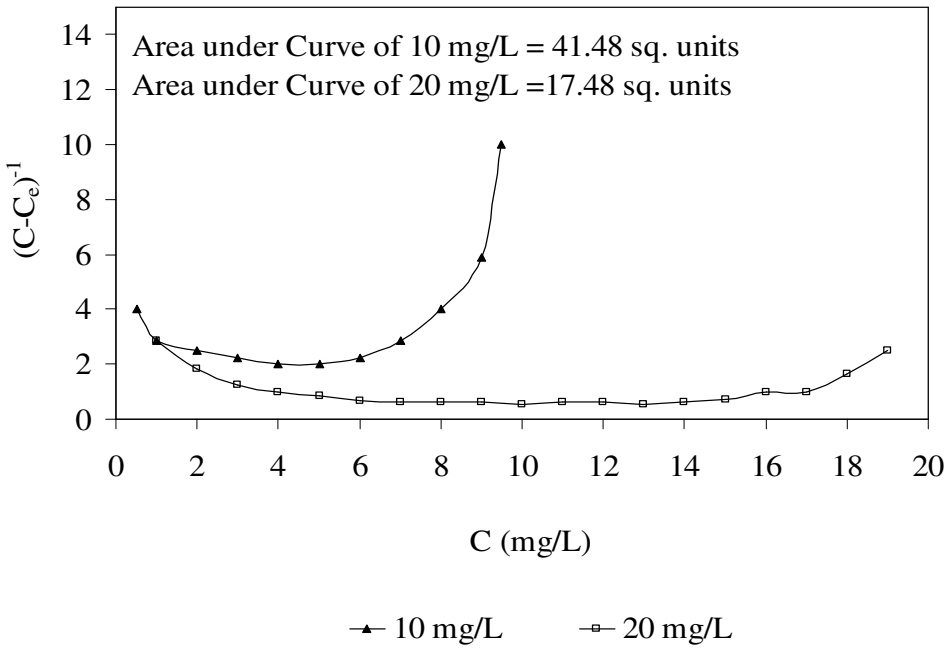

Figure 4.69: Curve area to evaluate for determination of theoretical breakthrough curve of total chromium

The theoretical breakthrough curves were generated by plotting $(V_t - V_B)/(V_E - V_B)$ versus (C/C_o) and is presented in Figure 4.70. For both the initial Cr(VI) of 10 mg/L and 20 mg/L, the experimental and theoretical breakthrough curves followed the same trend.

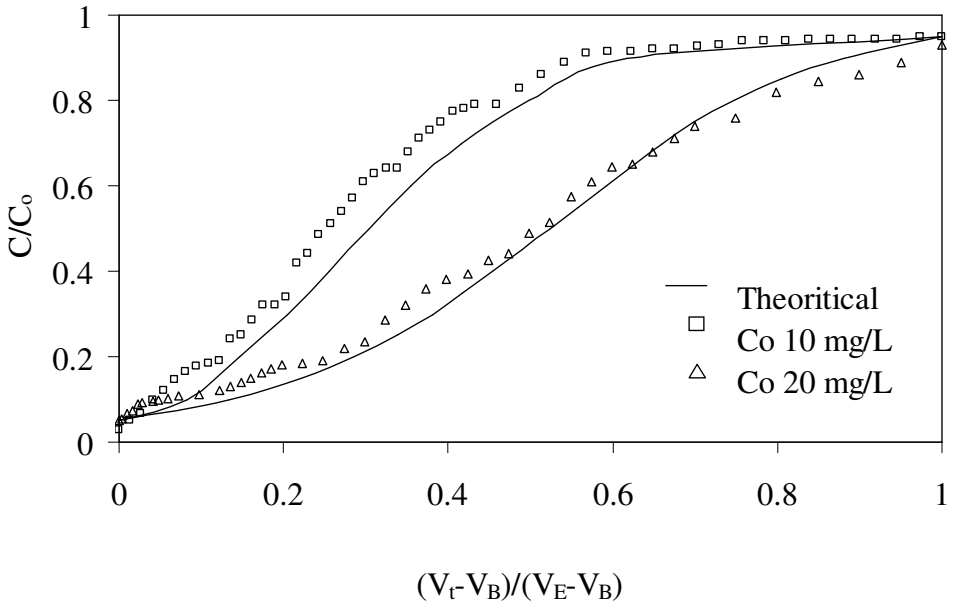

Figure 4.70: Theoretical and experimental breakthrough curve of total chromium

(g) Desorption and recovery

The recovery of metal ions from the metal saturated bed was another important aspect for reusability of adsorbent to reduce the process cost. Before starting the desorption experiment, one adsorption experiment was carried out with three column of 20, 30 and 40 cm depth initially fed with 20 mg/L Cr(VI) at 2.5 mL/min flow rate till exhaust. The exhausted adsorbent was used for desorption study. Desorption study was conducted with desorbent of 1 M NaOH at lower flow rate of 1 mL/min. Lower flow rate was applied so as to access more contact time and concentrate the chromate ions in possible minimum volume. A plot of throughput volume of desorbents versus concentration of total chromium recovered is shown in Figure 4.71.

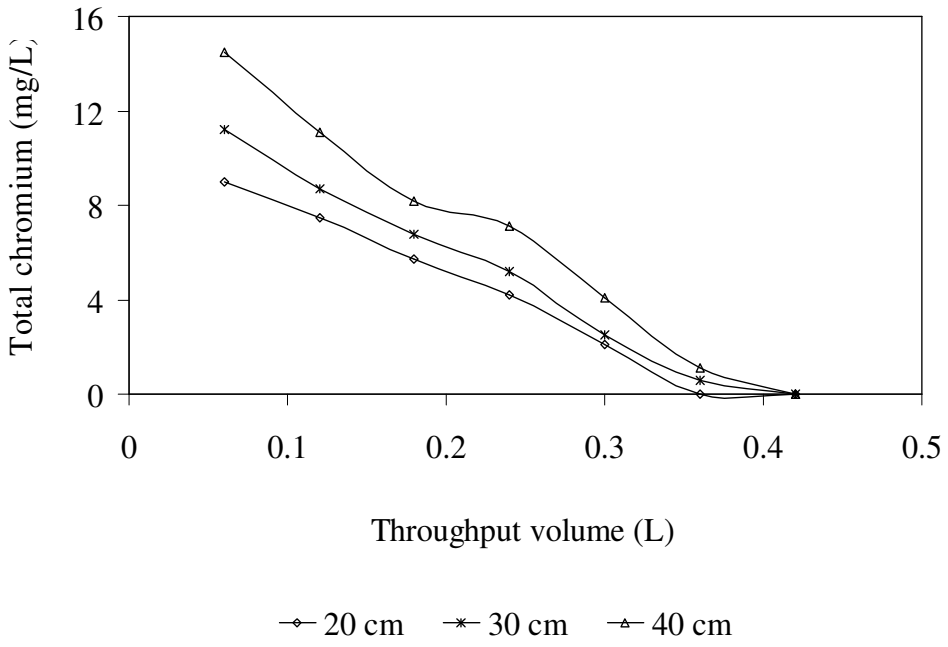

Figure 4.71: Desorption profiles of total chromium at different bed depth [Bed depth (cm): 20, 30 and 40 cm; Initial NaOH: 1 M; flow rate: 1 mL/min]

From the figure, effluent total chromium concentration was observed to be decreased with time elapsed. After throughput volume of 0.42 L (7 h of desorption operation), there were no further total chromium traced in the effluent. Thus all chromate ions were able to concentrate on 0.42 L of desorbent. 2.48%, 3.08% and 2.99% of total chromium were desorbed at 20, 30 and 40 cm of column bed depth respectively. This value was much lower than value observed in batch study of Cr(VI) removal by PANI-jute, where almost 83%

desorption was observed while using 2 M NaOH in 10 min. Probably increasing NaOH strength further or desorption in batch process may recover back more total chromium.

4.3 Studies with support less AFC

AFC coated silica gel and PANI-jute has been found a better alternative versatile adsorbent that can remove both anionic and cationic heavy metals at acidic and basic pH conditions respectively. However weight of support materials (silica gel/ jute fiber) also contributes to the weight of adsorbent. Therefore larger weight of own support material put several hurdles for its effective use. As such amount of metal ions removed per weight of adsorbent is lesser than the lone AFC polymer is supposed to achieve. Therefore efforts were made to make AFC an adsorbent without any base material support. It was observed that during the synthesis of AFC that if ratio between aniline to formaldehyde is more than optimum ratio of 1: 1.62, obtained AFC was in form of solid cakes. In order to achieved better adsorbent, alcohols were introduced to create more space and more viscous. Introduced alcohols during synthesis of AFC include t-butanol, methanol, isopropanol, n-octanol and glycerine.

4.3.1 Characterization of support less AFC synthesized with alcohols

Morphology of the polymers obtained were studied by employing scanning electron microscopic (Figures 4.72 & 4.73). SEM picture of the polymer synthesized in presence of t-butanol revealed the formation of micron sized spheroids which are almost uniform (almost uniformly 750 nm to 2 µm in size) (Figure 4.72) of polymers but morphologically different solid polymer in case of other alcohols. The presence of methanol, isopropanol, n-octanol and polyalcohols glycerine leads to amorphous polymer. The polymer formed due to glycerine was semi transparent gel which once dried breaks in to flakes/layers consistent with its SEM image.

4.3.2 Removal of Cr(VI) by support less AFC modified with alcohol

The results of the Cr(VI) binding for the polymers is shown in Table 4.35. All the polymers, except spheroids from t-butanol show effective removal of Cr(VI) with high q_e. In comparison, reported amine containing polymers acrilonitrile fibre and crosslink polymer

have q_e values 20.7 mg/g and 23 mg/g respectively (Deng and Bai 2004; Bayramoglu and Arica 2008). The present polymers are effective even at a low concentration of 9 mg/L and reduces Cr(VI) level by 70% (~ 3 mg/L) in case of polymer synthesized from isopropanol Table 4.35. The variation of q_e values for a particular initial concentration of Cr(VI) from polymer to polymer might be due to the differences in accessibility of the $-NH_3^+$ exchange sites. The removal is highest for polymers from methanol and isopropanol. The polymer from t-butanol shows considerably less removal of Cr(VI) compared to polymers synthesized from other alcohol. On the other hand, polymers from methanol, isopropanol or n-octanol due to their lack of seeding during formation yields exchange sites are more open for access to Cr(VI). The SEM photograph of the t-butanol sample after it was soaked in Cr(VI) solution for several hours followed by washing and vacuum drying (Figure 4.74) shows that some of the spheroids have been swollen to 2–3 µm size and burst open showing interiors as empty hollow sphere. Cr(VI) removal experiments were tested for both grinded and ungrinded form to check the effect of surface area (Table 4.35). Decreasing the surface area with large particle size (~ 100 mm^3 cubic blocks), the polymers remain effective in removing Cr(VI) (Table 4.36). Thus the polymers are porous enough to enable the solvent penetration through the matrix.

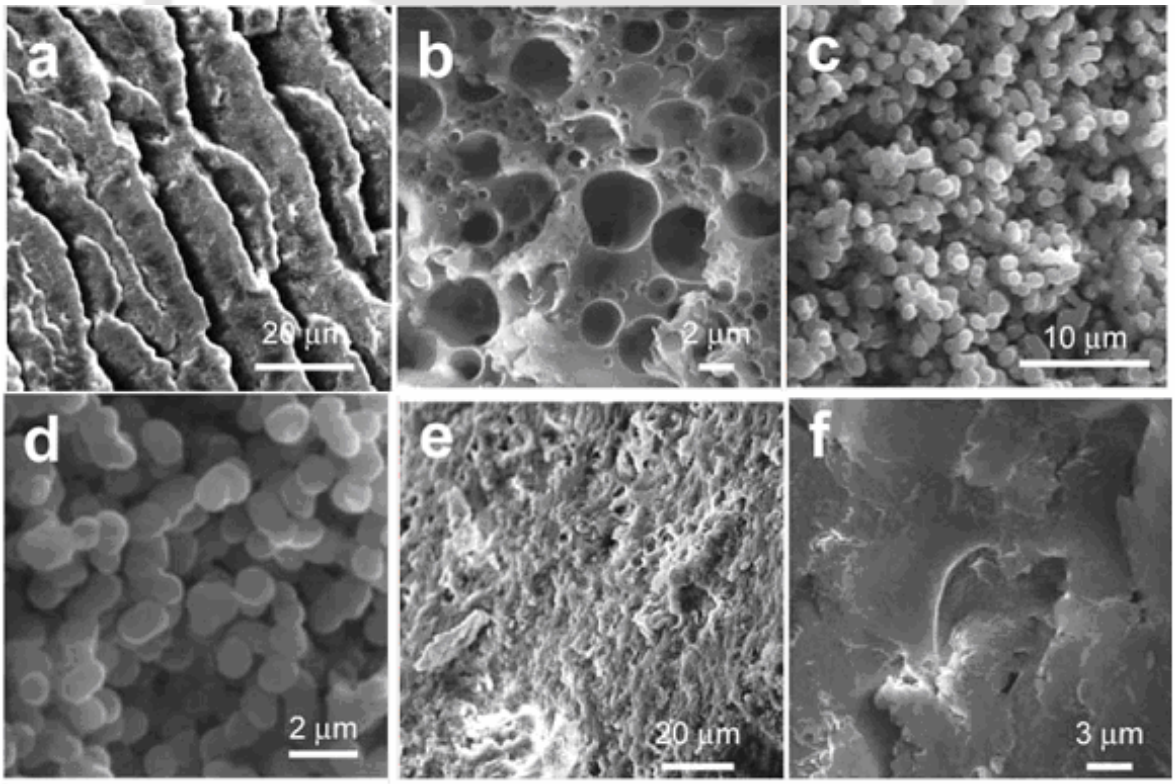

Figure 4.72: SEM images of the polymers formed in presence of (a) methanol, (b) isopropanol, (c,d) t-butanol, (e) noctanol and (f) glycerine.

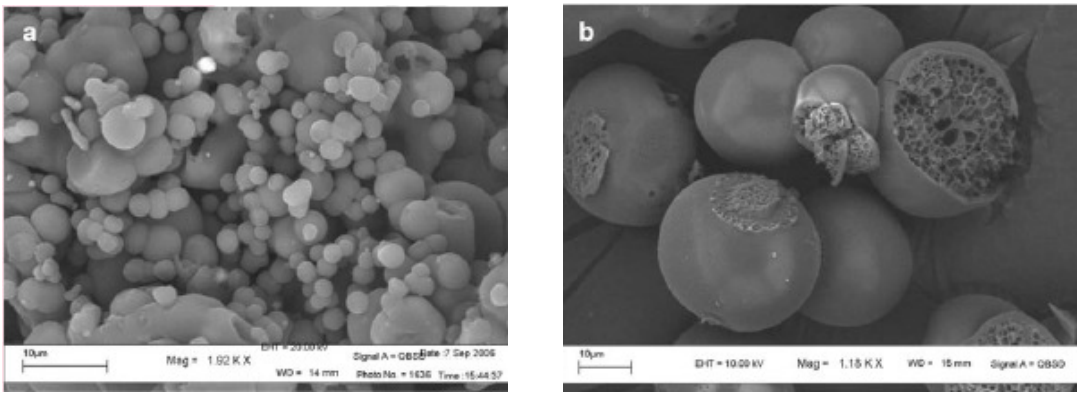

Figure 4.73: SEM images of (a) t-Butanol-AFC from concentrated medium (b) iso-Propanol-AFC from temperature controlled medium

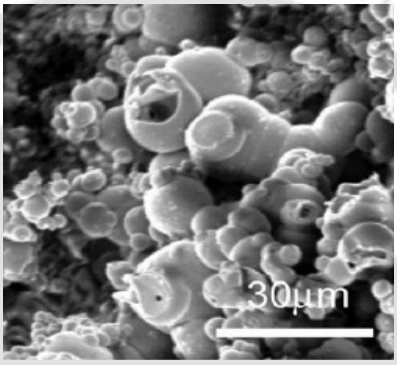

Figure 4.74 SEM images of the AFC polymer after chromium binding.

Table 4.35: Binding properties of the grinded polymers for Cr(VI) in different initial concentration at pH 3

Initial Cr(VI) Conc.	100 mg/L		50 mg/L		9 mg/L	
Polymer prepared from	Cr(VI) removal (%)	q_e (mg/g)	Cr(VI) removal (%)	q_e (mg/g)	Cr(VI) removal (%)	q_e (mg/g)
Methanol	68	68	66	33	61	2.7
Isopropanol	39	39	50	25	70	3.1
t-butanol	13	13	28	14	50	2.2
n-Octanol	66	66	76	38	49	2.2
Glycerine	44	44	66	33	69	3.1

Quantity of polymer used: 1g/L for initial conc. of 100 mg/L and 50 mg/L, and 2 g/L for 9 mg/L. Each set was allowed to equilibrate for 3 h.

Table 4.36: Binding properties of the large particles of polymers (~ 100 mm^3 cubic blocks) for Cr(VI) in different initial concentration at pH 3.

Initial Cr(VI) Conc.	100 mg/L		50 mg/L	
Polymer prepared from	Cr(VI) removal(%)	q_e (mg/g)	Cr(VI) removal(%)	q_e (mg/g)
Methanol	40	40	52	26
Isopropanol	40	40	60	30
t-butanol	30	30	24	12
n-Octanol	27	27	22	11
Glycerine	31	31	44	22

Quantity of polymer used: 1 g/L. Polymers used are ~ 3–5 mm square blocks. Each set was allowed to equilibrate for 3 h.

Chapter 5

Conclusions

This lab-scale study was conducted both in batch and column mode with synthetic wastewater containing heavy metals like hexavalent chromium [Cr(VI)], mercury [Hg(II)], trivalent chromium [Cr(III)], copper [Cu(II)], cadmium [Cd(II)] and lead [Pb(II)]. Two amine based functionalized polymers aniline formaldehyde condensate (AFC) coated on silica gel and polyaniline synthesized on jute fiber (PANI-jute) were prepared and employed for the removal of heavy metal ions. After studying the loop holes of both the polymers, a support less AFC was synthesized and preliminary investigation was carried out. From the present study, major conclusions were drawn and are listed below.

1. AFC polymer was synthesized using aniline and formaldehyde in acidic medium. Optimum ratio between aniline and formaldehyde for synthesis of AFC polymer was observed as 1.6:1. When aniline was higher than the optimum ratio, solubility of the polymer increased and more polymers was washed away during synthesis. However when the ratio decreased from optimum, polymer formation was hindered due to excessive cross linking of formaldehyde.

2. The obtained AFC polymer being resinous, support material was required to make granular adsorbent. Due to sticky nature of the AFC polymer, only silica gel was observed as the best support material. On characterization, pH_{ZPC} for AFC coated silica gel was observed as 6.2 suggesting favorable adsorption of anionic metals at pH < 6.2 and cationic metals above pH 6.2.
3. Optimum pH for removal of hexavalent chromium [Cr(VI)] by AFC was observed at pH 3 with maximum removal of 64.5 mg/g by electrostatic attraction of protonated amines (NH_3^+) of AFC with anionic acid chromate ion ($HCrO_4^-$). During desorption 0.5 M NaOH recovered 56% Cr(VI) whereas mineral acids recovered more than 80% chromium in the form of trivalent ion, due to reduction of Cr(VI) to Cr(III) by mineral acids.
4. During adsorption of trivalent chromium [Cr(III)] with AFC, removal increased with increase in pH achieving maximum removal of 25.31 mg/g at pH 6. Formation of multidentate coordination bonds between $[CrOH]^{2+}$ and $[Cr(OH)_2]^{1+}$ with deprotonated amine group ($–NH_2$) of AFC was the plausible mechanisms for removal of Cr(III) by AFC. Only 41.7% Cr(III) was able to recovered by desorption using mineral acids probably due to the high kinetic immobility of Cr(III).
5. Maximum removal of 174 mg/g of Hg(II) was observed in the pH range of 7- 9 and the main plausible mechanism is the binding of $Hg(OH)_2$ with amine group of AFC by ligand exchange process. Pottasium iodide and mineral acids both showed high desorption (90-100%) of Hg(II) from AFC. During desorption experiment, significant amount of polymer was released from surface of silica gel (as solution turn yellow). This polymer from mineral acid solution was extracted out using chloroform and recoated on silica gel. This regenerated AFC was further employed for Hg(II) adsorption with almost 80% Hg(II) removal for four cycles.
6. The coating of AFC on silica gel being a physical one was soluble in mild organic solvents like methanol and chloroform and during interaction of chromium-AFC, brown color effluent was generated probably due to degradation of AFC in strong acidic environment. From workability point of view, clogging of column bed with AFC coated silica gel occurred frequently probably due to its smaller effective size and gelling up of polymers inside column bed requiring maximum monitoring.
7. The second amine based polymer was synthesized using aniline and 1,4-phenylenediamine in acidic medium. This polymer, polyaniline (PANI) being resinous, required support medium. Jute fiber was observed as a suitable support material due to its light weight, easily availability and low cost. In order to improve the coating, PANI was directly synthesized over the jute surface. During

characterization, obtained polymer was identified as short chain polyaniline (oligoaniline) and its pH_{ZPC} was 6.6.

8. The optimum ratio of aniline to 1,4-phenylenediamine was obtained as 1: 0.14 in terms of metal removal. When amount of 1,4-phenylenediamine (chain length inhibitor) was increased, solubility of the polymer increased due to decrease in the chain length and washed out from jute fibre surface during synthesis. On the other hand when ratio was increased more, amount of chain inhibitor decreased increasing the chain length of polymer. However increase in chain length suggests availability of less amount of terminal amine group for metal binding.
9. When PANI-jute was employed for removal of hexavalent chromium, maximum removal of 62.9 mg/g was achieved at pH 3 by electrostatic attraction of protonated amines of PANI-jute with anionic specie of Cr(VI) $HCrO_4^-$. Desorption by mineral acids were able to recovered 83% Cr(VI) by NaOH whereas mineral acids recovered 93% in form of Cr(III).
10. During interaction of cationic metal ions Cr(III), Cu(II), Cd(II), Hg(II) and Pb(II) with PANI-jute, removal trend were almost similar for all metal ions, with removal increased with increase in pH achieving optimum pH in range of 6- 9. Removal mechanism was also observed similar for all cationic ions with coordination bond formation between cationic metal species and deprotonated amine ($-NH_2$) of PANI-jute. Maximum removal of Cu(II), Cd(II), Pb(II) and Hg(II) by PANI-jute were observed as 24.56, 18.79, 21.33 and 78.7 mg/g respectively.
11. Desorption studies of PANI-jute revealed 92 and 82% recover of Cu(II) and Pb(II) respectively and complete recovery for Hg(II) and Cd(II) by mineral acids. Since high desorption were obtained for all the metal ions, PANI-jute after desorption of metals ions were washed with water to neutralized its surface charge and further employed for adsorption of metal ions. Through this process of adsorption-desorption-adsorption cycle, PANI-jute could be used for more than six cycles without compromising metal removal efficiency.
12. Adsorption kinetics for all metal ions by both AFC coated silica gel and PANI-jute achieved within 120- 180 minutes suggesting rapid adsorption and obeyed Lagergren's pseudo second order kinetic model confirming chemisorption. A comparative study with mixed metal solutions also showed similar result for both the polymers with adsorption in the order of Cu(II) > Ni(II) > Cr(III) > Hg(II) > Pb(II) > Cd(II). Comparative adsorption of mixed metal ions was according to preferences dictated by the hard-soft theory of acids and bases and ligand exchange rate of metal ions.

13. Adsorption isotherm studies of metal ions by AFC shows adsorption Cr(VI), Cr(III) and Hg(II) on AFC can be well explained by Langmuir's isotherm even though adsorption of both Cr(III) and Cr(VI) fitted on Freundlich's isotherm. These finding suggest the nature of monolayer adsorption of these metal ions on AFC coated silica gel and insignificant interactions between the adsorbed metal ions on surface of AFC coated silica gel.
14. Adsorption isotherm of metal ions Cr(VI), Hg(II), Cu(II), Cd(II) and Pb(II) however was observed to be well fitted and can be explained better by Freundlich's isotherm as compared to Langmuir's isotherm suggesting the heterogenous surface of PANI-jute and lateral interactions between adsorbed metal ions.
15. Dynamic studies of column experiment revealed the achievement of removal of highly toxic Hg(II) by AFC coated silica gel and Cr(VI) by PANI-jute with effluent below the permissible limit of 0.05 µg/L for both the metal ions. For Hg(II), maximum uptake of 9.22 mg/g at column depth of 30 cm and initial Hg(II) 50 mg/L was achieved whereas 4.66 mg/g Cr(VI) removal was achieved by AFC coated PANI-jute at column bed depth of 60 cm and initial Cr(VI) of 120 mg/L. The experimental breakthrough profiles were in good agreement with theoretical breakthrough profile obtained from batch data.
16. AFC showed higher metal uptake as compared to PANI due to presence of more amines in the chain length as compared to terminal amine group in PANI-jute. However, from reusability point of view, PANI-jute showed more promising results than AFC. Thus the over all efficiency of PANI-jute can be increased by reusing in successive cycles without any regeneration thus decreasing the overall treatment cost. Besides, for metals with low desorption (like chromium), ignition of metal contaminated PANI-jute reduced the volume of spent adsorbent by more than 95- 99% solving the problem of solid waste disposal.
17. Presences by all metal ions on surface of polymers were examined by electron diffraction X-ray (EDX) before and after adsorption. Presence of Cu(II) and Cr(III) were further confirmed by employing electron spin resonance (ESR) technique.
18. As support material throws hurdles to effectivity of both AFC and PANI, third polymer, support less AFC was synthesized by increasing the amount of formaldehyde to have more cross linking and by introducing alcohols to create more voids. Introduced alcohols include t-butanol, methanol, isopropanol, n-octanol and glycerine. During preliminary investigation, support less AFC removed 68 mg/g Cr(VI) as against 25 and 23 mg/g by AFC coated silica gel and PANI-jute respectively under similar experimental conditions. However, synthesis of support less AFC seems to be

more sensitive than the two polymers. Temperature control during synthesis process of support less AFC was observed as very important which otherwise oxidized the polymer forming red flakes. Regarding its effective size, larger size of polymer yielded lesser removal of metal ions due to less surface area whereas grinding to smaller size polymer resulted floating of the polymer in solution resulting nonuniform mixing with metal solution. Therefore compromising between removal capacities and decreasing size of polymer was an important parameter to be considered for optimization. From commercialization point of view, AFC polymer both with and without support can be stored for six months time without degradation in metal removal capacity. PANI-jute however showed more stability and could be stored for 40 months time period without any degradation.

From the above discussions certain aspects of this work are suggested for future studies:

1. Optimization of synthesis procedure of support less AFC to obtain a reproducible polymer adsorbent.
2. Study on removal of metal ions (batch and column mode) with support less AFC.
3. Toxicity study on treated effluent of metal contaminated wastewater by AFC, PANI-jute and support less AFC.
4. To conduct metal removals study with actual industrial effluent wastewater.
5. To carried out pilot scale column study with objective of removing metal ions effectively.

Reference

1. Adak, A., and Pal, A. (2006). "Removal of phenol from aquatic environment by SDS-modified alumina: Batch and fixed bed studies." *Sep. Purif. Technol*., 50, 256-262.
2. Aderhold, D., Williams, C. J., and Edyvean, R. G. J. (1996). "The removal of heavy-metal ions by seaweeds and their derivatives." *Biores. Technol*., 58, 1-6.
3. Ajmal, M., Khan, A. H., Ahmad, S., and Ahmad, A. (1998). "Role of sawdust in the removal of copper(II) from industrial wastes." *Water Res*., 32, 3085–3091.
4. Aksu, Z., and Isoglu, I. A. (2005). "Removal of copper(II) ions from aqueous solution by biosorption onto agricultural waste sugar beet pulp." *Process Biochem*., 40, 3031–3044.
5. Aksu, Z., Kutsal, T., Gun, S., Haciosmanoglu, N., and Gholaminejad, M. (1991). "Investigation of biosorption of Cu(II), Ni(II) and Cr(VI) ions to activated sludge bacteria." *Environ. Technol.*, 12, 915–21.
6. Altundogan, H. S. (2005). "Cr(VI) removal from aqueous solution by iron (III) hydroxide-loaded sugar beet pulp." *Process Biochem*., 40, 1443-1452.
7. APHA, WEF, AWWA. (1988). Standard Methods for the Examination of Water and Wastewater, 20th ed., APHA, Washington, D.C. USA.
8. Arslan, G., and Pehlivan, E. (2008). "Uptake of Cr^{3+} from aqueous solution by lignite-based humic acids." *Biores. Technol*., 99, 7597-7605.
9. Atia, A. A., Donia, A. M., and Elwakeel, K. Z. (2005). "Selective separation of mercury (II) using a synthetic resin containing amine and mercaptan as chelating groups." *Reactive Functional Polymers*, 65, 267–275.
10. Baes, C. F., and Mesmer, R. E. (1976). The Hydrolysis of Cations, Wiley, New York, p. 311.
11. Bai, R. S., and Abraham, T. E. (2002). "Studies on enhancement of Cr(VI) biosorption by chemically modified biomass of *Rhizopus nigricans*." *Water Res*., 36, 1224–1236.
12. Bayramoğlu, G., and Arıca, M. Y. (2005). "Ethylenediamine grafted poly(glycidylmethacrylate-co-methylmethacrylate) adsorbent for removal of chromate anions." *Sep. Purif. Technol*., 45, 192-199.
13. Bayramoğlu, G., and Arica, M. Y. (2008). "Adsorption of Cr(VI) onto PEI immobilized acrylate-based magnetic beads: Isotherms, kinetics and thermodynamics study." *Chem. Eng. J*., 139, 20-28.
14. Bayramoğlu, G., Tuzun, I., Celik, G., Yilmaz, M., and Arica, M. Y. (2006). "Biosorption of mercury(II), cadmium(II) and lead(II) ions from aqueous system by microalgae

Chlamydomonas reinhardtii immobilized in alginate beads." *Int. J. Miner. Process*., 81, 35–43.

15. Benefield, L. D., Judkins, J. F., and Weand, B. L. (1982). Process Chemistry for Wastewater Treatment, Prentice-Hall, Englewood Cliffs, NJ, 433–439.
16. Bhattacharyya, K. G., and Sharma, A. (2004). "Adsorption of Pb(II) from aqueous solution by Azadirachta indica (Neem) leaf powder". *J. Hazard. Mater*., B113, 97-109.
17. Bohart, G. S., and Adams, E. Q. (1920). "Some aspects of behavior of charcoal with respect to chlorine." *J. Am. Chem. Soc*., 42, 523-529.
18. Bryson, W. G. (1980). "Application of electron spin resonance in the analytical chemistry of transition metal ions, Part 3. Determination of chromium(III) in aqueous solution [l]." *Anal. Chim. Acta*, 116, 353-357.
19. Chanda, M., and Rempel, G. L. (1995). "Polyethyleneimine gel-coat on silica: High uranium capacity and fast kinetics of gel-coated resin." *Reactive Polymers,* 25, 25-36.
20. Chen, H., and Wang, A. (2007). "Kinetic and isothermal studies of lead ion adsorption onto palygorskite clay." *J. Colloid Interface Sci*., 307, 309- 316.
21. Chen, J. P., Yoon, J. T., and Yiacoumi. S. (2003). "Effects of chemical and physical properties of influent on copper sorption onto activated carbon fixed-bed columns." *Carbon*, 41, 1635-1644.
22. Chen, J., Tao, X., Xu, J., Zhang, T., and Liu, Z. (2005). "Biosorption of lead, cadmium and mercury by immobilized Microcystis aeruginosa in a column." *Proc. Biochem.*, 40, 3675-3679.
23. Chiarle, S., Ratto, M., and Rovatti, M. (2002). "Mercury removal from water by ion exchange resins adsorption." *Water Res*., 34, 2971-2978.
24. Chiron, N., Guilet, R., and Deydier, E. (2003). "Adsorption of Cu(II) and Pb(II) onto a grafted silica: isotherms and kinetic models." *Water Res*., 37, 3079–3086.
25. Cho, H., Oh, D., and Kim, K. (2005). "A study on removal characteristics of heavy metals from aqueous solution by fly ash." *J. Hazard. Mater.*, 127, 187-195.
26. Christophi, C. A., and Axe, L. (2000). "Competition of Cd, Cu and Pb adsorption on goethite." *J. Environ. Eng*., 126, 66-74.
27. Cimino, G., Passerini, A., and Toscano, G. (2000). "Removal of toxic cations and Cr(VI) from aqueous solution by hazelnut shell." *Water Res*., 34, 2955-2962.
28. Connell, D. W., Morton, H. C., and Bycroft, B. M. (1984). Chemistry and ecotoxicology of pollution, John Wiley & Sons, Inc., New York.

29. Cooney, D. O. (1999). Adsorption design for wastewater treatment, CRC Press LLC, Boca Raton, Florida, USA.
30. Cotton, F. A., and Wilkinson, G. (1988). Advanced Inorganic Chemistry, 5th edition, John Wiley & Sons, New York, pp 679- 697.
31. Cox, M., Shafey, E. I., Pichugin, A. A., and Appleton, Q. (2000). "Removal of mercury(II) from aqueous solution on a carbonaceous sorbent prepared from flax shive." *J. Chem. Technol. Biotech.*, 75, 427–435.
32. Cruz, C. C. V., Costa, A. C. A. D., Henriques, C. A., and Luna, A. S. (2004). "Kinetic modeling and equilibrium studies during cadmium biosorption by dead *Sargassum sp.* Biomass." *Biores. Technol.*, 91, 249–257.
33. Dakiky, M., Khamis, M., Manassra, A., and Mer'eb, M. (2002). "Selective adsorption of chromium (VI) in industrial wastewater using low-cost abundantly available adsorbents." *Adv. Environ. Res.*, 6, 533-540.
34. Daneshvar, N., Salari, D., and Aber, S. (2002). "Chromium adsorption and Cr(VI) reduction to trivalent chromium in aqueous solution by soya cake." *J. Hazard Mater.*, B94, 49-61.
35. Deepa, K. K., Sathishkumar, M., Binupriya, A. R., Murugesan, G. S., Swaminathan, K., and Yun, S. E. (2006). "Sorption of Cr(VI) from dilute solutions and wastewater by live and pretreated biomass of *Aspergillus flavus*." *Chemosphere*, 62, 833–840.
36. Deng, S., and Bai, R. (2004). "Removal of trivalent and hexavalent chromium with aminated polyacrylonitrile fibers: performance and mechanisms." *Water Res.*, 38, 2424-2432.
37. Ekinci. E., Budinova, T., Yardim, F., Petrov, N., Razvigorova, M., and Minkova, V. (2002). "Removal of mercury ion from aqueous solution by activated carbons obtained from biomass and coals." *Fuel Processing Technol.*, 77–78, 437– 443.
38. Elangovan, R., Philip, L., and Chandraraj, K. (2008). "Biosorption of hexavalent and trivalent chromium by palm flower (*Borassus aethiopum*)." *Chem. Eng. J.*, 141, 99-111.
39. Ergican, E., Gecol, H., and Fuchs, A. (2005). "The effect of co-occurring inorganic solutes on the removal of arsenic (V) from water using cationic surfactant micelles and an ultrafiltration membrane." *Desalination*, 181, 9-26.
40. Farajzadeh, M. A., and Monji, A. B. (2004). "Adsorption characteristics of wheat bran towards heavy metal cations." *Sep. Purif. Technol.*, 38, 197-207.

41. Figueira, M. M., Volesky, B., Ciminelli, V. S. T., and Roddick, F. A. (2000). "Biosorption of metals in brown seaweed biomass." *Water Res*., 34,196–204.
42. Fourest, E., Chanal, C., and Roux, J. C. (1994). "Improvement of heavy metal biosorption by mycelial dead biomass (*R. arrhizus, Mucor miehei* and *Penicillium chrysogenus*)." *Microbial. Rev*., 14, 325-332.
43. Freundlich, H. M. F. (1906). "Uber die adsorption in losungen." *Zeitschrift für Physikalische Chemie (Leipzig)*, 57A, 385–470.
44. Gang, D., Banerji, S. K., and Clevenger, T. E. (2000). "Chromium (VI) removal by modified PVP-coated silica gel." *Practice Periodical of Hazardous, Toxic, and Radioactive Waste Mgmt.*, 4, 105-110.
45. Gode, F., and Pehlivan, E. (2003). "A comparative study of two chelating ion-exchange resins for the removal of chromium(III) from aqueous solution." *J. Hazard. Mater*., 100, 231-243.
46. Goel, J., Kadirvelu, K., Rajagopal, C., and Garg, V. K. (2005). "Removal of lead(II) by adsorption using treated granular activated carbon: Batch and column studies." *J. Hazard. Mater*., B125, 211–220.
47. Goel, P. K., (1997). Water Pollution Causes, Effects and Control, New age international publishers, New Delhi, India.
48. Gonza´le, J. R., Peralta-Videa, E., Rodrı´guez, M., and Delgado, J. L. (2006). "Potential of *Agave lechuguilla* biomass for Cr(III) removal from aqueous solutions: Thermodynamic studies." *Biores. Technol*., 97, 178–182.
49. Gündogan, R., Acemioglu, B., and Alma, M. H. (2004). "Copper (II) adsorption from aqueous solution by herbaceous peat." *J. Colloid Interface Sci*., 269, 303–309.
50. Gupta, V. K., Jain, C. K., Ali, I., Sharma, M., and Saini, V. K. (2003). "Removal of cadmium and nickel from wastewater using bagasse fly ash-a sugar industry waste." *Water Res.*, 37, 4038–4044.
51. Gupta, V. K., Rastogi, A., Saini, V. K., and Jain, N. (2006). "Biosorption of copper (II) from aqueous solutions by Spirogyra species." *J. Colloid Interface Sci*., 296, 59-63.
52. Guru, M., Venedikb, D., and Murathan, A. (2008). "Removal of trivalent chromium from water using low-cost natural diatomite." *J. Hazard. Mater*., 160, 318-323.
53. Hall, R. K., Eagleton, L. C., Acrivos, A., and Vermeulen, T. (1966). "Pore- and solid-diffusion kinetics in fixed-bed adsorption under constant-pattern conditions." *Ind. Eng. Chem. Fundamentals*., 5, 212-223.

54. Hamadi, N. K., Chen, X. D., Farid, M. M., and Lu, M. G. Q. (2001). "Adsorption kinetics for the removal of chromium (VI) from aqueous solutions by adsorbents derived from used tyres and saw dust." *Chem. Engg. J.*, 84, 95-105.
55. Herrero, R., Lodeiro, P., Rey-Castro, C., Vilarino, T., and Sastre de Vicente, M. E. (2005). "Removal of inorganic mercury from aqueous solutions by biomass of the marine macroalga *Cystoseira baccata*." *Water Res*., 39, 3199–3210.
56. Ho, Y. S. (2003). "Removal of copper ions from aqueous solution by tree fern." *Water Res*., 37, 2323–30.
57. Ho, Y. S. (2006). "Second order kinetic model for the sorption of cadmium onto tree fern: A comparison of linear and non-linear methods." *Water Res*., 40, 119-125.
58. Ho, Y. S., and McKay, G. (2003). "Sorption of dyes and copper ions onto biosorbents." *Process Biochem*., 38, 1047–1061.
59. Ho, Y. S., Chiu, W., and Wang, C. (2005). "Regression analysis for the sorption isotherms of basic dyes on sugarcane dust." *Biores. Technol*., 96, 1285-1291.
60. Horsfall, M. J., and Abia, A. A. (2003). "Sorption of cadmium(II) and zinc(II) ions from aqueous solutions by cassava waste biomass (*Manihot sculenta Cranz*)." *Water Res.,* 37, 4913–4923.
61. Hu, Z., Lei, L., Li, Y., and Ni, Y. (2003). "Chromium adsorption on high-performance activated carbons from aqueous solution." *Sep. Purif. Technol*., 31, 13-18.
62. Huang, C. P., and Ostovic, F. B. (1978). "Removal of cadmium (II) by activated carbon adsorption." *J. Env. Engg. Div, Proceedings of the Americal society of Civil Engineers*, 104, 863-878.
63. Huang, C., and Huang, C. P. (1996). "Application of *Aspergillus oryzae* and *Rhizopus oryzae* for Cu(II) removal." *Water Res*., 9, 1985-1990.
64. Huber, T. A. (2003). "A Literature Survey of Polyaniline, Part 1 Polyaniline as a Radar Absorbing Material, Defence R&D Canada – Atlantic, Technical Memorandum, DRDC Atlantic TM, pp. 2003-2014.
65. Hutchin, R. A. (1973). "New simplified design of activated carbon systems." *Am. J. Chem. Eng*., 80, 133–138. H.C.
66. Inbaraj, B. S., and Sulochana, N. (2006). "Mercury adsorption on a carbon sorbent derived from fruit shell of *Terminalia catappa.*" *J. Hazard. Mater*., B133, 283–290.
67. IS 10500:1991. Drinking water specifications, Bureau of Indian Standards, New Delhi.

68. Jeffery, G. H., Bassett, J., Mendham, J., and Denney, R. C. (1989). Vogel's textbook of quantitative chemical analysis, ELBS, Longman Group, 5th ed., pp 54-55 and 326.
69. Jeon, C., and Ho¨ll, W. H. (2003). "Chemical modification of chitosan an equilibrium study for mercury ion removal." *Water Res*., 37, 4770–4780.
70. Jezierska, J., Henryk, K., Kolarz, B. N. and Trochimczuk, A. (1991). "Electron paramagnetic resonance evidence for direct co-ordination of copper(II) ions by acrylic resins containing amine groups." *Polymer Bullet*, 26, 231-235.
71. Justi, K. C., Laranjeira, M. C. M., Neves, A., Mangrich, A. S., and Fa´vere, V. T. (2004). "Chitosan functionalized with 2[-bis-(pyridylmethyl) aminomethyl]4-methyl-6-formyl-phenol: equilibrium and kinetics of copper (II) adsorption." *Polymer*, 45, 6285-6290.
72. Kadirvelu, K., Kavipriya, M., Karthika, C., Vennilamani, N., and Pattabhi, S. (2004). "Mercury (II) adsorption by activated carbon made from sago waste." *Carbon*, 42, 745–752.
73. Kadirvelu, K., Namasivayam, C. (2003) "Activated carbon from coconut coirpith as metal adsorbent: adsorption of Cd(II) from aqueous solution" *Adv. Environ. Res.*, 7, 471–478.
74. Kaewsarn, P. (2002). "Biosorption of Copper(II) from aqueous solutions by pre-treated biomass of marine algae *Padina* sp.." *Chemosphere*, 47, 1081–1085.
75. Kalavathy, H. M., Karthikeyan, T., Rajgopal, S., and Miranda, L. R. (2005). "Kinetic and isotherm studies of Cu^{2+} adsorption onto H_3PO_4-activated rubber wood sawdust." *J. Colloid Interface Sci*., 292, 354-362.
76. Karthikeyan, T., Rajgopal, S. and Miranda, L. R. (2005). Chromium(VI) adsorption from aqueous solution by *Hevea Brasilinesis* sawdust activated carbon, *J. Hazard. Mater*., B124, 192-199.
77. Kedar, N. G., Inouea, K., Yamaguchia, H., Makinob, K., and Miyajimaa, T. (2003). "Adsorptive separation of arsenate and arsenite anions from aqueous medium by using orange waste." *Water Res.*, 37, 4945–4953.
78. Khezami, L., and Capart, R. (2005). "Removal of chromium(VI) form aqueous solution by activated carbons: kinetic and equilibrium studies." *J. Hazard. Mater*., 123, 223-231.
79. King, P., Rakesh, N., Beenalahari, S., Kumar P. Y., and Prasad, V. S. R. K. (2007). "Removal pf lead from aqueous solution using *Syzgium cumini* L, Equilibrium and kinetic studies." *J. Hazard. Mater*., 142, 340- 347.
80. Ko, D. C. K., Porter, J. F., and McKay, G. (2000). "Optimised correlations for the fixed-bed adsorption of metal ions on bone char." *Chem. Eng. Sci*., 55, 5819-5829.

81. Kratochvil, D., and Volesky, B. (1998). "Biosorption of Cu from ferruginous wastewater by algal biomass." *Water Res.*, 32, 2760-2768.
82. Kratochvil, D., Pimentel, P., and Volesky, B. (1998). "Removal of trivalent and hexavalent chromium by seaweed biosorbent." *Environ. Sci. Technol.*, 32, 2693-2698.
83. Kumar, G. P., Kumar, P. A., Chakraborty, S., and Ray, M. (2007). "Uptake and desorption of copper ion using functionalized polymer coated silica gel in aqueous environment." *Sep. and Purif. Technol.*, 57, 47- 56.
84. Kumar, U., and Bandyopadhyay, M. (2006). "Fixed bed column study for Cd(II) removal from wastewater using treated rice husk." *J. Hazard. Mater.*, 129, 253-259.
85. Kuyucak, N., and Volesky, B. (1988). "Biosorbents for recovery of metals from industrial solutions." *Biotechnol Lett.*, 10, 137-142.
86. Langmuir, I. (1918). "The adsorption of gases on plane surfaces of glass, mica and platinum." *J. Am. Chem. Soc.*, 40, 1361-1403.
87. Lazaridis, N. K., and Charalambous, Ch. (2005). "Sorptive removal of trivalent and hexavalent chromium from binary aqueous solutions by composite alginate–goethite beads." *Water Res.*, 39, 4385–4396.
88. Lazaridis, N. K., Bakoyannakis, D. N., and Deliyanni, E. A. (2005). "Chromium(VI) sorptive removal from aqueous solutions by nanocrystalline akaganeite." *Chemosphere*, 58, 65-73.
89. Lee, S. H., Jung, C. H., Chung, H., Lee, M. Y., and Yang, J. W. (1998). "Removal of heavy metals from aqueous solution by apple residues." *Process Biochem.*, 33, 205-211.
90. Lee, S. H., Shon, J. S., Chung, H., Lee, M., and Yang, J. (1999). "Effect of Chemical Modification of Carboxyl Groups in Apple Residues on Metal Ion Binding." *Korean J. Chem. Eng.*, 16, 576-580.
91. Li, Y., Liu, C., and Chiou, C. (2004). "Adsorption of Cr(III) from wastewater by wine processing waste sludge." *J. Colloid Interface Sci.*, 273, 95–101.
92. Lippard, S. J., and Berg, J. M. (1994). Principles of bioinorganic Chemistry. University Science Books, Mill Valley, California, USA, pp. 21-22 and 28-29.
93. Liu, G., and Freund, M. S. (1997). "New approach for the controlled Cross-Linking of Polyaniline: Synthesis and Characterization." *Macromolecules*, 30, 5660-5665.
94. Lorenzen, L., Deventer, J. S. J. V., and Landi, W. M. (1995). "Factors affecting the mechanism of the adsorption of arsenic species on activated carbon." *Miner. Engg.*, 8, 557-569.

95. Luo, F., Liu, Y., Li, X., Xuan, Z., and Ma, J. (2006). "Biosorption of lead ion by chemically-modified biomass of marine brown algae *Laminaria japonica*." *Chemosphere*, 64, 1122-1127.

96. Lyubchik, S. I., Lyubchik, A. I., Galushko, O. L., Tikhonova, L. P., Vital, J., Fonseca, I. M., and Lyubchik, S. B. (2004). "Kinetics and thermodynamics of the Cr(III) adsorption on the activated carbon from co-mingled wastes." *Colloids and Surfaces A: Physicochem. Eng. Aspects*, 242, 151–158.

97. Malkoc, E., Nuhoglu, Y., and Abali, Y. (2006). "Cr(VI) adsorption by waste acorn of *Quercus ithaburensis* in fixed beds: Prediction of breakthrough curves, *Chem. Eng. J.*, 119, 61–68.

98. Manuel, P.C., Martinez, J. M., and Macia, R. T. (1995). "Chromium(VI) removal with activated carbons." *Water Res*., 29, 2174-2180.

99. Martínez, M., Miralles, N., Hidalgo, S., Fiol, N., Villaescusa, I., and Poch, J. (2006). "Removal of lead(II) and cadmium(II) from aqueous solutions using grape stalk waste." *J. Hazard. Mater*., 133, 203-211.

100. Matheickal, J. T., Yu, Q., and Woodburn, G. M. (1999). "Biosorption of cadmium(II) from aqueous solution by pretreated biomass of marine algae *Durvillaea pota- torum*." *Water Res*., 33, 335-342.

101. Mathew, B., and Pillai, V. N. R. (1993). "Polymer-metal complexes of amino functionalized divinylbenzene-crosslinked polyacrylamides." *Polymer*, 34, 2650.

102. Mehrotra, A., Gopal, K., and Seth, P. K. (1999). Annual report VIO Hyderabad State. Indian Council of Agriculture Research, ICAR, New Delhi.

103. Melo, J. S., and D'Souza, S. F. (2004). "Removal of chromium by mucilaginous seeds of *Ocimum basilicum*." *Biores. Technol*., 92, 151-155.

104. Merrifield, J. D., Davids, W. G., MacRae, J. D., and Amirbahman, A. (2004). "Uptake of mercury by thiol-grafted chitosan gel beads." *Water Res*., 38, 3132–3138.

105. Metcalf and Eddy (2003). Wastewater Engineering Treatment and Reuse 4th edition, revised, Tata McGraw- Hill publications, New Delhi.

106. Michaels, A. S. (1952). "Simplified method of interpreting kinetic data in fluid bed ion exchange." *Ind. Eng. Chem*. 44, 1922.

107. Mohan, D., Gupta, V. K., Srivastava, S. K., and Chander, S. (2001). "Kinetics of mercury adsorption from wastewater using activated carbon derived from fertilizer waste." *Colloids and Surfaces A: Physicochem. Eng. Aspects,* 177, 169-181.

108. Mohan, D., Pittman, C. U., and Steele, P. H. (2006). "Single, binary and multi-component adsorption of copper and cadmium from aqueous solutions on Kraft lignin-a biosorbent." *J. Colloid Interface Sci*., 297, 489-504.

109. Mohanty, K., Jha, M., Meikap, B. C. and Biswas, M. N. (2005). "Removal of chromium (VI) from dilute aqueous solutions by activated carbon developed from *Terminalia arjuna* nuts activated with zinc chloride." *Chem. Eng. Sci*., 60, 3049 – 3059.

110. Namasivayam, C. and Ranganathan, K. (1995) "Removal of Cd(II) from wastewater by adsorption on waste Fe(III)/Cr(III) hydroxide", *Water Res.*, 29, 1737-1744.

111. Namasivayam, K., and Periasamy, K. (1994). "Adsorption of Pb(II) by peanut hull carbon from aqueous solutions." *Sep. Sci. Technol.*, 39, 2223-2237.

112. Navarro, R., Sump, K., Fujii, N., and Matsumura, M. (1996). "Mercury removal from wastewater using porous cellulose carrier modified with polyethyleneimine." *Water Res.,* 30, 2488-2494.

113. Noeline, B. F., Manohar, B. F., and Anirudhan, T. S. (2005). "Kinetic and equilibrium modelling of lead(II) sorption from water and wastewater by polymerized banana stem in a batch reactor." *Sep. Purif. Technol*., 45, 131–140.

114. Okieimen, J. F. E., Sogbaike, C. E., and Ebhoaye, J. E. (2005). "Removal of cadmium and copper ions from aqueous solution with cellulose graft copolymers." *Sep. Purif. Technol*., 44, 85–89.

115. Olad, A., and Nabavi, R. (2007). "Application of polyaniline for the reduction of toxic Cr(VI) in Water." *J. Hazard. Mater*., 147, 845-851.

116. Parab, H., Joshi, S., Shenoy, N., Lali, A., Sarma, U. S., and Sudersanan, M. (2006). "Determination of kinetic and equilibrium parameters of the batch adsorption of Co(II), Cr(III) and Ni(II) onto coir pith." *Process Biochem*., 41, 609–615.

117. Park, D., Yun, Y. S., and Park, J. M. (2004). "Reduction of hexavalent chromium with the brown seaweed *Ecklonia* biomass." *Environ. Sci. Technol*., 38, 4860-4864.

118. Park, D., Yun, Y. S., Jo, J. H., and Park, J. M. (2005a). "Mechanism of hexavalent chromium removal by dead fungal biomass of *Aspergillus niger.*" *Water Res*., 39, 533-540.

119. Park, D., Yun, Y. S., and Park, J. M. (2005b). "Use of dead fungal biomass for the detoxification of hexavalent chromium: screening and kinetics." *Process Biochem*., 40, 2559-2565.

120. Park, D., Yun, Y. S., and Park, J. M. (2005c). "Studies on hexavalent chromium biosorption by chemically-treated biomass of *Ecklonia* sp,." *Chemosphere*, 60, 1356-1364.

121. Park, D., Yun, Y. S., Yim, K. H., and Park, J. M. (2006). "Effect of Ni(II) on the reduction of Cr(VI) by *Ecklonia* biomass." *Biores. Technol*., 97, 1592-1598.

122. Park, D., Yun, Y. S., Yim, K. H., and Park, J. M. (2008). "How to study Cr(VI) biosorption: Use of fermentation waste for detoxifying Cr(VI) in aqueous solution." *Chem. Eng. J*., 136, 173- 179.

123. Pearson, R. G. (1963). "Hard and soft acids and bases." *J. Am. Chem. Soc*., 85, 3533-3539.

124. Periasamy, K. and Namasivayam, C. (1996) "Removal of copper (II) by adsorption onto peanut hull carbon from water and copper plating industry wastewater", *Chemosphere*, 32(4), 769-789.

125. Prado, A. G. S., and Airoldi, C. (2001). "Adsorption, preconcentration and separation of cations on silica gel chemically modified with the herbicide 2,4 dichloro phenol- xyacetic acid." *Analytica Chim. Acta*, 432, 201–211.

126. Prakasham, R. S., Merrie, J. S., Sheela, R., Saswathi, N., and Ramakrishna, S. V. (1999). "Biosorption of chromium VI by free and immobilized *Rhizopus arrhizus*." *Environ. Poll*., 104, 421-427.

127. Raji, C., and Anirudhan, T. S. (1998). "Batch Cr(VI) removal by polyacrylamide grafted sawdust: kinetics and thermodynamics." *Water Res*., 32, 3772-3780.

128. Ravi, S., Selvakumar, P. N., and Subramanian, P. (2006). "Electron paramagnetic resonance study of Cr^{3+} ions in $(NH_4)_2Co(SO_4)_2.6H_2O$ single crystal." *Solid State Communications,* 138, 129–131.

129. Rengaraj, S., Kim, Y., Joo, C. K., and Yi, J. (2004). "Removal of copper from aqueous solution by aminated and protonated mesoporous aluminas: kinetics and equilibrium." *J. Colloid Interface Sci*., 273, 14–21.

130. Ricordel, S., Taha, S., Cisse, I., and Dorange, G. (2001). "Heavy metals removal by adsorption onto peanut husks carbon: characterization, kinetic study and modeling." *Sep. Purif. Technol*., 24, 389–401.

131. Rivera-Utrilla, J., and Sanchez-Polo, M. (2003). "Adsorption of Cr(III) on ozonized activated carbon. Importance of Cpi–cation interactions." *Water Res*., 37, 3335–30340.

132. Saeed, A., Waheed, M., Akhter, and Iqbal, M. (2005). "Removal and recovery of heavy metals from aqueous solution using papaya wood as a new biosorbent." *Sep. Purif. Technol.*, 45, 25-31.

133. Sawyer, C. N., McCarty, P. L., and Parkin, G. F. (2003). Chemistry for Environmental Engineering and Science, 5th ed., Tata-McGraw-Hill, New Delhi, India.

134. Schaep, J., Van, D. B. B., Vandecasteele, C., and Wilms, D. (1998). "Influence of ion size and charge in nanofiltration." *Sep. Purif. Technol*., 14, 155.

135. Schwertmann, U., and Taylor, R. M. (1989). Iron oxides. In: Dixon, J.B., Weed, S.B. (Eds.), Minerals in Soil Environments, 2nd edn. Soil Sci. Soc. Am., Madison, WI, pp. 379–438.

136. Sekar, M., Sakthi, V., and Rengaraj, S. (2004). "Kinetics and equilibrium adsorption study of lead(II) onto activated carbon prepared from coconut shell." *J. Colloid Inter. Sci*., 279, 307–313.

137. Sharma, D. C., and Forster, C. E. (1996). "A Comparison of the sorbtive characteristics of leaf mould and activated carbon columns for the removal of hexavalent chromium." *Process Biochem*., 31, 213-218.

138. Sincero, A. P., and Sincero, G. A., (2003). Physical - Chemical treatment of water and wastewater, CRC press, Florida, USA, 401-402.

139. Singh, D. B., Rupainwar, D. C., Prasad, G., and Jayaprakash, K. C. (1998). "Studies on the Cd II/ removal from water by adsorption." *J. Hazard. Mater*., 60, 29–40.

140. Singh, K. K., Talat, M., and Hasan, S. H. (2006). "Removal of lead from aqueous solutions by agricultural waste maize bran." *Biores. Technol.*, 97, 2124-2130.

141. Stumm, W., and Morgan, J. J. (1996). Aquatic Chemistry, Chemical Equilibria and Rates in Natural Waters, 3rd Edition, John Willey and Sons.

142. Taty-Costodes, V. C., Fraduet, H., Porte, C., and Ho, Y. S. (2005). "Removal of lead(II) ions from synthetic and real effluents using immobilized Pinus sylvestris sawdust: Adsorption on a fixed-bed column." *J. Hazard. Mater*., B123, 135-144.

143. Thomas, (1994). "Heterogeneous ion exchange in a flowing system." *J. Am. Chem. Soc*. 66, 1664-1666.

144. Tokimoto, T., Kawasaki, N., Nakamura, T., Akutagawa, J., and Tanada, S. (2005). "Removal of lead ions in drinking water by coffee grounds as vegetable biomass." *J. Col. Inter. Sci.*, 281, 56–61.

145. Tunali, S., Kiran, I., and Akar, T. (2005). "Chromium(VI) biosorption characteristics of Neurospora crassa fungal biomass." *Minerals Eng.*, 18, 681–689.

146. Ucun, H., Bayhan, Y. K., Kayab, Y., Cakici, A., and Algurb, O. K. (2003). "Biosorption of lead (II) from aqueous solution by cone biomass of *Pinus sylvestris*." *Desalination*, 154, 233-238.

147. US Department of Health and Human Services. (1991). Toxicological Profile for Chromium. Public Health Service Agency for Toxic substances and Diseases Registry, Washington, DC.

148. Va´zquez, G., Gonza´lez-A´lvarez, J., Freire, S., Lo´pez-Lorenzo, M., and Antorrena, G. (2002). "Removal of cadmium and mercury ions from aqueous solution by sorption on treated *Pinus pinaster* bark: kinetics and isotherms." *Biores. Technol*., 82, 247–251.

149. Vasudevan, P., Padmavathy, V., Tewari, N., and Dhingra, S. C. (2001). "Biosorption of heavy metal ions." *J. Sci. Ind. Res*. 60, 112–120.

150. Veenstra, J. N. Sanders, D., and Ahn, S. (1999). "Impact of chromium and copper on fixed film biological systems." *J. Env. Eng.*, 125, 522–531.

151. Verma, S., Chakraborty, S., and Basu, J. K. (2006). "Adsorption study of hexavalent chromium using tamarind hull-based adsorbents." *Sep. Purif. Techno*l., 50, 336-341.

152. Viel, P., Palacina, S., Descoursb, F., Bureaub, C., Derf, F. L., Lyskawac, J., and Salle, M. (2003). "Electropolymerized poly-4-vinylpyridine for removal of copper from wastewater." *Appl. Surf. Sci*., 212, 792–796.

153. Vijayaraghavan, K., Jegan, J., Palanivelu, K., and Velan, M. (2005). "Batch and column removal of copper from aqueous solution using a brown marine alga *Turbinaria ornate*." *Chem. Eng. J.*, 106, 177-184.

154. Villaescusa, I., Fiol, N., MartInez, M., Miralles, N., Poch, J., and Serarols, J. (2004). "Removal of copper and nickel ions from aqueous solutions by grape stalks wastes." *Water Res*., 38, 992–1002.

155. Voice, T. C., and Weber, W. J. (1983). "Sorption of hydrophobic compounds by sediments, soils and suspended solids-I." *Water Res.*, 17, 1433-1441.

156. Volesky, B. (2001). "Detoxification of metal-bearing effluents: biosorption for the next century." *Hydrometallurgy*, 59, 203–216.

157. Walcarius, A., Etienne, M., and Delacote, C. (2004). "Uptake of inorganic Hg(II) by organically modified silicates: influence of pH and chloride concentration on the binding

pathways and electrochemical monitoring of the processes." *Anal. Chim. Acta*, 508, 87–98.

158. Warchoł, J., and Petrus, R. (2006). "Modeling of heavy metal removal dynamics in clinoptilolite packed beds." *Microporous Mesoporous Mater*., 93, 29-39.

159. Weber W. J. (1972). Physico-chemical Process for Water Quality Control, Wiley Inc., 261–305.

160. Weber, W. J., and DiGiano, F. A. (1995). Process Dynamics in Environmental Systems. , Wiley-Interscience, New York.

161. Wei, Y., Yang, C., and Ding, T. (1996). "A one-step method to synthesize N,N'-Bis(4'-aminophenyl)-1,4-quinonenediimine and its derivatives." *Tetrahedron letters*, 37, 731-734.

162. WHO (1993). Guidelines for drinking-water quality, World Health Organization, Geneva.

163. Wu, Y., Zhang, S., Guo, X., and Huang, H. (2008). "Adsorption of chromium(III) on lignin." *Biores. Technol*. 99, 7709-7715.

164. Yan, G., and Viraraghavan, T. (2003). "Heavy-metal removal from aqueous solution by fungus Mucor rouxii", *Water Res*., 37, 4486-4496.

165. Yang, X., Zhao, T., Yu, Y., and Wei, Y. (2004). "Synthesis of conductive polyaniline/epoxy resin composites: doping of the interpenetrating network." *Synthetic Mat*., 142, 57-61.

166. Yardim, M. F., Budinova, T., Ekinci, E., Petrov, N., Razvigorova, M., and Minkova, V. (2003). "Removal of mercury (II) from aqueous solution by activated carbon obtained from furfural." *Chemosphere*, 52, 835–841.

167. Zeroual, Y., Moutaouakkil, A., Dzairi, F. Z., Talbi, M., Chung, P. U., Lee, K., and Blaghen, M. (2003). "Biosorption of mercury from aqueous solution by *Ulva lactuca* biomass." *Biores. Technol.*, 90, 349–351.

168. Zhang, F. S., Nriagu, J. O., and Itoh, H. (2005). "Mercury removal from water using activated carbons derived from organic sewage sludge." *Water Res*., 39, 389–395.

169. Zheng, J. (2002). Studies of PF Resole/ Isocyanate hybrid adhesives. PhD dissertation, Virginia Polytechnic Institute and State University.

170. Zouboulis, A. I., Kydros, K. A., and Matis, K. A. (1995). "Removal of hexavalent chromium anions from solutions by pyrite fines." *Water Res*., 29, 1755-1760.